Role of EBAG9 in COPI-Dependent Glycoprotein Maturation and Secretion Processes in Tumor Cells

Dissertation

zur Erlangung des akademischen Grades

doctor rerum naturalium

(Dr. rer. nat.)

im Fach Biologie

eingereicht an der

Mathematisch-Naturwissenschaftlichen Fakultät I

der Humboldt-Universität zu Berlin

von

Diplom-Biologin Jana Wolf, geb. Göttert

Präsident der Humboldt-Universität zu Berlin

Prof. Dr. Dr. h.c. Christoph Markschies

Dekan der Mathematisch-Naturwissenschaftlichen Fakultät I

Prof. Dr. Andreas Herrmann

Gutachter/innen: 1. Prof. Dr. Thomas Börner

2. Prof. Dr. med. Bernd Dörken

3. PD Dr. Uta Höpken

Tag der mündlichen Prüfung: 21.10.2010

Index of contents

Abstract

The estrogen receptor-binding fragment-associated gene 9 (EBAG9) has received increased attention as an independent prognostic marker for disease-specific survival since in some human tumor entities high expression levels correlate with tumor progression and poor clinical prognosis. Interestingly, EBAG9 was identified as an ubiquitously expressed Golgi protein. Recent data demonstrate an involvement in regulated exocytosis in secretory cells and the cytotoxic functions of lymphocytes. However, EBAG9 is expressed in essentially all mammalian tissues, and in epithelial cells it has been identified as a modulator of tumor-associated O-linked glycan expression, a hallmark of many carcinomas.

This thesis addresses the pathogenetic link between EBAG9 expression and the alteration of the cellular glycome. To gain further insights into the cellular functions of EBAG9 in epithelial cells, tumor-associated EBAG9 overexpression was mimicked in living cells. It was demonstrated that EBAG9 associates with anterograde COPI-coated carriers and shuttles between the ER-Golgi intermediate compartment and cis-Golgi stacks. EBAG9 overexpression imposes a delay in anterograde ER-to-Golgi transport and mislocalizes components of the ER quality-control and glycosylation machinery. Conversely, EBAG9 downregulation accelerates glycoprotein transport through the Golgi and enhances mannosidase activity. Functionally, EBAG9 impairs ArfGAP1 recruitment to membranes and consequently, interferes with the disassembly of the coat lattice at the cis-Golgi prior to fusion.

Thus, EBAG9 acts as a negative regulator of a COPI-dependent ER-to-Golgi transport pathway in epithelial cells and represents a novel pathogenetic principle in which interference with intracellular membrane trafficking results in the emergence of a tumor-associated glycome.

Keywords: anterograde transport, COPI, EBAG9, glycosylation, immunomodulation, mechanisms of disease, secretory pathway, tumor pathogenesis, vesicle trafficking

Zusammenfassung

EBAG9 (estrogen receptor-binding fragment-associated gene 9) hat als unabhängiger prognostischer Marker viel Aufmerksamkeit erregt, da in einigen Tumoren hohe Expressionsraten und Tumorentwicklung korrelieren. In diesen Fällen ist eine hohe EBAG9 Expression häufig mit einer schlechten klinischen Prognose verbunden. EBAG9 ist ein ubiquitär exprimiertes Golgi Protein. Aktuelle Daten demonstrieren, dass es in sekretorischen Zellen an der regulierten Exozytose und an der zytotoxischen Funktion von Lymphozyten beteiligt ist. In epithelialen Zellen führt es zur Generierung von Tumor-assoziierten O-Glykanen, welche ein Erkennungsmerkmal vieler Krebsarten sind.

In dieser Arbeit wurde der pathogenetische Zusammenhang zwischen EBAG9 Expression und der Veränderung des zellulären Glykoms untersucht. Um einen tieferen Einblick in die zelluläre Funktion von EBAG9 in epithelialen Zellen zu gewinnen, wurden Zellen mit tumorähnlicher EBAG9 Expression verwendet. Innerhalb dieser Arbeit wurde demonstriert, dass EBAG9 mit anterograden COPI Vesikeln assoziiert und zwischen dem ER-Golgi intermediären Kompartiment und cis-Golgi pendelt. EBAG9 verursacht eine Verzögerung des anterograden Transportes vom ER zum Golgi und verändert die Lokalisation von Komponenten der ER Qualitätskontrolle und des Glycosylierungsapparates. Auf der anderen Seite beschleunigt die verminderte Expression von EBAG9 den Proteintransport durch den Golgi und verstärkt die Aktivität von Mannosidase II. Mechanistisch betrachtet verhindert EBAG9 die Rekrutierung von ArfGAP1 an die Membran. Dies beeinträchtigt das Auflösen der COPI Vesikelhülle und somit die Fusion von Vesikeln am cis-Golgi.

Damit agiert EBAG9 in epithelialen Zellen als negativer Regulator des COPI-abhängigen ER-Golgi Transportes und stellt damit ein neues phatogenetisches Prinzip dar, bei dem die Beeinflussung des intrazellulären Transportes zu der Entstehung von Tumor-assoziierten Glykanen führt.

Schlagwörter: anterograder Transport, COPI, EBAG9, Glykosylierung, Immunmodulation, Krankheitsmechanismen, sekretorischer Transportweg, Tumorpathogenese, intrazellulärer Proteintransport

1 Introduction

1.1 The tumor associated antigen EBAG9

Estrogen receptor-binding fragment-associated antigen 9 (EBAG9), which was isolated by the use of the CpG-genomic binding site cloning method (Watanabe, et al., 1998), was reported to be identical to RCAS1 (receptor-binding cancer antigen expressed on SiSo cells) (Ikeda, et al., 2000). RCAS1 was initially defined by the 22.1.1 monoclonal antibody (mAb), which was raised by immunization of mice with the human uterine cervical adenocarcinoma cell line SiSo (Sonoda, et al., 1996). Cell surface staining with mAb 22.1.1 was shown immunohistochemically in a large number of different tumor tissues, and in some tumor entities 22.1.1, staining correlated well with poor clinical prognosis (Izumi, et al., 2001; Nakakubo, et al., 2002). A soluble form of the 22.1.1 antigen was purified from the supernatant of cultured SiSo cells (Sonoda, et al., 1996). Expression cloning led to the isolation of a cDNA apparently encoding the 22.1.1 antigen (Nakashima, et al., 1999). However, recent studies demonstrated that the EBAG9 gene-product and the 22.1.1 defined antigen are structurally and functionally separate antigens (Reimer, et al., 2005). In fact, it was shown that EBAG9 is not recognized by the 22.1.1 mAb. Instead, the 22.1.1 mAb recognizes the Tn-glycan antigen, which appears upon EBAG9 overexpression on the cell surface of HEK293 cells (Engelsberg, et al., 2003).

1.1.1 Features of EBAG9 protein

EBAG9 is highly conserved in phylogeny, and data bank screens revealed that there are no homologies to any other known genes or proteins. The predicted amino acid sequences of murine and canine EBAG9 showed 98 % and 96 % homologies with those of human EBAG9, respectively (Sonoda, et al., 2008). Furthermore, evolutionary highly conserved proteins orthologous to EBAG9 are found in rat (*Rattus norvegicus*), canine (*Canis familiaris*), Xenopus (*Xenopus laevis*) und Zebrafish (*Danio rerio*). However, no homolog exists in yeast. Ikeda et al. (2000) discovered that the human EBAG9 gene is located at chromosome 8q23 and is frequently amplified in breast tumors. The EBAG9 cDNA sequence is 1060 bp long and includes a coding region of 639 bp. The protein itself consists of 213 amino acids and has a predicted molecular weight of 24 kDa. Using a polyclonal serum against recombinant EBAG9, in westernblot analysis a specific double band can be observed that migrates around

32 kDa (Tsuchiya, et al., 2001). This difference can not be explained either by N- or O-glycosylation of the protein (Engelsberg, et al., 2003). Additionally, Sonoda et al. (1996) showed that mAb 22.1.1 immunoprecipitates generated a 78-kDa signal in SDS-PAGE gels under reducing and non-reducing conditions. Here, a homodimerization via the C-terminal coiled-coil region was suggested (Nakashima, et al., 1999). According to sequence predictions, EBAG9 has been postulated to be a type II transmembrane (TM) protein with an N-terminal TM region (amino acids 8–27) and an extracellular C-terminal coiled-coil region (amino acids 179–206), which is also highly conserved in human EBAG9 (Fig. 1-1).

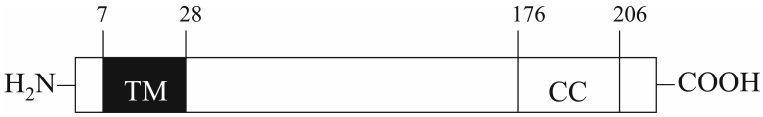

Fig. 1-1: Protein structure of EBAG9. Sequence prediction was carried out by „TMbase Server“ (Hofmann and Stoffel 1993) and „Coiledcoil prediction Server“ (Lupas, et al., 1991). TM = transmembrane domain; CC = coiled-coil domain.

EBAG9 mRNA as well as protein is ubiquitously expressed, but expression levels vary among tissues. The protein can be detected in the brain, spleen, lung, liver kidney, and testis as well as in the embryo at day 12, 14 and 16 dpc (days *post coitus*). Furthermore, relatively low expression levels were observed in the heart, uterus, and ovary, and at negligible levels in skeletal muscle (Tsuchiya, et al., 2001). Engelsberg et al. (2003) demonstrated that EBAG9 is predominantly localized in the Golgi. From deletion mutant studies it was concluded that the transmembrane domain of EBAG9 is responsible for its localization and sorting to the Golgi complex. Furthermore, Ruder et al. (2005) revealed that palmitoylation contributes to membrane association of EBAG9 and suggested that this anchor facilitates dynamic redistribution of EBAG9 in neuroendocrine cells.

1.1.2 EBAG9 and cancer

EBAG9 has been identified as a primary estrogen-responsive gene from a cDNA library of MCF-7 human breast cancer cell line (Watanabe, et al., 1998). Estrogen plays important roles in many biological processes, including the regulation of growth development and cell-type-specific gene expression in the reproductive tract (Couse and Korach, 1999), central nervous system (Simerly, et al., 1990), skeleton (Komm, et al., 1988), and immune system (Galien and

Garcia, 1997). These diverse functions are mediated by the estrogen receptors (ERα and β) which are members of the steroid-thyroid hormone receptor superfamily (Evans, 1988). The estrogen receptors bind to an estrogen responsive element (ERE) located in the promoters of responsive genes in a ligand-dependent manner and directly regulates their transcription (Nilsson, et al., 1998; Nilsson, et al., 2001). Furthermore, the estrogen receptors regulate gene expression by associating with other promoter-bound transcription factors. In MCF-7 cells it has been shown that EBAG9 mRNA is upregulated by estrogen and that its promoter responds to estrogen through the complete palindromic ERE, located in the 5´-upstream region of the gene. This binding increases the transcription rate by 0.5-3.2 times (Ikeda, et al., 2000; Watanabe, et al., 1998). Additionally, there might be estrogen-independent regulatory mechanisms of EBAG9 transcription, since putative binding motifs (*GC-boxes* and *E-boxes*) exist as well (Ikeda, et al., 2000). Alterations in the response to estrogen are associated with a variety of hormone-dependent diseases such as breast cancer, endometrial cancer, cardiovascular disease, and osteoporosis (Henderson and Feigelson, 2000; Ikeda, et al., 2000; Park, et al., 2005; Suzuki, et al., 2004; Tsuchiya, et al., 2001; Watanabe, et al., 1998).

EBAG9 overexpression has been recorded in a multitude of human epithelial cancers and has been proposed to correlate with tumor progression. Accordingly the molecule was introduced as an independent prognostic marker for disease-specific survival (Akahira, et al., 2004; Ogushi, et al., 2005; Suzuki, et al., 2004; Takahashi, et al., 2003; Tsuneizumi, et al., 2001). Interestingly, EBAG9 was shown to induce the surface deposition of the truncated O-linked glycans Tn (GalNAc) and the closely related TF (Thomsen-Friedenreich, Galβ1-3GalNAc) antigen at the cell surface in non-secretory cells (Engelsberg, et al., 2003). Using an Tn-antigen reactive antibody, elevated amounts of the truncated O-glycan Tn were detected in several tumor entities correlating with poor prognosis (Akashi, et al., 2003; Enjoji, et al., 2002; Okada, et al., 2003; Sonoda, et al., 1996). These results pointed towards an indirect, modulatory role of EBAG9 in the process of Tn antigen generation. Functionally, TF and Tn antigens were suggested to contribute to the pathogenesis of tumors through mediation of adhesion, invasion, and metastasis (Baldus, et al., 2000; Cavallaro and Christofori, 2001; Hakomori, 2002; Tsuiji, et al., 2003). Such glycan epitopes are normally cryptic in healthy and benign tissues, except in early embryonic stages (Springer, 1984). One conclusion has been that EBAG9 contributes indirectly to the antigenicity of tumor cells by modulating Tn and TF antigen expression (Engelsberg, et al., 2003).

1.1.3 Biological functions of EBAG9

Despite its putative role in tumor progression, the pathophysiological function of EBAG9 has not yet been well defined. Recombinantly expressed EBAG9 was suggested to bind to a yet unidentified receptor, which was supposed to be expressed on activated immune cells. Cell culture supernatant from SiSo cells inhibited proliferation of activated T cells and induced apoptotic cell death in receptor-bearing cells. Therefore, EBAG9 was proposed as a new death receptor ligand involved in tumor immune escape (Nakashima, et al., 1999). Moreover, it has been suggested that EBAG9 is involved in down-regulation of the maternal immune response during pregnancy (Ohshima, et al., 2001). Matsushima et al. (2001) demonstrated that EBAG9 expression by bone marrow macrophages is important in the regulation of erythropoiesis by induction of apoptosis in erythroid progenitor cells. Thereby the role of EBAG9 was extended to a general cell death-inducing system according to the Fas/Fas ligand system (Matsushima, et al., 2001). These studies mainly used the 22.1.1 antibody or the cell culture supernatant from SiSo cells. However, as already indicated, recent studies demonstrated that the EBAG9 gene-product and the 22.1.1 defined antigen are structurally and functionally separate antigens (Reimer, et al., 2005). This discrepancy sheds doubt on the proposed function of EBAG9 as an apoptosis-inducing death receptor ligand.

On the other hand, a recent study in neuroendocrine PC12 cells demonstrated that EBAG9 induces a downregulation of [Ca^{2+}] regulated secretion, but essentially no glycan alteration (Ruder, et al., 2005). Together with the identification of Snapin, a SNARE (soluble N-ethylmaleimide-sensitive factor attachment protein receptors) associated molecule as an interaction partner, these results pointed to a role for EBAG9 in the secretory pathway. Mechanistically, the phosphorylation of Snapin, which is a modulator of synaptotagmin-associated regulated exocytosis, was reduced. This in turn decreased the association of Snapin with the synaptosome-associated proteins of 23 and 25 kDa (SNAP23 and SNAP25), followed by a decrease in synaptotagmin recruitment. Enhancing the interaction between EBAG9 and Snapin inhibited the secretion of neuropeptide Y from PC12 cells *in vitro*, whereas constitutive secretion of α1-antitrypsin in HepG2 cells remained unaffected. From these data it was suggested that EBAG9 is a novel modulator of regulated exocytosis that acts upstream of Snapin and the SNARE complex (Ruder, et al., 2005).

However, a modulation of neurotransmitter release in cells equipped with a regulated exocytosis machinery could not be reconciled with the effects observed in epithelial cell lines, including O-linked glycan generation. This raises the question what physiological function EBAG9 in epithelial cells has, and whether this function relates to its proposed tumor association. Therefore, further analysis of the physiological role of EBAG9 in normal tissues and in tumor formation might be essential in order to understand general principles of oncogenic transformation.

1.2 The secretory pathway

1.2.1 From the endoplasmic reticulum to the cell exterior

In the biosynthetic secretory pathway of eukaryotic cells newly synthesized proteins are transported from the endoplasmic reticulum (ER), via the intermediate compartment (IC) and the Golgi apparatus to the plasma membrane (PM), or via late endosomes to lysosomes (Fig. 1-2) (Harter and Wieland, 1996; Saraste, et al., 2009). Between these compartments, vesicles continuously bud off from one membrane and fuse with another. There are three major classes of vesicles involved in protein trafficking, identified by their electron-dense "coats" COPI and COPII-coated vesicles (where COP stands for coat protein complex), and clathrin-coated vesicles (CCV). Each type is used for different transport steps in the cell and will be defined in detail in chapter 1.2.3.1 (Barlowe, 2000). During the stepwise transport of proteins through the secretory pathway, they are successively modified by means of glycosylation (Nilsson, et al., 2009). Transfer from one compartment to the next involves a delicate balance between forward (anterograde) and backward (retrograde) transport pathways. Here, transport vesicles select cargo molecules and move them to the next compartment in the pathway, while others retrieve escaped proteins and return them to a previous compartment where they usually function (Harter and Reinhard, 2000; Jackson, 2009).

1.2.1.1 Transport from the trans-Golgi-network

In general, the biosynthetic-secretory pathway allows the cell to modify the molecules it produces in a series of steps, store them until needed, and then deliver them to the exterior through a specific cell-surface domain in a process called exocytosis. At the trans-Golgi network (TGN), three main pathways of protein sorting can be distinguished (Fig. 1-2):

signal-mediated sorting into lysosomes, constitutive exocytosis and signal-dependent-regulated exocytosis (Gu, et al., 2001).

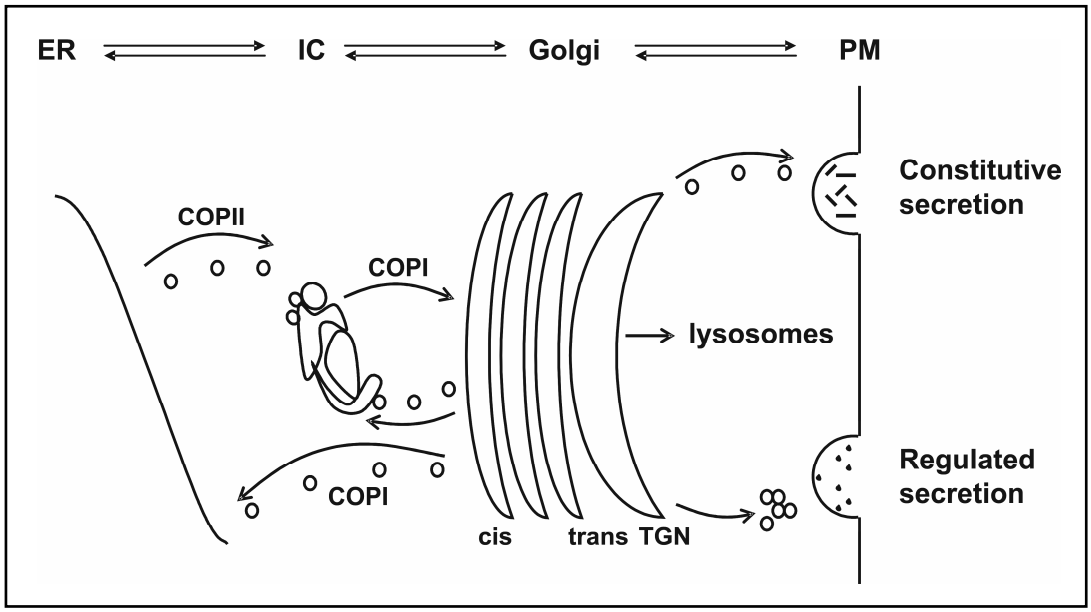

Fig. 1-2: The biosynthetic secretory pathway based on the stable compartment model. Newly synthesized proteins are transported from the endoplasmic reticulum (ER), via the intermediate compartment (IC) and the Golgi apparatus to the plasma membrane (PM) in an anterograde direction. They are first incorporated into COPII vesicles which bud from the ER and move towards the IC where a switch from COPII to COPI vesicles takes place (Scales, et al., 1997). From here tubulo-vesicular ER-to-Golgi carriers (EGCs) might move towards the cis Golgi in a COPI-dependent manner (Appenzeller-Herzog and Hauri, 2006). The sorting of mature proteins destined for lysosomes, constitutive or signal-mediated-regulated secretion takes place at the trans-Golgi-Network (TGN). In the retrograde direction Golgi resident and premature proteins that possess the C-terminal signal KDEL are retrieved from the IC/Golgi by KDEL-Receptor (KDELr) recycling back to the ER via retrograde COPI vesicles (Martinez-Menarguez, et al., 2001). The dual function of COPI might be made possible by the existence of different COPI vesicle sub-populations (Orci, et al., 1997).

The constitutive secretory pathway operates in all cells. Many soluble proteins are continually secreted from the cell by this pathway, which also supplies the plasma membrane with newly synthesized lipids and proteins. In contrast, specialized secretory cells also have a regulated secretory pathway, by which selected proteins at the TGN are diverted into secretory vesicles. In these vesicles, proteins are concentrated and stored until an extracellular signal induces a rise of cytoplasmic Ca^{2+}. This is followed by their fusion with the target membrane and finally, secretion (Burgoyne and Morgan, 2003). Although major differences between regulated and constitutive exocytosis have been established, a few regulatory molecules have been suggested to function in the switch between both processes. More specifically, the small Ras-like GTPase Rab11b has been demonstrated to function as a GTP-dependent switch between regulated and constitutive secretory pathways in neuronal but not in non-neuronal

cell lines (Khvotchev, et al., 2003). This observation suggested that the organization of the secretory pathway differs fundamentally between cells in which regulated and constitutive secretion coexist and, on the other hand, cells that are equipped only with a constitutive machinery.

One prominent example for regulated secretion is the cytotoxic response of cytotoxic T-lymphocytes (CTLs), which plays an important role in the killing of malignant and virally infected cells. Upon contact of T cells with antigen-presenting cells (APCs), a multimolecular assembly of receptors and adhesion molecules on both cells is induced, termed the immunological synapse (IS) (Friedl, et al., 2005). The antigen-specific cytotoxic response can be divided into three stages: 1. recognition and attachment of a CTL to a target cell, which is mediated through adhesion molecules and causes relocalization of the microtubule-organizing center (MTOC), the Golgi and lytic granules towards the IS (Kupfer and Singer, 1989; Stinchcombe, et al., 2001); 2. interaction of the T-cell receptor (TCR) with the peptide/MHC complex; 3. induction of target cell apoptosis via release of cytotoxic enzymes from lytic granules such as granzyme A and B and the pore-forming molecule perforin or Fas-L/Fas interaction (Montoya, et al., 2002; Reichardt, et al., 2007).

Multiple pathways to the endosomal system arise from the TGN and mediate delivery of essential components to various endosomal intermediates and finally, the lysosomes. Thus, proteins can reach lysosomes by both biosynthetic and endocytic pathways. Generally, membrane proteins are sorted by signals in their cytoplasmic tails recognized by the appropriate sorting machinery, including the adaptor complexes (AP) (Boehm and Bonifacino, 2001; Duffield, et al., 2008; Robinson and Bonifacino, 2001). However, some proteins do not possess a sorting signal; instead they are modified during biosynthesis by the addition of a mannose-6phosphate moiety, which is recognized by mannose-6-phosphate receptors (MPR). These transmembrane receptors cycle between the TGN and late endosomes and carry soluble proteins to lysosomes (Blott and Griffiths, 2002; van Meel and Klumperman, 2008).

1.2.1.2 Polarized transport

Many cell types of multicellular organisms are polarized and have two functionally distinct membrane domains to which different types of vesicles must be directed by the polarized transport machinery. A typical epithelial cell has an apical domain which faces the lumen and

often has specialized features such as cilia or a brush border of microvilli. Such a cell also has a basolateral domain, which covers the rest of the cell (Huet, et al., 2003). The two domains are separated by a ring of tight junctions which prevent proteins and lipids from diffusing between the two domains, so that the compositions of the two domains are different (Tanos and Rodriguez-Boulan, 2008). The transport routes of apically and basolaterally destined cargo diverge at the TGN in polarized cells (Ikonen and Simons, 1998; Rodriguez-Boulan and Powell, 1992; Schuck and Simons, 2004). From the TGN, cargo can be transported directly to the apical or basolateral membrane. Additionally, basolateral cargo can reach the plasma membrane through endosomes, whereas apical cargo can also be sorted to the apical membrane via the transcytotic route following initial transport to the basolateral membrane (Polishchuk, et al., 2004).

Basolateral sorting signals are confined to the cytosolic tails of membrane proteins. These signals are often tyrosine- or dileucine-based amino acid motifs that may be related to clathrin coated pit endocytic signals or PDZ-domain binding motifs (Duffield, et al., 2008; Rodriguez-Boulan, et al., 2005). Apical sorting signals are more variable, whereas basolateral determinants seem to dominate over apical ones (Schuck and Simons, 2004). The most notable difference between the apical and basolateral sorting principles seems to be that apical recognition is based not only on cytosolic protein-protein interactions, but also cooperative inter-lipid and protein-lipid affinities as well as carbohydrate recognition (Ikonen and Simons, 1998; Schuck and Simons, 2004). Both N- and O-glycosylation of the extracellular domain have been implicated in apical targeting (Scheiffele, et al., 1995). Here, 1-benzyl-2-acetamido-2-deoxy-α-D-galactopyranoside (GalNAc-α-*O*-bn), an inhibitor of O-gylcosylation, blocked cargo delivery to the apical surface in polarized cells (Delacour, et al., 2003). Mechanistically, GalNAcα-*O*-bn is converted into the benzyldisaccharide Galβ1–3GalNAcα-*O*-bn, which acts as a potent competitive inhibitor of α2,3-sialyltransferase (ST3Gal I) and is involved in the terminal elongation of *O*-linked glycans. However, there is also evidence that GalNAc-α-*O*-bn inhibits glycosylation in a cell-specific manner (Leteurtre, et al., 2003). Interestingly, GalNAc-α-*O*-bn was also shown to induce Tn and TF generation (Huet, et al., 2003).

Defects in trafficking pathways which maintain epithelial polarity can cause disease in organs in which epithelial cell polarity is crucial, such as the liver, kidney and intestines (Stein, et al., 2002). Thus, a loss of polarity is a hallmark of tumorigenesis in epithelial cells. However, it

remains unclear whether this is a consequence of or a prerequisite for oncogenic transformation (Fransen, et al., 1991; Hanahan and Weinberg, 2000; Moolenaar, et al., 1997; Tanos and Rodriguez-Boulan, 2008). Since EBAG9 is overrepresented in tumors of epithelial origin and an induction of tumor-associated glycans was observed, the question arose whether EBAG9 influences polarized transport.

1.2.2 Mechanisms of biosynthetic protein transport from the ER towards the Golgi

Currently, different models regarding the transport of anterograde and retrograde cargo through the secretory pathway are being considered. In general, cargo molecules move from the ER in vesicular or tubular shaped-transport intermediates, also called Vesicular Tubular Clusters (VTCs), to the Golgi complex, which involves the passage through an ER-Golgi intermediate compartment (ERGIC) or IC, the marker of which is the lectin ERGIC-53 (Fig. 1-2) (Polishchuk, et al., 2009; Presley, et al., 1997; Scales, et al., 1997; Schweizer, et al., 1991; Stephens and Pepperkok, 2001). Recent reports argue against mobile transport complexes but favour a stationary IC where anterograde and retrograde sorting of proteins occurs (Appenzeller-Herzog and Hauri, 2006). Furthermore, the IC also contributes to the concentration, folding, and quality control of newly synthesized proteins (Hauri, et al., 2000; Hebert, et al., 2005).

Subsequently, a secretory cargo arrives at the cis side of a Golgi stack and then travels across the stack to the opposite, trans side before being exported from the trans-Golgi network (TGN). It is still uncertain how the Golgi apparatus achieves and maintains its polarized structure and how molecules move from one cisterna to another. One view is that vesicles might transport proteins between the cisternae, budding from one cisterna and fusing with the next. According to this vesicular transport model, the Golgi apparatus is a relatively static structure, with its enzymes held in place, while the molecules in transit are moved through the cisternae in sequence, carried by transport vesicles (Nickel, et al., 1998; Orci, et al., 1997; Palade, 1975; Pepperkok, et al., 1993; Volchuk, et al., 2000). Retrograde flow retrieves escaped ER and Golgi proteins and returns them to preceding compartments. Directional flow is achieved as forward-moving cargo molecules are selectively packaged into forward-moving vesicles, whereas proteins to be retrieved are selectively packaged into retrograde vesicles.

However, the cisternal maturation mode of cargo transport is now the favoured model (Barr, 2002). This cisternal maturation model assumes that Golgi cisternae form *de novo*, progressively mature, and ultimately dissipate (Bonfanti, et al., 1998; Glick, et al., 1997; Martinez-Menarguez, et al., 1999; Stephens, et al., 2000). In a stacked Golgi, vesicular tubular clusters that arrive from the ER would fuse with one another to become a cis-Golgi network. This new cisternae would progress through the stack, and peel off from the trans face. Secretory cargo proteins are thought to be carried forward by this process of cisternal progression. Meanwhile, the progressing cisternae would mature by the recycling of resident Golgi proteins from older to younger cisternae via retrograde vesicle flow (Rabouille and Klumperman, 2005; Storrie and Nilsson, 2002; Ungar, et al., 2006). A combination of both models, the percolating vesicle model, integrates the advantages of rapid anterograde transport mediated by vesicles, as opposed to the higher capacity of cisternal maturation that accounts for the transport of large cargo (Bethune, et al., 2006; Pelham and Rothman, 2000).

1.2.3 From budding to fusion: components of the secretory pathway

1.2.3.1 Coat proteins

Coat proteins play a key role in intracellular transport by coupling vesicle formation with cargo sorting. This process involves coat binding to specific sequences in the cytoplasmic domains of cargo proteins for their proper packaging into nascent vesicles. Most transport vesicles form from specialized, coated regions of membranes. They bud off as coated vesicles (COPI, COPII or CCV) that have a distinctive cage of proteins covering their cytosolic surface. Before the vesicle fuses with a target membrane, the coat is discarded. This is required to allow the two cytosolic membrane surfaces to interact directly and fuse (Barlowe, et al., 1994; Malhotra, et al., 1989).

Clathrin-coated vesicles (CCV) have been demonstrated to mediate transport from the Golgi apparatus and from the plasma membrane (Hanover, et al., 1984). Here, clathrin as a central organiser concentrates cargo adaptor protein (AP) complexes such as AP1, AP2 and AP3 (Robinson, 2004). Most AP complexes link clathrin to selected membrane cargo and lipids and bind accessory proteins that regulate coat assembly and disassembly. It has been shown that there is structural and functional homology between COPI coats and clathrin-adaptor

coats (Fig. 1-3) (Boehm and Bonifacino, 2001; Bonifacino and Lippincott-Schwartz, 2003; Hoffman, et al., 2003; McMahon and Mills, 2004; Robinson and Bonifacino, 2001; Serafini, et al., 1991).

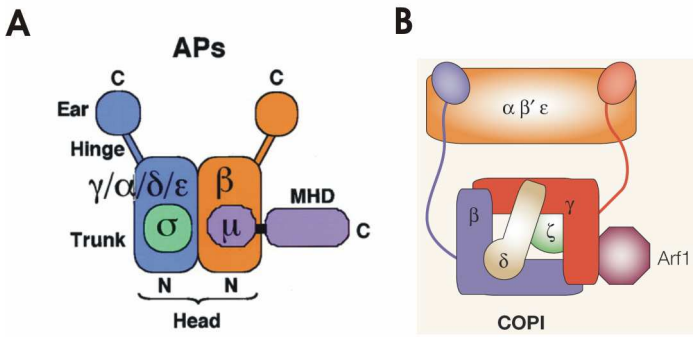

Fig. 1-3: Schematic representation of adaptins and coatamer protein I. (A) N and C indicate the amino- and carboxy-termini of the proteins, respectively; γ-adaptin earhomology domain; MHD, μ-homology domain (Boehm and Bonifacino, 2001). (B) The structure of the coatomer protein (COPI) βγδζ subcomplex is based on the model of AP2 because of the homology of their subunits. The arrangement of the other COPI subunits has not been elucidated (Bonifacino and Lippincott-Schwartz, 2003).

In contrast, COPI- and COPII-coated vesicles commonly mediate transport from the ER and the Golgi cisternae (Fig. 1-2). COPI is composed of seven conserved subunits (α, β, β´, δ, γ, ε and ζ) divided into two subcomplexes: the F subcomplex (β δ, γ and ζCOP), and the B subcomplex (α, β´, ε). The former subcomplex probably has a topology similar to the AP complex and the latter is likely to be the functional equivalent of clathrin (Fig. 1-3) (McMahon and Mills, 2004; Schledzewski, et al., 1999; Takatsu, et al., 2001; Waters, et al., 1991). Coatomer subunits recruit cargo by directly binding to dilysine motifs (KKXX, KXKXX) or to a motif containing two arginine and phenylalanine moieties, both located at the carboxy terminus (Cosson and Letourneur, 1994; Letourneur, et al., 1994). Moreover, cargos are captured by adaptor transmembrane proteins, such as the KDEL receptor (KDELr), that communicate with the COPI coat at their cytosolic site. KDELr recognizes the K(H)DEL sequence at the carboxy terminus of many ER-resident proteins and thus retrieves them from the Golgi (Lewis and Pelham, 1992; Semenza, et al., 1990). The COPII coat structure was found to consist of the subcomplexes Sec23/24p and Sec13/31p. For cargo proteins a DxE-type motif was found to interact with COPII subunits (Bonifacino and Lippincott-Schwartz, 2003; Harter and Wieland, 1996; Nishimura, et al., 1999).

While COPII functions in ER export in the anterograde transport direction (Budnik and Stephens, 2009; Hughes and Stephens, 2008), the interpretation of the role of COPI-coated transport carriers is made complex by the existence of different COPI vesicle sub-populations.

Their distribution is statistically significantly segregated within the Golgi complex (Beck, et al., 2009; Malsam, et al., 2005; Moelleken, et al., 2007; Orci, et al., 1997). COPI acts primarily in the retrieval of ER-derived resident proteins from later compartments. More recent studies have revealed that mammalian cells contain at least three distinct isoforms of coatomers that appear to assemble separately and regionally within the Golgi (Moelleken, et al., 2007). These findings suggested that COPI may carry traffic in both the anterograde and retrograde direction within a stack, depending on the COPI population involved (Lee, et al., 2004). This second function of COPI transport carriers was proposed because they were shown to serve the anterograde route as well. Using vesicular stomatitis virus G protein (VSVG) as anterograde transport marker, it was demonstrated that COPII is lost rapidly after vesicle budding from ER exit sites. At the boundary between ER exit sites and the IC, the COPII coat is replaced by COPI coat components. Depending on the COPI population, these vesicular tubular clusters move either towards the Golgi, or recycle back to the ER (Bannykh and Balch, 1997; Beck, et al., 2009; Griffiths, et al., 1995; Scales, et al., 1997; Stephens, et al., 2000). Direct evidence for a role of coatomer in ER-to-Golgi transport was provided by the demonstration that VSVG transport to the Golgi is inhibited by antibodies directed against the βCOP subunit of coatomer (Pepperkok, et al., 1993; Peter, et al., 1993). Furthermore, in *Saccharomyces cerevisiae*, a block of anterograde transport is observed in mutants of COPI subunits (Hosobuchi, et al., 1992). Additionally, COPI has also been implicated in post-Golgi trafficking steps such as the maintenance of endosomal/lysosomal function (Aniento, et al., 1996; Razi, et al., 2009).

However, many reports point toward a more complex structure of the secretory pathway, since an additional pathway for Golgi-to-ER transport has been discovered (Girod, et al., 1999; Storrie, et al., 2000; White, et al., 1999). Girod et al. (1999) provided evidence for a COPI-independent transport pathway which is specifically regulated by Rab6 and is used by Golgi glycosylation enzymes and Shiga toxin.

1.2.3.2 The vesicle machinery: from Arfs to SNAREs

Targeting of COPI vesicles to a particular destination in the Golgi or ER is a multistep process in which tethers and members of the Rab- and Adenosine diphosphate-ribosylation factor (Arf)- families play a leading role in vesicle tethering, followed by vesicle docking, and

ultimately a SNARE-dependent membrane fusion event (Bonifacino and Glick, 2004; Cai, et al., 2007).

In general, each vesicle transport reaction can be divided into four essential steps (Fig. 1-4) (Bonifacino and Glick, 2004). First, the assembly of protein coats which are dynamic structures that cycle on and off membranes. Recruitment of the coat components from the cytosol onto donor membranes is regulated by the small guanosine triphosphatases (GTPases) ADP-Ribosylation Factor 1 (ARF1) for COPI vesicles and Sar1 for COPII vesicles (Cai, et al., 2007; Donaldson, et al., 1992). These in turn are activated by Guanine-nucleotid-exchange factors (GEFs) which replace GDP by GTP (Chardin, et al., 1996; Jackson and Casanova, 2000; Peyroche, et al., 1996). Coatomer-Arf1-GTP complexes then undergo low affinity interactions to generate a membrane-deforming lattice capable of budding-coated carriers (Bremser, et al., 1999; Goldberg, 2000).

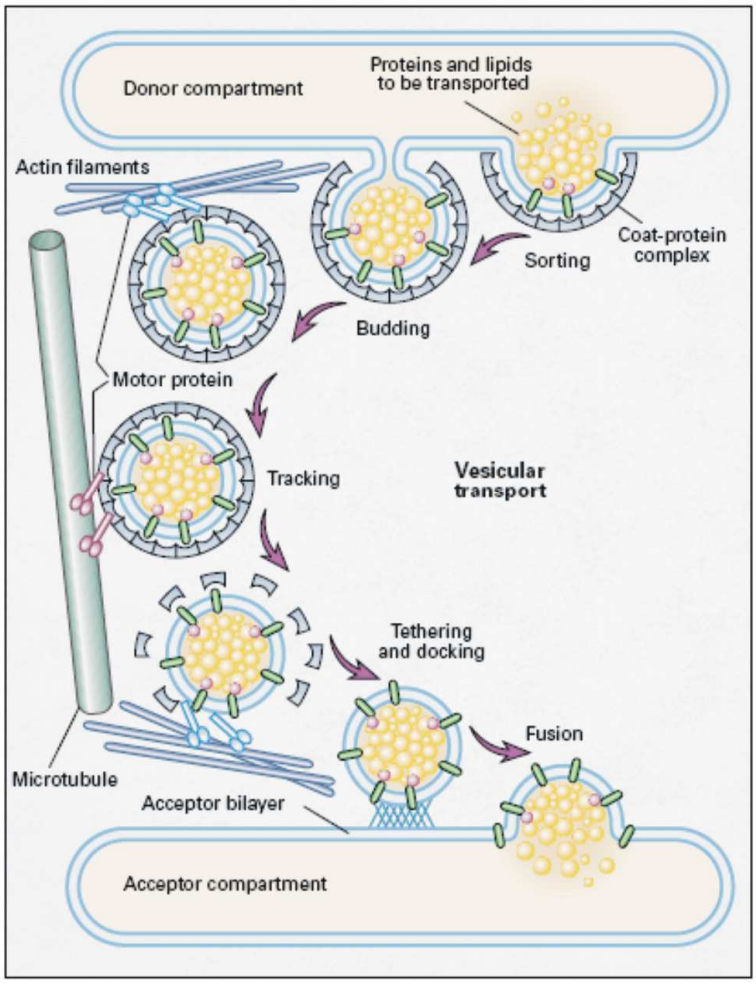

Fig. 1-4: From budding to fusion. Each vesicle transport reaction can be divided into four essential steps that include coatomer recruitment, vesicle budding, vesicle transport, tethering and fusion. Briefly, proteins and lipids are sorted to specific sites on the donor membrane, transport vesicles bud with the aid of cytosolic complexes of coat proteins and vesicles move along cytoskeletal tracks. The vesicle is tethered and docked near the target membrane and subsequently fuses with the acceptor bilayer, releasing its contents (after Olkkonen and Ikonen (2000).

Second, after budding, vesicles are transported to their final destination by diffusion or by motor-mediated transport along a cytoskeletal track (microtubules or actin). The molecular motors kinesin, dynein, and myosin have all been implicated in this process (Lippincott-Schwartz, 1998; Mermall, et al., 1998). Prior to vesicle tethering, ARF1 or Sar1, respectively, are inactivated by GTPase activating proteins (GAPs), which hydrolyze GTP on Arf1 leading to release of Arf1-GDP and disassembly of the coatomer complex (Bigay, et al., 2003; Cukierman, et al., 1995; Liu, et al., 2005; Makler, et al., 1995; Randazzo and Kahn, 1994; Reinhard, et al., 2003; Tanigawa, et al., 1993).

Third, the Rab proteins of the ras superfamily of small GTPases, are key regulators of tethering and fusion by facilitating docking of vesicles at the target membrane (Zerial and McBride, 2001). They bind to GEFs and are activated by the exchange of GDP to GTP. Finally, Rab binds to Rab effectors at the target membrane and facilitates the attachment of SNARE proteins (Ohya, et al., 2009). The complexity of the Rab protein family in mammalian cells correlates with the diversity of vesicle transport routes displayed in a variety of mammalian cell types (Simons and Zerial, 1993). Individual Rab proteins are localized to distinct, characteristic organelles, suggesting that each type regulates a particular membrane traffic step (de Renzis, et al., 2002; Rink, et al., 2005).

The last step in vesicle-mediated transport is the fusion of the vesicle with its target membrane. The fusion of two lipid bilayers is catalyzed by the assembly of the SNARE complex. Here a SNARE molecule on a transport vesicle (v-SNARE) pairs with its cognate SNARE-binding partner (t-SNARE) on the appropriate target membrane (Sollner, et al., 1993; Sollner, et al., 1993). However, recent findings indicate that it is not the pairing of SNAREs that drives the specificity of vesicle targeting, but rather tethers like Rab proteins, which act further upstream (Burgoyne and Morgan, 2003; Cai, et al., 2007; Chavrier, et al., 1990; Jahn and Scheller, 2006; Olkkonen and Ikonen, 2000; Sudhof, 1995).

SNAREs are a family of membrane proteins that are related to three different neuronal proteins: Syn1 (syntaxin 1), VAMP (vesicle-associated membrane protein)/synaptobrevin, and SNAP25 (synaptosome-associated protein-25) (Bennett, et al., 1992; Cai, et al., 2007; Oyler, et al., 1989; Trimble, et al., 1988). Individual family members function in distinct vesicular trafficking pathways. Thus, Syn1, VAMP2 and SNAP25 are required for synaptic vesicle exocytosis in neurons, where SNARE-mediated vesicle fusion has been extensively studied.

Here, Snapin has been reported to be a neuron-specific component of synaptic vesicles that interacts with isolated SNAP25 as well as with the assembled synaptic SNARE complex to modulate the interactions between SNAREs and synaptotagmin (Buxton, et al., 2003; Ilardi, et al., 1999; Sudhof, 1995). Synaptotagmin plays a crucial role in regulated exocytosis by binding Ca^{2+} and functions as a Ca^{2+} sensor that triggers neurotransmitter release (Andrews and Chakrabarti, 2005; Chapman, 2002). As has been described in chapter 1.1.3, this step was shown to be regulated by EBAG9.

1.2.4 Retrograde transport

Control of membrane traffic has a major role in maintaining the composition of various cell membranes. To maintain the composition of each membrane-enclosed compartment in the secretory pathway at a constant size, the balance between the "forward" and "backward" flow needs to be precisely regulated. Thus, simultaneously to the anterograde transport, there is a constant retrograde flow of proteins and membrane lipids which are either taken up at the plasma membrane by endocytosis, or of Golgi resident proteins which need to be retrieved (Sannerud, et al., 2003).

The intracellular retrograde transport routes between the plasma membrane and the endoplasmic reticulum have been insufficiently explored. Bacterial toxins, such as the Shiga toxin subunit B (STB) produced by *Shigella dysenteriae*, have become a powerful tool to study this pathway. STB enters the cell through clathrin-independent endocytosis and is transported directly to the Golgi via the retrograde pathway, which is distinct from the well-known route used by the MPR (chapter 1.2). However, the Golgi-to-ER transport route appears to be independent of classic recycling markers, such as the KDELr and COPI. Instead, it was demonstrated that the STB reaches the ER via a Rab6-dependent retrograde pathway, which is also used by several Golgi glycosylation enzymes (Girod, et al., 1999; Johannes, 2002; Mallard, et al., 1998).

On the other hand, proteins can also bind directly to COPI coats by signals, such as the KKXX sequence, at C-terminus forming retrograde directed vesicles. In contrast, soluble ER resident proteins containing the lysine-aspartate-glutamate-leucine (KDEL) or related sequences bind to specialized receptor proteins such as the KDEL receptor (Lewis and Pelham, 1990; Munro and Pelham, 1987). This retrieval receptor is a multipass

transmembrane protein that binds to the KDEL sequence and packages any protein displaying this residue into COPI-coated retrograde transport vesicles. To accomplish this task, the KDEL receptor itself cycles between the ER and the cis-Golgi apparatus via the IC, where it is mainly localized (Majoul, et al., 1998; Martinez-Menarguez, et al., 2001; Orci, et al., 1997). The receptor has a high affinity for the KDEL sequence in vesicular tubular clusters and the Golgi apparatus. There it captures escaped ER resident proteins that are present in VTC and the Golgi at low concentration. Subsequently, in the ER the KDELr has a low affinity for the KDEL sequence to unload its cargo in spite of the very high concentration of KDEL-containing resident proteins. This is accomplished by different pH values established in the different compartments, regulated by H^+ pumps in their membranes. The KDELr could bind the KDEL sequence under the slightly acidic conditions in vesicular tubular clusters and the Golgi compartment, but could release it at the neutral pH in the ER. Such pH-sensitive protein-protein interactions form the basis for many protein sorting steps in the cell (Harter and Wieland, 1996; Pelham, 1996).

So far, three KDEL receptor proteins with a significant degree of conservation have been identified, suggesting that they might have some redundant functions (Capitani and Sallese, 2009; Raykhel, et al., 2007). In addition, the retrieval of KDEL-tagged proteins contributes to the protein quality-control (Yamamoto, et al., 2001). Quality control checkpoints exist in many organelles along the secretory pathway. In the ER, proteins deemed defective by the quality control process are sorted for degradation by the cytosolic 26S proteasome through a process termed ER-associated protein degradation (ERAD). Properly folded proteins are directed to ER exit sites for export. Once in the IC or cis-Golgi, aberrant proteins that have escaped earlier checkpoints can also be selectively returned to the ER. Here, proteins that fail the quality control test can be retained and prevented from traversing the secretory pathway. The ER retention of a substrate is mediated by its binding to resident ER proteins that possess ER retention signals, such as the KDEL sequence. Thus, retrieval from the IC or Golgi is mediated by the recycling of the KDELr back to the ER. These substrate-KDELr complexes are selectively included in COPI coated vesicles, which bud from the cis-Golgi (Beck, et al., 2009; Daniels, et al., 2004; Ellgaard, et al., 1999).

Moreover, recent literature suggests that KDELr exhibits properties of a signalling protein (Pulvirenti, et al., 2008; Sallese, et al., 2009; Yamamoto, et al., 2003). Here, ER chaperones that arrive at the Golgi activate a KDELr-dependent phosphorylation cascade, involving the

Src family kinases (SFKs), which control intra-Golgi trafficking (Asp and Nilsson, 2008; Pulvirenti, et al., 2008; Sallese, et al., 2009; Yamamoto, et al., 2003).
On the other hand, KDELr was also demonstrated to regulate the secretory pathway through its interaction with ARFGAP1. Aoe et al. (1997) could show that KDELr oligomerizes and interacts with ARFGAP1, which in turn recruits cytosolic GAP to membranes and induces ARF1 inactivation (Inoue and Randazzo, 2007; Liu, et al., 2005).

1.3 Biosynthetic transport and glycosylation

The Golgi complex is a major site of carbohydrate synthesis. The oligosaccharide processing steps occur in a correspondingly organized sequence in the Golgi stack, with each cisterna containing a characteristic abundance of processing enzymes. Proteins are modified in successive stages as they move from cisterna to cisterna across the stack, so that the stack forms a multistage processing unit. This compartmentalization might seem unnecessary, since each oligosaccharide processing enzyme can accept a glycoprotein as a substrate only after it has been properly processed by the preceding enzyme. Nonetheless, it is clear that processing occurs in a spatial as well as a biochemical sequence: enzymes catalyzing early processing steps are concentrated in the cisternae toward the cis face of the Golgi stack, whereas enzymes catalyzing later processing steps are concentrated in the cisternae toward the trans face. To generate such ordered distribution, enzymes must first be transported to specific Golgi cisternae, and subsequently their localization must be maintained through a combination of retention, retrieval or replacement (Brockhausen, 2006; Rabouille and Klumperman, 2005; Sannerud, et al., 2003; Ungar, et al., 2006).

1.3.1 N- and O-glycosylation

Two types of glycan modifications can be distinguished. Firstly, in N-linked glycosylation oligosaccharides are uniquely added to asparagines found in Asn-X-Ser/Thr recognition sequences in proteins. Secondly, in O-linked glycosylation, carbohydrates are attached to hydroxyl groups of mainly serine or threonine residues. The latter begins in the cis-Golgi, whereas N-glycosylation takes place throughout the ER and the Golgi (Brockhausen, 1999; Helenius and Aebi, 2001).

The processing pathway of both is highly ordered so that each step is dependent on the previous one. Processing of N-glycans is initiated in the ER with the attachment of N-linked oligosaccharide onto the protein, which is then trimmed while the protein is still in the ER (Molinari, 2007). Further modifications and additions occur in the Golgi apparatus. Here, the last enzyme in the sequential action of three enzymes, Mannosidase II, removes two mannoses to yield the final core of three mannoses that is present in a complex oligosaccharide (Tulsiani, et al., 1982). At this stage, the bond between the two N-acetylglucosamines in the core becomes resistant to attack by a highly specific endoglycosidase (Endo H) (Fig. 1-5). Since all later structures in the pathway are also Endo H-resistant, treatment with this enzyme can be used as a marker for intra-Golgi transport (Matlin and Simons, 1983). Finally, additional N-acetylglucosamines, galactoses, and sialic acids are added depending on the protein and tissue. Sialic acids are negatively charged and can be cleaved by the enzyme neuraminidase (Kornfeld and Kornfeld, 1985; Moremen, 2002; Roth, 2002; Zhang, 2006).

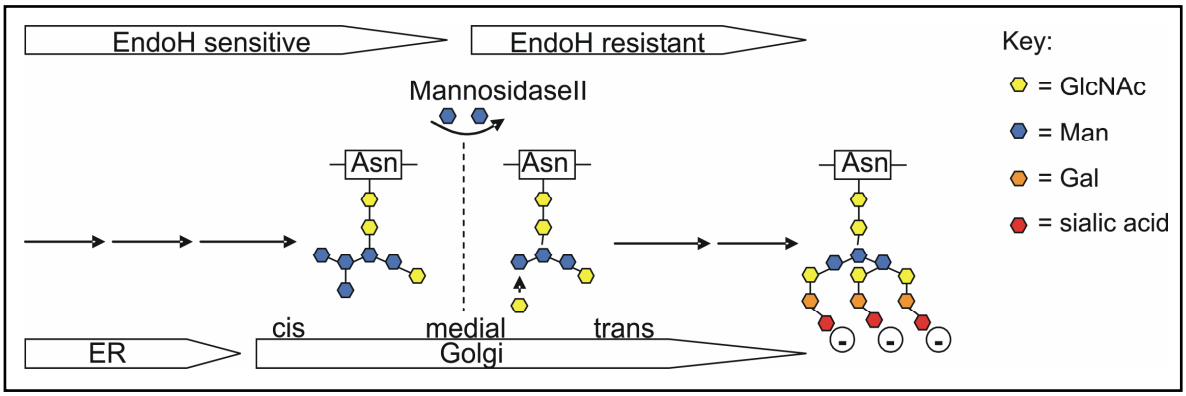

Fig. 1-5: Selected steps of N-glycosylation in eukaryotic cells. The sequential action of enzymes in the ER and Golgi, including Mannosidase II (Man II), yields the final core of three mannoses of complex oligosaccharides. These are further processed in the Golgi and glycosylation is terminated by addition of sialic acids. GlcNAc = N-acetylglucosamine, Man = mannose, Gal = galactose, sialic acid = N-acetylneuraminic acid [modified after (Alberts, 2002)].

O-Glycans are assembled by a series of reactions catalyzed by glycosyltransferases and sulfotransferases in the Golgi. Depending on the nature of the amino acid residue and sugar group involved in the carbohydrate-protein linkage, O-glycans can be divided into multiple subgroups: (1) in mucin-type *O*-glycoproteins, GalNAc is linked to serine or threonine residues; mucins are defined as cell surface or secreted glycoproteins with large numbers of clustered *O*-glycans; (2) for intracellular-glycoproteins, *N*-acetylglucosamine is linked to serine or threonine; and (3) for proteoglycans, xylose is linked to serine or threonine (Zhang, 2006). Many O-glycans are extended into long chains with variable termini that may be

similar to the termini of N-glycans. Usually, processing of O-glycans is initiated in the cis-Golgi by the addition of *N*-acetylgalactosamine (GalNAc) by polypeptide GalNAc-transferases (GalNAcT), expressed in a tissue-specific fashion. Altogether, eight O-glycan core structures can then be synthesized. The most common O-glycan core structures are cores 1 and 2. Core structures 1 to 4 in particular are elongated by Gal- and GlcNAc-transferase and/or terminated by Fucose-, sialyl-, Galactose-, *N*-acetylglucosamine-, GalNAc- and/or sulfo-transferases in many different ways to form functional carbohydrate structures (Brockhausen, 1999).

1.3.2 Functional role of glycosylation

Glycans have been shown to play a pivotal role in the folding, oligomerization, sorting, and transport of proteins. In addition, they influence cell-cell adhesion, cell-surface signalling, protein quality control and immune system functions including the mediation of cell death and antitumor responses (Bax, et al., 2007; Fukuda, 2002; Helenius and Aebi, 2001; Julien, et al., 2007; Priatel, et al., 2000; Rudd, et al., 2001; Toscano, et al., 2007; Tsuboi and Fukuda, 1998; Zhang, 2006).

The most important indirect effect of glycans on folding involves the quality control checkpoints, where N-linked carbohydrates act as maturation tags (Helenius and Aebi, 2001). Quality control in the ER is mediated via the Calnexin-calreticulin cycle, whereas quality control in the IC or Golgi depends on efficient retention of immature proteins primarily mediated by recycling of the KDELr as described in chapter 1.2.4 (Hebert, et al., 1995; Helenius and Aebi, 2004; Ou, et al., 1993; Peterson, et al., 1995).

On the other hand, glycosylation is also involved in the selective anterograde trafficking of glycoproteins. Hauri, Appenzeller et al. (2000) suggested that the mannose-binding lectin ERGIC-53 serves as a cargo capture and transport receptor for trafficking from the ER to the IC. In this study, ERGIC-53 has been shown to associate with human cathepsin C and accelerate its transport to the Golgi in a glycan-dependent fashion (Hauri, et al., 2000; Hauri, et al., 2000; Hebert, et al., 2005).

Furthermore, increasing evidence has been provided for an important role of glycosylation in the function of the immune system. Almost all of the key surface molecules involved in the

regulation of the innate and adaptive immune response are glycoproteins. Glycans and glycopeptides not only influence the structure and function of immune molecules, but also influence the immune response leading to tumor immunity (Bax, et al., 2007; Irimura, et al., 1999; Rudd, et al., 2001; Toscano, et al., 2007; Tsuboi and Fukuda, 1998; Zhang, 2006). Thus, O-glycans as well as N-glycans have been demonstrated to affect T and B cell functions, but also the complement pathway. More specifically, glycans have been shown to modulate ligand binding to the CD8αβ coreceptor of T cells (Moody, et al., 2001) and play an important role in the differentiation of T lymphocytes as demonstrated in ST6Gal I-deficient mice (Alvarez, et al., 1999; Marino, et al., 2008). Additionally, it has been established that glycans play a role in the generation and loading of antigenic peptides onto MHC class I molecules. Thus, Calnexin and ERp57 assist in the early folding events of the MHC class I heavy chain (HC). Here, unassembled HCs interact with membrane-bound Calnexin through a monoglycosylated N-linked glycan at Asn86 of the MHC class I HC (Peaper and Cresswell, 2008; Wearsch, et al., 2004). Moreover, glycans also influence the range of antigenic peptides generated in the endosomal pathway for presentation by MHC class II (Bax, et al., 2007; Rudd, et al., 2001; Toscano, et al., 2007; Tsuboi and Fukuda, 1998; Zhang, 2006).

1.4 The secretory pathway and disease

The biosynthetic secretory pathway is an essential processes for the correct localization and function of molecules within the cell. Disturbances in the function of the biosynthetic transport pathway can lead to a variety of diseases, including cancer (Aridor and Hannan, 2000; Olkkonen and Ikonen, 2000). One example linking exocytosis and tumor development is the EWS-WT1 gene-fusion (Palmer, et al., 2002). The EWS-WT1 product in desmoplasmic small round cell tumors induces the overexpression of the Munc13-1-related molecule BAIAP3. Since BAIAP3 has been implicated in regulated exocytosis and tumor growth, it has been assumed that modulation of exocytosis *per se* might play a role in tumor development. However, the process by which cancer is linked to the modulation of the secretory pathway is still poorly understood and might provide a novel pathogenetic principle.

Targeting the function of biosynthetic transport often causes interference with the coordinated spatial and functional arrangement of the glycosylation machinery, which has global effects since glycans are involved in many biological processes (chapter 1.3.2). Failure to maintain

glycosylation pathways is associated with deregulated expression of naturally occurring glycans, abnormal branching of glycoproteins and glycolipids, and neoexpression of sugars normally restricted to embryonic tissue (Dube and Bertozzi, 2005; Hakomori, 1989; Newsom-Davis, et al., 2009). Changes of the resulting glycome are a hallmark of cancer cells; functional consequences may include modulation of metastasis and evasion from immunosurveillance (Cavallaro and Christofori, 2001; Ohtsubo and Marth, 2006; Rudd, et al., 2001; Toscano, et al., 2007; Tsuboi and Fukuda, 1998; Zhang, 2006). Many tumor cells have altered biosynthetic pathways of glycans and aberrant mRNA expression levels or activities of glycosyltransferases, leading to the disturbance of the cellular glycome (Brockhausen, 2006; Brockhausen, et al., 1998; Brockhausen, et al., 1995; Dennis, et al., 1999; Field and Wainwright, 1995; Freire, et al., 2005; Julien, et al., 2001; Sewell, et al., 2006; Whitehouse, et al., 1997). The most common tumor-associated glycan antigens are the O-linked blood group precursor structures Tn (GalNAc) and TF (Galβ1-3GalNAc), which have been recorded in several carcinoma entities and have been introduced in chapter 1.1.2 (Brockhausen, 1999; Ohtsubo and Marth, 2006).

In normal epithelial cells of the breast O-glycan structures are mainly core 2-based, resulting from the activity of 2-β6-N-acetylglucosaminyltransferase (C2GnT1) on core 1 O-glycans. In contrast, in breast carcinoma cells shorter O-glycans are added. These result from chain termination by sialylation of GalNAc or core1 by α2,6-sialyltransferase (ST6GalNAc-I) or α2,3 sialyltransferase (ST3Gal-I), respectively (Fig. 1-6).

Mechanistically, either C2GnT1 could be lost or the upregulation of ST6GalNAc-I/II and ST3Gal-I accounts for the switch from core 2 to sialylated core 1 O-glycans in breast cancer cells (Dalziel, et al., 2001; Julien, et al., 2007; Sewell, et al., 2006). Likewise, the downregulation of the core 1 enzyme β1,3galactosyltransferase (T-synthase) would lead to an accumulation of truncated Tn-glycans (Freire, et al., 2005). Recent reports provide evidence that T-synthase requires a unique molecular chaperone, Cosmc, which is an endoplasmic reticulum ER-localized adenosine triphosphate binding chaperone. In the ER this chaperone interacts with the nascent polypeptide of human T-synthase and assists its proper folding. Native T-synthase, which occurs mainly as a homodimer, then exits the ER. When Cosmc is mutated and dysfunctional, the nascent polypeptides of T-synthase form inactive aggregates or oligomers. These associate with the chaperone GRP78 (BiP) and are subsequently proceeded

to the ERAD pathway. Here they are retrotranslocated from the ER to the cytosol, ubiquitinated, and finally degraded by the proteasome (Ju, et al., 2008). Accordingly, Ju and Cummings (2002) demonstrated that a mutated chaperone, Cosmc, accounts for the increased amount of inactive T-synthase in Jurkat cells.

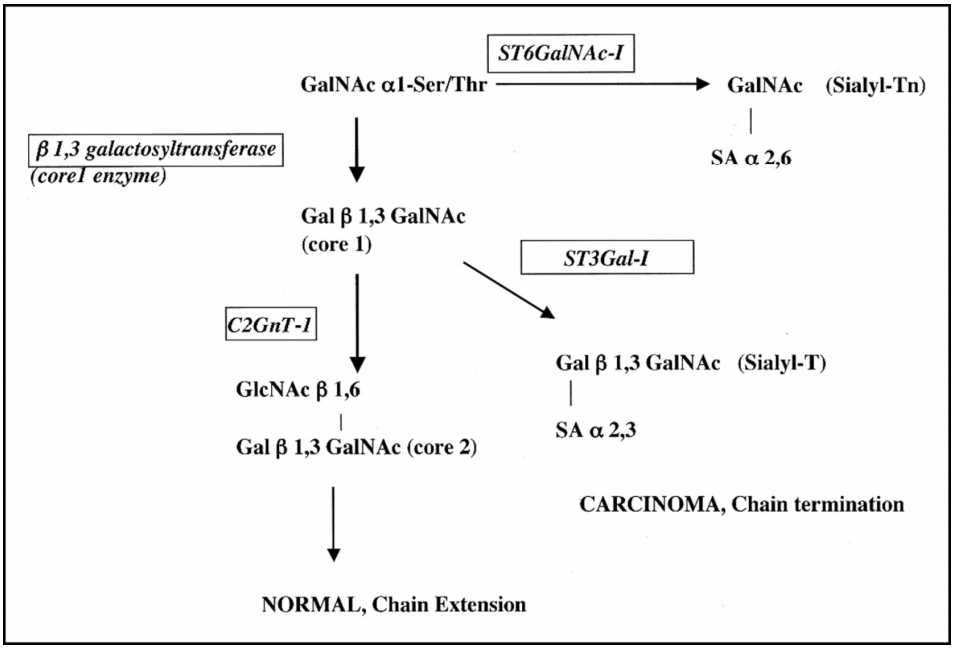

Fig. 1-6: Glycosylation and cancer. In breast cancer cells a switch from core 2 to core 1 O-glycans takes place (Sewell, et al., 2006).

In general, alterations in glycan structures *per se* have numerous biological and pathological consequences in cancer, because potential ligands and receptors responsible for interactions between cancer cells and their microenvironment are changed. This influences the growth and survival of the cell, its ability to invade and metastasize, and its interactions with lectins and cell-surface receptors or cells of the immune system (Glinskii, et al., 2004; Hanahan and Weinberg, 2000; Springer, 1984; Tsuiji, et al., 2003). However, whereas the genetic dissection of pathogenetic events in tumor cell transformation has made tremendous progress, more complex traits of malignancy, including modulatory effects on the secretory pathway and glycosylation, have proven difficult to analyse (Schietinger, et al., 2006).

1.5 Aims

The tumor-associated antigen EBAG9 has been identified as a primary estrogen-responsive gene (Park, et al., 2005; Suzuki, et al., 2004; Tsuchiya, et al., 2001; Watanabe, et al., 1998).

EBAG9 overexpression has been recorded in a multitude of human epithelial cancers and was shown to correlate with tumor progression (Akahira, et al., 2004; Ogushi, et al., 2005; Suzuki, et al., 2004; Takahashi, et al., 2003; Tsuneizumi, et al., 2001). Previously, it was demonstrated that EBAG9 induces the surface deposition of common tumor-associated glycan antigens, such as the O-linked blood group precursor structures Tn (GalNAc) and TF (Galβ1-3GalNAc) at the cell surface in non-secretory cells (Engelsberg, et al., 2003). Despite its putative role in tumor progression, the pathophysiological function of EBAG9 has not yet been well defined. In neuroendocrine PC12 cells, EBAG9 induces a downregulation of Ca^{2+} regulated secretion (Ruder, et al., 2005), but essentially no glycan alteration. However, modulation of neurotransmitter release in cells equipped with a regulated exocytosis machinery could not be reconciled with the effects observed in epithelial cell lines, including O-linked glycan generation.

In this project, I aimed for elucidation of the functional role of EBAG9 within the Golgi apparatus and how this function might be correlated with glycome alteration and tumor progression in epithelial cells. First, I planned to examine the putative pathophysiological implications of EBAG9 for the biosynthetic pathway including constitutive and regulated exocytosis. Here, I wanted to use EBAG9 overexpression to mimic crucial events during tumor cell pathogenesis, since EBAG9 is overrepresented but not deleted in tumors. As a further assessment of the physiological role of EBAG9, I intended to apply siRNA-mediated depletion of EBAG9. Second, with regard to proteins associating with EBAG9, I meant to develop a detailed understanding of the underlying mechanism of EBAG9 function in epithelial cells.

2 Materials

All enzymes, chemicals and materials not listed were purchased from Amersham Bioscience (Freiburg), BioRad (München), Boehringer (Mannheim), Clontech (Palo Alto, USA), Fluka (Neu-Ulm), Gibco/BRL (Eggenstein), Merck (Darmstadt), NEB (Schwalbach), NEN (Köln), Promega (Mannheim), Qiagen (Hilden), Roche (Mannheim), Roth (Karlsruhe), Serva (Heidelberg) or Sigma (Taufkirchen).

2.1 Cells

Cos-7	African green monkey kidney cells	ATCC CRL-1651
Hek293	Human embryonic kidney cell	ATCC CRL-1573
Hela	Human cervix carcinoma	ATCC CCL-2
MCF-7	Human breast adenocarcinoma	ATCC HTB-22
MDA-MB435	Human breast adenocarcinoma or Human melanoma cells (under debate)	ATCC HTB-129
MDCK	Madin Darby Canine kidney cells	ATCC CCL-34
PC12	Rat adrenal pheochromocytoma	ATCC CRL-1721

EBAG9 or GFP stably transfected MDA-MB435 cells were provided. Stably εCOPI-YFP, EBAG9-Δ176-213-GFP and EBAG9-Δ30-213GFP expressing MDA-MB435 cells were generated within this work as described in chapter 3.3.3.

2.2 Viruses

Adenovirus for human EBAG9 (Ad-EBAG9) or LacZ (Ad-LacZ) were provided by Dr. Arne Engelsberg (AG Dr. Armin Rehm). The plasmid contains a CMV promoter for efficient EBAG9 or LacZ expression. Adenovirus for basolateral or apical directed VSVG-ts045-GFP

(Schuck, et al., 2007) and GST-rGH12 were provided by Dr. Sebastian Schuck (AG Prof. Kai Simons) as well as fowl plaque virus (FPV) described in (Matlin and Simons, 1983).

2.3 Bacterial strains

E.*coli* DH5α (Stratagene): F^-, ϕ80d*Lac*ZΔM15, Δ(*Lac*ZYA-*arg*F)U169, *deo*R, *rec*A1, *end*A1, *hsd*R17(r_k^- , m_k^*), *pho*A, *sup*E44, *thi*-1, *gyr*A96, *rel*A1, λ^-

E.*coli* XL1-Blue (Stratagene): *sup*E44, *hsd*R17, *rec*A1, *end*A1, *gyr*A46, *thi*, *rel*A1, *Lac*F´[*pro*AB^+, *Lacl*^{q}ZΔM15, Tn10(tet^r)]

2.4 Mice strains

C57BL/6 and BALB/c mice were obtained from Charles River Laboratories (Sulzfeld). EBAG9-deficient mice were provided by Dr. Constantin Rüder (AG Dr. Armin Rehm). Severe Combined Immunodeficient (SCID) mice, strain B6.CB17-Prkdc^{scid} /SzJ, were purchased from Jackson Laboratory.

2.5 Expression constructs

Tab. 1: Vectors

Vector	Reference	Description
pcDNA3.1(+)	Invitrogen	Eukaryotic expression vector, Amp^r, Neo^r
pEGFP-N3	Clontech	Eukaryotic expression vector with GFP-tag 3´of MCS, , Kan^r, Neo^r
pDsRed2-N1	Clontech	Eukaryotic expression vector with DsRed-tag 3´of MCS, , Kan^r, Neo^r

Tab. 2: Expression constructs

Plasmid	Reference	Description
C2GnT1	(Dalziel, et al., 2001)	C2GnT1 in pcDNA Neo
EBAG9-C-FLAG	(Ruder, et al., 2005)	Human EBAG9 in pFlag
EBAG9-GFP	(Engelsberg, et al., 2003)	Human EBAG9 in pEGFP-N3
EBAG9-Δ1-27-GFP	(Engelsberg, et al., 2003)	Deletion mutant of EBAG9-GFP (AS 28-213)
EBAG9-Δ1-163-GFP	(Engelsberg, et al., 2003)	Deletion mutant of EBAG9-GFP (AS 164-213)
EBAG9-Δ30-213GFP	(Engelsberg, et al., 2003)	Deletion mutant of EBAG9-GFP (AS 1-29)
EBAG9-Δ176-213-GFP	(Engelsberg, et al., 2003)	Deletion mutant of EBAG9-GFP (AS 1-175)
EBAG9-Δ1-27/Δ176-213-GFP	(Ruder, et al., 2009)	Deletion mutant of EBAG9-GFP (AS 28-175)
εCOPI-YFP	(Presley, et al., 2002; Ward, et al., 2001)*[1]	Bovine εCOPI in pEYFP
GalT-DsRed	Clontech (Verviers, Belgium)	Human GalT in DsRed
GalNAcT2-CFP	(White, et al., 1995) *[2]	Human GalNAcT2 in pECFP
pHGHCMV5	(Khvotchev, et al., 2003)	Human GH in pCMV5
ST6GalNAcII-FLAG	(Sewell, et al., 2006) *[3]	ST6GalNacII in pFLAG
T-synthase-HPC4	(Ju and Cummings, 2002) *[4]	Human C1β3Gal-T HPC4 tagged in pcDNA4
VSVG-TsO5-GFP	(Cao, et al., 2000) *5	VSVG in pEGFP
Expression plasmids generated within this work (as described in chapter 3.1.9):		
C2GnT1-DsRed2	C2GnT1 with DsRed-tag in pDsRed2-N1	
EBAG9-DsRed2	EBAG9 with DsRed-tag in pDsRed2-N1	
ST6GalNAcII-DsRed2	ST6GalNacII with DsRed-tag in pDsRed2-N1	

Kindly provided by:
*[1] Dr. Jennifer Lippincott-Schwartz
*[2] Dr. Sebastian Schuck
*[3] Dr. Joyce Taylor-Papadimitriou
*[4] Prof. Richard D. Cummings
*[5] Dr. M.A. McNiven

2.6 Oligonucleotides

All nucleotides were purchased from BioTeZ GmbH (Berlin-Buch). Underlined bases label restriction sites.

Tab. 3: Primer for cloning of expression plasmids

Name	Sequence (5´→ 3´)
C2GnT1-KpnI-fw	5´-GGGGTACCATGCTGAGGACGTTGCTGCGA-3´
C2GnT1-BamHI	5´-CGGGATCCCCGTGTTTTAATGTCTCCAAAGC-3´
EBAG9-KpnI-fw	5´-CGGGGTACCATGGCCATCACCCAGTTT-3´
EBAG9-BamHI-rev	5´-CGCGGATCCCCTGAAAGTTTCACACCA-3´
EBAG9-1-29-BamHI-rev	5´-CGGGGTACCATGGCCATCACCCAGTTT-3´
EBAG9-1-175-BamHI-rev	5´-CGCGGATCCCCCTGTCTCAGAACTTCT-3´
ST6GalNAcII-Kpn-fw	5´-GGGGTACCATGGGGCTCCCGCGCGGGTCG-3´
ST6GalNAcII-BamHI-rev	5´-CGGGATCCCCGCGCTGGTACAGCTGAAGG-3´

2.7 Antibodies

Tab. 4: Primary antibodies

(anti -) Name (clone)	Isotyp / specificity	Source / reference
ArfGAP1 (S17)	Rabbit-anti-human	Santa Cruz Biotechnology (Santa Cruz, CA)
βCOPI (maD)	Mouse Ascites Fluid, monoclonal	Sigma (Deisenhofen, Germany)
Calnexin	Rabbit polyclonal; anti-human	Stressgen (Ann Arbor, MI)
Cathepsin D (1C11)	Mouse IgG_1 mAK; anti-human	Zymed Laboratories
Cosmc (P-14)	Goat polyclonal; anti-human	Santa Cruz Biotechnology
EBAG9 serum	Rabbit polyclonal; anti-human	(Engelsberg, et al., 2003)
EEA1 (14)	Mouse IgG_1 mAK; anti-human	BD Bioscience (Heidelberg, Germany)
ERGIC-53	Mouse IgG_1; anti-human	Alexis Biochemicals (San Diego, CA)
FLAG-tag (M2)	Mouse-IgG	Sigma
GalNAcT1	Mouse IgG_1; anti-human	(Rottger, et al., 1998) *[1]
γCOPI (19)	Mouse IgG, anti-human	Santa Cruz Biotechnology

GAPDH	Rabbit polyclonal; anti-human	Biozol (Eching, Germany)
GFP	Mixture of two mouse $IgG_1\kappa$ monoclonal antibodies	Roche (Basel, Switzerland)
GFP-biotin	Goat polyclonal	Vector Laboratories (Burlingame, CA)
GM130	Mouse IgG_1; anti-human	BD Bioscience
Granzyme B-Alexa Fluor 647 (16G6)	Rat IgG2b; anti-mouse	eBioscience (San Diego, CA)
KDELr	Mouse monoclonal; anti-human	Stressgen (Ann Arbor, MI)
Lck	Mouse IgG1; anti-human	BD Bioscience
Mannosidase II	Rabbit polyclonal; anti-human	Chemicon (Hampshire, UK)
MHC-class I (W6/32HL)	Mouse IgG_{2a}; anti-human MHC class I heavy chain	(Barnstable, et al., 1978)
P230 (15)	Mouse IgG_1; anti-human	BD Bioscience
PDI (SPA-890)	Rabbit-anti-human	Stressgen
Peanut Agglutinin (PNA)	Anti-Gal-β1,3GalNAc (TF); biotin linked	Vector Laboratories
Protein C (HPC4)	Rabbit IgG; anti-Protein C epitope tag peptide	GenScript (Piscataway, NJ)
Sec23 (E19)	Goat IgG, anti-human	Santa Cruz Biotechnology
TF (5f4)	Mouse-anti-human	Donated by Dr. Uwe Karsten
Tn (22.1.1)	Mouse IgM; anti-human	MBL (Naka-ku Nogoya, Japan)
C1GALT1 (T-synthase)	Rabbit, anti-human	Sigma
Vivia Villosa Lectin (VVA)	Anti-GalNAc (Tn); biotin linked	Vector Laboratories
VSVG (P5D4)	Mouse IgG_1 ; anti-human	Sigma
VSVG (TKG, clone 17.2.21.4)	Mouse-anti-human	(Goldenberg and Silverman, 2009)*[2]

Kindly provided by: *[1] Prof. Nilsson
*[2] Jean Gruenberg

Appropriate isotype controls for flow cytometry were purchased from BD Biosciences or Caltag Laboratories (Hamburg, Germany).

Tab. 5: Secondary antibodies and streptavidin conjugates

Name	Isotyp / specificity	Source / reference
Anti-goat-Alexa Fluor 568	Donkey-anti-goat IgG	Molecular Probes (Karlsruhe, Germany)
Anti-goat-HRP	Donkey-anti-goat IgG	Southern Biotechnology (Birmingham, AL)
Anti-mouse-Alexa Fluor 488	Goat-anti-mouse IgG	Molecular Probes
Anti-mouse-Alexa Fluor 568	Goat-anti-mouse IgG	Molecular Probes
Anti-mouse APC	Goat anti-mouse IgG	BioLegend (San Diego, CA)
Anti-mouse-biotin	Goat anti-mouse IgGs	DakoCytomation (Glostrup, Denmark)
Anti-mouse-cy5	Goat anti-mouse IgG + IgM (H+L)	Jackson ImmunoResearch (West Grove, PA)
Anti-mouse-HRP	Goat anti-mouse IgG H+L)	Southern Biotechnology
Anti-rabbit-Alexa Fluor 488	Goat-anti-rabbit IgG	Molecular Probes
Anti-rabbit-Alexa Fluor 568	Goat anti-rabbit IgG H+L)	Molecular Probes
Anti-rabbit-biotin	Goat anti-rabbit IgGs	DakoCytomation
Anti-rabbit-cy5	Goat-anti-rabbit IgG	Jackson ImmunoResearch
Anti-rabbit-HRP	Goat anti-rabbit IgG H+L)	Southern Biotechnology
Anti-rat-Alexa Fluor 568	Goat-anti-rat IgG	Molecular Probes
Anti-rat-HRP	Goat-anti-rat IgG	Southern Biotechnology
Anti-rat-cy5	Donkey-anti-rat-cy5	Jackson ImmunoResearch
Streptavidin-Alexa Fluor 568	Streptavidin linked	Molecular Probes
Streptavidin-cy2	Streptavidin linked	Jackson ImmunoResearch
Streptavidin-cy5	Streptavidin linked	Jackson ImmunoResearch
Streptavidin-HRP	Peroxidase linked	Southern Biotechnology

Tab. 6: Fluorescently labeled proteins

Name	Source / reference
BODIPY TR C_5-Cermide	Molecular Probes
Shiga Toxin B subunit – cy3 *[1]	(Mallard, et al., 1998)
Transferrin-Alexa Fluor 633	Molecular Probes
Transferrin-Alexa Fluor 568	Molecular Probes

Kindly provided by: *[1] Prof. Ludger Johannes and Prof. Brian Storrie

2.8 Reagents

Cycloheximide (Sigma) was prepared as stock solution in DMSO (100 mg/ml). Nocodazole (Sigma) was prepared as stock solution in DMSO (5 mg/ml) and BFA (Sigma) in EtOH (5 mg/ml). MG-132 (Calbiochem) was kindly provided by Dr. Stephan Matthas. Mannosidase II substrate p-nitrophenyl-alpha-D-mannopyranoside was from Sigma, Endoglycosidase H (EndoH) and neuraminidase (NANA) were from New England Biolabs (NEB, Frankfurt, Germany). Protein A- and G-Sepharose, and glutathione-Sepharose were purchased from Amersham Biosciences (Buckinghamshire, UK).

2.9 Buffer and media

Buffer and solutions not listed can be found within the respective method section.

Adenovirus storage buffer: 15 mM Tris pH 8.0, 150 mM NaCl, 0.15 % BSA, 50% Glycerol

DNA-Sample buffer (10×): 0,25 % Bromphenolblue, 0,25 % Xylene-Cyanole, 30 % Glycerin

EB-buffer: 10 mM Tris/HCl, pH 7.5

IEF sample buffer: 9.5M Urea, 2 % Ampholine, pH 3.5-10 (v/v), 2 % NP-40 (v/v), 5 % β-Mercaptoethanol (v/v)

LB-Medium (Agar): 10 g Baco-Trypton, 5 g Yeast-extract, 10 g NaCl, ad 1 l H_2O, (15 g Agar)

NET-buffer (10×):	0.5 M Tris/HCL pH 7.5, 1.5 mM NaCl, 50 mM EDTA, 5 % NP-40
NP-40 Lysisbuffer:	50 mM Tris/HCL pH 7.4, 5 mM Mg_2Cl, 0.5 % NP-40 (add before use: 1 mM PMSF, 5 µg/ml Aprotinin)
PAA for IEF:	30% Acrylamid (v/v), 1.6% N,N-Methylenbisacrylamid (w/v), stir with active carbon overnight 4°C, filter
PBS(T):	140 mM NaCl, 2.7 mM KCl, 8.1 mM Na_2HPO_4, 1.5 mM KH_2PO_4, ad 1 l H_2O, pH 7.2 (0,05 % Tween-20)
Protein-Sample buffer (2×):	125 mM Tris pH 6.8, 4 % SDS, 0,002% Bromphenolblue, 20 % Glycerin, 5 % β-Mercaptoethanol
RIPA-Lysisbuffer:	50 mM Tris/HCL pH 7.5, 50 mM NaCl, 0.5 mM EDTA, 0.5 % NP-40, 0.25 % Na-deoxycholate (add before use: 1 mM PMSF, 5 µg/ml Aprotinin)
Running buffer (Lämmli):	250 mM Tris, 2.5 M Glycin, 1 % SDS
Stripping buffer:	0.1 M Glycin, 0.15 M NaCl, ad 1 l H_2O pH 2.5
TAE (50×):	2 M Tris, 5.71 % (v/v) Eisessig, 50 mM EDTA pH 8.0
TBS(T):	50 mM Tris/HCL pH 7.4, 50 mM NaCl, (0,05 % Tween-20)
TE:	10 mM Tris/HCL, 1 mM EDTA, ad 1 l H_2O, pH 7.4
TX-100-Lysisbuffer:	50 mM Hepes pH 7.4, 150 mM NaCl, 10 % Glycerin, 1 % Triton X-100 (add before use: 1 mM PMSF, 5 µg/ml Aprotinin)
TX-100-buffer for IP:	20 mM Hepes pH 7.4, 140 mM KCl, 20 mM NaCl, 0.5 mM $MgCl_2$, 0.5 % Triton X-100 (add before use: 1 mM PMSF, 5 µg/ml Aprotinin)
WBT:	20 % Methanol, 250 mM Tris, 2.5 M Glycin

Medium for cell culture

DMEM:	500 ml DMEM (PAA, Cölbe), 5 ml Penicillin/Streptomycin (10000 U/ml; PAA), 5 ml 200 mM Glutamin (PAA), 5 ml 100 mM Sodium-Pyruvat (Gibco/BRL), 5 ml 100 mM non-essential aminoacids (Gibco/BRL) for some cell lines
RPMI:	500 ml RPMI (PAA, Cölbe), 5 ml Penicillin/Streptomycin (10000 U/ml; PAA), 5 ml 200 mM Glutamin (PAA), 5 ml 100 mM Sodium-Pyruvat (Gibco/BRL), 500 µl 50 mM β-Mercaptoethanol (Gibco/BRL)
Trypsin-solution:	0.05 % Trypsin, 0.02 % EDTA (PAA)
Freezing media:	90 % FCS, 10 % DMSO

3 Methods

3.1 Molecular biology

3.1.1 Culture of bacteria

To amplify plasmids LB-medium was inoculated with bacteria of E.coli strain E.*coli* DH5α or E.*coli* XL1-Blue or spread on LB-Agarplates and incubated overnight at 37 °C. Clones were selected by addition of 100 µg/ml Ampicillin (Roth, Karlsruhe) or 30 µg/ml Kanamycin (Roth).

3.1.2 Transformation of *E.coli*

For transformation an aliquot of chemo-competent *E.coli* bacteria was incubated with DNA (10 µl of ligation or 5-20 ng plasmid-DNA) for 20 min on ice. After heat shock of 30 s at 42 °C the mixture was cooled on ice for 2 min. After adding 200 µl LB-Medium and incubation for 60 min at 37 °C, 50-200 µl of Bacteria suspension was distributed on LB-agarplates supplemented with Ampicillin or Kanamycin.

3.1.3 Isolation of plasmid DNA from *E.coli* cells

Analytic preparation of small quantities of plasmid DNA was done using the principle of alkaline lysis and was done to test for designated product of ligation. Transformed E.coli bacteria were grown overnight and 1.5 ml centrifuged at 13000 rpm for 30 s. The pellet was resupended in 300 µl P1-buffer, 300 µl P2-buffer were added and cells were lysed for 5 min at RT. After addition of 300 µl P3-buffer the suspension was neutralized, incubated for 15 min on ice and centrifuged at 13000 rpm, 4 °C for 20 min. The plasmid DNA was precipitated from the supernatant by using 0.7 Vol Isopropanol for 5 min on ice. After centrifugation and washing with 70 % EtOH, the plasmid DNA was air dried and dissolved in 50 µl EB buffer.

P1-buffer: 50 mM Tris/HCL pH 8.0, 10 mM EDTA pH 8.0, 100 µg/ml RNaseA

P2-buffer: 200 mM NaOH, 1 % SDS

P3-buffer: 3 M Potassiumacetate pH 5.5

The preparative isolation of plasmid DNA was done using DNA-affinity columns from JETSTAR (Genomed, Bad Oeynhausen, Germany) or QUIAGEN (Hilden, Germany) "Plasmid Maxi- Kit" according to manufacturer's instructions.

3.1.4 Polymerase chain reaction (PCR)

Polymerase chain reaction was used to amplify certain DNA sections and to introduce direct mutations. To ensure high fidelity of DNA polymerisation a polymerase with 3´-5´-*proof-reading* activity (PFU; Roboklon, Berlin, Germany) was chosen and the PCR-reaction was performed according to manufacturer's instructions using the buffer provided.

3.1.5 Restriction digest

Cleavage of DNA was carried out using restriction enzymes and buffer provided by New England Biolabs (NEB, Schwalbach). For 1 µg plasmid DNA 1-5 U restriction enzyme was used and incubated for at least 3 h or overnight. After linearization the vector was incubated with Calf Intestine Phosphatase (CIP) (1 U/5 µg DNA; NEB, Schwalbach) for 30 min at 37 °C to dephosphorylate the 5´-end. This procedure inhibits re-ligation of the linearized vector without incorporation of a DNA fragment and enhances the efficiency of ligation. Afterwards the phosphatase was inactivated at 75 °C for 15 min. Finally, the cleavage products were isolated by agarose gel electrophoresis (chapter 3.1.6) and DNA was purified from the gel as described in chapter 3.1.7.

3.1.6 Agarose gel electrophoresis

Analysis and purification of DNA was performed by horizontal electrophoresis in an 0.8 % - 2 % Agarosegel (0.8-2 g Agarose/100 ml 1x TAE, 0.5 µg/ml Ethidiumbromide). DNA-probes were mixed with 10x DNAsample buffer and the probe was separated by electrophoresis (4-8 V/cm) in 1x TAE buffer. Excitation of the intercalating dye Ethidiumbromide by UV-light (254-366 nm) allows the analysis of DNA bands. The size of DNA-fragments was determined by comparison with a 1 kb-DNA-Ladder (Gibco/BRL;

Eggenstein). The amount of DNA was estimated by comparison with SmartLadder (Eurogentec, Seraing, Belgien).

3.1.7 Isolation of DNA from agarose gels

DNA separated by Agarose gel electrophoresis was quickly cut out under a UV-light using a scalpel. The DNA was isolated using the „QIAquickTM Gel-Extraction Kit“ (Qiagen) according to manufacturer's instructions.

3.1.8 Ligation of DNA

Ligation of Vector and DNA to obtain the desired expression construct was performed in a total volume of 20 µl (1 U T4-DNA-Ligase, 2 µl 10x Ligationbuffer; Roche) overnight at 16 °C for sticky ends. Vector and DNA were added in a molar ratio of 1:3, 1:1 and 3:1, whereas the amount of vector was 50-150 ng.

3.1.9 Cloning

EBAG9, C2GnT1 or ST6GalNAcII were amplified by PCR (chapter 3.1.4) using the primers shown in Tab. 3 and subcloned into KpnI and BamHI restriction sites of pDsRed2-N1 (Clontech). All constructs generated were verified by sequencing.

3.2 Protein biochemistry

3.2.1 Protein isolation and determination of protein concentration

Cells were trypsinized and counted using a Neubauer haemocytometer. After collecting the cells by centrifugation at 1100 rpm for 5 min, the pellet was washed twice with PBS and resuspended in the appropriate cold lysis buffer (NP40, RIPA or TX-100) to a final concentration of 4×10^6/100 ml. This was followed by 30 min rotation at 4 °C. Finally, cell lysate was centrifuged at 13000 rpm for 10 min to pellet unsoluble cell material and nuclei. The supernatant was stored at -20 to -80 °C or directly used for SDS-PAGE (chapter 3.2.2),

coimmuniprecipitation (chapter 3.3.6) or Mannosidase activity assay (chapter 3.3.13). If required, protein concentration was determined by Bradford assay using the „BIO-RAD Protein Assay“ (BioRad) according to manufacturer’s instructions. Bovine serum albumin (BSA) was used as standard to plot a calibration curve.

3.2.2 SDS-polyacrylamide-gelelectrophoresis (SDS-PAGE)

For protein separation by SDS-PAGE 2x protein sample buffer was added and probes were boiled for 5 min. Equal amounts of protein were loaded on 8 %, 10 % or 12 % reducing SDS-polyacrylamide gel. A 4.5 % stacking gel served to focus the probes before separation. To determine the molecular weight of proteins „RainbowTM coloured protein molecular weight marker, high molecular weight range“ (Amersham) was separated on the same gel. Electrophoresis was carried out in 1x Laemmli-buffer at 5-8V/cm. Resolving gel (RG) and stacking gel (SG) were prepared according to the following recipe.

Tab. 7: Composition of SDS-polyacrylamide gels

Gel	12 % RG	10 % RG	8 % RG	4.5 % SG
H_2O	16.75 ml	19.80 ml	23.20 ml	7.5 ml
Rotiphorese® Gel30 (30 % Acrylamid, 0.8 % Bisacrylamid; Roth)	20.75 ml	16.7 ml	13.30 ml	1.875 ml
1.5 M Tris/HCl pH 8.8, 0.4 % SDS	12.5 ml	12.5 ml	12.5 ml	-
0.5 M Tris/HCl pH 6.8, 0.4 % SDS	-	-	-	3.125 ml
10 % APS	250 µl	250 µl	250 µl	90 µl
TEMED (Roth)	25 µl	25 µl	25 µl	9 µl

3.2.3 Immunoblot (westernblot analysis)

After separation by SDS-PAGE proteins were transferred to nitrocellulose membranes (Schleicher & Schuell, Dassel, Germany) at 400 mA for 2-3 h in WBT using a „Trans-Blot®SD“ westernblot chamber (BioRad).

The blots were blocked in 1× TBST with 5 % milk for 30 min to saturate unspecific protein binding and washed three times with 1× TBST, followed by incubation with primary antibody (Tab. 4) in 1× TBST with 2.5 % milk for 1-2 h at RT or overnight at 4 °C. After washing four times with 1× TBST for 5-10 min, the blots were probed with a secondary antibody conjugated to horseradish peroxidase (Tab. 5) in 1× TBST with 2.5 % milk for 45 min at RT

and washed again four times with 1× TBST for 5-10 min. Protein bands were visualized by chemiluminescence (ECL kit, Amersham Biosciences, Braunschweig, Germany), exposed to an X-ray (Kodak X-OMAT LS) film and developed.

For further analysis the membrane was incubated in stripping buffer (chapter 2.9) for 30 min to strip all bound antibody off the membrane. After washing twice with H_2O the membrane could be re-probed again.

3.2.4 One-dimensional (1d)-isoelectric focusing gel electrophoresis (IEF)

Isoelectric focusing separates proteins according to their charge. Immunoprecipitates were dissolved in IEF sample buffer and loaded into gel pockets. Samples were overlaid with ~ 1:4 diluted sample buffer, including Bromphenol blue, followed by adding Kathode buffer (50mM NaOH) into the upper chamber. Then, chambers were filled with Anode buffer (20 mM H_3PO_4) and electrophoresis was carried out at 1000 V for 12-13 h overnight. The IEF gel was prepared according to the following recipe.

Tab. 8: Composition of 1d-isoelectric focusing gel

	Gel
H2O	16.5 ml
Urea	41.25 g
10 % NP-40	15 ml
PAA	11.25 ml
Dissolve slowly at 30 °C under frequent stirring	
Add ampholine:	
pH 5-7	3 ml
pH 3.5-10	0.75 ml
pH 7-9	0.75 ml
10% APS	150 µl
TEMED (Roth)	75 µl

3.2.5 Autoradiography

To enhance the detection of [^{35}S]-labeled proteins, the SDS-PAGE gel was incubated twice with DMSO for 30 min to dehydrate the gel and then incubated in the scintillator 2,5-Diphenyloxazol/DMSO (PPO; Roth) for 1 h. Afterwards the gel was washed in H_2O for 30 min to precipitate PPO and dried for 2 h on Whatman-paper (Schleicher&Schuell) at 68 °C

under vacuum. Finally, radioactive labeled proteins were visualized by exposure to an X-ray (Kodak X-OMAT AR) film at -80 °C. Sometimes, gels were exposed to a Phosphoimager-Plate (Fuji), and analysis was done using a „Fujix BAS 2000 Phospho-Imager“ (Fuji).

3.2.6 Quantification of protein bands

Band intensities were quantified by densitometry using the program „Tina 2.0“ (Raytest). The intensity values obtained were adjusted to background intensity values.

3.3 Cell biology

3.3.1 Cell culture and transfections

HEK293, HeLa, MDA-MB435, and COS7 were grown in DMEM medium (chapter 2.9; PAA Laboratories, Cölbe, Germany) supplemented with 10 % FCS (Foetal Calf serum inactivated for 20 min at 55 °C; Biochrom, Berlin, Germany) in a humidified incubator at 37 °C and 5 % CO_2. PC12 cells were grown on collagen coated plates [10 µg/ml Collagen Typ I (Sigma) in 0.1 M acetic acid] in RPMI-medium supplemented with 10 % horse serum (Invitrogen, Carlsbad, CA) and 10 % FCS. MDCK cells strain II were maintained as described (Benting, et al., 1999). Cells were grown to confluency and generally passaged 1:3 to 1:6. They were washed with PBS, trypsinised and resuspended in fresh medium. For cryoconservation, 5×10^6 cells/ml were resuspended in freezing medium, followed by transfer to a -80 °C freezer and ultimately stored in liquid nitrogen one day later.

3.3.2 Transfection of mammalian cells

Cells were transfected with plasmid DNA by using LipofectAMINE 2000 (Invitrogen, Karlsruhe) or Fugene (Roche, Basel, Switzerland) according to manufacturer’s instructions by using generally a ratio 1:1 of DNA (µg) : Lipofectamine (µl). Transfection was done in OptiMEM (Gibco/BRL) for 5-6 h, then medium was changed to normal growth medium and plasmids were expressed for 24-36 h.

3.3.3 Generation of stable cell lines

After transfection of 2×10^6 cells in a 10 cm dish with 15 µg of plasmid DNA as described above (chapter 3.3.1), cells were grown for 24 h at 37 °C in normal growth medium to allow expression of the plasmid. Then cells were split into five 24 well plates in normal growth medium. Medium was changed after 6 h to fresh medium containing 700 µg/ml geneticin-sulphate (G-418; PAA, Pasching, Austria). Cells were fed with selective medium every 3-4 days until untransfected control cells died. Finally, G418 resistant clones were picked, expanded and tested for gene-product expression by FACS analysis. Stable clones were maintained in the presence of 400 µg/ml G-418.

3.3.4 Amplification and transduction of cell lines with adenovirus

To amplify EBAG9-encoding adenovirus, HeK293A cells (~ 60-80 % confluent) were infected with purified virus in DMEM supplemented with 2 % FCS for 90 min at 37 °C. Cells were grown for 2-7 days in normal growth medium until they began to detach. Cells and supernatant were collected, centrifuged at 1500 rpm, and cell pellet was resuspended in DMEM supplemented with 2 % FCS, followed by three thaw (37 ºC) and freeze (-70 ºC) cycles. Then, cells were centrifuged at 3500 rpm at 4 °C for 20 min and the supernatant purified via a discontinuous CsCl-gradient consisting of CsCl 1.4 M solution (53 g CsCl, 87 ml 10 mM Tris-HCl, pH 7.9) and CsCl 1.2 M solution (26.8 g CsCl, 92 ml 10 mM Tris-HCl, pH 7.9). The first gradient was centrifuged for 90 min at 26.000rpm at 4 ºC (deceleration rate = 0) using a SW 28/Beckman swinging bucket rotor. Afterwards, the tube was punctured below the lowest bluish white band containing the virons using a 5 ml syringe with an 18G needle. The viral band was aspirated and loaded on a second discontinuous CsCL gradient, followed by centrifugation overnight at 28.000 rpm at 4 ºC (deceleration rate = 0) using a SW 40/Beckman swinging bucket rotor. The purified virons were isolated as described above and diluted 1:1 with TE. To remove the CsCl, the purified virus was loaded on an equilibrated 10 ml Sephadex G25 column in PBS and fractions (~ 0.5 ml) were collected. Virus concentration was determined by optical density analysis at 260 nm. Fractions with the highest virus concentration were pooled, 10 % Glycerol was added and stored at -80 °C. Virus

infectivity was determined empirically and by titration as described previously (Cichon, et al., 1999; Ruder, et al., 2005).

3.3.5 Pulse-chase experiments

Cells were incubated in methionine- and cysteine-free RPMI medium for 45 min at 37°C. After starvation, cells were centrifuged at 1100 rpm for 5 min and resuspended in 500 µl in methionine- and cysteine-free RPMI, followed by incubation with 500 µCi [^{35}S]methionine-cysteine (Expre labeling mix, Perkin Elmer, Waltham, MA) for 10 min to label the cells (Pulse). Then medium supplemented with excess of unlabeled methionine (1.5 mM) and cysteine (0.5 mM) was added and cells were chased at either 19.5 °C or 37 °C for various times. For each time point, 1 ml sample was taken, centrifuged and cells were lysed in NP-40 buffer (chapter 3.2.1). After centrifugation, preclearing of the supernatant was done by addition of 80 µl Staph.A (Staphylococcus aureus, Pansorbin, Calbiochem) 5 µl rabbit serum. Then, the sample was centrifuged and MHC class I heavy chain was immunoprecipitated (chapter 3.3.6). To investigate the ER to Golgi transport, immunoprecipitates were digested with Endoglycosidase H (EndoH$_f$, NEB) or neuraminidase (NEB) as described elsewhere (Rehm, et al., 2001). Samples were analysed by SDS-PAGE (chapter 3.2.2) or 1d-IEF-gel (chapter 3.2.4). Gels were fixed and subjected to autoradiography (chapter 3.2.5).

3.3.6 Immunoprecipitation (IP) and co-immunoprecipitation

To isolate specific proteins from cell lysates (chapter 3.2.1), 5 µl antigen-specific antibody and 120 µl protein A-Sepharose (Amersham Biosciences) or protein G-Sepharose (Amersham Biosciences) were added and rotated for at least 2 h at 4 °C. After centrifugation at 13000 g for 1min and washing four times with 1× NET buffer (for pulse chase experiments), immunoprecipitates were analyzed as described in chapter 3.2.2.

If the immunoprecipitated protein interacts with other proteins *in vivo*, these associated proteins might be co-immunoprecipitated. For coimmunoprecipitation, HeLa cells were transiently transfected with EBAG9-GFP or GFP. Cells were lysed in 0.5 % TX-100 lysis buffer for 30 min at 4 °C. Solubilized proteins were incubated with anti-GFP monoclonal

antibody and protein A- or G-Sepharose for 3 h at 4°C. Beads were washed 10 times with 0.4 % TX-100 lysis buffer, and bound proteins were separated by SDS-PAGE (chapter 3.2.2) and analysed by immunoblotting (chapter 3.2.3). Primary antibodies used for blots were biotinylated anti GFP and anti-βCOP.

3.3.7 Subcellular fractionation

Hela cells transfected with T-synthase for 48 h (chapter 3.3.2) and infected with murine Ad-EBAG9 or Ad-LacZ for 18 h (chapter 3.3.4) were resuspended in 1.5 ml homogenization buffer (HB). Resuspended cells were homogenized by 30 strokes in a glass-teflon homogenizer with a tight-fitting pestle (B. Braun, Melsungen). Afterwards, the homogenate was centrifuged at 3000 rpm for 7 min at 4 °C to remove nuclei and unbroken cells. Then the postnuclear supernatant (PNS) was centrifuged at 60.000 rpm for 50 min at 4 °C using a table-top ultra centrifuge to obtain microsomal membranes and cytosolic fractions.

For investigation of ArfGAP1 or βCOP, the microsomal fraction was directly resuspended in sample buffer, whereas proteins of the cytosolic fraction were precipitated quantitatively with 20 % TCA for 1-3 h, washed once with ice-cold EtOH before they were resuspended and finally analysed by SDS-PAGE and immunoblot (chapter 3.2.3).

For analysis of T-synthase distribution, the microsomal fraction was homogenized in 850 µl HB and loaded on a discontinuous Optiprep (Axis-Shield, Po CAS, Oslo, Norway) gradient (bottom – 50, 40, 30, 20, 10 % - top) followed by centrifugation at 21.000 rpm at 4 °C overnight using a SW40 rotor. Fractions 1-14 (785 µl) were carefully removed from top to bottom, precipitated as described, washed once with ice cold acetone, once with EtOH and finally analysed as described before.

Homogenizing buffer (HB): 10 mM Tris/HCl pH 7.4, 250 mM Sucrose, protease inhibitors and 1 mM EDTA (only for ArfGAP1)

3.3.8 Fluorescence activated cell sorting (FACS)-analysis

Cells for analysis were once washed with cold FACS-buffer, transferred into round-bottom microtiterplates and blocked for 20 min. After centrifugation at 1500 rpm for 1 min, cells were washed once with FACS-buffer, blocked with normal goat serum (NGS) for 20 min and then incubated with primary antibody for 30 min on ice. This was followed by two washing steps and incubation with the secondary antibody for 30 min on ice. For determination of cell death, one aliquot of cells was also stained with PI (Bender MedSystems, Vienna, Austria) according to manufacturer's instructions. Finally, cells were washed three times and analysed on a FACSCalibur (Becton-Dickinson) or FACS Canto (Becton-Dickinson). Data were analysed using "Cell Quest" (BD Biosciences, Heidelberg) or FlowJo (BD Biosciences, Heidelberg) software.

FACS-buffer: PBS, 0.5 % BSA, 0.05 % NaN_3

3.3.9 Immunofluorescence

0.7×10^5 (12 well) or 3.6×10^4 (24 well) cells were grown on glass coverslips (Roth). 24 h later they were washed with PBS, fixed with 2-4 % PFA for 10 min on ice, washed twice and permeabilized for 5 min with 0.25 % Triton X-100 in PBS. Afterwards cells were washed twice for 5 min with PBS and blocked in 2.5 % milk powder in PBS for 30 min to avoid unspecific binding of antibodies. Slides were then incubated with primary antibodies (Tab. 4) in 2.5 % milk powder in PBS for 1-2 h at RT, washed twice for 5 min with PBS, followed by incubation with secondary antibody (Tab. 5**Tab. 5**) conjugated with fluorescence dye in 2.5 % milk powder in PBS for 45 min at RT. Finally, cells were washed twice for 5 min in PBS and covered with Mowiol on a microscope slide. Treatment with nocodazole (10 µM) or BFA (5 µg/ml) was carried out for 1 h prior to fixation of cells.

Mowiol solution: 0.2 M Tris/HCl pH 8.5, 50 % Glycerin, 20 % w/v Mowiol 4-88 (Calbiochem)

3.3.10 Lectin staining

Cells were fixed in cold acetone for 7 min on ice, washed twice with PBS, permeabilized with 0.25% TritonX-100 for 10 min and blocked with 5% BSA for 60 min. Then, cells were washed in special washing medium (WM) and stained with VVA, PNA (Tab. 4) and GM130 in special binding medium (BM) for 90 min. After washing twice for 5 min with WM the cells were incubated with secondary antibody in BM for 45 min. Finally, cells were washed twice for 5 min in WM, and covered with Mowiol on a microscope slide.

Washing Medium (WM): 10 mM Hepes, pH 7,5; 0,15 M NaCl

Binding Medium (BM): 10 mM Hepes, pH 7,5; 0,15 NaCl; 0,08 % NaN_3; 0,1 mM $CaCl_2$; 0,01 mM $MnCl_2$

3.3.11 Confocal image acquisition and correlation analysis

Images were acquired with a Zeiss LSM510Meta confocal setup on an Axiovert 200M inverted microscope (Zeiss, Göttingen, Germany) equipped with an argon and helium/neon I or II laser for double or triple fluorescence at 488 nm, 543 nm and 635 nm using a 63x or 100x phase contrast plan-apochromat oil immersion objective. For double and triple staining GFP, Alexa Fluor 568 or 647, cy3, DsRed and cy5 signals were recorded sequentially (multi track) to minimize potential cross-talk between the fluorophores. Main beam splitter was HFT UV/488/543/633, HFT UV 488/543 or HFT UV 458/514 with following parameters for each fluorochrome: GFP, λ_{exc} = 488 nm and λ_{em} = BP500-530 nm or Metadetector 494.7-505.4 nm (double staining with DsRed); CFP, λ_{exc} = 458 nm and λ_{em} = Metadetector 462.6-473.3 nm; Alexa Fluor 568, Cy3 and DsRed, λ_{exc} = 543 nm and λ_{em} = LP560 nm (double staining with GFP) or λ_{em} = BP565-615 nm (triple staining); Cy5 and Alexa Fluor 647, λ_{exc} = 633 nm and λ_{em} = LP650 nm. All images were processed using LSM Examiner 3.2 and LSM Browser software (Zeiss) or ImageJ (open source). To better visualize colocalization of proteins, the cy5 / Alexa Fluor 647 were reassigned to green or red colours when appropriate.

Colocalization was quantified calculating the Pearson's correlation coefficient (R) according to the following formula (Ch, channel; values are pixel intensities):

$$R_P = \frac{\sum \left(Ch1_i - Ch1_{aver}\right)\left(Ch2_i - Ch2_{aver}\right)}{\sqrt{\sum \left(Ch1_i - Ch1_{aver}\right)^2 \sum \left(Ch2_i - Ch2_{aver}\right)^2}}$$

The Golgi was marked as region of interest (ROI) using the LSM software. For each ROI the software calculated R. In all experiments the intensity of signals was kept equal. The Pearson's correlation coefficient takes into consideration similarities between shapes, while ignoring the intensities of signals, and thus is applicable when fluorescence intensities are equal (Zinchuk and Zinchuk, 2008; Zinchuk, et al., 2007). For the calculation of the relative Golgi fluorescence (RGF) ImageJ software was used. The Golgi or whole cell was marked as ROI and the sum of the values of the pixels in the selection (Integrated Density) was quantified. RGF was calculated according to the following formula:

$$RGF = \frac{Fluorescence\ Golgi}{Fluorescence\ total\ cell}$$

Selective photobleaching of the Golgi complex was performed using 30-50 consecutive scans of the appropriate laser line at full power (Ward, et al., 2001). Recovery was then monitored by time-lapse imaging at low-intensity illumination. Images of cells were captured with a 100x phase contrast plan-apochromat oil immersion objective using a pinhole diameter equivalent to 1 Airey unit. All figures were assembled with Corel Draw (Corel).

3.3.11.1 Time-lapse imaging

To observe live-cells, we used 15 µ-slides for live cell imaging (Ibidi). MDA-MB435 cells stably expressing EBAG9 were grown on these dishes for 24 h, then medium was changed to fresh complete medium with 5 µg/ml transferrin conjugated to Alexa Fluor 568 for 20 min at 37 °C, washed once with medium without transferrin, followed by addition of fresh medium supplemented with 10 mM Hepes. The cells were viewed with a Zeiss LSM 5 Live confocal microscope equipped with a 63× objective lens (Plan-Apochromat; Carl Zeiss). GFP was excited by the 488 nm line of an Argon laser and detected through a BP500-525 nm band-pass filter, and Alexa Fluor 568 was excited by the 532 nm line and detected through the 550 nm

long-pass filter. Cells were scanned with the multitrack mode with 5.2 or 5.0 s of interval time.

3.3.12 Transport assays

3.3.12.1 Human growth hormone release assay

For detection of constitutive exocytosis $5x10^5$ EBAG9-GFP and GFP stably transfected mamma carcinoma (MDA-MB435) cells or $3x10^6$ PC12 cells were seeded in untreated or collagen coated wells, respectively. MDA-MB435-EBAG9 and MDA-MB435-GFP cells were transfected with human growth hormone (hGH) alone, whereas PC12 cells were transiently cotransfected with hGH and EBAG9-GFP or GFP using LipofectAMINE2000 (chapter 3.3.2). 48 h after transfection, cells were stimulated with low KCl buffer or high KCl buffer for 30 min (constitutive release) or 10 min (regulated secretion) at 37 °C. Cell culture supernatant and transfected cells were collected, and cells were broken in PBS by three cycles of freeze-thawing. The resulting cell extracts were cleared by centrifugation at 13000 rpm for 10 min, and the amounts of hGH in the medium and in the cell extracts were quantified by hGH specific ELISA, according to the manufacturer's instructions (Biosource, Nivelles, Belgium). Regulated release of hGH from PC12 cells was effectuated with high KCl secretion buffer for 10 min, essentially as described (Khvotchev, et al., 2003).

Low KCL buffer: 140 mM NaCl, 5.6 mM KCl, 2.2 mM $CaCl_2$, 0.5 mM $MgCl_2$, 5.6 mM glucose, 15 mM Hepes, pH 7.4

High KCL buffer: 95 mM NaCl, 56 mM KCl, 2.2 mM $CaCl_2$, 0.5 mM $MgCl_2$, 5.6 mM glucose, 15 mM Hepes, pH 7.4

3.3.12.2 Polarized transport assay

The VSVG transport assay was carried out as described (Schuck, et al., 2007). MDCKII cells grown to confluence on coverslips were infected with EBAG9 adenovirus (chapter 3.3.4) for 1 h, grown for 12 h, reinfected with apical or basolateral VSVG-encoding adenovirus for 2 h

and incubated at 39.5 °C for 6 h. Cells were then shifted to 32 °C, chased in the presence of 40 µg/ml cycloheximide for the time intervals indicated and analysed by widefield microscopy (chapter 3.3.11).

To monitor Golgi to plasma membrane transport of apical VSVG, cells were incubated at 19.5 °C in CO_2-independent medium containing 40 µg/ml cycloheximide. After 90 min the protein was allowed to exit the Golgi at 32 °C for the times indicated.

3.3.12.3 rGH transport assay

The rGH transport assay was modified after (Scheiffele, et al., 1995). MDCKII cells were seeded on 24-mm polycarbonate filters (Costar) and grown for 24 h (Fig. 3-1). Then cells were incubated in PBS without $MgCl_2$ and $CaCl_2$ (PBS-) for 15 min to open tight junctions and to facilitate virus infection, followed by cotransfection of control and GST-rGH12 adenovirus or EBAG9 and GST-rGH12 adenovirus for 1 h. After 14 h incubation at 37 °C cells were washed in PBS with $MgCl_2$ and $CaCl_2$, radioactively labeled (chapter 3.3.5) and chased for the indicated times. Medium was harvested from the apical and basolateral side of the filter, cells were lysed in 0,5 % Triton-X-100 in PBS-containing 10× CLAP (NEB) for 10 min at RT and the protein containing supernatant was collected. Finally, rGH12 was precipitated with glutathione beads, resolved by SDS-PAGE and analysed by phosphorimager (chapter 3.2.5).

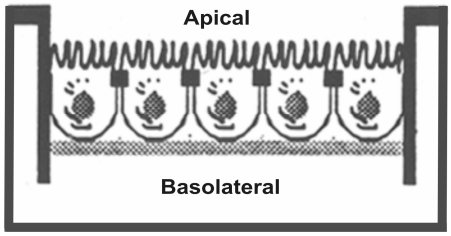

Fig. 3-1: Filter grown MDCK cells. Medium from apical and basolateral side is separated by filter.

3.3.12.4 HA transport assay

Influenza hemagglutinin transport in filter-grown MDCK cells was modified after (Schuck, et al., 2007). MDCKII cells were seeded on 24-mm polycarbonate filters (Costar) and grown for 24 h. Then cells were incubated in PBS without $MgCl_2$ and $CaCl_2$ (PBS-) for 15 min to open tight junctions and to facilitate virus infection, followed by transfection with EBAG9

adenovirus for 1 h at 37 °C. After 12 h incubation at 37 °C cells were washed in PBS with $MgCl_2$ and $CaCl_2$ (PBS+), infected with Fowl plaque virus [FPV; 0.45 ml virus / filter (about 10-20 PFU/cell)] for 1 h and incubated in fresh infection medium for 3 h. Then, filters were washed in PBS+, radioactively labeled (chapter 3.3.5) for 8 min, washed in PBS+ and chased for the indicated times to measure ER to PM transport. After washing the filter with cold PBS+, cells were trypsinized from the apical and basolateral side so that the total surface delivery of hemagglutinin (HA) could be measured. Cells were lysed in 2 % NP-40 in PBS-containing 1× CLAP, 0,2 % SDS for 10 min at RT and the protein containing supernatant was collected. Finally, HA was resolved by SDS-PAGE and analysed by phosphorimager (chapter 3.2.5).

3.3.12.5 VSVG transport assay

For transport assays of VSVG-GFP, COS7 cells were transiently cotransfected using LipofectAMINE2000 or Fugene with VSVG-GFP and either EBAG9, EBAG9-DsRed2 or empty vectors pcDNA3.1 and pDsRed2, respectively (chapter 3.3.2). Cells were cultured for 16-24 h at 40°C in a humidified atmosphere, 100 µg/µl cycloheximide were added, followed by incubation for 3 h at 15°C before shifting cells to 32°C to resume transport, as described (Rojo, et al., 1997). At defined time intervals, cells were processed for immunofluorescence as described in chapter 3.3.9.

3.3.12.6 siRNA treatment and VSVG-transport analysis

MDA-MB435 cells, stably expressing EBAG9, or MCF7 cells were transfected with Alexa Fluor 647 labeled siRNA against EBAG9 (3´-AAGATGCACCCACCAGTGTAA-5´) or Alexa Fluor 647 labeled "all star negative control" using Oligofectamin (Invitrogen) according to manufacturer's instructions and incubated at 37 °C. After 24 h cells were retransfected with siRNA and cells were analysed for EBAG9-GFP expression by FACS analysis 24 h later. MCF7 cells were collected after 48 h of siRNA expression, and protein lysates (section 3.2.1) were analysed for EBAG9 expression by SDS-Page (chapter 3.2.2) and westernblot (chapter 3.2.3).

For VSVG-transport analysis cells were re- and co-transfected with siRNA and GFP-tagged VSVG-ts045 for 5 h at 37 °C, and finally incubated at 39.5 °C to accumulate VSVG in the ER. After 48 h siRNA expression, 100 µg/µl cycloheximide was added, followed by incubation for 30 min at 32 °C to allow ER export and subsequent transport beyond the Golgi. Cells were fixed in PFA at the times indicated, permeabilized and stained with an antibody against GM130. Colocalization was analysed by confocal microscopy (chapter 3.3.11). The kinetics of Golgi transition was quantitatively determined by measuring the ratio of fluorescence intensity in the Golgi versus the whole cell at 30 min as described in chapter 3.3.11.

3.3.12.7 Shiga toxin transport assay

HeLa cells were transiently transfected with EBAG9-GFP or GFP. After 24 h cells were incubated with media containing Cy3-Shiga toxin B-fragment (1:1000 dilution of concentrated stock) for 45 min on ice as described (Yoshino, et al., 2005). Cells were washed twice with cold PBS to remove unbound STB. Warm medium was added, followed by a chase at 37 °C. Cells were fixed and processed for immunofluorescence as described in chapter 3.3.9 and analysed by confocal microscopy (chapter 3.3.11).

3.3.13 Mannosidase activity assay

Stable EBAG9-GFP or GFP expressing MDA-MB435 cells were lysed in 10 mM KH_2PO_4 buffer, pH 6.8, containing 0.5 % Triton X-100 and 1 mM NaN_3 for 30 min at 4 °C. After centrifugation, protein concentration of the lysate was determined by Bradford assay (chapter 3.2.1). For the Mannosidase activity assay (Jelinek-Kelly, et al., 1985), 1 mg of protein lysate was incubated with 0, 2, 4, 6, 8, 10 or 12 mM p-nitrophenyl-alpha-D-mannopyranoside at 37 °C. After 0, 30, 60, 90 and 120 min aliquots were taken and mixed with an equal volume of 0.5 M Na_2CO_3 buffer to terminate the enzymatic reaction. Optical density of reaction products was measured at 405 nm in a plate reader. To plot enzyme activity as Michaelis-Menten kinetics, the optical density was plotted against time and the velocity of the reaction calculated from the gradient of the linear regression.

3.3.14 Lymphocyte activation

Cytotoxic T lymphocytes (CTL) were derived by activation of 4×10^6 splenocytes/ml from effector strain C57BL/6 (H-2^b haplotype) (*Ebag9*$^{+/+}$ and *Ebag9*$^{-/-}$) with 4×10^6 irradiated (3,000 rads) splenocytes/ml as stimulators from BALB/c (H-2^d haplotype) mice in complete RPMI medium supplemented with β-mercaptoethanol. For confocal microscopy analysis, naive $CD8^+$ T cells were stimulated by culturing cells for 3-4 days with plate-bound anti-CD3ε mAb (3 µg/ml) and anti-CD28 mAb (2 µg/ml) in the presence of 50 U/ml IL-2. $CD8^+$ cells were purified by negative selection with magnetic beads (Miltenyi Biotec or Dynal), followed by 1-2 days of culture in the presence of IL-2 and IL-7 (Peprotech; 50 U/ml). Purity of $CD8^+$ cells was usually greater than 90 %.

3.3.15 Immunological synapse formation

Dynabeads (4.5 µm) precoated with CD3/CD28 antibodies (Invitrogen) were used to initiate synapse formation. 5×10^5 CTLs were mixed with 5×10^5 coated beads and incubated for 5 min at 37 °C in complete RPMI, allowing the formation of conjugates. After centrifugation for 4 min at 2000 rpm (Eppendorf-centrifuge), the pellet was responded in RPMI without FCS and distributed into wells of collagen coated plates followed by 30 min incubation at 37 °C. Next, cells were fixed in either acetone or 2 % PFA and subjected to immunofluorescence staining as described in chapter 3.3.9, except that cells were blocked with 5 % BSA. Antibodies were incubated in 1 % BSA in PBS and the second antibody was pre-absorbed with hamster serum for 30 min at RT.

3.3.16 *In vivo* tumor growth

Immunodeficient B6.CB17-Prkdc^{scid} /SzJ homozygous mice (Charles River, Sulzfeld, Germany) were transiently anesthetized. Then $2x10^6$ MDA-MB435-GFP or MDA-MB435-EBAG9-GFP cells in 100 µl PBS were injected into the mammary fat pad. Tumor volume was frequently monitored and followed up to 92 days or till a maximum tumor size of 15 mm (measured in two rectangular dimensions) was reached. Tumor volume was calculated according to the formula: V = longest diameter x (smallest diameter)^2.

3.4 Statistical analysis

Results are expressed as mean ± S.D or SEM, as indicated. Data were considered statistically significant for $p < 0.05$, which was determined using the two-tailed unpaired Student's *t* test or the Wilcoxon-sign-rank test, where appropriate.

4 Results

To investigate the physiological role of the tumor-associated antigen EBAG9 in epithelial cells, mamma carcinoma cells that stably express EBAG9-GFP (MDA-MB435-EBAG9-GFP) were used. This situation is analogous to EBAG9 overexpression in tumor cells. In general, EBAG9 protein expression levels vary strongly in diverse cancer cells and tissues (Akahira, et al., 2004; Reimer, et al., 2005; Takahashi, et al., 2003; Tsuchiya, et al., 2001). This is also reflected in a broad range of native EBAG9 protein expression levels in diverse epithelial cell lines (Fig. 4-1A).

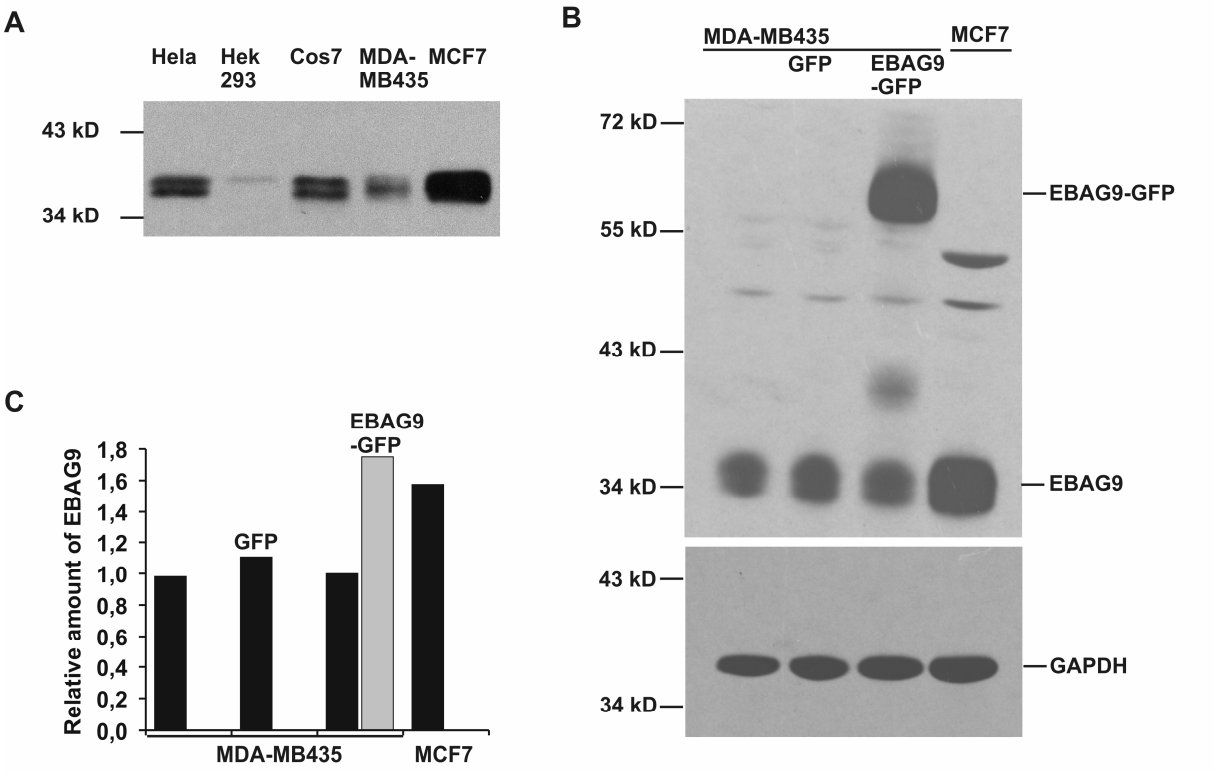

Fig. 4-1: EBAG9 overexpression in different cell lines. Indicated cell lines either expressing endogenous EBAG9 only (A) or stably expressing GFP and EBAG9-GFP (B) were lysed in a buffer containing 25 mM Hepes, pH 7.4, 140 mM KCl, 20 mM NaCl, 0.5 mM $MgCl_2$, 0.8 mM PMSF, aprotinin 5 µg/ml, 0.5 % TX-100 for 30 min at 4 °C. Lysates were spun to deplete nuclei and insoluble material, and 100 µg of each probe was resolved by SDS-PAGE and analysed by immunoblotting using rabbit-anti-EBAG9 serum or rabbit-anti-GAPDH (loading control). (C) Densitometry analysis of (B) showing the amount of EBAG9 relative to endogenous EBAG9 in MDA-MB435 cells normalized to GAPDH. Black bars, endogenous EBAG9; grey bar, overexpressed EBAG9-GFP.

Here, westernblot analysis demonstrated that the expression level of stably transfected EBAG9 was 1.7× fold higher than endogenous EBAG9, but still in the range of endogenous EBAG9 in another mamma carcinoma cell line, MCF-7 (Fig. 4-1B, C). Thus, referring to

endogenous EBAG9 expression in MCF-7 cells, EBAG9-GFP stably expressing MDA-MB435 cells mimic EBAG9 expression in a range similar to primary human tumors.

4.1 Golgi association of EBAG9

4.1.1 Subcellular localization and morphology of EBAG9

Since a detailed understanding of the subcellular localization of a protein should provide an indication of the physiological process it might be involved in, the localization and dynamics of EBAG9 were thoroughly analysed. First, a subcellular localization analysis of EBAG9 by confocal microscopy revealed a strong colocalization of EBAG9 with the cis-Golgi marker GM130 and with the IC marker ERGIC-53 (Fig. 4-2). The latter was identified as a cargo-specific transport receptor for ER-to-Golgi traffic known to continuously cycle between these two compartments (Appenzeller-Herzog and Hauri, 2006).

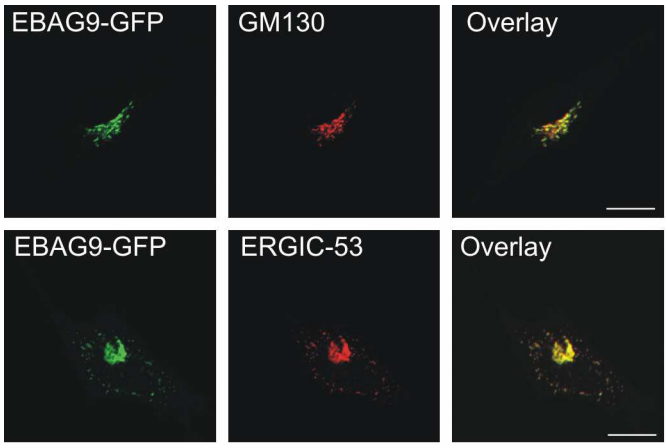

Fig. 4-2: EBAG9 localizes to the Golgi as well as to the intermediate compartment. MDA-MB435 cells stably expressing EBAG9-GFP were fixed in PFA, permeabilized and stained with antibodies against GM130 or ERGIC-53. The subcellular distribution of EBAG9-GFP (green) and GM130 or ERGIC-53 (red) was analysed by confocal microscopy. Merged images are shown on the right. Scale bars, 10 µm.

In the overlay images, it could be seen that cis-Golgi ($GM130^+$) and IC ($ERGIC\text{-}53^+$) were not resolved sufficiently as separated compartments. A more detailed analysis, using an EBAG9 construct that exhibits a substantially smaller epitope tag (FLAG-tag, 12 aa), demonstrated that EBAG9 stronger colocalized with ERGIC-53 (at 37 °C, mean R = 0,60; at 15 °C, mean R = 0,57) than with GM130 (at 37 °C, mean R = 0,28; at 15 °C, mean R = 0,18) as quantified by the Pearson`s correlation coefficient (R) (Fig. 4-3). This is consistent with earlier studies demonstrating that ERGIC-53 is present in tubulo-vesiclular membrane profiles predominantly near the cis-side of the Golgi stack at 37 °C. Theses ERGIC clusters have been shown to move even closer to the Golgi apparatus at 15 °C (Klumperman, et al., 1998;

Schweizer, et al., 1988). Furthermore, it was noted that the morphological integrity of the Golgi was not altered by EBAG9 overexpression.

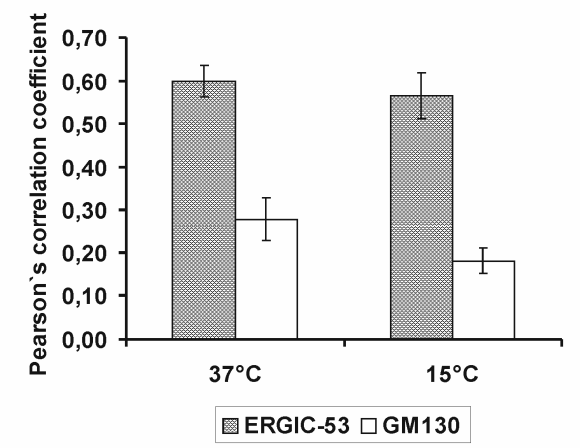

Fig. 4-3: EBAG9 colocalizes stronger with ERGIC-53 than GM130. HeLa cells were transiently transfected with EBAG9-C-Flag. After 24 h, cells were either chased at 15 °C for 3 h, or directly fixed and stained with antibodies against EBAG9, ERGIC-53 and GM130. Colocalization of EBAG9 with ERGIC-53 and GM130 was assessed by determining the Pearson`s correlation coefficient. Data represent mean values ± SEM of 16 cells.

4.1.2 Dynamic redistribution of EBAG9 in epithelial cells

Dynamic molecular interactions are fundamental for many cellular processes. To address whether EBAG9 is permanently or dynamically associated with Golgi membranes, fluorescence recovery after photobleaching (FRAP) analysis was applied. In FRAP, fluorescent molecules are permanently bleached at a region of interest. The rate of fluorescence recovery provides a measure of how fast fluorescent molecules move into the bleached region and depends on the rates of passive diffusion and active transport of the fluorescent molecule through the cell. Secondly, mobility is also influenced by binding interactions, which prevent molecules from free diffusion (Sprague and McNally, 2005).

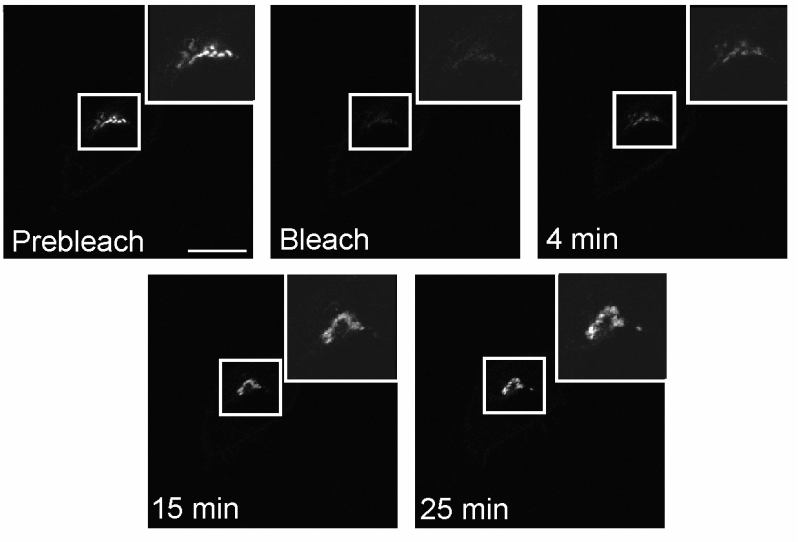

Fig. 4-4: Dynamic association of EBAG9 with Golgi membranes. MDA-MB435-EBAG9-GFP stably transfected cells were photobleached in the Golgi area, and the recovery of fluorescence in the selected area was monitored. Images show representative time points postbleach. Recovery of EBAG9 fluorescence can be readily seen after 15-25 min. Insets show a higher magnification of the indicated area. Scale bar, 10 µm.

After photobleaching of Golgi located EBAG9-GFP, full fluorescence recovery was obtained within 15 to 20 min (Fig. 4-4). These data were comparable to those obtained in published experiments using tagged p58/ERGIC-53 protein (Tisdale, et al., 1997; Ward, et al., 2001), and clearly differed from the much slower transport of a Golgi-resident (GalT) molecule or the extremely fast transport of a cytoplasmic protein (εCOPI) (Presley, et al., 1998). These results indicated that EBAG9 could traffic between the ER and the Golgi apparatus like ERGIC-53, continuously cycling between these two compartments.

Additionally, the behaviour of EBAG9 was investigated by live cell imaging of MDA-MB435 cells stably expressing EBAG9-GFP. Many cells exhibited a perinuclear staining pattern corresponding to the Golgi, and in some cells budding and fusion reactions of vesicular and tubular structures could be observed (indicated by an arrow) (Fig. 4-5).

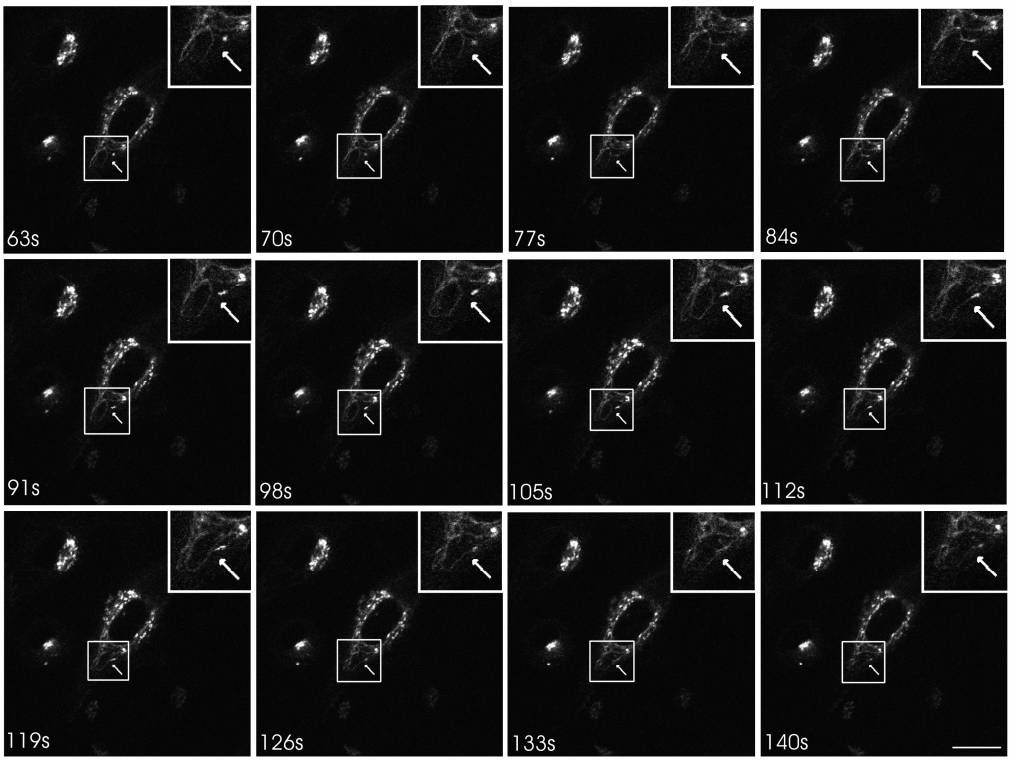

Fig. 4-5: Vesicular and tubular structures in EBAG9-overexpressing cells. Representative pictures from a **t**ime-lapse sequence showing movement of EBAG9 containing structures. MDA-MB435 cells stably expressing EBAG9-GFP were imaged in Hepes buffered medium with a confocal microscope with a stage heated to 37 °C using a 488 nm laser excitation. Sixty frames were collected. Insets show higher magnification of the area indicated by a square. Budding and fusion reactions of vesicular and tubular structures are indicated by an arrow. Scale bar, 10 µm.

This demonstrated that EBAG9 moves with vesicles involved in protein trafficking, in which budding and fusion events take place continuously. These vesicles might belong to any of the

three major classes of coated vesicles: COPI, COPII or Clathrin coated vesicles. Clathrin-coated vesicles can be distinguished from other vesicle populations, since transferrin is specifically endocytosed by clathrin-coated endosomal vesicles (Hanover, et al., 1984; Kirchhausen, et al., 2005). Time-lapse imaging of EBAG9 and transferring-containing vesicles showed that transferrin-labeled endosomal carriers were clearly separate from EBAG9-GFP stained vesicles (Fig. 4-6A).

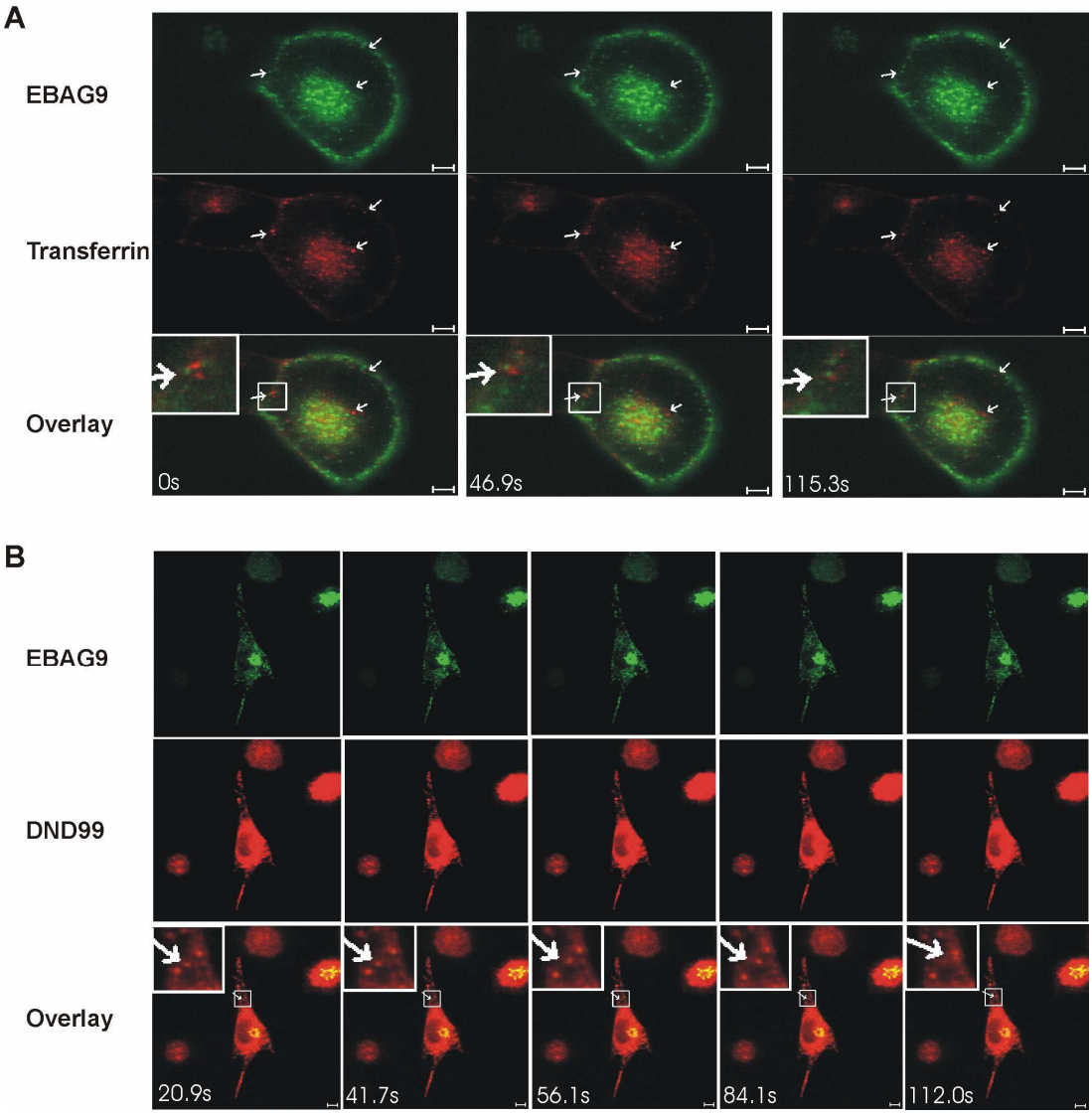

Fig. 4-6: EBAG9 localizes to DND99 positive compartments, but not to clathrin-coated vesicles containing transferrin. (A) Representative images of a time-lapse sequence showing movement of EBAG9-GFP and transferring-containing vesicles. MDA-MB435 cells stable expressing EBAG9-GFP were imaged in Hepes buffered medium with a confocal microscope with a stage heated to 37 °C using a 488 nm and 532 nm laser excitation. 40 frames were collected. Insets show higher magnification of the area indicated by a square. Scale bar, 5 µm. (B) Representative images of a time-lapse sequence showing movement of EBAG9-GFP and DND99 containing vesicles. MDA-MB435 cells stably expressing EBAG9-GFP were imaged in Hepes buffered medium with a confocal microscope with a stage heated to 37 °C using a 488 nm and 532 nm laser excitation. 20 frames were collected. Insets show higher magnification of the area indicated by the square. Scale bar, 5 µm.

In contrast, a strong overlap of EBAG9 with DND99 was found (Fig. 4-6B). DND99 consists of a fluorophore linked to a weak base that is only partially protonated at neutral pH and thus freely permeate to cell membranes, whereas in cellular compartments with low internal pH, such as lysosomes, it accumulates selectively.

Taken together, these results indicated that EBAG9 moves with non-clathrin coated vesicles within the cell and is only transiently associated with the Golgi, presumably shuttling between the ER and the Golgi. Furthermore, EBAG9 might associate with lysosomes.

4.2 EBAG9 associates with coatomer complex I

To obtain mechanistical insight into the cellular function of EBAG9 within the secretory pathway, I searched for interaction partners. A former interaction screen employing an EBAG9-GST fusion protein pull-down assay, which used a bait different from that previously used for a yeast-two hybrid screen (Ruder, et al., 2005), pointed towards a possible interaction with COPI. In this screen, COPI complex subunits δCOP, γ2COP, γCOP, β2COP, βCOP, β´COP and αCOP were identified by mass spectrometry (data generated by Dr. Tatjana A. Reimer, AG Dr. A. Rehm).

To confirm that EBAG9 and COPI can associate in epithelial cells, coimmunoprecipitation studies in EBAG9-GFP expressing HeLa cells were performed (Fig. 4-7).

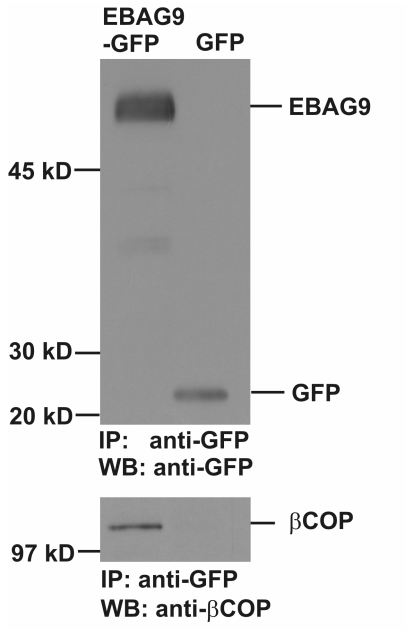

Fig. 4-7: EBAG9 associates with βCOP. HeLa cells were transiently transfected with EBAG9-GFP or GFP. After 24 h, EBAG9-GFP or GFP were immunoprecipitated from TX-100 lysates with an anti-GFP antibody (IP). Samples were washed and analysed by SDS-PAGE and immunoblotting (WB) using anti-βCOP or biotinylated anti-GFP antibodies.

An association between full length EBAG9-GFP and endogenous βCOP could be detected in those cells, but not in GFP control cells.

To map a possible interaction site, stable MDA-MB435 cell lines expressing mutant EBAG9 (Δ176-213 or Δ30-213) were generated and used for coimmunoprecipitation experiments. Additionally, transiently overexpressed, truncated forms of EBAG9 (Δ1-27, Δ1-163 and Δ1-27/Δ176-213) were employed as a bait to capture interacting endogenous βCOP. However, none of these EBAG9 mutants coimmunoprecipitated with endogenous βCOP (Fig. 4-8).

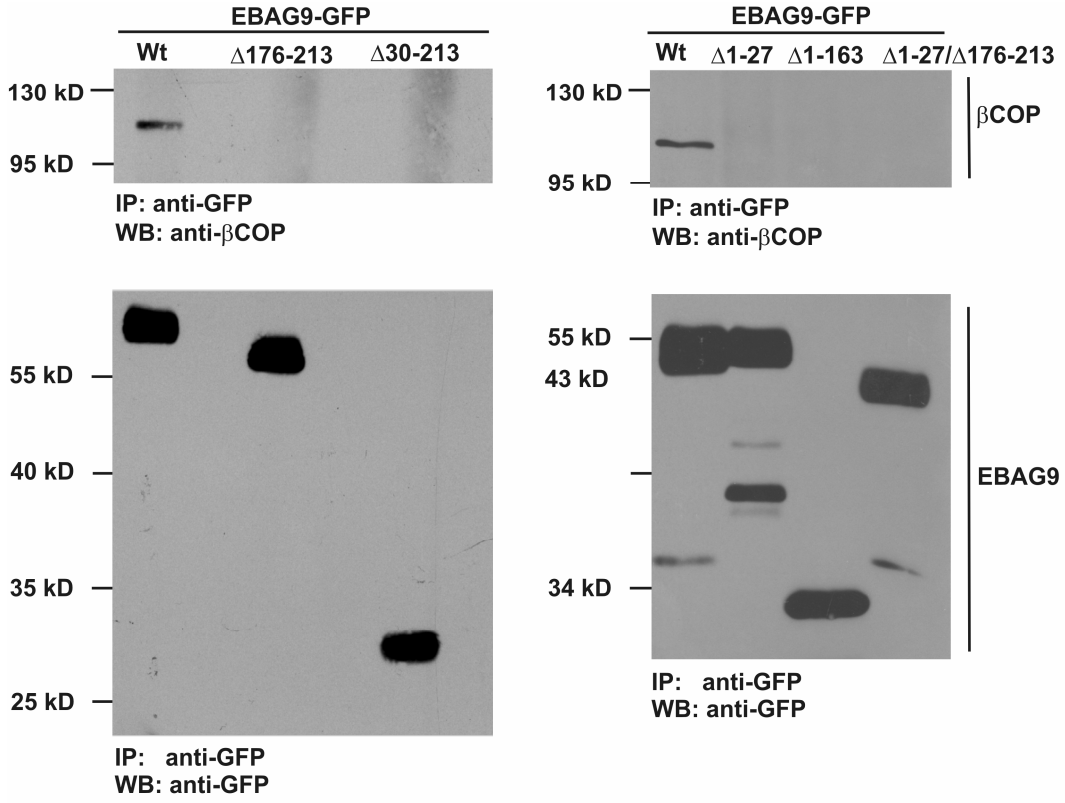

Fig. 4-8: Only full length EBAG9 interacts with βCOP. MDA-MB435 cells stably expressing EBAG9-GFP (Wt), GFP, EBAG9-Δ176-213-GFP, EBAG9-Δ30-213-GFP or MDA-MB435 cells transiently transfected with EBAG9-GFP, GFP, EBAG9-Δ1-27-GFP, EBAG9-Δ1-163-GFP, EBAG9-Δ1-27/Δ176-213-GFP were used. After 24 h, GFP constructs were immunoprecipitated from TX-100 lysates with an anti-GFP antibody (IP). Samples were washed and analysed by SDS-PAGE and immunoblotting (WB) using anti-βCOP or biotinylated anti-GFP antibodies.

Next, the presence of EBAG9 on COPI transport carriers was tested by immunofluorescence. MDA-MB435 cells stably expressing EBAG9 were treated with nocodazole to better visualize a possible colocalization. Nocodazole is a microtubule depolymerising agent which causes the Golgi apparatus to break down into functional ministacks (Dinter and Berger, 1998). Here, numerous vesicles were found to be double positive for EBAG9-GFP and γCOP (Fig. 4-9).

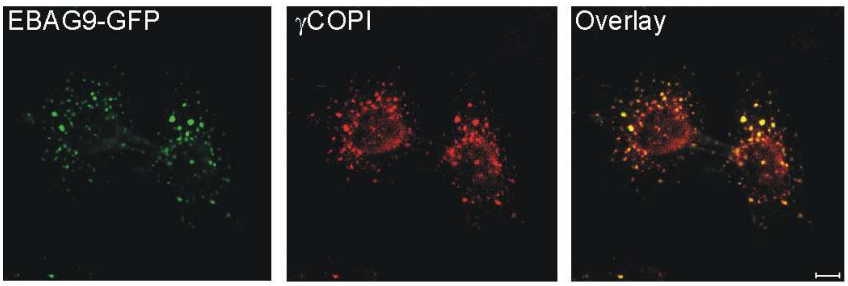

Fig. 4-9: EBAG9 is localized on COPI transport carriers. MDA-MB435 cells stably expressing EBAG9-GFP were treated with nocodazole for 2 h, fixed in PFA, permeabilized and stained with an antibody against γCOPI. Subcellular distribution of EBAG9-GFP (green) and γCOPI (red) was analysed by confocal microscopy. Merged images are shown on the right. Scale bars, 5 µm.

This observation suggested that COPI-coated transport carriers were also positive for EBAG9. In summary, these data indicated that EBAG9 associates with COPI coats *in vitro* and *in vivo*.

4.3 EBAG9 impairs the anterograde transport route

The dynamic redistribution of EBAG9 within the ER-cis-Golgi trafficking route and the identified COPI association pointed towards a potential function of EBAG9 in biosynthetic cargo transport. Thus, constitutive and regulated secretion as well the anterograde transport between the ER and the Golgi were thoroughly investigated.

4.3.1 EBAG9 inhibits protein transport before the medial Golgi in a cell-type dependent manner

4.3.1.1 EBAG9 affects regulated secretion in secretory as well as constitutive secretion in epithelial cells

To see whether EBAG9 might influence cargo delivery, epithelial non-secretory MDA-MB435-EBAG9-GFP cells, equipped only with a constitutive pathway, were transfected with a reporter vector encoding human growth hormone (hGH). Then the secretion of hGH into cell culture supernatant was measured over 30 min. In EBAG9-GFP transfectants, constitutive exocytosis was 61.4% lower than in GFP-expressing control cells (Fig. 4-10 A).

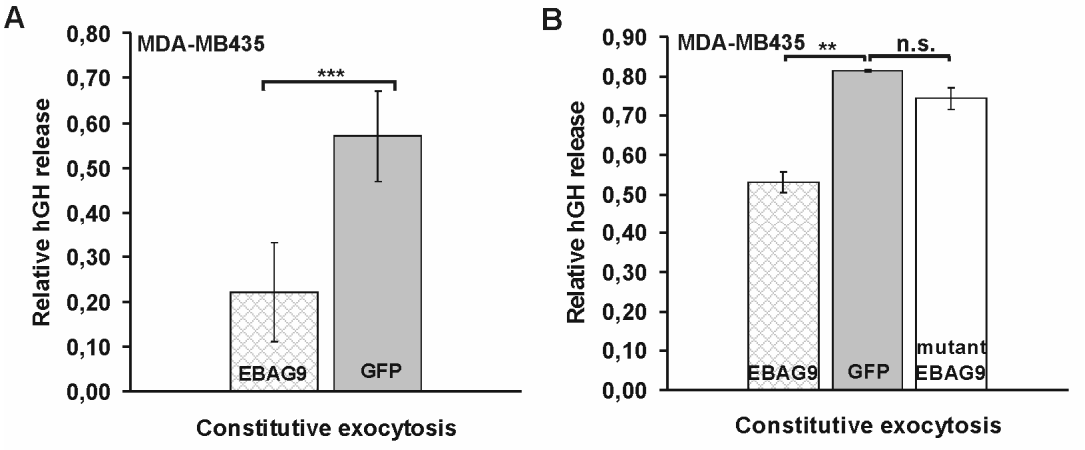

Fig. 4-10: EBAG9 decreases constitutive release of hGH in epithelial cells. (A, B) MDA-MB435-EBAG9-GFP, -GFP or -EBAG9-Δ30-213-GFP stably transfected mamma carcinoma cells were transfected with human growth hormone (hGH). hGH secretion was stimulated by incubation in low KCl (5.6 mM) containing secretion buffer for 30 min. Release of hGH into culture supernatant and total cell lysate associated hGH was determined by ELISA. All data are means ± S.D. of three independent experiments, performed in triplicate and normalized to total hGH. *** p≤ 0,0005; ** p≤ 0,005; Student's unpaired *t* test; n.s., non significant.

Furthermore, a hGH release assay was carried out in PC12 cells, to reconcile the finding that EBAG9 controls regulated synaptic-like vesicle release in neuroendocrine PC12 cells (Fig. 4-11). This neuroendocrine cell line is equipped with a regulated as well as a constitutive pathway. The assay applied here induces [Ca^{2+}] regulated secretion of hGH by high [K^+] concentration. Potassium depolarizes the membrane and triggers exocytosis by gating [Ca^{2+}] influx via [Ca^{2+}] channels (Khvotchev, et al., 2003).

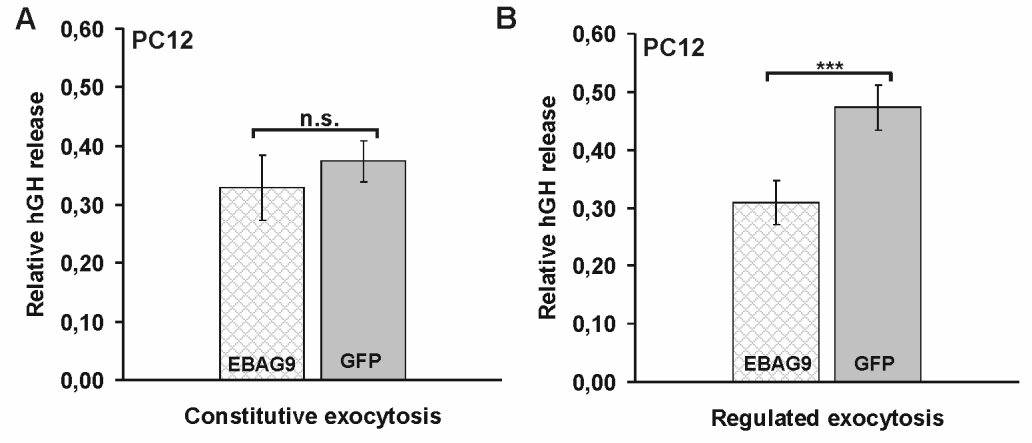

Fig. 4-11: EBAG9 impairs the regulated, but not the constitutive release of hGH in neuroendocrine cells. (A, B) PC12 cells were transiently cotransfected with hGH and EBAG9-GFP or GFP. After 48-72 h, hGH secretion was stimulated with low KCl solution for 30 min (constitutive secretion) (A), or for 10 min in high KCl solution (56 mM, regulated secretion) (B). Release of hGH was measured as described in Fig. 4-10. All data are means ± S.D. of three independent experiments, performed in triplicate and normalized to total hGH. *** p≤ 0,0005; Student's unpaired *t* test; n.s., non significant.

In contrast to non-secretory cells, the constitutive pathway was unaltered, whereas regulated secretion upon transient EBAG9 transfection was inhibited as shown before (Ruder, et al., 2005).

As an additional control, a truncated variant of EBAG9, the EBAG9-Δ30-213-GFP mutant was used to rule out that the inhibition of secretion results from local overloading with transfected EBAG9-GFP (Fig. 4-10B). However, although still attached to Golgi membranes due to a membrane anchor, this mutant behaved essentially as it did in GFP control cells. In agreement, EBAG9-Δ30-213-GFP also failed to cause a significant increase of the Tn- and TF-epitope (Fig. 4-12), whereas full length EBAG9 overexpression in epithelial cell lines generated cell surface deposition of Tn- and TF-glycans (Engelsberg, et al., 2003).

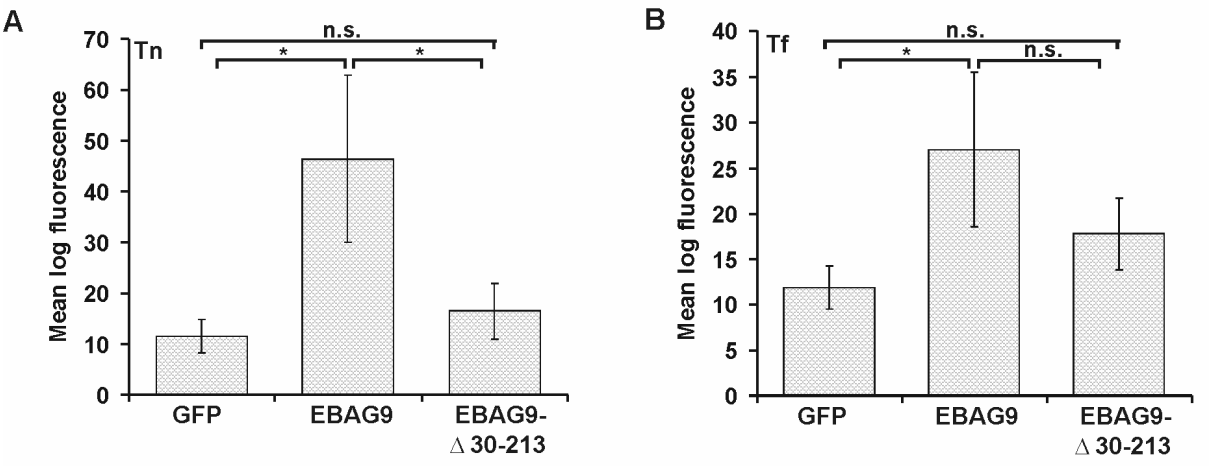

Fig. 4-12: Aberrant expression of cell surface glycans caused by EBAG9 overexpression. HEK 293 cells were transfected with EBAG9-GFP, EBAG9-Δ30-213-GFP, or GFP as a control. After 48 h cells were processed for immunofluorescence staining. Cells were incubated with primary antibodies including mouse IgM (isotype control), anti 22.1.1 Ab (A) and anti TF mAb (B) on ice. After 30 min, cells were washed and incubated with goat-anti-mouse-IgG/IgM-APC (FL4) for 30 min on ice. Cells were analysed by flow cytometry. To exclude damaged cells from evaluation, cells were costained with propidium iodide. Background staining for isotype controls was always in the same range between differently transfected cells. Tn and TF cell surface expression was significantly upregulated in EBAG9-GFP expressing cells, compared to control GFP transfected cells or truncated mutant EBAG9-Δ30-213-GFP transfected cells. Data represent the mean values ± S.D. of three independent experiments. * $p \leq 0{,}05$; Student's unpaired *t* Test.

To revisit this antibody based assay, specific lectins were applied. Lectins are proteins able to bind specifically and reversibly to mono- or oligosaccharides. Confocal microscopy demonstrated a significant accumulation of intracellular VVA^+ ($GalNAc^+$; Tn^+) stained structures. These structures were reminiscent of the ER and mostly separated from EBAG9-GFP staining (Fig. 4-13).

Similarly, EBAG9 overexpression led to expanded PNA^+ (Gal^+; Gal-β-1,3$GalNAc^+$; TF^+) glycan structures within the cell in stably transfected mamma carcinoma cells.

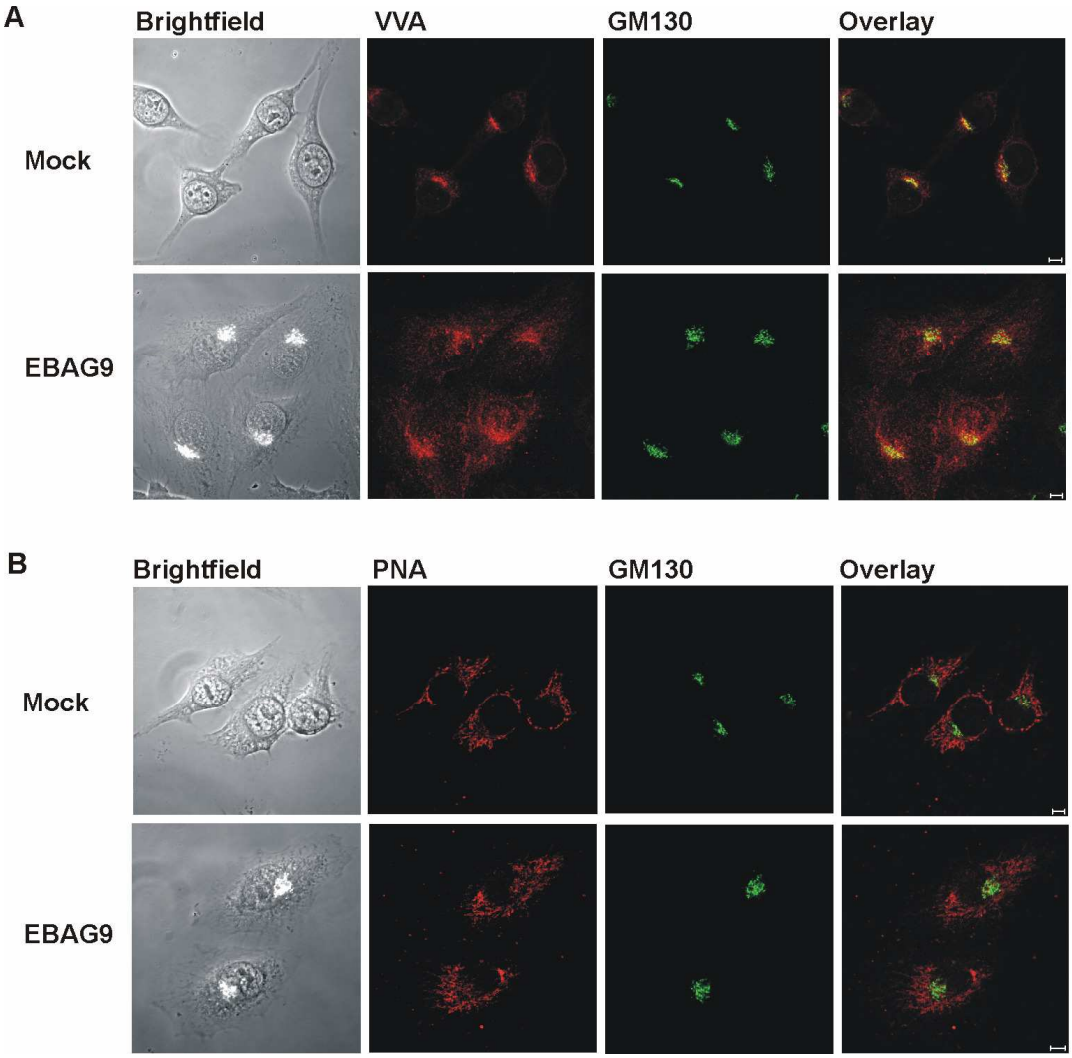

Fig. 4-13 Truncated O-glycan structures accumulate within the cell by EBAG9 overexpression. (A, B) MDA-MB435 cells stably expressing EBAG9-GFP (white) or GFP were fixed in cold acetone for 7 min, permeabilized with 0.25 % TritonX-100 and blocked with 5 % BSA for 60 min. Cells were washed in special washing medium (10 mM Hepes, pH 7,5; 0,15 M NaCl) and stained with lectins against VVA (A), PNA (B) and GM130 in special binding medium (10 mM Hepes, pH 7,5; 0,15 M NaCl; 0,08 % NaAzide; 0,1 mM $CaCl_2$; 0,01 mM $MnCl_2$). Scale bars, 5 µm.

These results suggested that EBAG9 modulates the secretory pathway in a cell-type-specific manner depending on the unique molecular composition of the cell. Furthermore, they indicated that the aberrant expression of glycans in EBAG9-overexpressing cells could be related to disturbances within the biosynthetic secretory pathway.

4.3.1.2 Transport polarity of apical and basolateral cargo is unaltered

Loss of polarity is a hallmark of tumorigenesis in epithelial cells. N-linked glycans as well as O-linked glycans have been shown to provide sorting signals for apical protein transport in polarized Madin-Darby canine kidney (MDCK) and Caco-2 cells (Benting, et al., 1999; Monlauzeur, et al., 1998). To investigate the late stages of membrane glycoprotein transport and sorting between plasma membrane domains, the MDCK cell line is a useful model system. MDCK cells exhibit the properties of a polarized transporting epithelium (Matlin and Simons, 1983). Since EBAG9 is overexpressed in several tumors of epithelial origin and induces the expression of tumor-associated glycans, the question of whether EBAG9 might influence polarized transport in MDCK cells was addressed. First, two variants of the temperature-sensitive O45 strain of vesicular stomatitis virus glycoprotein (VSVG-tsO45) coupled to GFP were used to monitor basolateral and apical transport. The apical VSVG (aVSVG) mutant travels selectively to the apical surface, whereas the basolateral VSVG (bVSVG) mutant is transported to the basolateral surface (Keller, et al., 2001). Both glycoproteins have a reversible folding defect at 39.5 °C, causing them to accumulate in the ER. Shifting to the permissive temperature of 32 °C induces rapid folding, export from the ER and delivery to the corresponding plasma membrane. If the temperature shift is combined with cycloheximide treatment to block protein biosynthesis, ER-accumulated VSVG can be chased through the secretory pathway as a synchronous wave. Polarized MDCK cells infected with EBAG9-encoding adenovirus sorted VSVG to the basolateral (Fig. 4-14A) or apical (Fig. 4-14B) membrane, but transport was strongly delayed. In control cells, most of the bVSVG was delivered to the basolateral membrane within 40 min after the temperature shift. In contrast, in EBAG9-overexpressing cells, even after 90 min the majority of bVSVG was still intracellular and only a small fraction was found at the basolateral membrane (Fig. 4-14A). To investigate the transport between Golgi and plasma membrane in more detail, cells were incubated for 90 min at 19.5 °C to accumulate aVSVG in the Golgi before chasing it at the transport permissive temperature. At 45 min, significant levels of aVSVG signals were still associated with the Golgi area. This clearly visible difference as compared to control cells was resolved after 60 min when aVSVG reached the plasma membrane at a similar rate (Fig. 4-14B).

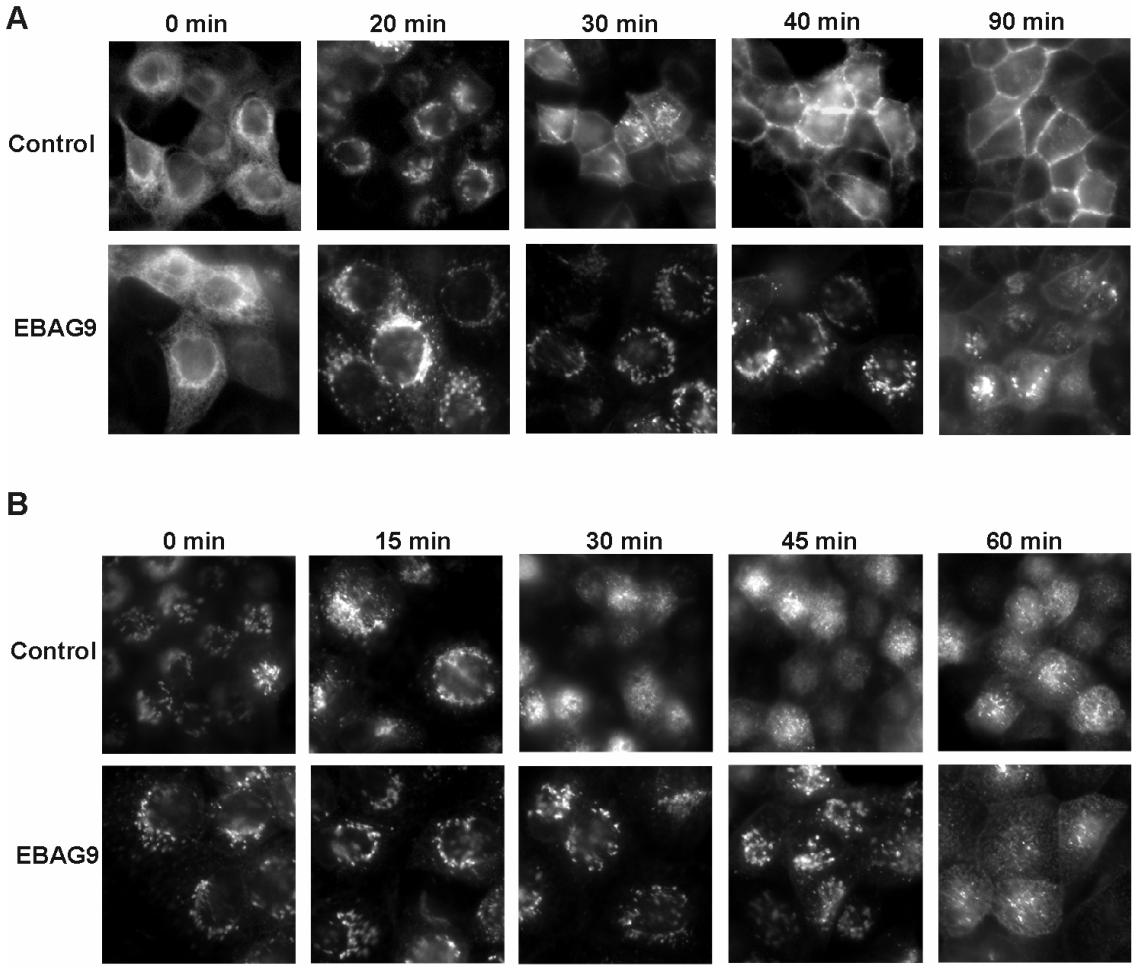

Fig. 4-14: EBAG9 delays surface transport of basolateral and apical VSVG in polarized MDCK cells. (A, B) Coverslip-grown MDCK cells expressing adenovirally-encoded EBAG9 were infected with a second adenovirus encoding GFP-tagged (A) basolateral or (B) apical VSVG-ts045. Cells were incubated at 39.5 °C to accumulate VSVG in the ER (0 min panel A) or, if further incubated for 90 min at 19.5 °C, in the Golgi (0 min panel B). Subsequently, cells were shifted to the transport-permissive temperature of 32 °C, and transport kinetics of VSVG-GFP from the ER to the basolateral (A) or from the Golgi to the apical (B) surface was followed for different time intervals. Cells were fixed in PFA, and analysed by widefield microscopy.

Additionally, a GST-coupled, glycosylated variant of rat growth hormone (rGH) that is secreted mostly from the apical membrane was investigated (Guan, et al., 1985). Here, MDCK cells were grown on filters to separately collect apical and basolateral medium containing radioactively labeled rGH. Consistent with the results above, polarized MDCK cells overexpressing EBAG9 sorted rGH correctly, but secretion was decreased (Fig. 4-15). Within an observation period of 60 min, only approximately 20 % of the rGH was secreted, 73 % of it into the apical medium, when EBAG9 was overexpressed (Fig. 4-15B). Whereas in control cells, approximately 70 % (apical and basolateral) of the rGH was secreted, 77 % of it from the apical medium (Fig. 4-15A).

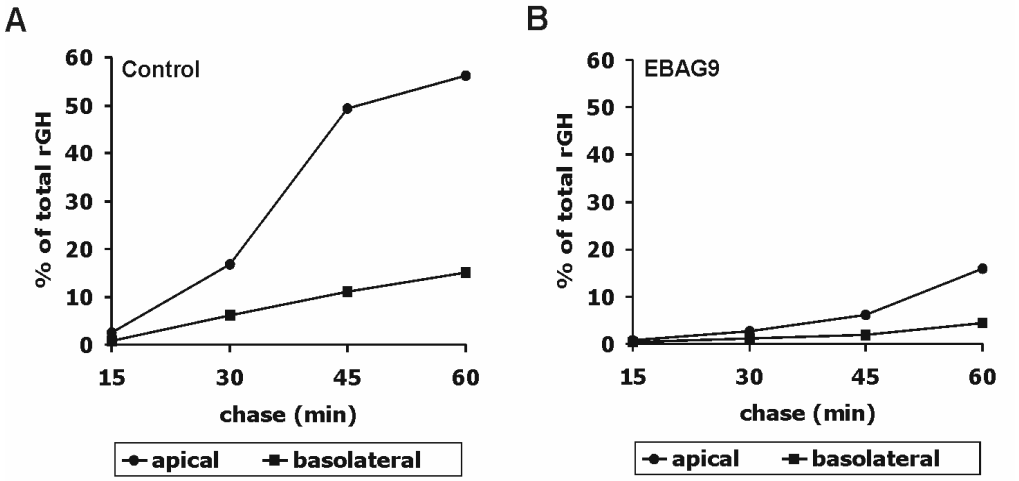

Fig. 4-15: EBAG9 decreases surface transport of rGH in polarized MDCK cells. (A, B) Filter-grown MDCK cells expressing adenovirally-encoded EBAG9 or control cells were infected with a second adenovirus encoding GST-tagged rat growth hormone (rGH). Newly synthesized protein was radiolabeled. After the time intervals indicated, apical and basolateral media as well as total cell lysates were collected, the amount of labeled rGH in all three fractions was determined by pull-down of rGH with gluthathione beads, SDS-PAGE and autoradiography. The percent transport to the apical and basolateral side is calculated and shown for control and EBAG9, respectively.

In agreement with these findings, a strong delay in ER-to-plasma-membrane transport in EBAG9-overexpressing MDCK cells was also observed for influenza hemagglutinin, another marker for biosynthetic surface transport (Fig. 4-16). When MDCK cells are infected with influenza A viruses, the spike glycoproteins are inserted predominantly in the apical cell surface, leading to virus assembly at the apical plasma membrane domain. The cell surface transport of hemagglutinin can be easily measured by a sensitive tryptic assay (Matlin and Simons, 1983; Rodriguez Boulan and Sabatini, 1978). After a chase for 60 min of infected pulse-labeled cells, the amount of hemagglutinin precursor (HA, HA_0) was diminished. Instead, the polypeptides HA_1 and HA_2 appeared (Fig. 4-16A). These are formed by a cell-dependent cleavage during transport of the precursor to the plasma membrane and remain associated by disulfide bonding. The HA_1 harbours the original amino terminus of the hemagglutinin precursor and is a peripheral membrane protein, localized on the outside of the infected cell. The HA_2 is a transmembrane polypeptide with about 11 amino acid residues exposed on the cytoplasmic membrane face. Both HA_1 and HA_2 are glycosylated (Matlin and Simons, 1983). After 60 min chase, 73,7 % of the hemagglutinin A had reached the plasma membrane in control cells, whereas in EBAG9-overexpressing cells only 7,6 % were transported to the surface (Fig. 4-16B).

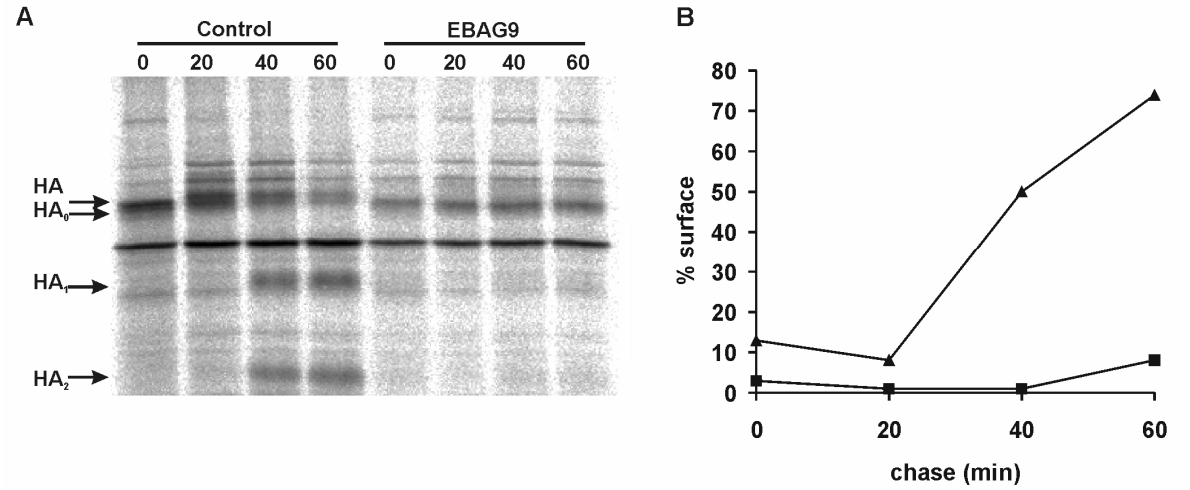

Fig. 4-16: EBAG9 overexpression blocks transport of hemagglutinin and VSVG-GFP. (A) Influenza hemagglutinin transport in filter-grown MDCK cells was assayed as described (Schuck, et al., 2007), except that trypsin was applied from both the apical and the basolateral side so that the total surface delivery of hemagglutinin was measured. HA = full-length hemagglutinin, HA_0 = unglycosylated HA, HA_1 and HA_2 = trypsin cleavage products of HA. In control cells, HA became accessible to trypsin cleavage within 40 min, whereas even after 60 min almost no HA had reached the cell surface in EBAG9-overexpressing cells, as shown by lack of HA1 and HA2 cleavage products. (B) Quantification of hemagglutinin surface transport shown in (A). EBAG9 (■), and control cells (▲).

Taken together, this provided evidence, that EBAG9 overexpression inhibits protein transport but does not influence biosynthetic sorting routes at the TGN. However, this transport block might result in a short-term alteration of cell surface protein composition caused by EBAG9 overexpression.

To analyse the kinetics of the EBAG9-imposed transport block, the refill of anterograde transported VSVG-GFP into the Golgi region after photobleaching was determined (Fig. 4-17).

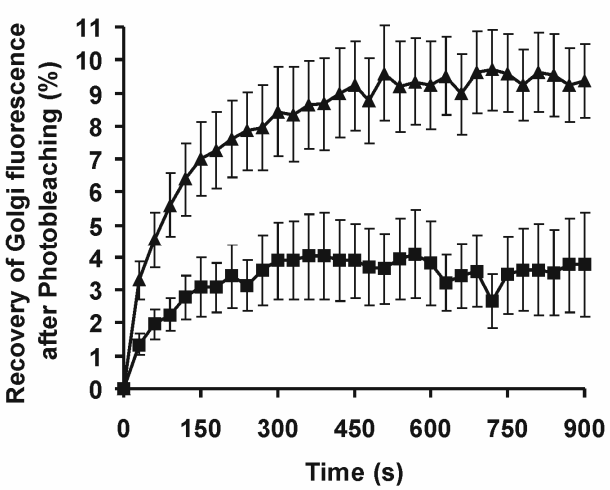

Fig. 4-17: EBAG9 overexpression inhibits transport of VSVG-GFP. COS7 cells were cotransfected with VSVG-GFP and EBAG9-DsRed2 or empty vector. After 48 h at 40 °C, 20 mM Hepes was added and cells were moved to a confocal microscope, equipped with a stage heated to 32°C. Using the 488 nm laser line at full power, selective photobleaching of GFP within the Golgi was performed and the recovery monitored by time lapse imaging at 30 s intervals at low intensity illumination. Fluorescence quantification was done using Zeiss LSM software. The recovery of VSVG-GFP Golgi fluorescence was twofold faster in control than in EBAG9 expressing cells. Data represent mean values ± SEM of a total of 6 cells from three independent experiments, *** p≤ 0,0005; Student's unpaired *t* Test. EBAG9 (■) and mock control (▲).

In accordance with previous results, VSVG transport into the Golgi area exhibited a substantially faster kinetics in control cells than in EBAG9-overexpressing cells. Here, 2.5 times less VSVG reached the Golgi within a 15 min observation period.

4.3.1.3 Anterograde transport is accelerated by EBAG9 downregulation

To analyse the physiological role of EBAG9 in epithelial cells and to confirm the observed transport block, siRNA mediated depletion of EBAG9 was applied. Efficiency of siRNA-mediated downregulation was verified in EBAG9-GFP transfected cells by loss of GFP-fluorescence intensity, which was about 50% (Fig. 4-18).

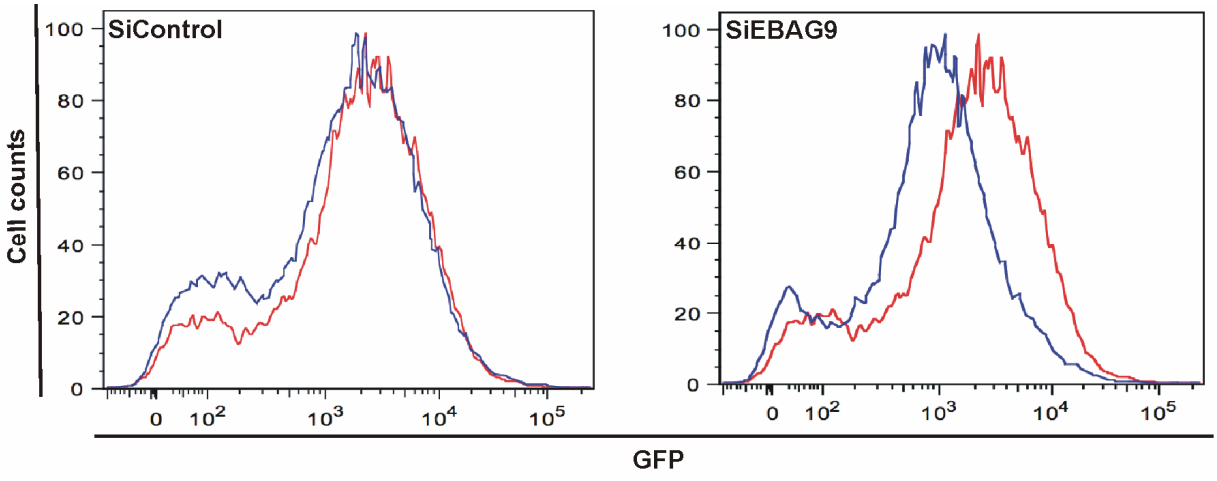

Fig. 4-18: Downregulation of overexpressed EBAG9-GFP by EBAG9 specific siRNA. MDA-MB435 cells stably transfected with EBAG9-GFP were transfected with Alexa Fluor 647 labeled siRNA against EBAG9 or Alexa Fluor 647 labeled "all star negative control" (Quiagen) using Oligofectamin (Invitrogen) according to the manufacturer's instructions. After 24 h cells were re-transfected and incubated again for 24 h. Cells were collected, washed, and levels of EBAG9-GFP expression in cells were analysed by flow cytometry on a FACSCalibur™ flow cytometer (BD Biosciences), using CellQuest analysis software. Representative graphs from the three experiments that were performed are shown. Blue curves, EBAG9-GFP (siRNA control or siRNA EBAG9 as indicated); red curves, EBAG9-GFP (isotyp control).

In addition, immunoblotting followed by densitometry analysis revealed a reduced expression of endogenous EBAG9 in HeLa cells of about 73% (Fig. 4-19).

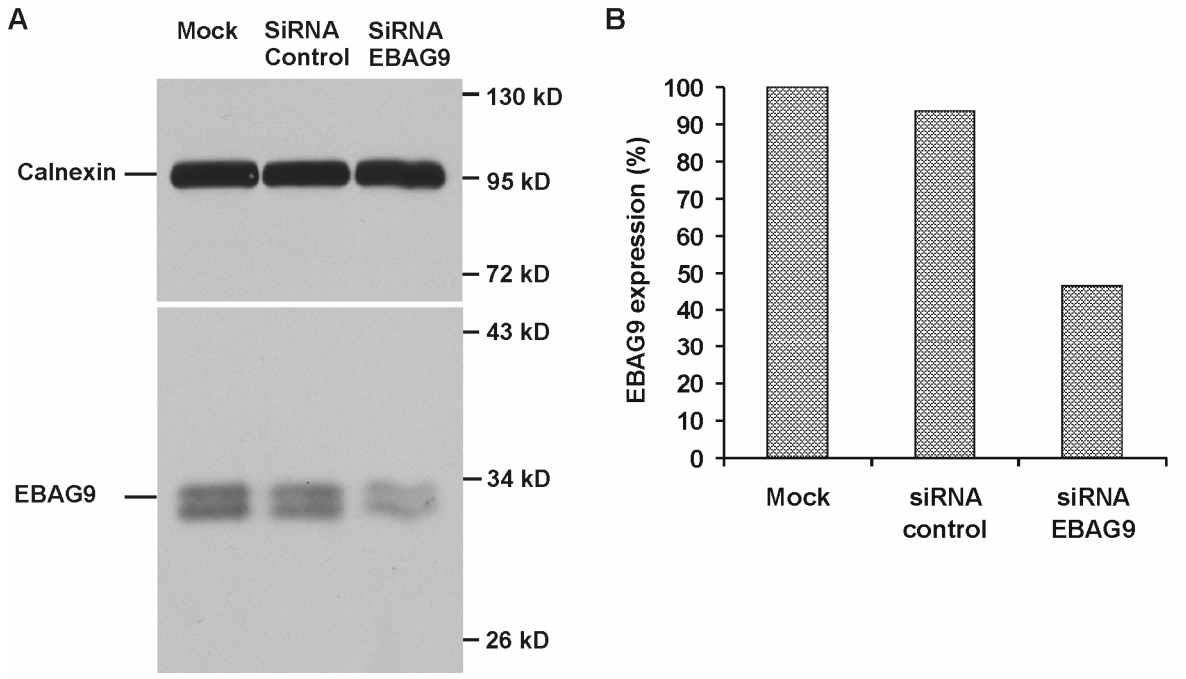

Fig. 4-19: Downregulation of endogenous EBAG9 by EBAG9 specific siRNA. (A) HeLa cells were transfected with siRNA EBAG9-Alexa Fluor 647, siRNA Control-Alexa Fluor 647 and mock control as described in Fig. 4-18. Cells were lysed for 30 min at 4°C. Lysates were spun to deplete nuclei and insoluble material, and 100 µg of each probe was resolved by SDS-PAGE and analysed by immunoblotting using rabbit-anti-EBAG9 serum or rabbit-anti-Calnexin. Protein bands were quantified by densitometric scanning and are shown in (B).

Next, it was tested whether the delivery of VSVG-GFP to the plasma membrane (PM) might be accelerated in EBAG9-specific siRNA treated MDA-MB435 cells. After release of the temperature block, VSVG was chased until all cargo had reached the Golgi (10 min), followed by emergence of cargo carriers at the PM (30 min). At 30 min, more VSVG containing vesicles moving towards the plasma membrane could be seen in siRNA EBAG9 transfected cells than in control cells (Fig. 4-20A). To quantitatively measure the kinetics of Golgi transition, the ratio of fluorescence intensity in the Golgi versus the whole cell was determined at 30 min (Fig. 4-20B; chapter 3.3.11). This was consistent with the assumption that VSVG was transported through the Golgi significantly faster in EBAG9 siRNA treated than control cells.

Additionally, effectiveness of VSVG delivery to the plasma membrane was determined by using an antibody against an extracellular epitope of VSVG. The percentage of cells with VSVG on the plasma membrane at 30 min was quantified after the shift to 32 °C (Fig. 4-21).

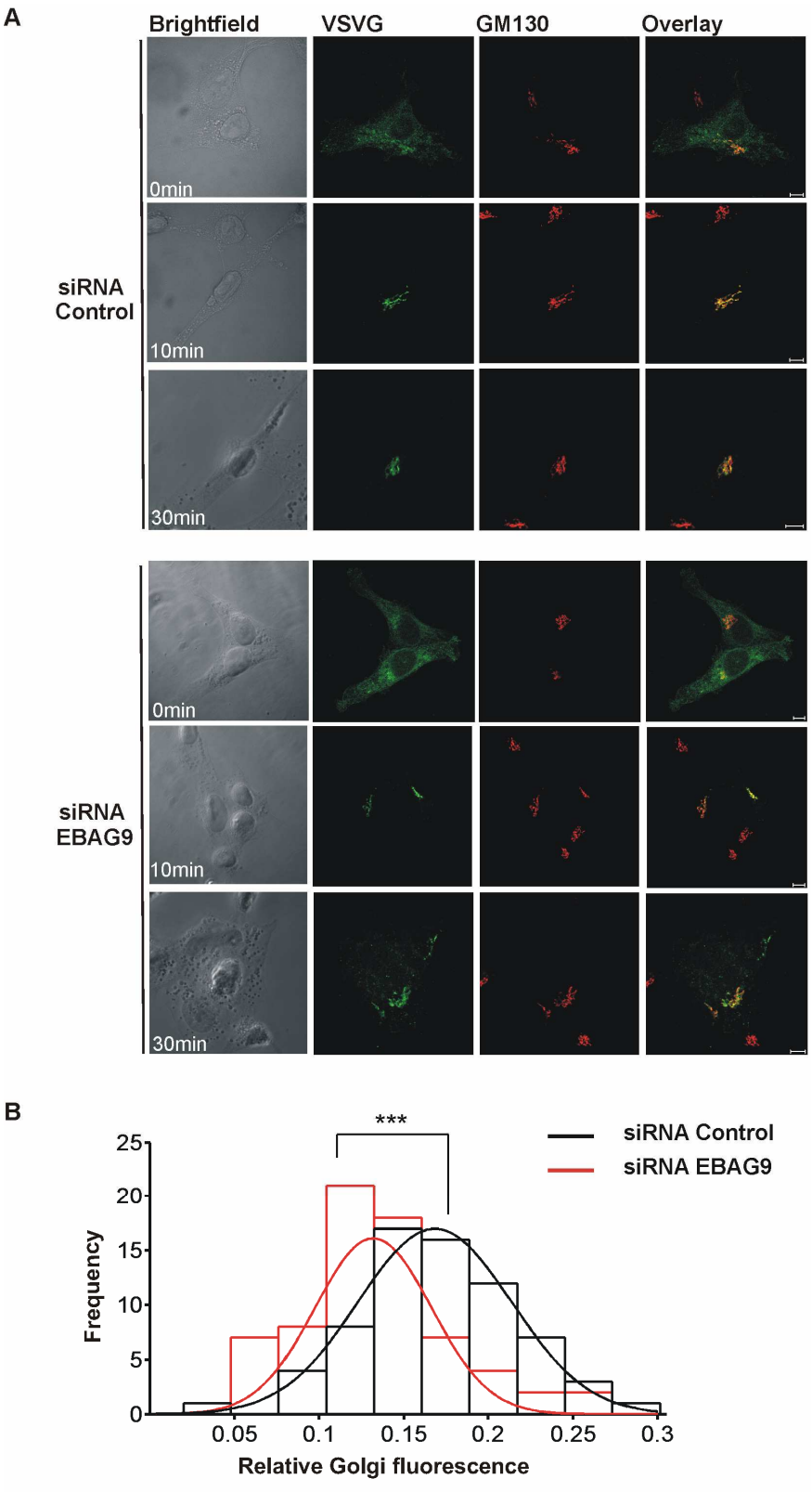

Fig. 4-20: VSVG transport is accelerated by EBAG9 downregulation. (A) MDA-MB435 cells were transfected with fluorescently labeled siRNA and incubated at 37 °C. After 24 h cells were re- and co-transfected with siRNA and GFP-tagged VSVG-ts045 (green) for 5 h and finally incubated at 39.5 °C to accumulate VSVG in the ER (0 min). After 48 h siRNA expression, 100 µg/µl cycloheximide was added and cells were shifted to 32 °C for up to 30 min to allow ER export and subsequent transport beyond the Golgi. Cells were fixed in PFA, permeabilized and stained with an antibody against GM130 (red) and analysed by widefield microscopy. (B) Shown is the number of cells (frequency) for each group of Golgi versus total cell fluorescence (Relative Golgi fluorescence). Data are means ± S.D. 60 cells each of two independent experiments; ***p≤ 0,0005; Student's unpaired *t* test; Scale bars, 5 µm.

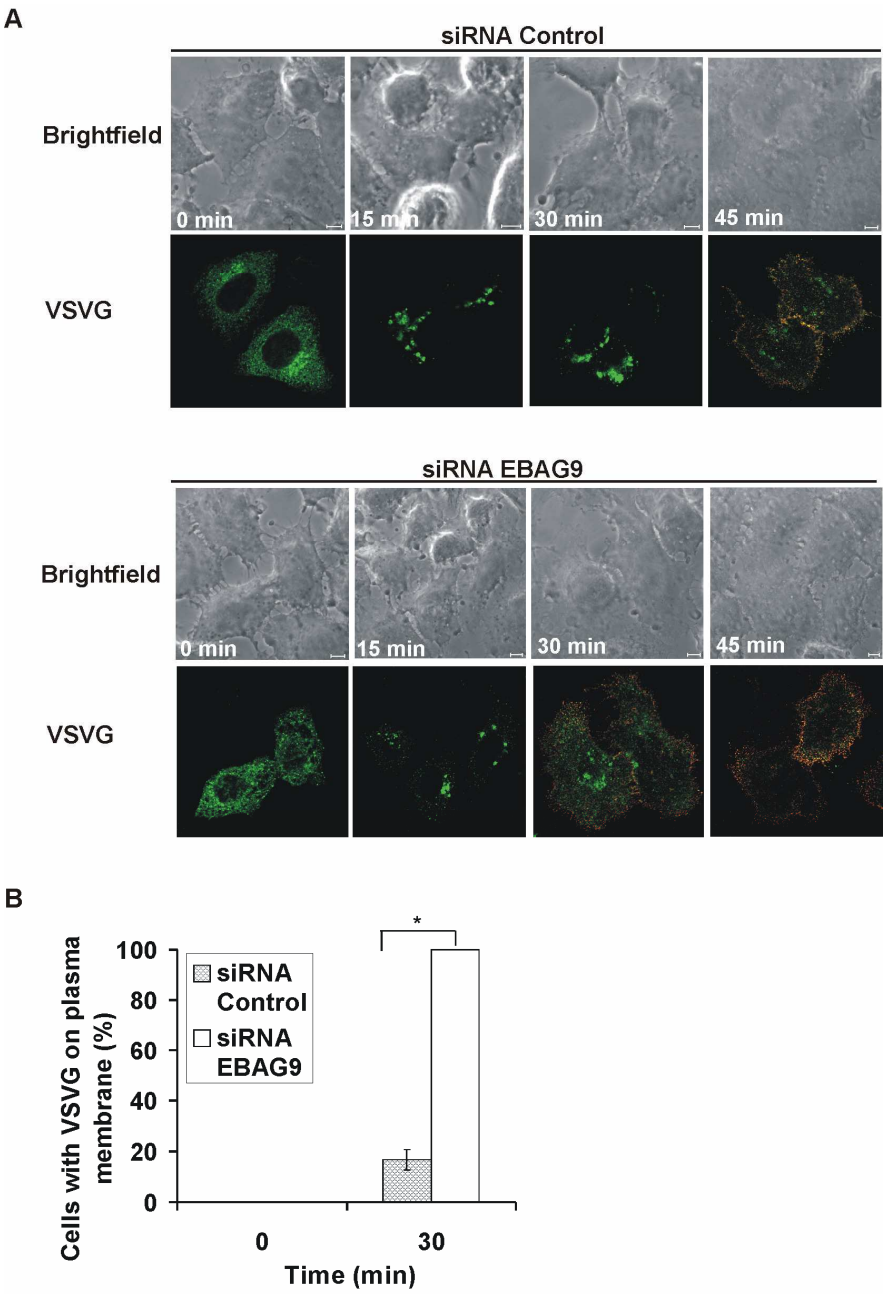

Fig. 4-21: Surface transport of VSVG is accelerated in EBAG9 depleted cells. (A) Hela cells were transfected with fluorescently labeled siRNA and 24 h later co-transfected with siRNA and GFP-tagged VSVG-ts045 (green) for 4 h. Then, cells were shifted to 39.5 °C to accumulate VSVG in the ER (0 min). After 48 h, 50 µg/µl cycloheximide was added and cells were shifted to 32 °C for up to 45 min to allow ER to Golgi transport (15 min), and subsequent transport beyond the Golgi (30 min). Cells were placed on ice at the times indicated, stained with anti-VSVG antibody (TKG) directed against an extracellular epitope of VSVG to label VSVG protein at the cell surface (red), fixed and followed by widefield microscopy analysis. (B) Quantification of cells chased for 30 min. Shown is the percentage of cells with VSVG surface staining. Data are means ± S.D. from n = 18 or 12 cells in each group (n = two independent experiments), *p≤0,05; Student's unpaired *t* test; Scale bars, 5 µm.

In cells treated with siRNA EBAG9, essentially all cells expressed VSVG on the plasma membrane within 30 min. In contrast, only 16,7 % of control cells showed cell-surface deposited VSVG at 30 min. In control cells, it took even 45 min till all VSVG molecules had reached the plasma membrane (Fig. 4-21). Thus, it can be concluded that EBAG9 impairs the secretory pathway in a cell-type-specific and dose-dependent manner.

4.3.2 EBAG9 inhibits the biosynthetic transport at a step between the IC and medial-Golgi

4.3.2.1 EBAG9 affects transport of a membrane glycoprotein at a pre-medial Golgi step

To further localize the EBAG9-imposed transport block in epithelial cells, the sensitivity of major histocompatibility complex (MHC) class I antigen to Endoglycosidase H (EndoH) digestion was examined (Fig. 4-22).

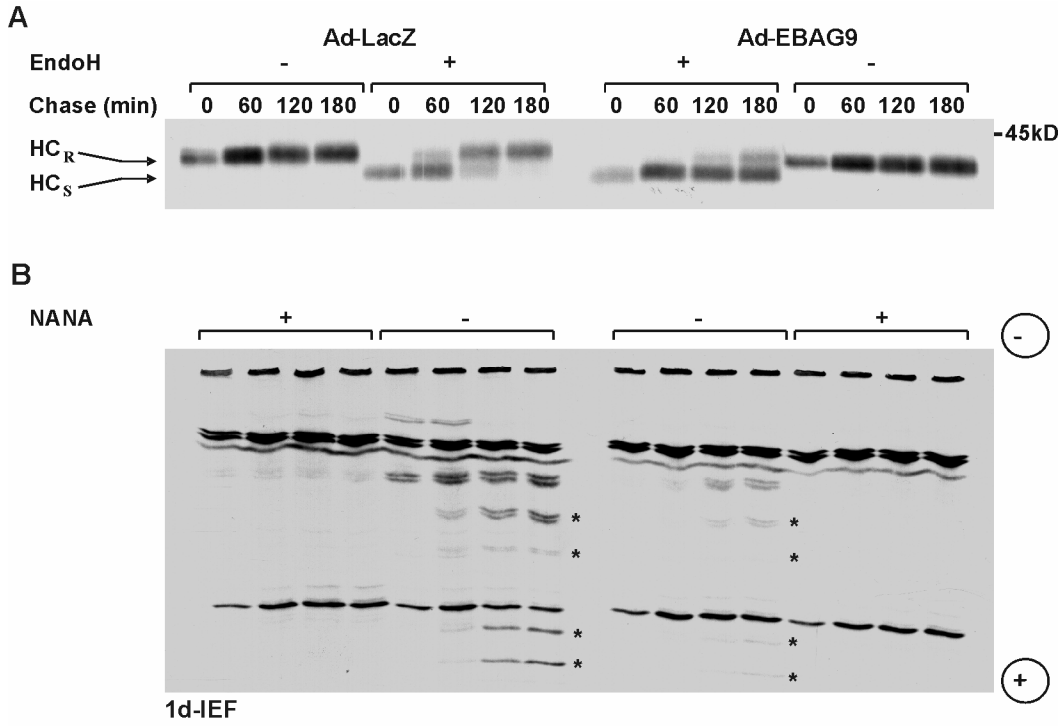

Fig. 4-22: MHC class I transport is inhibited in a pre-medial Golgi compartment by EBAG9 overexpression. (A) HeLa cells were infected with EBAG9- or LacZ-encoding adenovirus (MOI 5-20) for 14-16 h. Cells were labeled with [^{35}S]-methionine/cysteine for 10 min at 37 °C, followed by a chase at 19.5 °C for the times indicated. MHC class I was immunoprecipitated from NP-40 lysates with W6/32 antibody which recognizes properly folded MHC class I complexes, samples were treated (+/-) with EndoH and analysed by SDS-PAGE. HC_R = Endo H resistant heavy chain, HC_S = Endo H sensitive heavy chain. Light chain, β_2m, was omitted from the gel. (B) An aliquot of the immunoprecipitates was subjected to neuraminidase treatment or was mock treated (NANA), followed by 1-d isoelectric focusing gel analysis (*sialylated forms).

HeLa cells were transduced with EBAG9- or β-galactosidase encoding adenovirus, followed by metabolic labelling for 10 min, and chased up to 180 min at 19.5 °C. At 19.5 °C, transport processes within the Golgi are significantly delayed and allow a higher resolution of glycan-modifying enzyme activities. MHC class I molecules were recovered from cell lysates using the W6/32 antibody. Immunoprecipitates were split, and aliquots were treated with EndoH or

neuraminidase, followed by SDS-PAGE (Fig. 4-22A) and 1d-isoelectric focusing gel (1d-IEF) analysis (Fig. 4-22B). In control cells, the acquisition of EndoH resistance was detected after 60 min and finally, after 180 min all molecules had passed the medial Golgi. In EBAG9 transduced HeLa cells Endo H resistant forms were not detected until 120 min. Even after 180 min only 1/3 of MHC class I molecules had acquired Endo H resistance and substantial amounts of EndoH-sensitive heavy chains persisted (Fig. 4-22A). This suggested that the EBAG9-imposed transport block must occur before the medial Golgi. In contrast, the addition of sialic acids occurs within the trans-Golgi and leads to a negative charge shift. This can be visualized by treatment of the samples with neuraminidase (NANA), since the enzyme cleaves sialic acids of branched glycans. In agreement with a transport block at a level prior to the medial Golgi, 1-d isoelectric focusing gel analysis revealed a transfer of sialic acids in Ad-EBAG9 transduced cells only at 120 and 180 min of chase (indicated by * Fig. 4-22B).

In summary, it can be inferred that MHC class I molecules that pass the EBAG9-induced transport block in a pre-medial Golgi compartment finally undergo sialylation in the trans-Golgi compartment.

4.3.2.2 The delivery of anterograde cargo from the ER to the IC is not delayed by EBAG9

To address whether the ER exit of cargo protein is already disturbed by EBAG9 overexpression, a transport assay with VSVG-GFP on a short time scale was performed. Transiently transfected COS7 cells were rapidly shifted from 40 °C to 32 °C for 3 min to allow release of newly folded VSVG from ER exit sites. After 3 min, VSVG was already clearly separated from Sec23 positive vesicles in all cells. Thus in EBAG9-overexpressing cells, cargo loading and the budding and scission of VSVG-containing COPII vesicles had occurred in a proper sequence (Fig. 4-23A, B top row). Additionally, a partial overlap of VSVG with γCOPI and ERGIC-53 was observed in most cells. This pointed toward an accurately accomplished coat switch between COPII and COPI carriers. VSVG entered the IC at a similar rate in all cells. However, VSVG-containing transport intermediates often appeared densely clustered in the presence of EBAG9, whereas in control cells smaller vesicles predominated (Fig. 4-23A, B row 2, 3).

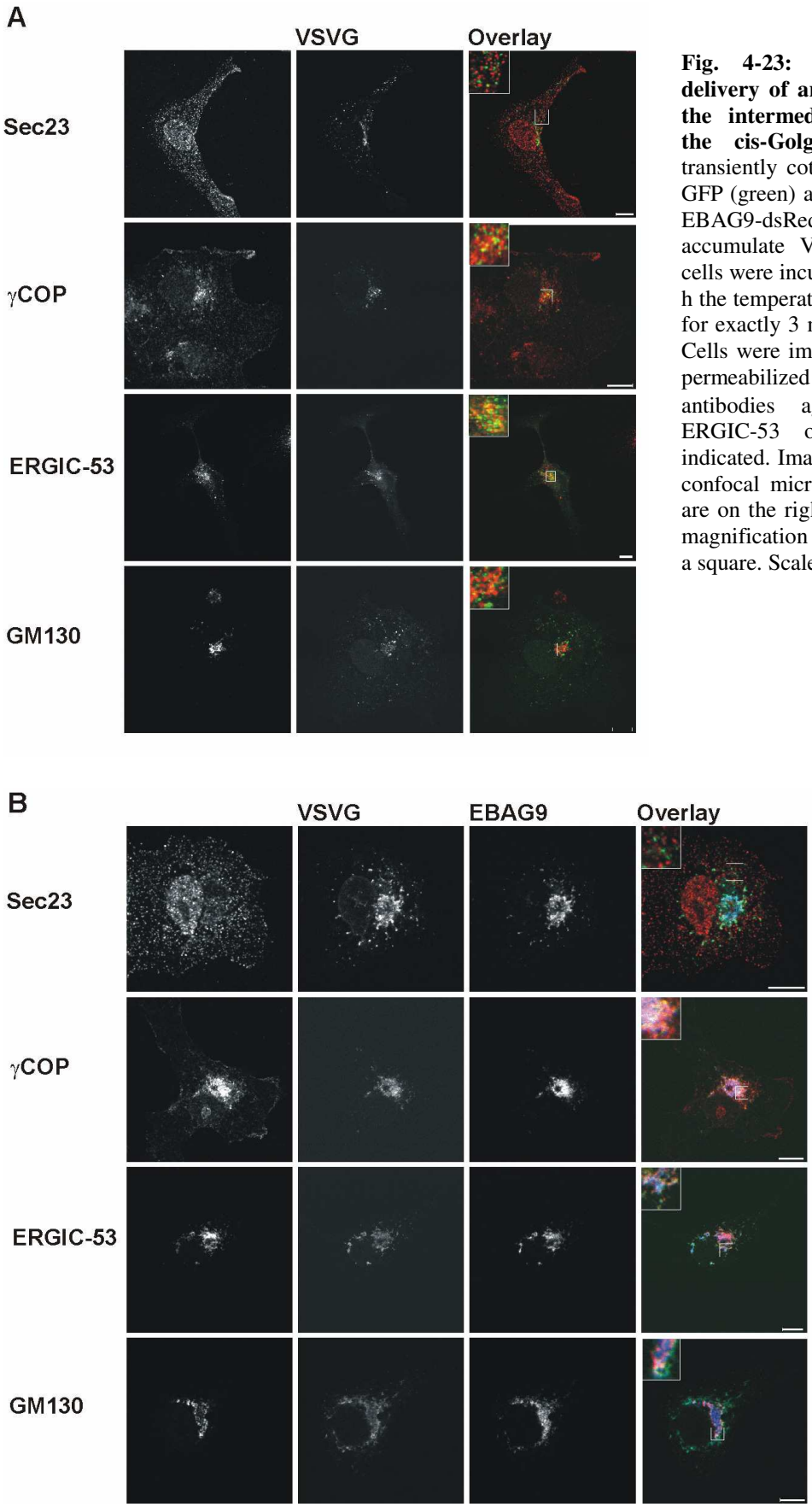

Fig. 4-23: EBAG9 targets the delivery of anterograde cargo from the intermediate compartment to the cis-Golgi. COS7 cells were transiently cotransfected with VSVG-GFP (green) and empty vector (A), or EBAG9-dsRed (blue) (B). To accumulate VSVG-GFP in the ER, cells were incubated at 40 °C. After 24 h the temperature was shifted to 32 °C for exactly 3 min to release the cargo. Cells were immediately fixed in PFA, permeabilized and stained with antibodies against Sec23, γCOP, ERGIC-53 or GM130 (red), as indicated. Images were acquired using confocal microscopy. Merged images are on the right. Insets show a higher magnification of the area indicated by a square. Scale bars, 10 µm.

These structures resemble pleiomorphic tubulovesicular ER-to-Golgi carriers (EGCs) (Marra, et al., 2007; Polishchuk, et al., 2009; Presley, et al., 1997), which appeared significantly expanded in EBAG9-overexpressing cells compared to controls.

In agreement with these results, EBAG9 overexpression itself had no effect on the recruitment of εCOP-YFP onto Golgi membranes, as shown by FRAP analysis of double transfected MDA-MB435 cell lines (Fig. 4-24).

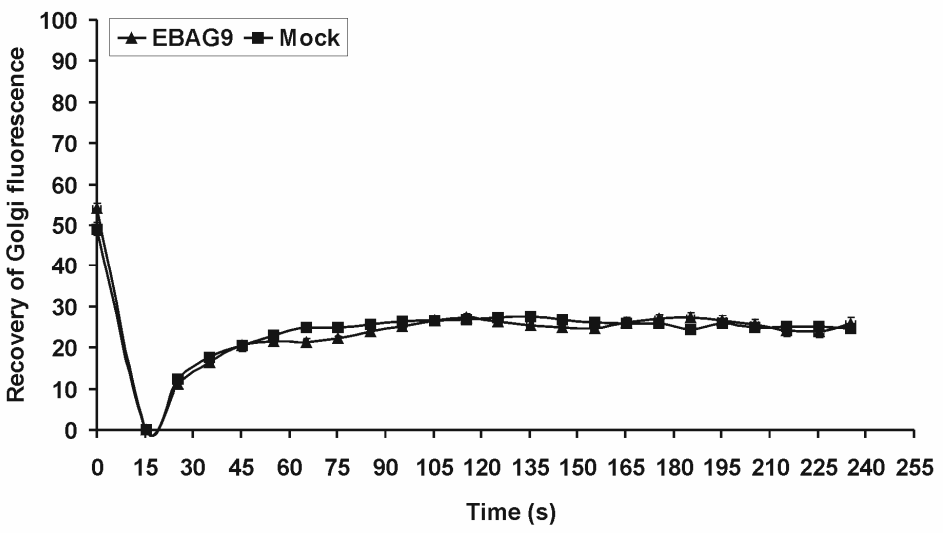

Fig. 4-24: Recruitment of coatomer subunits to Golgi membranes remains unaltered in the presence of EBAG9. MDA-MB435 cells stably expressing εCOPI-YFP were transfected with EBAG9-DsRed2 or empty vector. After 24 h cells were imaged in Hepes buffered medium with a confocal microscope, equipped with a stage heated to 37 °C. Excitation of YFP was done with a 514 nm laser excitation wavelength, and 543 nm excitation wavelength was used for DsRed2. Selective photobleaching of YFP within the Golgi was performed using the appropriate laser line at full power. Recovery was then monitored by time lapse imaging at 15 s intervals at low intensity illumination. Fluorescence quantification was done using Zeiss LSM software. Data represent mean values ± SEM of a total of 26 cells from three independent experiments.

Here, the εCOP-YFP fluorescence signal within the Golgi region was selectively bleached and recovery was measured over time in EBAG9 or control transfected cells. However, this assay measures only the recruitment of cytoplasmic coatomer components, but not the fusion of COPI coated carriers with target membranes.

Taken together, the results suggested that EBAG9 is present on COPI-coated carriers that transport VSVG beyond the intermediate compartment without any delay.

4.3.2.3 Priming and docking of vesicles is undisturbed by EBAG9

According to Ruder et al. (2005) and confirmed by the EBAG9-imposed inhibition of hGH secretion in neuroendocrine PC12 cells, EBAG9 also delays regulated secretion. Most recent literature has shown that COPI components are involved in the maintenance of endosomal/lysosomal sorting (Razi, et al., 2009). Hence, another system of regulated cytotoxic secretion, the response of cytotoxic T-cells (CTL), was investigated to gain more mechanistic insight into EBAG9 function.

Ruder et al. (2009) demonstrated in EBAG9 KO mice that the loss of EBAG9 confers an enhanced cytolytic capacity on CTLs. The transfer of cytolytic agents from secretory lysosomes in CTLs is critically dependent on the cell's capacity to form a so-called immunological synapse. The immunological synapse is a stable region of contact between a T cell and an antigen-presenting cell that forms through cell–cell interactions of adhesion molecules. The mature immunological synapse contains two distinct, stable membrane domains: a central cluster of TCRs, known as the central supramolecular activation cluster (cSMAC), and a surrounding ring of adhesion molecules known as the peripheral supramolecular activation cluster (pSMAC). In turn, this polarization of the T cell allows effector molecules to be focused directly toward the antigen-bearing target cell (Montoya, et al., 2002; Reichardt, et al., 2007). To address a potential influence of EBAG9 on the formation of the immunological synapse, an immunofluorescence staining of CTLs conjugated with anti-CD3/CD28-conjugate microbeads was performed. These beads engage the T cell receptor and induce the regulated secretion of lytic granule content. A simultaneous detection of lytic granule reorientation and localization of the signalling zone molecule Lck was performed. CTLs were allowed to form conjugates with anti-CD3/CD28 mAb-coated microbeads, which acted as surrogate APCs, for 15 min, followed by anti-granzyme B and anti-Lck staining. Synapse formation for bead-conjugated T cells was assessed by the reorientation of both markers. Clusters of coalesced Granzyme B-stained lytic granules could be identified exclusively in conjugated T cells, surrounded by Lck staining (Fig. 4-25B). This pattern differed markedly from unconjugated, nonpolarized T cells in which granules were scattered at the cell periphery (Fig. 4-25A). Consistent with the short duration of conjugate formation, in rare cases conjugated T cells contained single, nonpolarized lytic granules.

Among the conjugates analysed (n = 10 for each group), similar numbers of granules in Wt and KO CTLs showed a tight polarization of the majority of granules at the synapse.

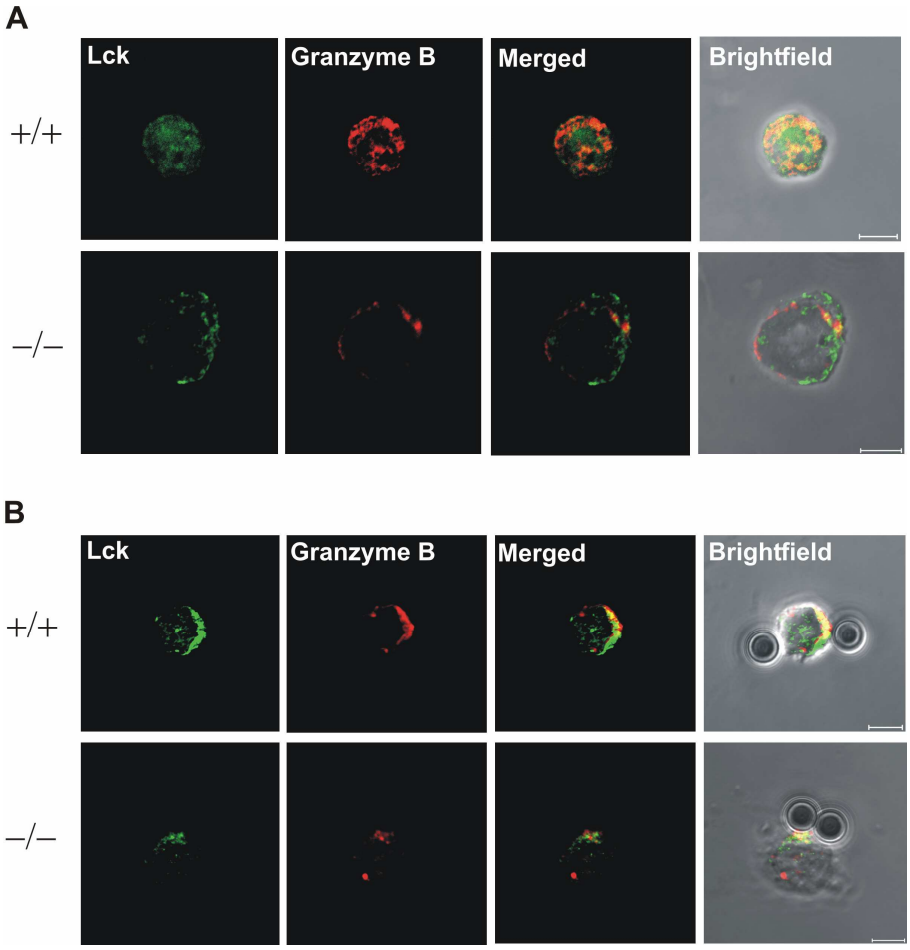

Fig. 4-25: Immunological synapse formation is indistinguishable between Wt and EBAG9-/- CTLs. CTLs from EBAG9 Wt and KO mice were generated and purified as described in methods. CTLs were mixed in a 1:1 ratio with CD3/CD28 precoated Dynabeads, centrifuged for 5 min, and incubated for another 5 min at 37 °C. Conjugates were plated on poly-L-lysine coated coverslips, and incubated for additional 15 min before fixation with PFA and permeabilization. Granules were visualized by intracellular staining with the secretory lysosome marker Granzyme B-Alexa Fluor 647 (reassigned to red), and the signaling zone molecule Lck (green). Representative images are shown. At the 15 min time point, unconjugated T cells could be easily identified and exhibited a scattered, non-polarized distribution of lytic granules at the cell periphery (A). In T cells conjugated with microbeads, in both genotypes a clearly visible focusing of lytic granules toward the T cell-microbead interface occurred. In this polarized cluster of granules, substantial accumulation of Lck-positive structures was visible (B, Merged images). Data are representative of one experiment with CTLs from n = 3 animals per genotype, with at least 20 conjugates analysed. Polarization was identified in 6 synapses per group. Bar 5µm.

These data indicate that EBAG9 is not involved in the secretion process at the plasma membrane itself, but rather acts upstream through regulation of trafficking steps toward the maturation of secretory lysosomes.

In addition, the redistribution of EBAG9-GFP upon the formation of the immunological synapse was investigated (Fig. 4-26). Granule polarization to the contact site between T cell

and CD3/CD28-coated microbeads was assessed by anti-cathepsin D staining. Whereas in nonpolarized CTLs cathepsin D-positive organelles were distributed clearly separately from the perinuclear staining pattern of EBAG9-GFP, upon polarization EBAG9-GFP was relocated towards the synapse. The EBAG9-GFP-positive organelles surrounded the cathepsin D-containing granules, but a fusion between both compartments was rarely seen (Pearson's correlation coefficient r = -0.10 ± 0.18).

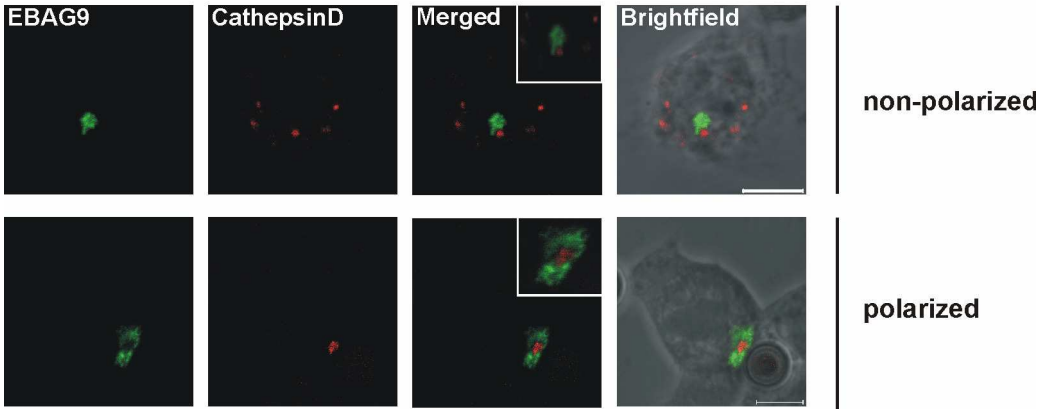

Fig. 4-26: EBAG9 moves to the immunological synapse upon polarized stimulation of CTLs. CTLs were generated and transfected with EBAG9-GFP (green) as described in Methods. CTLs were mixed with CD3/CD28-precoated Dynabeads, incubated for 5 min at 37 °C, plated on coverslips, and incubated for another 30 min before fixation and permeabilization. Lytic granules were stained with anti-cathepsin D antibody (red). Representative images of non-conjugated and non-polarized T cells are shown in the top row. Polarized T cells with conjugated beads is shown below. Data are from one experiment with CTLs from n = 3 animals. At least 20 conjugates were analysed (r =-0.10 ± 0,18). Scale bars: 5 µm. Insets have additional magnifications of 2- to 3-fold.

Taken together, this provides evidence that EBAG9 is not involved in priming and docking of vesicles before fusion and release. Therefore the underlying cause must lie within a process further upstream, either within the Golgi or the endosomal transport.

4.4 Lack of tumor-promoting effect of EBAG9 in immunodeficient mice

To investigate a putative role of EBAG9 overexpression in tumor pathogenesis in further detail, the influence of EBAG9 on *in vivo* tumor growth of mamma carcinoma cells in severe combined immunodeficiency (SCID) mice was analysed. In this T- and B-lymphocyte deficient model, no significant difference in tumor growth kinetics between control and MDA-MB435-EBAG9-overexpressing tumor cells was seen until day 35. However, at later time points, MDA-MB435-EBAG9 tumor growth was significantly delayed compared to

control tumors (Fig. 4-27). These data were in accordance with the cell biological data on a disturbed biosynthetic transport pathway.

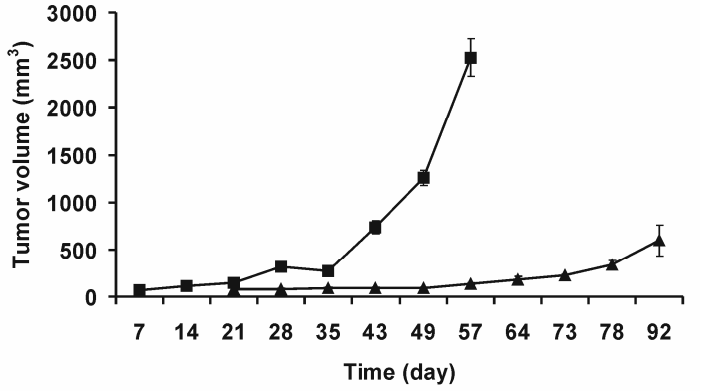

Fig. 4-27: EBAG9 delays tumor growth in SCID mice. B6.CB17-Prkdc^{scid} /SzJ homozygous mice were temporarily anesthetized and 2x10^6 MDA-MB435 cells, stably transfected with GFP or EBAG9-GFP, in 100µl PBS injected into the mammary fat pad. EBAG9-overexpressing tumors grew much slower than control tumors. One representative experiment out of two experiments that were performed. Data are mean tumor volumes ± SEM from n = 8 animals per group. Control (■) and EBAG9 (▲).

4.5 EBAG9 targets selectively COPI-dependent ER-to-Golgi transport

The data obtained thus far in epithelial cells suggested an inhibitory role of EBAG9 in a COPI-dependent, ER-to-Golgi trafficking route. However, since the anterograde and retrograde transport route are closely connected, Golgi-to-ER transport was investigated as well. Trafficking and distribution of KDELr is recognized as a function of a COPI-dependent retrograde trafficking route.

4.5.1 KDEL-receptor redistributes towards the ER

EBAG9-GFP or GFP transiently transfected HeLa cells were incubated for various times at 15 °C. At this temperature, protein is expected to accumulate in the intermediate compartment (Hauri, et al., 2000) and thus also in the ER (Luna, et al., 2002) permitting an investigation of retrograde transport only. Cells were fixed and the kinetics of Golgi to ER/IC transport of KDELr were monitored by immunofluorescence staining with antibodies against KDELr and the ER marker Calnexin (Fig. 4-28).

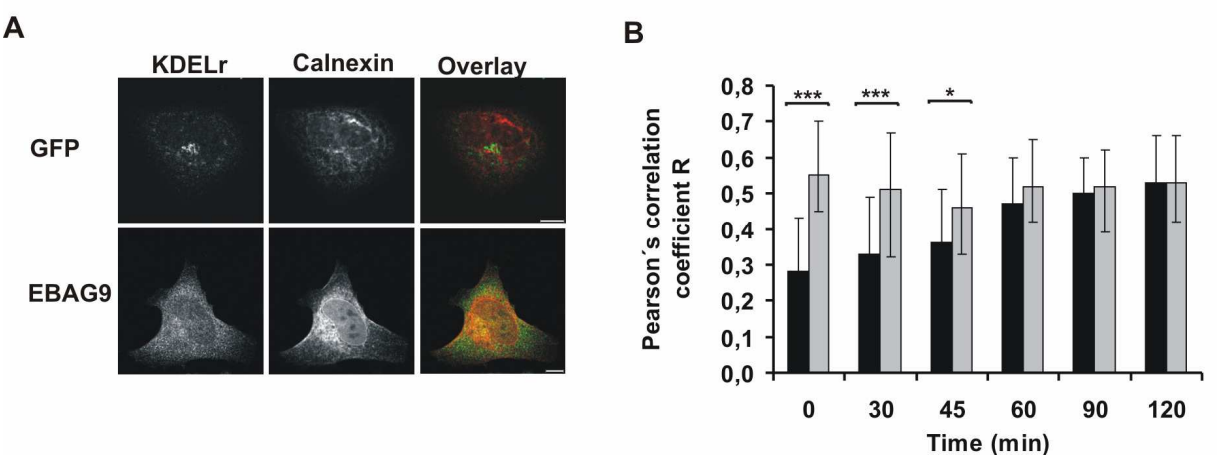

Fig. 4-28: EBAG9 shifts the steady-state distribution of KDELr towards the ER. (A, B) HeLa cells were transiently transfected with EBAG9-GFP or GFP. After 24 h, cells were chased at 15 °C for the times indicated, fixed in PFA, permeabilized and stained with antibodies against KDELr (green) and Calnexin (red). (B) Kinetics of retrograde transport via COPI vesicles was assessed by determining the Pearson`s correlation coefficient of KDELr and Calnexin. Data represent the mean values ± S.D. of 30 cells from three independent experiments. Black bars, GFP control; grey bars, EBAG9-GFP. The steady-state level of KDELr in the ER was significantly higher in EBAG9 expressing than in control cells. ***p≤ 0,0005; **p≤ 0,05; Student's unpaired *t* Test. Scale bars, 10 µm.

As expected, KDELr distribution in control cells changed from a predominant Golgi steady-state distribution (0 min) to a peripheral punctuate staining pattern after a 2 h incubation at 15 °C. In contrast, in EBAG9-overexpressing cells the steady-state distribution of KDELr was already found to be redistributed into punctuate peripheral structures at 0 min (Fig. 4-28 A). The Pearson's correlation coefficient (R) of KDELr and Calnexin was calculated for different time points for each cell analysed. This quantitative evaluation revealed increasing R values over time in control cells (R = 0.28 at 0 min to R = 0.53 at 120 min), indicating a slow accumulation of KDELr in the ER (Fig. 4-28 B), as expected. However, in EBAG9-overexpressing cells high R values (R = 0.55) at the steady-state level at 0 min pointed towards the presence of significant quantities of KDELr in the ER at the beginning of the chase. No further increase of ER colocalization was observed, thus precluding an acceleration of the retrograde trafficking route. Therefore it could be concluded that KDELr distribution is affected by an EBAG9-induced disturbance of the anterograde transport between ER and Golgi, rather than by enhanced retrograde transport.

Additionally, EBAG9 exhibited a compact perinuclear localization corresponding to the Golgi apparatus with some surrounding vesicular structures at 0 min (Fig. 4-29). After a temperature switch (120 min) to 15 °C, the localization of EBAG9 changed to an intensely dotted Golgi-peripheral labeling, pointing towards a redistribution to the IC. Under these conditions,

proteins that normally recycle between the ER, IC and the Golgi, such as ERGIC or the KDELr, accumulate in the IC. These results supported the view that EBAG9 shuttles between the ER and the Golgi.

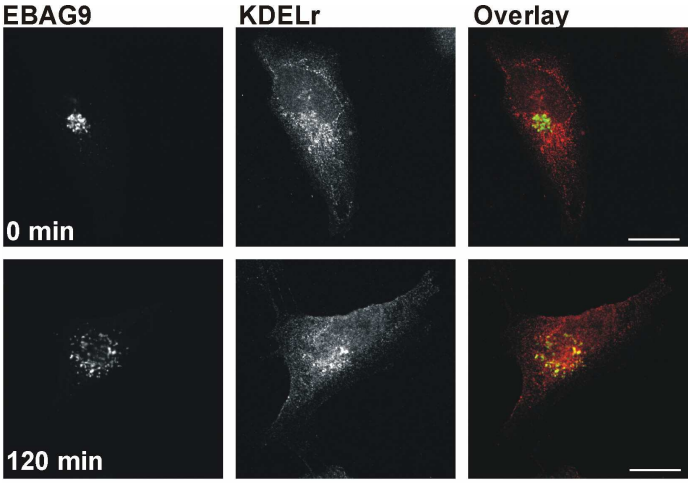

Fig. 4-29: EBAG9 redistributes towards the IC at 15°C. HeLa cells were transiently transfected with EBAG9-GFP. After 24 h, cells were incubated at 15 °C for the indicated times, fixed and stained for KDELr. Merged images are shown on the right, EBAG9 (green) and KDELr (red). Scale bars, 10 µm.

4.5.2 Retrograde transport of Shiga-toxin B subunit is not disturbed

To substantiate the specificity and topology of this block, a second retrograde transport route was analysed. Transport of Shiga toxin B-fragment (STB), which enters the cell through clathrin-independent endocytosis, was shown to reach the ER via a Rab6-dependent pathway that appears to be separate from those employed by classic recycling markers, such as the KDELr and COPI coated carriers (Girod, et al., 1999; Johannes, 2002). Using confocal microscopy and colocalization analysis, kinetics of retrograde transport of STB was found to be similar in EBAG9 expressing and control cells (Fig. 4-30). In control as well as in EBAG9-overexpressing cells vesicles, containing STB, had entered the cell within 20 min. Then, after 60 min STB had reached the Golgi, colocalizing with cis-Golgi marker GM130. After 90 min, the toxin had been transported to the IC as indicated by the colocalization with ERGIC-53. Finally, at 180 min, STB distributed in a ER like pattern (Calnexin^{+}). Thus, EBAG9 overexpression does not affect a COPI-independent retrograde transport route.

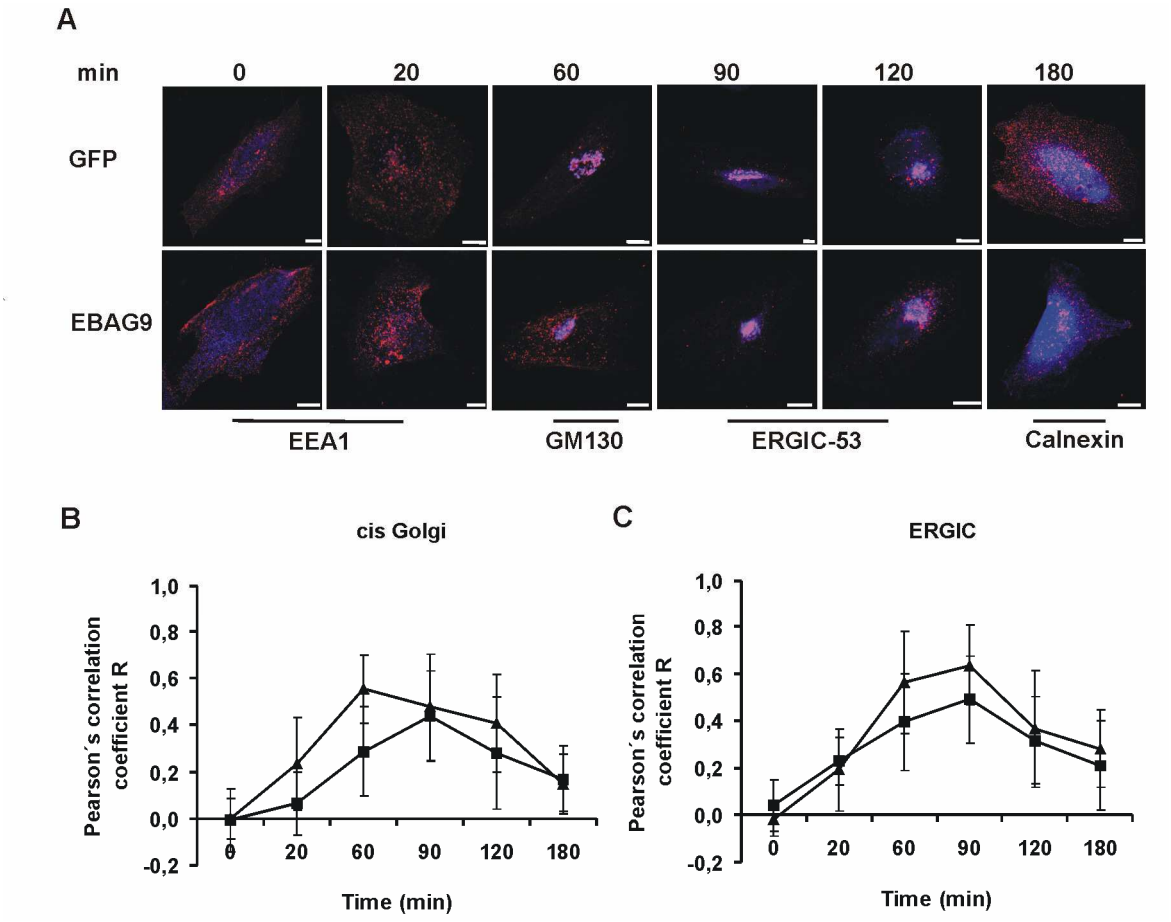

Fig. 4-30: EBAG9 does not affect retrograde transport of Shiga-toxin B fragment. (A - C) HeLa cells were transiently transfected with EBAG9-GFP (■) or GFP (▲). After 24 h, cells were incubated with cy3-coupled Shiga-toxin B-fragment (STB) (red) for 45 min on ice, followed by a chase at 37 °C for the times indicated. Cells were fixed in PFA, permeabilized and stained with antibodies against EEA1, GM130, ERGIC-53 or Calnexin (blue). Retrograde transport was followed by confocal microscopy analysis. (B, C) Colocalization of STB with the markers indicated was determined by calculating the Pearson`s correlation coefficient (data shown for GM130 and ERGIC-53). Data represent the mean values ± S.D. of 12 cells from two independent experiments. Differences were not significant between EBAG9 and control cells. Scale bars, 10 µm.

The conserved oligomeric Golgi (COG) complex is thought to function in retrograde vesicular trafficking and to influence the expression levels of Golgi resident integral membrane proteins (Ungar, et al., 2006). COG-deficient cells have multiple glycosylation defects, similar to EBAG9-overexpressing cells. Thus, based on this phenotypic similarity, it was interesting to see whether EBAG9 also affected expression levels of proteins that were shown to be COG sensitive markers, among them ERGIC-53, or COG insensitive marker proteins. The latter included Calnexin, PDI (ER), GM130, P230 (Golgi), and vesicle markers (SNARE molecule GS27). In immunoblot analysis, differences between EBAG9-overexpressing and control cells were not detectable (Fig. 4-31).

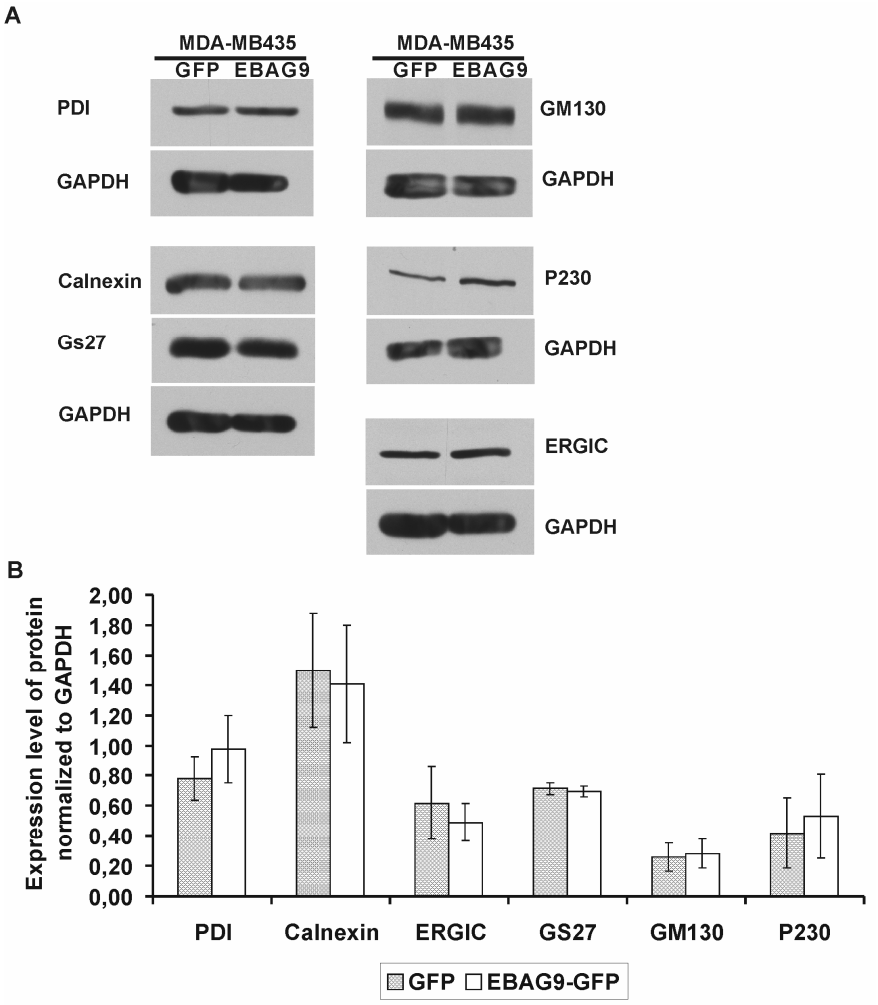

Fig. 4-31: Expression levels of proteins involved in secretory pathway functions are undisturbed in EBAG9-overexpressing cells. (A) Protein lysates from equal numbers of EBAG9-GFP or control stably transfected MDA-MB435 cells were analysed by SDS-PAGE, followed by immunoblotting with the indicated antibodies. Expression levels of ER (Calnexin, PDI), IC (ERGIC-53), Golgi (GM130, P230) and SNARE proteins (GS27) were indistinguishable between EBAG9-overexpressing and control cells. Protein bands were quantified by densitometric scanning and are depicted in (B). Data represent mean values ± SEM of two independent experiments.

4.5.3 Enzymatic processing of ceramide and endosomal uptake of transferrin remain unaffected by EBAG9 overexpression

To strengthen the specificity of the inhibition of COPI-dependent transport by EBAG9 that has been observed, the endosomal transport route as well as the transport of ceramide were analysed. Cell-surface transferrin receptors deliver transferrin with its bound iron to early endosomes by receptor-mediated endocytosis. The low pH in the endosome induces transferrin to release its bound iron, but the iron-free transferrin itself (apotransferrin) remains bound to its receptor. The receptor-apotransferrin complex enters the tubular extensions of the early endosome and from there it is recycled back to the plasma membrane. Here, the complex dissociates into the extracellular fluid. EBAG9 or control transfected HeLa or MDA-

MB435 cells were incubated with fluorescently labeled transferrin and the uptake was followed by FACS for 1 h. After the removal of labeled transferrin and competition with the unlabeled version, the recycling of labeled transferrin was retraced and measured as loss of cell-associated fluorescence (Fig. 4-32). No difference in the uptake and recycling of transferrin was seen between low- and high-EBAG9 expressing cells.

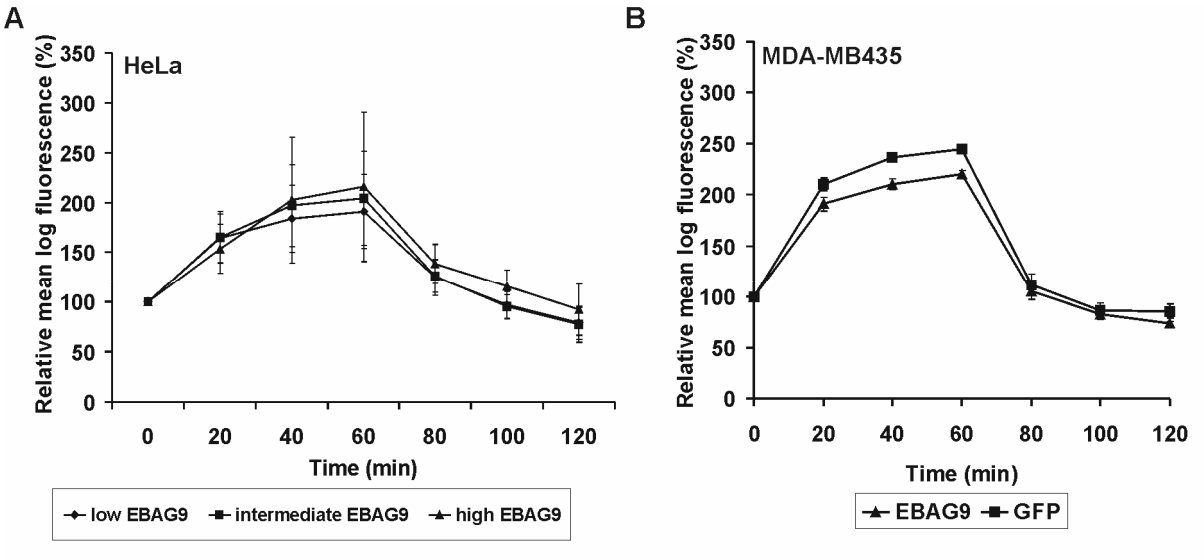

Fig. 4-32: Transferrin uptake and recycling is not impaired upon EBAG9 overexpression. (A) HeLa cells were transiently transfected with EBAG9-GFP and incubated with 10 µg/ml Alexa Fluor-633-labeled transferrin at 37 °C for 60 min. The recycling phase was induced by briefly washing the cells, followed by competition with excessive unlabeled transferrin (10x excess molar ratio). Cells were fixed in 1 % glutaraldehyde/PBS at various time points, followed by flow cytometry analysis to determine cell-associated fluorescence activity. Transiently transfected HeLa cells were grouped according to their GFP intensity (FL1), and uptake (0-60 min) versus recycling values (> 60-120 min) for fluorescently labeled transferrin (FL4) are given according to low, intermediate and high EBAG9-GFP levels. Data represent the mean values ± S.D. of five independent experiments. No difference in the uptake and recycling of transferrin was seen between low- and high-EBAG9 expressing cells. Thus, endosomal uptake and recycling are not compromised in the presence of EBAG9. (B) EBAG9-GFP and GFP stably transfected MDA-MB435 cells were labeled and analysed as described above. Data represent the mean values ± S.D. from three independent experiments.

From theses data the possibility was excluded that the endosomal uptake and recycling route of transferrin was influenced by EBAG9 in epithelial cell lines.

Similarly, the transport route taken by the fluorescently labeled ceramide analogue BODIPY TR C_5-ceramide, which is used as a marker for a post-medial Golgi processing, was not impaired (Fig. 4-33) (Ktistakis, et al., 1995; Martin and Pagano, 1994). BODIPY TR C_5-ceramide molecules combine an endogenous lipid, ceramide, with a fluorophore moiety (BODIPY). Like their cellular counterparts, these molecules are metabolized intracellular to fluorescent sphingomyelin and glycosylceramide. Both metabolites are then transported from the Golgi complex to the cell surface (Ktistakis, et al., 1995). The transport of BODIPY TR

C_5-ceramide to the cell surface and its subsequent loss from the cell is a time-dependent process which was measured as loss of cell-associated fluorescence by FACS. In both stably transfected control and EBAG9-overexpressing cells BODIPY TR C_5-ceramide was transported at the same rate (Fig. 4-33).

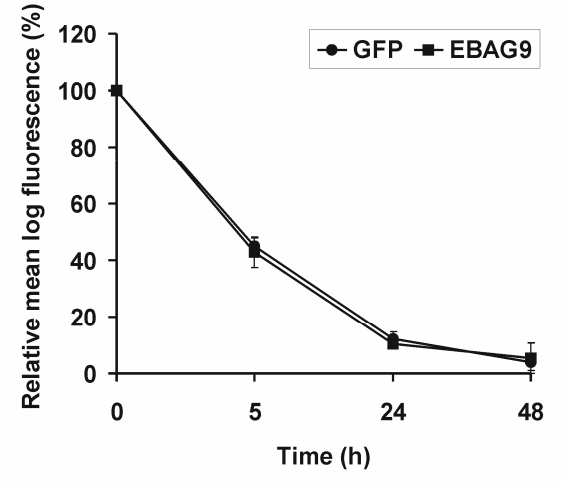

Fig. 4-33: Ceramide transport is not affected by EBAG9 overexpression. EBAG9-GFP and GFP stably transfected MDA-MB435 cells were incubated with BODIPY-TR-C_5-ceramide in serum-free DMEM for 30 min, washed and incubated for the indicated time points at 37 °C. Loss of fluorescence intensity was measured by FACS. There was no difference in kinetics of ceramide transport between EBAG9-overexpressing and control cells. Data represent mean values ± S.D. of three independent experiments.

Taken together, these data further support the specificity of the EBAG9-imposed transport block, which has to occur upstream of ceramide processing and transferrin recycling.

4.6 EBAG9 controls the spatial distribution and function of a cis-Golgi localized enzyme

Subsequently, the spatial distributions of different Golgi enzymes were analysed. Proper spatial and functional arrangement of Golgi glycan-modifying enzymes is most important for the function of the Golgi complex and the subsequent formation of mature glycoconjugates. Mannosidase II (Man II), mainly localized within the cis-Golgi, and β-1-4 Galactosyltransferase (GalT), a marker for the trans-Golgi, were explored (Brockhausen, 2006). Both enzymes are involved in N-glycosylation. In contrast, the UDP-N-acetyl-α-D-galactosamine: polypeptide N Acetyl-galactosaminyl-transferase (GalNAc-T2), located predominantly in the medial-Golgi complex (Storrie and Nilsson, 2002), and the UDP-galactose:glycoprotein-N-acetyl-D-galactosamine 3-β-D-galactosyltransferase (core 1 β3-Gal-T or T-synthase), localized between the cis-medial Golgi compartment (Brockhausen, 2006), are both involved in O-glycosylation.

The T-synthase generates the core 1 disaccharide O-glycan Galβ1-3GalNAcα1-Ser/Thr (T-antigen, Thomson-Friedenreich antigen), which is a precursor for many extended O-Glycans (Ju and Cummings, 2002; Ju, et al., 2002). Loss or downregulation of this protein would favour the generation of the Tn-antigen (Ju, et al., 2008; Sewell, et al., 2006). However, this is not the only pathway for Tn formation. The human lymphoblastoid T cell line Jurkat has been demonstrated to contain higher amounts of inactive T-synthase, which is subject to quick ubiquitination and a subsequent degradation by the proteasome (Ju and Cummings, 2002). These cells lack T-synthase activity and express the Tn antigen, although they contain a normal gene and mRNA encoding the enzyme. Ju and Cummings (2002) demonstrated that a mutated chaperone, Cosmc, accounts for the increased amount of inactive T-synthase.

Hence, the expression of Cosmc was investigated by confocal microscopy. However, no difference in the amount or distribution of Cosmc could be found between EBAG9-overexpressing MDA-MB435 and control cells (Fig. 4-34).

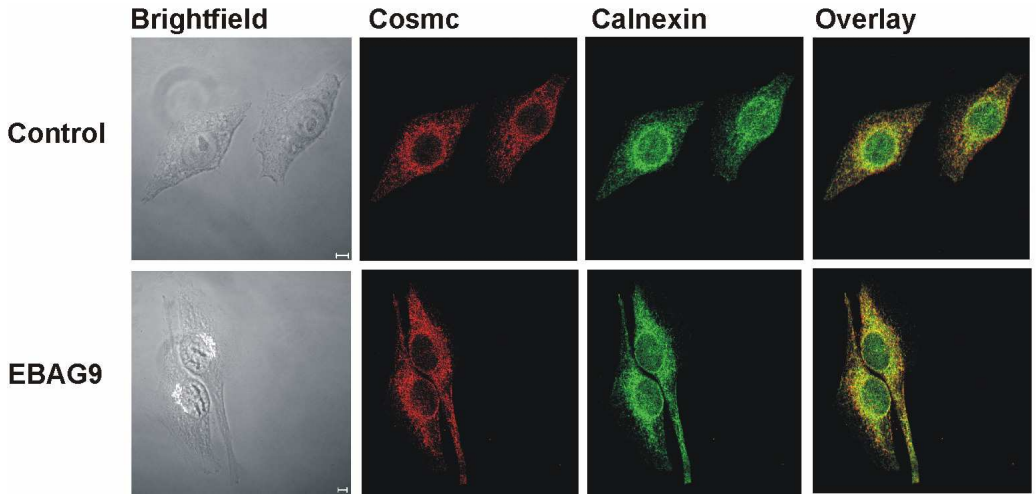

Fig. 4-34: Cosmc expression and distribution is not altered by EBAG9 expression. MDA-MB435 cells stably expressing EBAG9-GFP (white) or GFP (not shown) were fixed in cold methanol, permeabilized and stained with antibodies against Cosmc (red) and Calnexin (green). Analysis was done by confocal microscopy analysis. Scale bars, 5 µm.

Furthermore, the expression and distribution of either transfected or endogenous T-synthase was analysed first by confocal microscopy and subsequently by subcellular fractionation. Confocal microscopy revealed no difference in the Golgi distribution of T-synthase in stably EBAG9-GFP and GFP-expressing cells (Fig. 4-35).

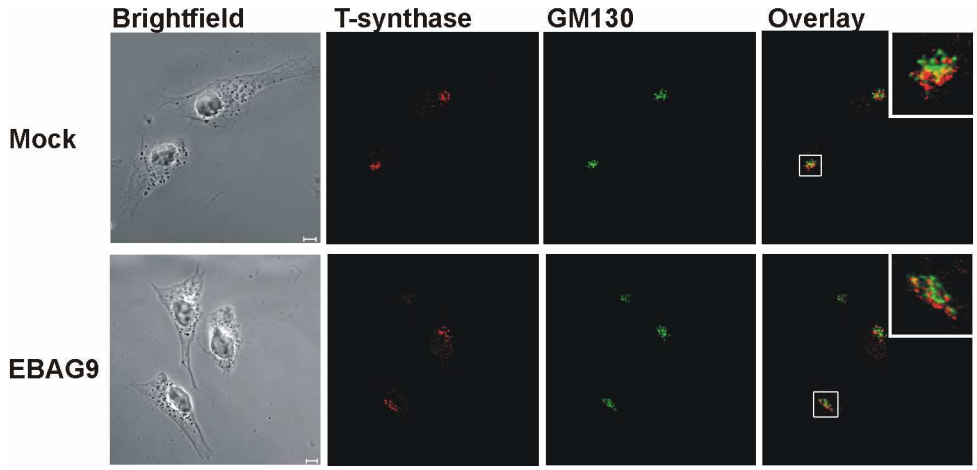

Fig. 4-35: Distribution of endogenous T-synthase is not affected by EBAG9 overexpression. MDA-MB435 cells stably expressing EBAG9-GFP (white) or GFP (not shown) were fixed in cold 2 % PFA, permeabilized and stained with antibodies against T-synthase (red) and GM130 (green). Analysis was done by confocal microscopy. Insets show a higher magnification of the indicated area. Scale bar, 5 µm.

Additionally, the spatial distribution of T-synthase was analysed after 1 h of nocodazole and Brefeldin A (BFA) treatment, respectively. After 1 h of nocodazole treatment, T-synthase did not colocalize with either the cis-Golgi marker GM130 or the trans-Golgi marker P230 (data not shown), but was rather localized throughout the ER, including the nuclear envelope. In contrast, EBAG9 had already accumulated in numerous discrete structures distributed throughout the cell (Fig. 4-36A). Thus, EBAG9 overexpression had no affect on T-synthase redistribution. However, the data also demonstrated that EBAG9 and GM130 redistributed to peripheral sites at a much faster rate than the Golgi resident T-synthase. This agrees with Cole et al. (1996) showing that itinerant (ERGIC-53) and resident (GalT) Golgi markers redistribute at distinct rates and supports our previous results that EBAG9 only transiently associated with the Golgi. Similarly, after 1 h of BFA treatment, T-synthase also redistributed towards ER-like structures, whereas EBAG9 colocalized with GM130 in non-ER discrete structures throughout the cell (Fig. 4-36B).

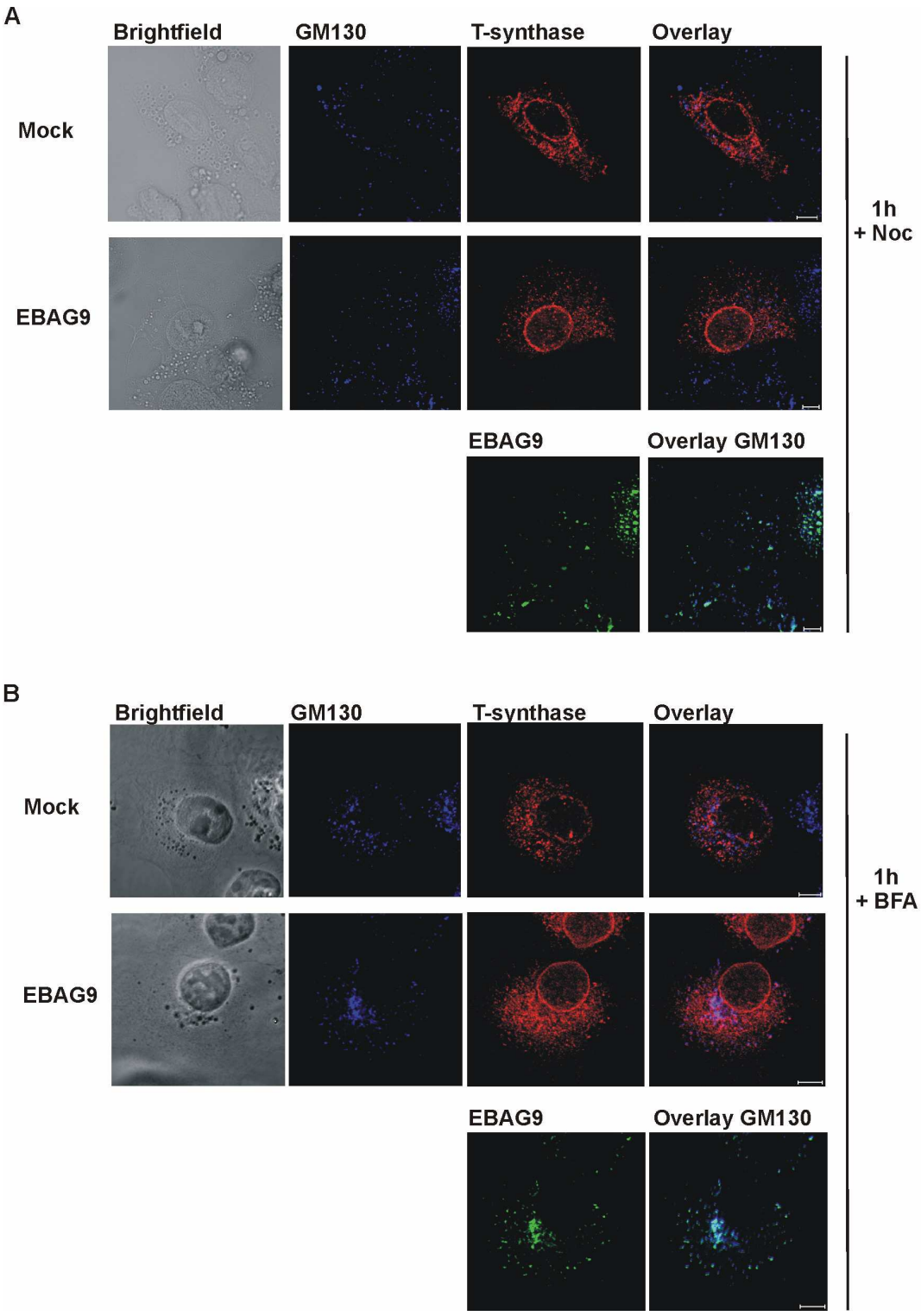

Fig. 4-36: Nocodazole or BFA treatment do not reveal an affect of EBAG9 overexpression on T-synthase localization. (A, B) MDA-MB435 cells stably expressing EBAG9-GFP (green) or GFP (not shown) were transfected with T-synthase-HPC4 (red) and after 48 h of expression nocodazole (10 µM) (B) or BFA (5 µg/ml) (B) was added for 1 h. Cells were permeabilized and stained with antibodies against HPC4 and GM130 (blue). Scale bars, 5 µm.

To test whether active T-synthase might be partially mislocalized, subcellular fractionation of T-synthase was applied to separate ER from Golgi membranes (Fig. 4-37A).

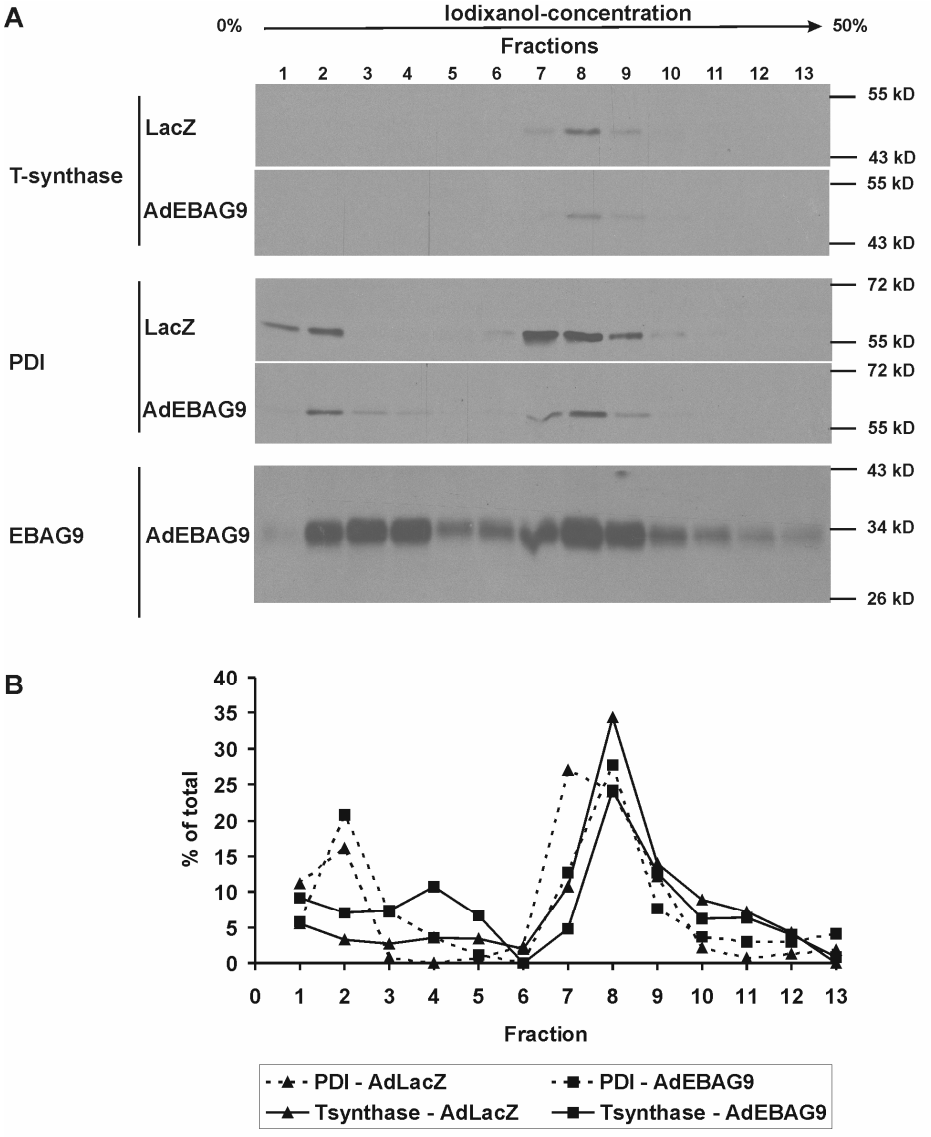

Fig. 4-37: Subcellular fractionation of T-synthase transiently expressed in Hela cells. (A) Hela cells were transfected with T-synthase-HPC4 for 48 h and infected with adenovirus LacZ (control) or EBAG9 for 18 h. Then the postnuclear supernatant was fractionated using a discontinuous iodixanol density gradient. Fractions were analysed by immunoblot using antibodies against HPC4, PDI and EBAG9. (B) Distribution of T-synthase and PDI in adenovirus LacZ or EBAG9 infected cells in percent. Protein bands were quantified by densitometric scanning.

The postnuclear supernatant of Hela cells, transfected with T-synthase-HPC4 and infected with either EBAG9 or control adenovirus, was fractionated using a discontinuous iodixanol density gradient. Due to different densities, cellular components sediment at a position where the density of the solution is equal to their own. The buoyant density of subcellular membranes in iodixanol gradients increases in the following order: PM < early endosomes < Golgi < ERGIC < ER. The fractions collected were then analysed by immunoblot to detect the distribution of T-synthase, PDI as an ER marker, and the distribution of EBAG9. However, PDI distributed in two peaks, the first corresponding to Golgi (lower density, fraction 1-3) and

the second corresponding to the ER fraction (higher density, fraction 7-9) (Fig. 4-37B). Densitometry analysis showed that the distribution was similar in both LacZ and EBAG9-overexpressing cells. Recent literature gives evidence that PDI is also found in the rest of the endomembrane system, including the Golgi, secretory vesicles, plasma membrane and mitochondria (Sun, et al., 2006; Turano, et al., 2002). Separate from the fractionation profile of PDI, T-synthase distributed in one main peak corresponding to an ER localization (fraction 7-9) in both cell lines explored (Fig. 4-37B). However, this distribution might be an artefact of T-synthase overexpression, since endogenous T-synthase was predominantly localized to the Golgi as shown before (Fig. 4-36A). Furthermore, EBAG9 was found in two major peaks (fraction 2-4 and fraction 7-9), which might indicate Golgi/IC and ER localization. This agrees with previous results suggesting that EBAG9 shuttles between the ER and the Golgi.

These results suggested that the function of T-synthase is not influenced by EBAG9 expression. Currently, it is unknown whether T-synthase is subject to anterograde COPI-dependent transport processes.

Likewise, confocal microscopy analysis revealed no difference in the Golgi localization of GalT and GalNAc-T2 in EBAG9 expressing and control MDA-MB435 cells (Fig. 4-38A, B).

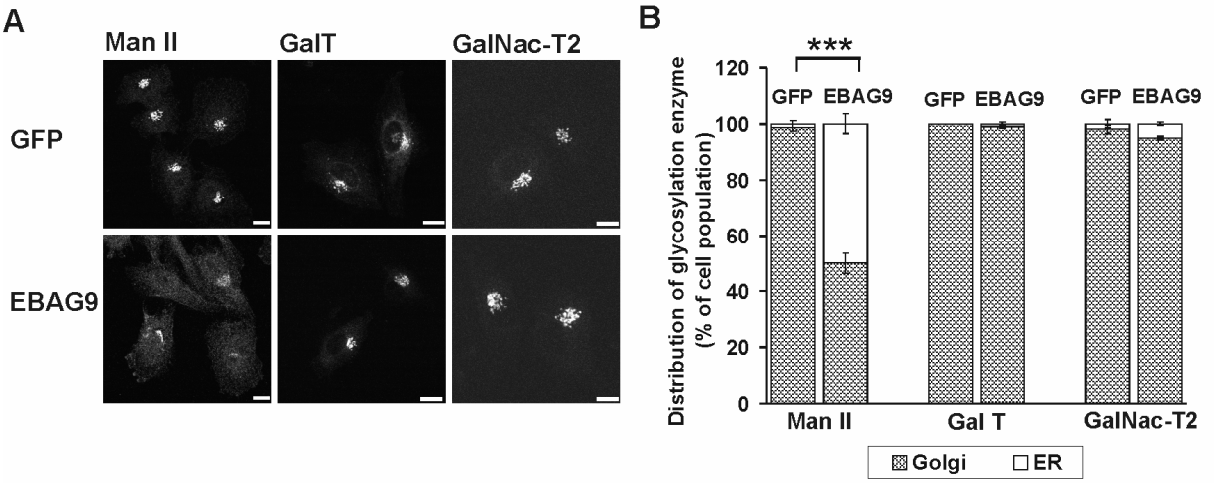

Fig. 4-38: EBAG9 overexpression affects distribution of mannosidase II, whereas GalT and ppGalNacT2 remain unaffected. (A) EBAG9-GFP and GFP stably transfected MDA-MB435 cells were transfected with GalT-dsRed or GalNacT2-CFP. After 24 h, cells were fixed in PFA and permeabilized, and untransfected cells stained with an antibody against mannosidase II (Man II). All cells were costained with GM130 antibody, and the distribution of enzymes was analysed by confocal microscopy. Shown is the distribution of the indicated enzyme in white. (B) Quantitative analysis of the percentage of cells with predominant ER or Golgi-like staining pattern. Data represent the mean values ± S.D. of two (GalT, GalNacT2) or three (Man II) independent experiments, in which 50 cells were counted for each experiment. ***p≤ 0,0005; Student's unpaired *t* Test. Scale bars, 10 µm.

In contrast, the distribution of the endogenous cis/medial Golgi marker Mannosidase II (Man II) (Cole, et al., 1996; Pernet-Gallay, et al., 2002), changed from a Golgi staining pattern ($GM130^{+}$) in control cells to a predominant ER-like staining pattern in about 50 % of EBAG9-overexpressing cells, indicating a redistribution of Man II towards the ER (Fig. 4-38A, B).

Since a correct Golgi localization is indispensable for proper enzymatic activity of these enzymes, the consequences of Man II relocalization were investigated in an enzyme assay using 4-nitrophenyl-alpha-D-mannopyranoside as substrate. The amount of the enzymatic cleavage product 4-Nitrophenol can be determined by spectral absorption at 405 nm. The velocity of each reaction was calculated and expressed as Michaelis-Menten-Kinetics. In EBAG9-expressing cells, the enzymatic activity of Man II was decreased by 60 % compared to control cells (Fig. 4-39).

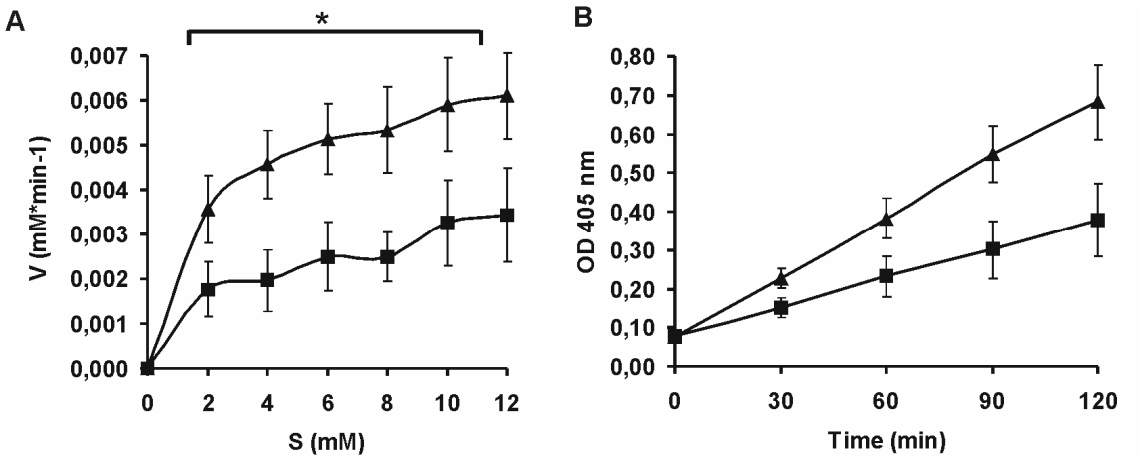

Fig. 4-39: Mannosidase II activity is reduced in EBAG9-overexpressing cells. (A) Equal amounts of lysate from EBAG9-GFP (■) and GFP (▲) stably transfected MDA-MB435 cells were incubated with 0, 2, 4, 6, 8, 10 or 12 mM p-nitrophenyl-alpha-D-mannopyranoside at 37 °C for 0, 30, 60, 90 and 120 min, and the optical density of the reaction product was determined at 405 nm. Data show a representative Michaelis-Menten-Kinetics, determined from the velocity of each reaction and calculated for each concentration over time. Data represent the mean values ± SEM of three independent experiments. * p≤ 0,05; Student's unpaired *t* Test. (B) Equal amounts of lysate from EBAG9-GFP (■) and GFP (▲) stably transfected MDA-MB435 cells were incubated with 6 mM p-nitrophenyl-alpha-D-mannopyranoside at 37 °C for 0, 30, 60, 90 and 120 min, and the optical density of the reaction product was determined at 405 nm. Data represent the mean values ± SEM of three independent experiments.

Consistently, treatment with siRNA EBAG9 resulted in a significantly increased Man II activity. Thus, Man II converted its substrate about 33% faster in siRNA EBAG9 treated cells compared to control (Fig. 4-40).

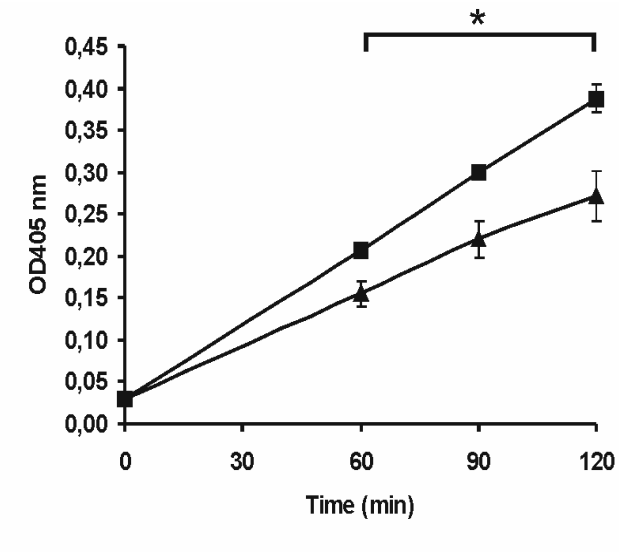

Fig. 4-40: Mannosidase II activity is enhanced by EBAG9 depletion. MDA-MB435 were transfected with fluorescently labeled siRNA EBAG9 (■) and control siRNA (▲) for 48 h. Then, MDA-MB435 cells were lysed in 10 mM KH_2PO_4 buffer, pH 6.8, containing 0.5 % Triton X-100 and 1 mM NaN_3 for 30 min at 4 °C. Protein concentration was determined by Bradford assay. For the Mannosidase activity assay, 1 mg of protein lysate was incubated with 6 mM 4-nitrophenyl-alpha-D-manno-pyranoside at 37 °C. After 0, 60, 90 and 120 min, aliquots were taken and mixed with an equal volume of 0.5 M Na_2CO_3 buffer to terminate the enzymatic reaction. Optical density of reaction products was measured at 405 nm in a plate reader. Shown is the mean of three independent experiments. Gradient between 60 and 120 min is significantly different. * p≤ 0,05; Student's unpaired *t* Test.

In summary, these results suggested that EBAG9 shuttles between the ER and the Golgi and specifically targets anterograde COPI-dependent processes.

4.7 EBAG9 impairs recruitment of cytosolic GAP to membranes

Mechanistically, the data generated suggested that EBAG9 inhibits anterograde transport by interfering with a process prior to fusion and release of vesicles.

The disassembly of the coatomer complex occurs prior to vesicle tethering and is an essential step in the final fusion of Golgi vesicles with target membranes. Disassembly in turn, depends on ArfGAP1 which is thought to catalyze Arf1 GTP hydrolysis (Beck, et al., 2009; Liu, et al., 2005; Spang, 2002). The binding of ArfGAP1 to Golgi membranes is mediated through interactions between its noncatalytic domain and the KDELr (Aoe, et al., 1997). Since a redistribution of KDELr toward the ER was seen, the distribution of ArfGAP1 by subcellular fractionation was determined. The ratio of cytosolic and membrane-bound ArfGAP1 shifted toward the cytosol upon EBAG9 overexpression (Fig. 4-41A, B). The increased ArfGAP1 in the cytosol reflects its impaired recruitment from the cytosol to membranes and not its increased synthesis, since the total pool of ArfGAP did not change upon EBAG9 overexpression (Fig. 4-41A). In confocal microscopy, an enhanced cytosolic and decreased membrane-bound staining of ArfGAP1 was confirmed (Fig. 4-41C).

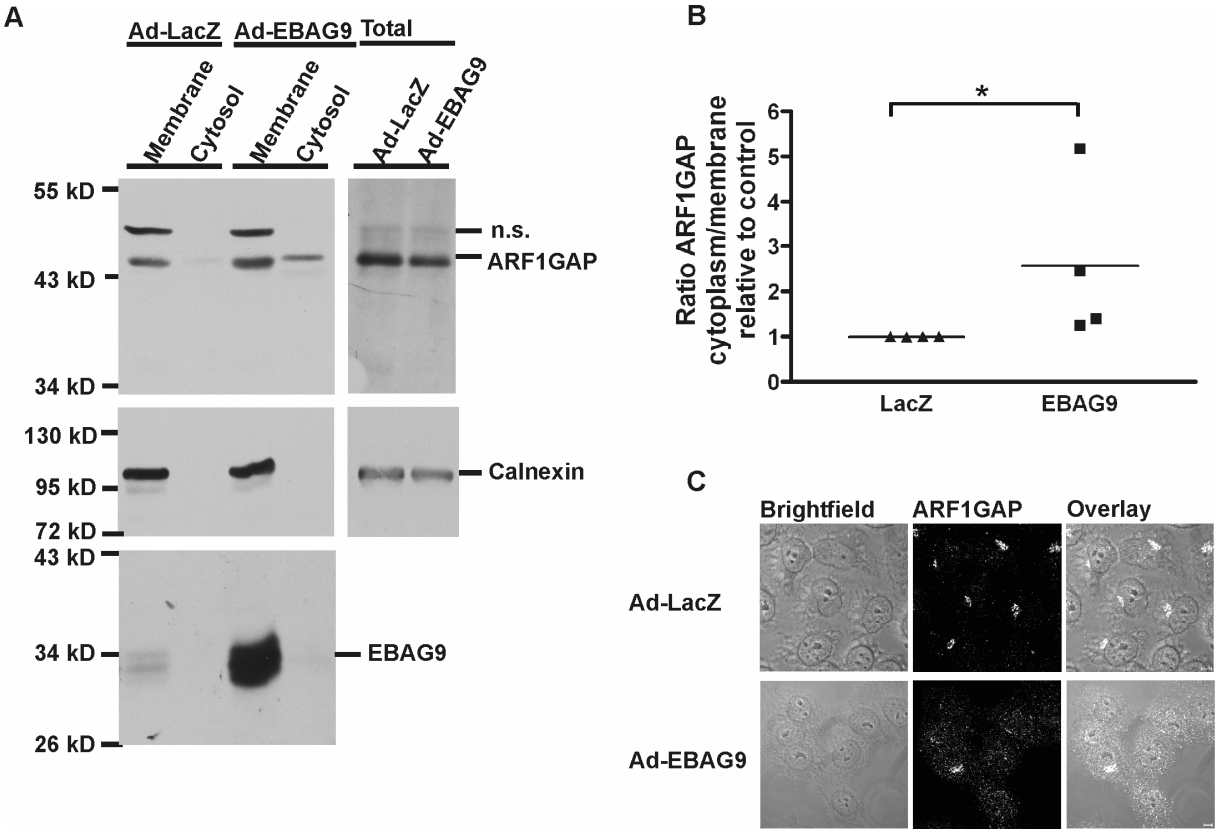

Fig. 4-41: EBAG9 affects the recruitment of cytosolic GAP to membranes. (A, B) Hela cells infected with adenovirus EBAG9 or control were analysed for the distribution of ArfGAP1 to membranes or cytosol by subcellular fractionation. Cellular fractions (total, cytosolic, membrane) were immunoblotted for ArfGAP1, and also for Calnexin as loading control. (B) Quantification was done by densitometric scanning of bands. Shown is the ratio of cytosolic and membrane-bound ArfGAP1 of four independent experiments. * p≤ 0,05; Mann-Whitney *U* test. A representative blot is shown in (A). (C) Hela cells infected with adenovirus EBAG9 or control were fixed after 18 h in methanol, permeabilized, stained with an antibody against ArfGAP1 and analysed by confocal microscopy. Shown is the representative distribution of ArfGAP1 in white, n = 30 cells analysed. Scale bars, 5 µm.

Since ArfGAP1 relocalization could impair coat disassembly, the amount of βCOP on microsomal membranes was determined. In fact, subcellular fractionation of EBAG9 expressing cells confirmed a higher amount of βCOP associated with microsomal membranes (Fig. 4-42). The increased βCOP represents its impaired dissociation from the microsomal membranes and not its increased synthesis, since the total pool of βCOP did not change upon EBAG9 overexpression. Both observations, ArfGAP1 and βCOP localization, implicate a direct effect of EBAG9 overexpression on the uncoating reaction of COPI vesicles, which is a prerequisite for fusion of vesicles with target membranes.

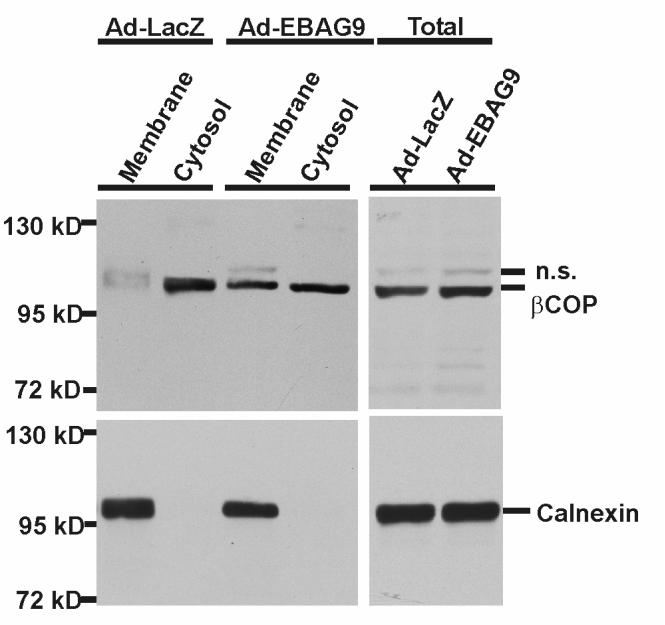

Fig. 4-42: EBAG9 impairs βCOP release from microsomal membranes. HeLa cells infected with adenovirus EBAG9 or control were analysed for the localization of βCOP to microsomal membranes or cytosol. Cellular fractions (total, cytosolic, microsomal membranes) were immunoblotted for βCOP, and for Calnexin as loading control. A representative blot of two independent experiments performed is shown.

In summary, these results suggested that EBAG9 overexpression, by interfering with the distribution of KDELr, impairs GAP recruitment to membranes and thus inhibits the dissociation of coat proteins from Golgi structures. This in turn inhibits the fusion of IC-derived Golgi vesicles with cis-Golgi membranes, a process that results in a delay of COPI-dependent vesicle transport.

5 Discussion

To gain insight into the pathophysiological function of EBAG9 in view of its role in glycome alteration in epithelial cells, the role of EBAG9 in vesicular trafficking was investigated.
In this work, COPI-dependent vesicular transport processes were identified as a target for EBAG9 activity. This interaction resulted in the mislocalization of components of the ER quality control and glycosylation machinery in epithelial cell lines. The observations do not only add a new molecule involved in the regulation of the secretory pathway in epithelial cell types, but also links the modulation of exocytosis with tumor pathogenesis. In several primary tumors and tumor cell lines, defects for specific steps in the sequential order of glycosylation have been found (Brockhausen, 2006; Whitehouse, et al., 1997). However, these mechanisms apply to single, specific tumor entities, and not to others. In contrast, EBAG9 has a 3-to-5-fold increased level of expression in a multitude of human epithelial cancers compared to benign tissues (Akahira, et al., 2004; Ogushi, et al., 2005; Takahashi, et al., 2003; Tsuneizumi, et al., 2001). An overexpression model such as that used in the current work could be a concern since the transfected gene product might titrate out interacting factors required for the activity or transport of other proteins. However, the application of such a system seems appropriate to mimic crucial events during tumor cell pathogenesis, since EBAG9 is overrepresented but not deleted in tumors. Secondly, from this epidemiological survey it can be inferred that EBAG9 overexpression defines a broadly applicable pathogenic principle.

5.1 Characterisation of EBAG9-COPI association

To address the molecular pathways of by which EBAG9 modulates essential trafficking steps in epithelial cell lines, a biochemical interaction screen that had been previously carried out was confirmed by co-immunoprecipitation experiments. From several COPI-coat components retrieved by the former screen, which included αCOP, γCOP, βCOP, β´COP and δCOP, endogenous βCOP was demonstrated to co-immunoprecipitate with EBAG9. This result is consistent with a recent proteomics approach where EBAG9 was found in purified COPI vesicles (Gilchrist, et al., 2006). The exact contribution of COPI to intra Golgi transport is still being debated. Several reports suggested the existence of distinct sub-populations of COPI-

coated vesicles involved in bidirectional transport, but also in post-Golgi trafficking steps. Regarding ER to Golgi trafficking, Scales et al. (1997) and Stephens et al. (2000) have demonstrated that after COPII mediated ER exit, subsequent transport is carried out by tubulovesicular intermediates that stained also for the COPI coat. In this thesis, EBAG9 has been observed in such vesiclular-tubular structures as well, which points towards a function of EBAG9 in ER to Golgi transport. Currently, compelling evidence for an important function of COPI in ER to Golgi transport exists (Duden, et al., 1994; Hosobuchi, et al., 1992; Pepperkok, et al., 1993; Peter, et al., 1993). These authors showed that VSVG transport to the Golgi is inhibited by antibodies directed against the βCOP subunit of coatomer. The relation to my work on EBAG9 could lie in an association of EBAG9 with βCOP, which has an impact on anterograde COPI-dependent transport. This is supported by the fact that EBAG9 colocalizes with γCOP on transport vesicles, suggesting that COPI-coated transport carriers are also positive for EBAG9. Furthermore, this vesicle population was clearly separate from another class of coated vesicles, CCV. On the other hand, EBAG9 was also found on lysosome-like vesicles. Most interestingly, Aniento et al. (1996) implicated COPI in transport events into and through early endosomes and the maintenance of lysosomal function. This raises the question of whether EBAG9 might play a role in post-Golgi trafficking steps as well. In this view, EBAG9 would be able to associate with different COPI sub-populations.

To map a possible interaction site of EBAG9 with endogenous COPI, the association of EBAG9 truncation mutants with COPI was investigated. Only the full length protein but none of the mutants coimmunoprecipitated with endogenous βCOP. This implies that more than one interaction site for EBAG9-βCOP interaction exists or that a certain conformation is required for successful interaction. Alternatively, EBAG9 might associate with βCOP via an indirect protein-protein interaction or EBAG9 interacts with the assembled COPI coat only. In summary, these data indicated that full-length EBAG9 associates with COPI coats *in vitro* and *in vivo* and it can be inferred that EBAG9 might influence COPI-dependent transport processes.

5.2 EBAG9 dynamically associates with the Golgi

To address the molecular function of EBAG9, its localization and dynamic behaviour was investigated in more detail. To this end, pharmacological agents, such as BFA or nocodazole, have proven to be powerful tools. The fungal metabolite BFA triggers rapid COPI dissociation and reversible redistribution of Golgi enzymes into the ER by inhibiting a guanine nucleotide exchange factor (GEF) of ARF-1. On the other hand, matrix proteins, like GM130 or GRASP65, are forced to disperse throughout the cytoplasm without merging with the ER (Dinter and Berger, 1998). In contrast, nocodazole, a microtubule depolymerising agent, causes the Golgi apparatus to break down into functional ministacks that become redistributed from the juxtanuclear region to random sites throughout the cytoplasm. Secretory and biosynthetic activities of the Golgi apparatus remain remarkably unaffected upon nocodazole treatment (Dinter and Berger, 1998). Cole et al. (1996) showed that this is a two-step process. First, Golgi membrane components gradually redistribute to ER exit sites upon microtubule disruption accompanied by a significant block in secretory trafficking. Subsequently, a regeneration of small Golgi stacks in these peripheral sites re-establishes secretory flow from the ER to the Golgi and result in “Golgi fragmentation" (Cole, et al., 1996).

As seen before, EBAG9 colocalized with the cis-Golgi marker GM130 even when the Golgi complex was disassembled with nocodazole or BFA (Engelsberg, et al., 2003; Reimer, et al., 2005). At the same time after treatment, when T-synthase was rather localized throughout the ER, including the nuclear envelope, EBAG9 had already accumulated in numerous discrete $GM130^{+}$ structures distributed throughout the cell. These data also demonstrated that EBAG9 and GM130 redistributed to peripheral sites at a much faster rate than the Golgi resident T-synthase. This agrees with Cole et al (1996) showing that itinerant (ERGIC-53) and resident (GalT) Golgi markers redistribute at distinct rates that are comparable to those of EBAG9 and T-synthase. Thus, it can be inferred that EBAG9 only transiently associates with the Golgi complex. In conclusion, EBAG9 behaves in a way similar to ERGIC-53, which was shown to recycle constitutively between the IC and ER (Aridor, et al., 1995; Itin, et al., 1995; Lippincott-Schwartz, et al., 1990; Saraste and Svensson, 1991).

In support of this conclusion, strong colocalization was also obtained with proteins cycling between the ER and the Golgi complex, such as ERGIC-53 and KDELr. This observation was especially pronounced under conditions that enhance the formation of the IC. In fact, as

shown by FRAP analysis, EBAG9 is not stably associated with the Golgi, but rather traffics between the ER and the Golgi apparatus. The kinetic behaviour of EBAG9 is similar to tagged p58/ERGIC-53 protein (Tisdale, et al., 1997; Ward, et al., 2001). By way of comparison, Ward et al. (2001) showed that GalT recovers much slower (50 min) after selective photobleaching of the Golgi area, as expected for a Golgi resident protein. In contrast, εCOPI recovery was very rapid within 20 s. COPI components are known for their binding and release from Golgi membranes. They are recruited from a cytoplasmic pool, a process which is very rapid since it does not require any transport intermediates (Presley, et al., 1998). This comparison suggests that EBAG9 behaves like ERGIC-53, which was shown to reside only transiently at the Golgi complex and recovers within 15 min. Based on the very distinct recovery times after photobleaching of Golgi resident, cytoplasmic and cycling molecules, it can be inferred that EBAG9 traffics between the ER/IC and the Golgi system.

This fine-tuned localization analysis under dynamic conditions and the association between EBAG9 and COPI, prompted me to explore transport processes between the ER and the Golgi complex in more detail.

5.3 EBAG9 is a regulator of the biosynthetic pathway

5.3.1 EBAG9 influences the anterograde secretory pathway

While a significant inhibition of constitutive hGH release was found in EBAG9-GFP transfectants, this was not the case in neurosecretory PC12 cells. In agreement with a previous study (Ruder, et al., 2005), only the regulated release was decreased in these cells. Consistent with this observation, the regulated secretion of Granzyme B and A from secretory lysosomes was strongly enhanced in EBAG9-deleted cytotoxic T lymphocytes, whereas the constitutive pathway remained unaltered (Ruder, et al., 2009). These results implied that EBAG9 modulates the secretory pathway in a cell type-specific manner, depending on the unique composition of the exocytosis machinery. Such promiscuous binding and trafficking behaviour was also shown for syntaxin 6 which was found to associate with different partners depending on the intracellular compartment and the cell line explored (Wendler and Tooze, 2001). A similar function has been suggested previously for Rab11b, which was demonstrated

to function as a GTP-dependent switch between regulated and constitutive secretory pathways in neuronal, but not in non-neuronal cell lines (Khvotchev, et al., 2003).

To exclude the possibility that EBAG9 transfection might cause antigen overload at the Golgi complex with subsequent artefacts on cellular transport assays, a Golgi-localized truncation mutant was employed. Consistent with its inability to induce truncated O-linked glycan formation, this mutant failed to inhibit hGH secretion in mamma carcinoma cells. These observations imply that the aberrant expression and intracellular accumulation of glycans in EBAG9-overexpressing cells might be related to disturbances within the biosynthetic secretory pathway.

In general, EBAG9 imposed a transport block which exhibited a two-fold decreased in kinetics in VSVG Golgi accumulation. Despite the significant delay of apical and basolateral targeting of VSVG, rGH and HA in EBAG9-overexpressing polarized cells, no disturbance of polarity was detected. Polarized transport mainly diverges at the TGN (Ikonen and Simons, 1998; Nelson and Yeaman, 2001) and is apparently unaffected by EBAG9. Failure to cause alterations in transferrin recycling or transport and the metabolism of BODIPY TR C_5-ceramide supports our contention that EBAG9 overexpression does not impose nonselective effects on the secretory or endocytic pathway in epithelial cell lines (Koval and Pagano, 1991; Ktistakis, et al., 1995; Martin and Pagano, 1994). However, a delay, but not the complete abolishment of transport, might be of functional relevance for short-lived cell surface proteins, proteins to be replaced, or proteins to be secreted, such as cytokines and growth factors, and also gap junctional proteins and plaques (Berthoud, et al., 2004).

In support of this functional specificity, siRNA-mediated downregulation of EBAG9 expression accelerated VSVG transport along the secretory transport route. Hence, EBAG9 behaves physiologically as a negative regulator of the constitutive secretory pathway in epithelial cells. However, the secretion block in EBAG9-overexpressing tumor cells seems to be contradictory to the observed accelerated growth kinetics of $EBAG9^+$ tumors when transplanted into immunocompetent mice. In general, solid tumor progression requires secretion of matrix-degrading enzymes, cytokines, and angiogenetic factors for rapid expansion (Bergers and Coussens, 2000; Coussens and Werb, 1996; Coussens and Werb, 2002; Hong, et al., 2009; Johnsen, et al., 1998; Ogushi, et al., 2005; Rak, et al., 1995). Interestingly, this growth-promoting effect of EBAG9 disappeared in T and B lymphocyte-

deficient SCID mice. This is in accordance with the report of Ogushi, Takahashi et al. (2005) on the growth kinetics of transfected renal cell carcinoma cells in immunodeficient BALB/c nude mice. In this thesis, the growth of EBAG9-overexpressing tumors was retarded, which is consistent with the protein transport block that was observed in EBAG9-overexpressing cells *in vitro*. Thus, it can be concluded that the tumor-promoting effect of EBAG9 does not rely on autonomy in growth signals, insensitivity to growth-inhibitory signals, evasion of apoptosis or a limitless replicative potential typical for many carcinomas (Hanahan and Weinberg, 2000), but rather on the suppression of antitumor immunity. In agreement with several reports on a modulatory function of altered glycan antigens during T cell recognition or activation (Cudic, et al., 2002; Jensen, et al., 2001; Marth and Grewal, 2008; Rubinstein, et al., 2004; Rudd, et al., 2001; Tsuboi and Fukuda, 1997; van Kooyk and Rabinovich, 2008), it might be hypothesized that EBAG9 modulates the recognition of tumor cells by T lymphocytes that attack, most likely by tuning the secretory pathway and subsequently altering the cellular glycome, a process commonly referred to as immune evasion.

.

5.3.2 EBAG9 selectively affects IC-to-cis Golgi transport

The delayed acquisition of EndoH resistance of MHC class I molecules revealed the topology of the EBAG9-associated transport inhibition. EndoH resistance is acquired as a function of enzymes located in the cis-medial Golgi compartment (Tarentino, et al., 1978), thus it can be concluded that EBAG9 acts prior to this step. Consistent with a selective effect of EBAG9 on an earlier Golgi route, but not on overall Golgi integrity, the TGN- associated sialylation of MHC class I heavy chains occurred in the proper manner. The phenotype that was observed might be caused either by a direct interaction of EBAG9 with MHC class I-loaded COPI vesicles, or alternatively, indirectly by the partial relocalization of Man II, which contributes to the synthesis of EndoH resistant glycoproteins. Currently, neither possibility can be discounted. However, regarding the interaction of EBAG9 and βCOP, it is interesting to note that the injection of βCOP specific antibodies induces VSVG arrest at the interface ER/Golgi stack and the inhibition of the acquisition of EndoH resistance, a phenotype comparable to the effects seen in EBAG9-overexpressing cells (Pepperkok, et al., 1993).

To further dissect the topology of the EBAG9-associated transport block, VSVG transport steps between the ER and the IC were analysed. As mentioned before, ER export is mediated by vesicles coated with COPII coatamer, which is lost before fusion with the IC. Subsequent transport events between the IC and the cis-Golgi are likely to be mediated by a COPI-dependent step (Bannykh and Balch, 1997; Presley, et al., 1997; Scales, et al., 1997; Stephens, et al., 2000). In EBAG9-overexpressing cells, the loading of VSVG-containing cargo and the formation of COPII coated vesicles occurred properly. Thus, processes at ER exit sites appear to remain unaffected, including vesicle budding and scission. Subsequently, VSVG was found in COPI and ERGIC-53 positive structures, which implies that the switch between COPII and COPI coat components was undisturbed and the transport of anterograde cargo from the ER towards the IC was not inhibited by EBAG9. Therefore, the function of EBAG9 is separate from p53/58, which had been proposed to function in the coupled exchange of COPII for COPI (Tisdale, et al., 1997). Furthermore, as shown by FRAP analysis, EBAG9 did not interfere with the recruitment of cytosolic coatomer components onto Golgi membranes. Thus, inhibition of coat assembly seems unlikely, including inhibitory functions on GEFs, as has been shown for the enterovirus 3A protein (Wessels, et al., 2006).

On the other hand, the formation of densely clustered, COPI and VSVG double-positive carriers that were still separated from the cis-Golgi marker GM130 suggest that EBAG9 targets a step in cargo delivery immediately prior to fusion with the cis-Golgi. These structures resemble pleiomorphic, tubulo-vesicular ER-to-Golgi carriers (EGCs) or vesicular-tubular-clusters (VTC), respectively (Marra, et al., 2007; Polishchuk, et al., 2009; Presley, et al., 1997). EGCs mature into larger and more homogeneous membrane units, and are destined for the incorporation into the cis-Golgi, a process controlled by GM130. It has been shown that inhibition of the tethering molecule GM130 delayed anterograde transport of VSVG and caused KDELr accumulation in peripheral structures, a phenotype also observed for EBAG9 overexpression. In contrast to the loss of GM130 function, EBAG9 overexpression does not cause a gross modification of Golgi biogenesis. Interestingly, partially uncoated vesicles tend to form large aggregates (Rutz, et al., 2009), which is consistent with what can be seen for VSVG carriers in the presence of EBAG9.

Additional insight into EBAG9 behaviour was gained from the regulated cytotoxic response of CTLs. As shown by TCR-induced relocalization toward the immunological synapse, the localization of EBAG9 is also dynamic within CTLs. This relocalization in CTLs is consistent

with the colocalization between EBAG9 and GM130 and the known polarization of the microtubule-organizing center and associated organelles toward the signaling platform at the T cell–target cell contact site (Kupfer and Singer, 1989; Stinchcombe, et al., 2001). Interestingly, EBAG9 positive organelles surrounded cathepsin D-containing granules. Since both compartments did not fuse and the polarization of lytic granules toward the immunological synapse was unaltered in *Ebag9–/–* mice, it appears that vesicle docking and tethering are not influenced in CTLs. Provided that similar mechanisms of EBAG9 function apply in CTLs and epithelial cells, it can be inferred from these observations that EBAG9 regulates trafficking steps further upstream in both model systems.

Taken together, the data presented here suggest that EBAG9 overexpression blocks VSVG transport at a step between the IC/ERGIC and cis-Golgi. More specifically, EBAG9 might target a step in cargo delivery immediately prior to fusion with the cis-Golgi complex. Furthermore, it seems likely that EBAG9 exists in a macromolecular complex with COPI on coated carriers. On these carriers, the molecule might interfere with essential COPI interactions required for the uncoating reaction and subsequent vesicle tethering and docking.

5.4 Aberrant expression of EBAG9 mislocalizes components of the ER quality control and glycosylation machinery in a COPI-dependent manner

In principle, the inhibition of anterograde transport could depend on a disturbance of the retrograde route (Bannykh and Balch, 1997; Luna, et al., 2002; Pernet-Gallay, et al., 2002). In yeast, defects in anterograde transport due to COPI mutations are thought to be an indirect effect of the failure to retrieve an anterograde machinery (Lee, et al., 2004). In the present work, the trafficking of two substrates of the retrograde pathway, STB and the KDELr, were addressed. While there were no differences in the dynamics of the retrograde transport of the STB subunit towards the Golgi and ER in EBAG9-overexpressing and control cells, a disturbance of the steady state distribution of KDELr was seen. This difference is best explained by a selective effect of EBAG9 on a COPI-dependent transport route. KDELr is known to be transported within COPI vesicles (Capitani and Sallese, 2009; Martinez-Menarguez, et al., 2001) In contrast, STB employs an alternative, Rab6-dependent pathway (Girod, et al., 1999; Mallard, et al., 1998; White, et al., 1999). The finding that KDELr

distribution at steady-state conditions was already shifted towards a predominant ER localization and was not subject to further relocalization might imply that EBAG9 affects the COPI-dependent transport between the ER and Golgi rather than the reverse route. The overexpression of the Golgi Microtubule-Associated Protein-210 (GMAP-210) leads to a transport phenotype similar to that seen for EBAG9, but an important distinction remains the combined effect of GMAP-210 on the anterograde and retrograde route (Pernet-Gallay, et al., 2002). Alternatively, KDELr is involved in ER quality control through the retrieval of KDEL-tagged proteins from the IC or cis-Golgi back into the ER. This mechanism ensures that only correctly folded proteins are exported from the ER, whereas misfolded proteins are degraded by the ERAD pathway (Beck, et al., 2009; Capitani and Sallese, 2009; Yamamoto, et al., 2001). Yamamoto et al. (2001) demonstrated that a significant amount of unassembled TCR α chain is exported from the ER and then returned to the ER from the post-ER compartments by retrograde transport. This recycling is mediated by the KDELr, and when interrupted, a high amount of TCRα was found to escape ERAD. Thus, retrieval by the KDEL receptor contributes to mechanisms by which the ER monitors newly synthesized proteins for their proper disposal. In view of the EBAG9-induced accumulation and prolonged resident time of premature proteins at the IC/cis-Golgi interface, with a subsequent inhibition of N-linked glycan maturation functioning as quality-control tags (Daniels, et al., 2004; Hebert, et al., 2005; Helenius and Aebi, 2001), it might be possible that by retrieving many of these proteins, KDELr itself accumulates in the ER. However, this hypothesis seems unlikely, since no degradation of premature MHC class I molecules, uncovered by EndoH treatment, was observed over time in EBAG9-overexpressing cells.

An additional function of KDELr was demonstrated by Aoe et al. (1999). This study showed that ligand binding on the luminal side of the KDELr also induces its interaction with ARFGAP1 on the cytoplasmic side of the receptor. As a result, ARFGAP1 is recruited from the cytosol to the membranes to activate GAP activity on ARF1. Currently, the role of ARFGAP1 in COPI vesicle biogenesis is still under debate. On the on hand, it has been demonstrated that coat disassembly depends on GTP hydrolysis by ARF1, catalyzed by ARF1 GTPase-activating proteins (ArfGAPs) (Tanigawa, et al., 1993). This uncoating reaction is a prerequisite for vesicle fusion. Reinhard, Schweikert et al. (2003) found that vesicles can be formed when liposomes are incubated with ARF1 and coatomer in the presence of GTP only. The subsequent addition of ARFGAP1 induces the release of ARF1 and coatomer to inhibit

vesicle formation (Reinhard, et al., 2003). Another study reported that GAP activity triggers the release of coatomer from liposomal membranes by sensing membrane curvature (Bigay, et al., 2003). In contrast to this view, studies from Hsu et al. (2009) have proposed the involvement of ArfGAP1 in multiple stages of COPI vesicle formation, including budding, cargo selection and fission (Hsu, et al., 2009). Based on in vitro budding assays, Yang, Lee et al. (2002) have suggested that ArfGAP1 is an essential and stoichiometric component of the coat of Golgi-derived COPI vesicles (Yang, et al., 2002). This role is contrary to reports defining the minimal machinery for the formation of COPI vesicles from liposomal membranes (Bremser, et al., 1999; Spang, et al., 1998), or from Golgi membranes in the absence of cytosol (Beck, et al., 2009; Beck, et al., 2008; Malsam, et al., 2005; Weimer, et al., 2008). Furthermore, the study of Yang et al. (2002) disagrees that ARFGAP1 acts as an uncoating enzyme (Bigay and Antonny, 2005; Reinhard, et al., 2003). In fact, the use of GTP-γS to block GAP activity in early studies resulted in the stabilization of coatomer on the Golgi membrane (Donaldson, et al., 1992; Palmer, et al., 1993). In addition, ArfGAP2/3, but not ArfGAP1, was detected on reconstituted COPI vesicles (Frigerio, et al., 2007). Finally, individual ArfGAPs, including ArfGAP1, can be depleted from cells without compromising cell viability, suggesting that none of these GAPs is an essential coat component (Frigerio, et al., 2007; Saitoh, et al., 2009).

Within this work the recruitment of ArfGAP1 but not COPI onto Golgi membranes was found to be impaired by EBAG9 overexpression, arguing against ArfGAP1 as an essential component of COPI vesicles. Instead, an increase of the amount of βCOP on microsomal membranes points toward an essential function of ArfGAP1 in the disassembly of the coat lattice as demonstrated before (Aoe, et al., 1999; Liu, et al., 2005). In this thesis, KDELr relocalization had profound consequences, since KDELr regulates ArfGAP1 recruitment onto Golgi membranes through interaction with GAP1. Thus, the EBAG9 imposed relocalization of KDELr interferes with ArfGAP1 recruitment and subsequently, the lack of ArfGAP1 activity delays COPI lattice disassembly on membranes, and carriers fail to fuse with their target membrane (Fig. 5-1). In agreement, densely clustered VSVG carriers were observed in EBAG9-overexpressing cells, resembling large aggregates of partially uncoated vesicles as described Rutz et al. (2009).

At present we cannot definitively say whether KDELr redistribution is the cause or consequence of the transport block imposed by EBAG9 overexpression. Three possible

scenarios could be envisioned. In the first, KDELr accumulates in the ER by retrieving premature proteins as already discussed; in the second overexpressed EBAG9 replaces KDELr as a vesicle constituent because of its stoichiometric advantage and KDELr stays behind in the ER; in the third, EBAG9 facilitates phosphorylation of KDELr by protein kinase A (PKA), which is required for receptor-mediated trafficking from the Golgi to the ER (Cabrera, et al., 2003). EBAG9 itself is predicted to exhibit six phosphorylation sites (PhosphoSitePlus, 6 predicted phosphorylation sites). Hence, it can be hypothesised that EBAG9 might recruit kinases which subsequently phosphorylate KDELr.

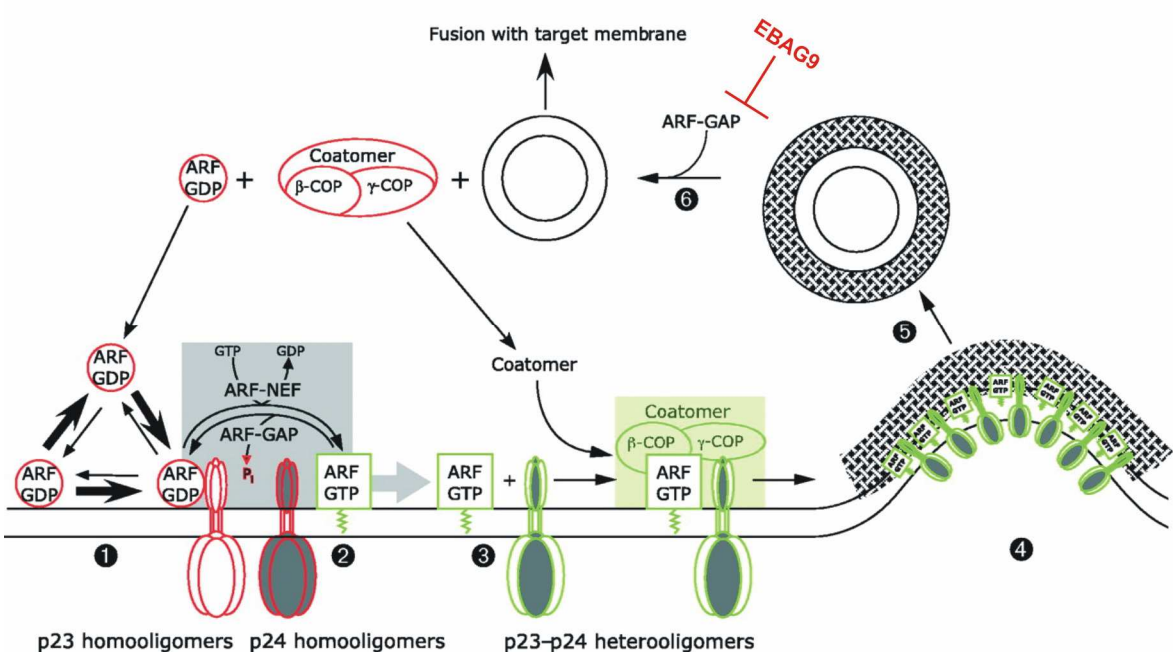

Fig. 5-1: EBAG9 impairs ARFGAP1 recruitment to membranes, subsequently interfering with uncoating of COPI. Recruitment of coat proteins is initiated by ARF-GDP binding to p23 (1). Upon nucleotide exchange, ARF-GTP dissociates from p23, resulting in its stable association with the membrane (2). Multiple cycles of GTP hydrolysis and GDP to GTP exchange are likely to occur (grey box), possibly causing rearrangements of p23/p24 oligomers (3). The products of these processes are ARF-GTP and presumably a p23/p24 heterooligomer, which triggers coatomer binding and coat polymerization (4). Following budding (5), the catalytic domain of ARF-GAP is sufficient to trigger uncoating; the recruitment of ARFGAP1 to membranes mediated through KDELr is impaired by EBAG9 overexpression (6). Active components are shown in green; inactive components are shown in red [modified after (Nickel, et al., 2002)].

Furthermore, KDELr exhibits features of a G protein-coupled receptor with some characteristics of signalling receptors and was shown to activate a phosphorylation cascade that controls intra-Golgi trafficking (Capitani and Sallese, 2009; Pulvirenti, et al., 2008). The signal generated by the incoming traffic at the cis-Golgi complex is provided by the chaperones that exit the ER during the secretory process, as has been demonstrated for the immunoglobulin-binding protein BiP (Yamamoto, et al., 2003). KDELr binding of these chaperones at the cis-Golgi then activates Src family kinases and hence a phosphorylation on

the Golgi complex, as has been demonstrated by Pulvirenti et al. (2008). These kinases positively regulate the intra-Golgi transport machinery. More specifically, it was demonstrated that inhibition of Src kinases by chemical agents or siRNA impaired intra-Golgi trafficking. The inhibition of KDELr itself had the same impact (Pulvirenti, et al., 2008; Sallese, et al., 2009). Accordingly, KDELr redistribution to the ER imposed by EBAG9 could provide a signal to decelerate the biosynthetic pathway and might amplify the phenotype of constitutive transport inhibition.

Consistent with the suggestion that EBAG9 influences a COPI-dependent transport route, a diminished Golgi localization, activity, and redistribution towards the ER was observed for the cis/medial Golgi marker Man II in EBAG9-overexpressing epithelial cells. In agreement, EBAG9 knockdown increased Man II activity. Since COPI-dependent transport is likely to play a role in the correct steady-state distribution of proteins within the Golgi stack (Rabouille and Klumperman, 2005; Schmitz, et al., 2008; Tu, et al., 2008), EBAG9 might have a direct impact on enzyme localization and activity by interfering with COPI-dependent transport processes.

A shift in distribution was not observed for GalT and GalNAc-T2, which were hypothesized to recycle via a COPI-independent pathway (Girod, et al., 1999; Storrie, et al., 1998). In contrast, it is largely accepted that Man II employs a COPI-dependent transport route (Martinez-Menarguez2001, Lanoix2001). Another O-glycosylating enzyme, T-synthase, and its chaperone Cosmc were found to be unaffected by EBAG9 overexpression. However, this analysis is not complete. Different mechanisms involving other enzymes may account for aberrant gylcosylation in cancer cells (Brockhausen, et al., 1998; Brockhausen, et al., 1995; Julien, et al., 2007; Sewell, et al., 2006); therefore a disturbance of O-glycosylating enzymes by EBAG9 overexpression could be induced. Glycosylation is a very complex process involving dynamically changing pathways whose control mechanisms are poorly understood (Brockhausen, 2006). On the other hand, it is not known whether O-glycosylating enzymes such as T-synthase are transported via a COPI-dependent anterograde transport route, or what amount of time they spend at the Golgi complex.

These data indicate that EBAG9 overexpression causes a severe interference with the highly ordered sequence of enzymatic reactions necessary to catalyze glycan modifications. In spite of many reports on a genetic deregulation of enzymes involved in tumor-associated glycan

synthesis (Dennis, et al., 1999; Hakomori, 1996; Whitehouse, et al., 1997; Zhang, 2006), to my knowledge EBAG9 is the first example of a tumor-associated antigen that interferes with the topological hierarchy of glycan-modifying enzymes. Consequently, the spatial rearrangement of enzymes may lead to a failure to synthesize essential intermediates, or may block further conversions through the premature synthesis of terminal glycan structures. A relocalization of a cis-Golgi protein (GM130), as well as the Tn antigen from the Golgi to the ER has been observed in human colon cancer cells. It has been suggested that these alterations induce abnormal protein or lipid glycosylation (Egea, et al., 1993).

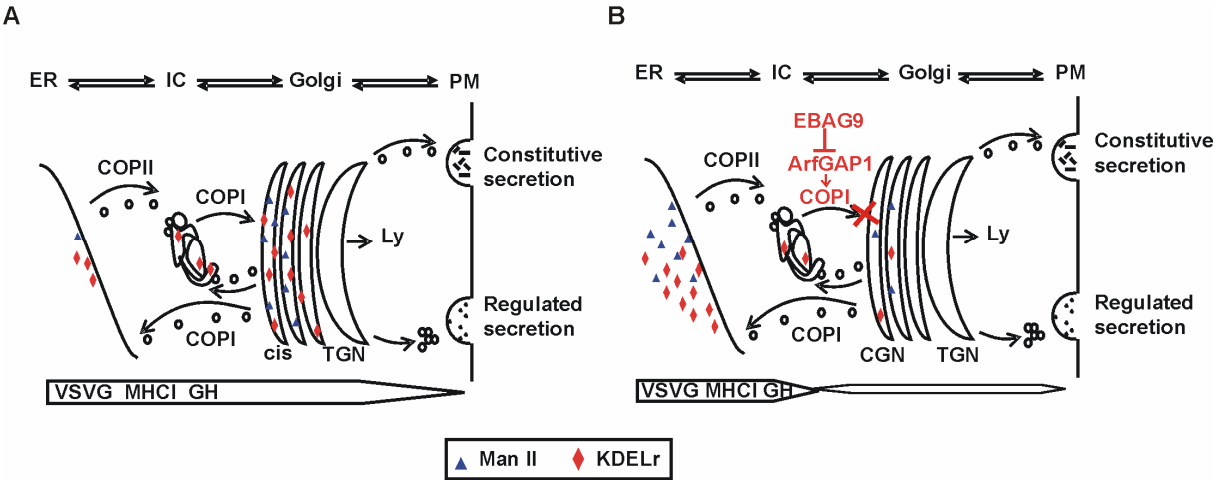

Fig. 5-2: Model of EBAG9 action within the secretory pathway. (A) The involvement of EBAG9 within the biosynthetic secretory pathway based on the stable compartment model (Appenzeller-Herzog and Hauri, 2006). Newly synthesized proteins, such as VSVG, MHC class I, growth hormone (GH), or Golgi resident proteins, like Mannosidase II, undergo anterograde transport and are incorporated into COPII vesicles which bud from the ER and move towards the IC, where a switch from COPII to COPI vesicles takes place. From here, tubulo-vesicular ER-to-Golgi carriers (EGCs) move toward the cis Golgi in a COPI-dependent manner. The sorting of mature proteins destined for lysosomes (Ly), constitutive or signal mediated regulated secretion takes place at the trans-Golgi-Network (TGN). In the retrograde direction, Golgi resident and pre-mature proteins that possess the C-terminal signal KDEL are retrieved from the IC/cis-Golgi by the KDEL-Receptor (KDELr), recycling back to the ER via retrograde COPI vesicles. The dual functions of COPI might be possible because of the existence of different COPI vesicle sub-populations. (B) EBAG9 associates with COPI on anterograde-moving vesicles, fine-tuning the secretory pathway between the IC and cis-Golgi by negative regulation. Here, it might interfere with ArfGAP1 recruitment required for the uncoating reaction and subsequent vesicle tethering and docking. EBAG9 overexpression, which is likely in some tumors, inhibits the transport of biosynthetic cargoes such as (VSVG), (MHCI), growth hormone (GH) or Golgi resident protein Mannosidase II (Man II) at the level of IC/cis-Golgi. Thus, Man II is redistributed towards the ER, disturbing the glycosylation of proteins and delaying protein maturation. This might also contribute to a block of anterograde cargo transport. Transport inhibition, on the other hand, causes proteins to accumulate and prolongs the resident time of premature proteins. Here, KDELr functions in retrieving proteins with the KDEL signal as a quality-control mechanism of the secretory pathway and might accumulate itself in the ER. Finally, the transport block has global effects on the glycosylation of proteins which might cause changes in the migratory, adhesive or invasive behaviour of cells and which might suppress anti-tumor immunity, leading to tumor progression.

In summary (Fig. 5-2), the data in this thesis are in agreement with reports demonstrating that protein transport from the IC to cis-Golgi is mediated by a COPI-dependent mechanism

(Bannykh and Balch, 1997; Presley, et al., 1997; Scales, et al., 1997). Upon EBAG9 overexpression in experimental cell lines and potentially in tumor tissues as well, the molecule causes the relocalization of KDELr towards the ER. It follows that ArfGAP1 recruitment to $COPI^+$ vesicles is diminished, which leads to partially uncoated vesicles. These vesicles tend to form aggregates and are unable to fuse with the cis-Golgi. Subsequently, anterograde transport through the Golgi is downregulated. As a result, COPI-dependent cargo, including enzymes such as Man II, is strongly affected in localization and activity. This relocalization has tremendous consequences for the glycosylation of a wide range of proteins and lipids with diverse functions and destinations.

5.5 The evolving understanding of EBAG9 function – current views and future prospects

In recent years EBAG9 has been implicated in several functions, as described in chapter 1.1.3. Within this work, novel mechanistic insight into EBAG9 function in epithelial cells is provided, since it could be shown that this molecule acts as a negative regulator of the COPI-dependent anterograde transport pathway (Tab. 9). How does this fit into current concepts on EBAG9 function in mammalian cells and in tumor tissues?

COPI, as one of three known coatamer protein complexes involved in vesicle transport, has been shown to play a role not only within the biosynthetic secretory pathway but also within the endosomal transport route towards the plasma membrane. Thus, COPI-coated vesicles might be as diverse as CCV, where each subpopulation is specialized for a different transport step (Boehm and Bonifacino, 2001). Regarding COPI-mediated transport, such diversity could arise from different coatomer subcomplexes (Bednarek, et al., 1996; Orci, et al., 1997). Since EBAG9 was shown to associate with COPI, which is known to play a role in transport steps beyond the Golgi as well, EBAG9 might not only have an impact on COPI-dependent biosynthetic transport as demonstrated in this work, but also in post-Golgi trafficking. In fact, live-cell imaging of EBAG9-GFP in epithelial cells shows a predominant Golgi staining, but also EBAG9 positive vesicles moving throughout the cytoplasm, including even including areas close to the plasma membrane. There is evidence for a promiscuous behaviour on the part of other proteins of the secretory pathway as well. Syntaxin 6, for example, is found in many intracellular compartments, including the TGN and endosomal structures in fibroblast

cell lines, secretory granules in PC12 cells, and locations at the plasma membrane in neutrophiles, and can associate with multiple partners (Wendler and Tooze, 2001).

Tab. 9: Recent studies on EBAG9 regarding its cellular function

Cell type	EBAG9	Interaction partner	Phenotype
Renca cells in Balb/c mice *[1]	overexpression		Accelerated EBAG9 tumor growth; number of infiltrating $CD8^+$ T lymphocytes was decreased in EBAG9-overexpressing tumors
Neuroendocrine cells *[2]	Overexpression	Snapin	Inhibition of regulated, but not constitutive secretion; EBAG9 inhibits Snapin phosphorylation and subsequently binding to SNAP25
4T1mouse (Balb/c) mammary carcinoma model *[3]	Downregulation by siRNA		Suppression of tumor growth and metastasis; Strong specific cytotoxic T lymphocyte activity and enhanced γ-interferon and interleukin-2 production; induction of intensive infiltration of $CD8^+$ T cells in tumor mass
4T1 cells in Balb/c	Overexpression		Faster tumor growth and metastasis
4T1/T-lymphocyte co-culture	Overexpression		Induction of T cell apoptosis, enhancement of glycogen synthase kinase 3" phosphorylation; Inhibition of γ-interferon production of T cells; enhanced expression of chemokine receptor 4
Cytotoxic T lymphocytes *[4]	Ebag9 KO mice	γ2Adaptin	Enhanced cytolytic capacity of CTLs; enhanced cytolytic primary and memory T cell response; EBAG9 involvement in endosomal-lysosomal biogenesis and membrane fusion
Epithelial cells *[5]	Overexpression	COPI	Cell surface expression of truncated O-linked-glycans Tn and TF; EBAG9 shuttles between the ER and cis-Golgi; Delay of constitutive ER-to-Golgi transport; regulated secretion unaffected; mislocalisation of KDELr and ArfGAP1 disturbs COPI uncoating; altered distribution and decreased activity of Man II
	Downregulation by siRNA		Acceleration of ER-to-Golgi transport, increased activity of Man II

*[1]Ogushi et al. (2005), *[2] Rüder et al. (2005), *[3] Hong et al. (2009), *[4] Rüder et al. (2009), *[5] Wolf et al. (in press)

For this versatility two main properties are necessary: mobility and the ability to bind and regulate different proteins. In the case of EBAG9, the dynamic behaviour was not only demonstrated in this study, in which EBAG9 was shown to cycle between the ER and the

Golgi in epithelial cells, but also during relocalization toward the immunological synapse in CTLs upon polarized stimulation. Furthermore, EBAG9 was shown to redistribute toward secretory vesicles in nerve growth factor (NGF)-activated neuroendocrine cells in the vicinity of the plasma membrane (Ruder, et al., 2005). In support of this flexibility, redistribution of EBAG9 in CTLs towards the plasma membrane was demonstrated (Ruder, et al., 2009). The mobility of proteins can be achieved by diverse posttranslational modifications, including acetylation, methylation and palmitoylation (Bijlmakers, 2009; Zhang and Wang, 2008). The latter is a lipid anchor by which proteins are attached to the inner surface of membranes, allowing them to become recruited to membranes only when necessary. More specifically, it has been demonstrated that the dynamic turnover of palmitate regulates the intracellular trafficking of Ras to and from the Golgi (Baekkeskov and Kanaani, 2009; Goodwin, et al., 2005). Since EBAG9 exhibits a palmitoylation anchor and is subject to phosphorylation, it can be suggested that these modifications contribute to EBAG9 relocalization in epithelial as well as in T cells. Such a relocalization would also be consistent with the colocalization between EBAG9 and GM130, on the one hand, and the polarization of the microtubule-organizing centre including associated organelles toward the T cell synapse (Ruder, et al., 2009).

However, dynamic and promiscuous behaviour could not only be explained by posttranslational protein modifications but also by different interaction partners which might be similar in sequence and structural motifs. Since the molecular equipment of a cell differs depending on its specialized functions, regulatory proteins such as EBAG9 might associate with diverse partners in different cell types. EBAG9 has been suggested to play a role in both the regulated and constitutive secretion pathways. Similarly, Rab11b has been suggested to have diverse functions in neuronal and non-neuronal cells and was shown to function as a GTP-dependent switch between the regulated and constitutive secretory pathways (Khvotchev, et al., 2003). For EBAG9, different interaction partners involved in different transport pathways have been identified. Rüder et al. (2005) have shown that in neuroendocrine cells EBAG9 negatively modulated regulated secretion by interacting with Snapin. For CTLs it has been suggested that EBAG9 is involved in the endosomal-lysosomal transport route (Ruder, et al., 2009). In this cell type, EBAG9 exerted its effects through interaction with the adaptor molecule γ2-adaptin, which is normally localized to the cis-Golgi in epithelial cells (Lewin, et al., 1998). Functionally, the loss of EBAG9 conferred CTLs with

enhanced cytolytic capacity through improved Granzyme release, another example of regulated secretion. In contrast, in epithelial cells equipped only with a constitutive secretory machinery, this pathway was negatively regulated by EBAG9 via COPI association. Interestingly, γ2-adaptin and βCOP share structural similarities. Adaptins and COPI are distantly related and share 16-21 % identity at the amino acid level (Boehm and Bonifacino, 2001). The large AP subunits are related to the βCOP and γCOP subunits of COPI, while the medium and small AP subunits are related to the δCOP and ζCOP subunits of COPI, respectively. γ2-adaptin belongs to the large AP subunits and has been identified as a homolog of γ1-adaptin, a constituent of the AP1 complex, which mediates sorting events at the TGN and/or endosomes (Boehm and Bonifacino, 2001). However, γ2-adaptin appears to function independently of AP1 and γ1-adaptin. Major differences include subcellular localization, a lack of dependency on the GTPase ARF1 for recruitment onto TGN membranes (Fig. 5-3), and the inability of γ2-adaptin to substitute for the loss of γ1-adaptin in gene-deleted mice. Thus, γ2-adaptin may not act as a typical vesicle-forming adaptor, and γ2-adaptin–containing AP complexes have not yet been identified (Boehm and Bonifacino, 2001; Bonifacino and Lippincott-Schwartz, 2003; Hirst, et al., 2003; McMahon and Mills, 2004; Takatsu, et al., 1998; Zizioli, et al., 1999). Instead, a sorting function of γ2-adaptin within the endosomal-lysosomal compartment has been suggested (Rost, et al., 2006). From these publications, it might be inferred that the structural similarities between βCOP and the large AP subunits or γ2-adaptin, respectively, favour the promiscuous behaviour of EBAG9. However, whether the regulatory mechanisms are the same remains to be investigated Whereas BFA treatment resulted in impaired recruitment and dissociation of γ1-adaptin (AP1) from TGN, γ2-adaptin recruitment to membranes was not inhibited. Thus, the membrane association of γ2-adaptin appears to be regulated in a manner different from that of AP-1 and COPI (Takatsu, et al., 1998). Since EBAG9 affected COPI membrane association through the inhibition of ArfGAP1 recruitment, a similar mechanism of EBAG9 on γ2-adaptin-dependent transport processes seems unlikely. However, it might be envisioned that EBAG9 influences AP1-dependent transport processes as well (Fig. 5-3).

Mechanistically, EBAG9 is not involved in the secretion process at the plasma membrane of CTLs itself, but rather acts upstream through the regulation of trafficking steps and the maturation of secretory lysosomes (Ruder, et al., 2009). For CTLs, it might be envisioned that

EBAG9 will reduce cytolytic capacity by acting at different sites. First, EBAG9 affects the efficiency of transport of effector molecules through the secretory pathway at the cis-Golgi level. In this context, Vollenweider et al. (1998) demonstrated that the disturbance of ER-Golgi trafficking had an impact on the targeting of cathepsin C, which is normally destined for lysosomes. Alternatively, it has been suggested that EBAG9 acts as a negative regulator of vesicle secretion by suppressing cargo transfer, as well as fusion/exocytosis of these vesicles, by targeting their partner molecules at the post-Golgi level (Kino and Chrousos, 2009).

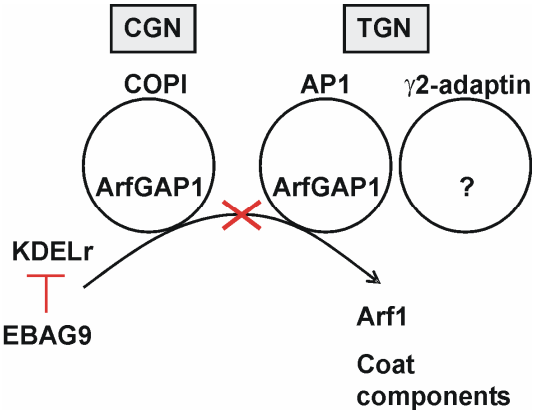

Fig. 5-3: Role of ARF1 for AP1 assembly at the TGN. Whereas COP1 and AP1 membrane association depends on ArfGAP1, γ2-adaptin recruitment seems to be independent of Arf1. Subsequently, EBAG9 might influence AP1 mediate transport processes via inhibition of KDELr dependent ArfGAP1 recruitment and impaired uncoating, as well. For EBAG9 action on γ2-adaptin mediated transport processes a different mechanism must be supposed. CGN = cis-Golgi network, TGN = trans-Golgi network.

In the concept that has emerged from this thesis, EBAG9 influences the secretory pathway in a cell-type-dependent manner. The capacity to shuttle between the ER and the Golgi might specifically enable the molecule to act on the COPI-dependent anterograde transport route between the IC and the Golgi. In this scenario, EBAG9 targets a step prior to the priming and docking of vesicles, and thus prevents fusion and release in epithelial cells. Mechanistically, EBAG9 interferes with the uncoating reaction of COPI vesicles prior to fusion with the cis-Golgi by impairing the recruitment of ArfGAP1 to Golgi membranes (chapter 5.4), which is a prerequisite for vesicle docking and finally fusion. Consequently, this activity inhibits not only the transport of proteins to be secreted, but leads also to a mislocalization of factors/components necessary for ER quality control and glycosylation.

In order to gain more insight into the molecular processes in which EBAG9 is involved in epithelial cells, it might be interesting to investigate whether γ2-adaptin, its interaction partner in T cells, influences the constitutive secretory pathway as well. Additionally, the association of COPI and EBAG9 could be reconfirmed by applying fluorescence resonance energy transfer (FRET) analysis using confocal microscopy or flow cytometry.

How can the regulatory role of EBAG9 within the secretory pathway be reconciled with its association with tumors?

Malignant transformation is accompanied by a modulation of the secretory pathway in a manner which promotes the development and proliferation of tumors as well as metastasis. Thereby, the expression of cell surface molecules is disturbed as well as the synthesis and release of a diverse range of growth factors and cytokines. Subsequently, responses to apoptotic signals and growth control are lost (Chan and Weber, 2002).

As has been demonstrated in this study, the deregulation of a transport pathway can have extensive consequences. This disturbance can cause the deposition of aberrant glycans on the plasma membrane (chapter 1.4); functionally, this alteration may impose a failure of a protective T cell immune response. As has been described in chapter 1.1.2, EBAG9 has been correlated with tumor progression. In immunocompetent BALB/c mice, EBAG9 overexpression promoted tumor growth (Hong, et al., 2009; Ogushi, et al., 2005). In this thesis, it was shown that in immunodeficient SCID mice, EBAG9 impaired the growth of tumor cells, which is in agreement with the observed secretion block. These results in animal models raise the question as to why EBAG9 expression significantly correlates with the progression of malignant tumors, including breast (Suzuki, et al., 2001), ovarian (Akahira, et al., 2004), prostate (Takahashi, et al., 2003), hepatocellular (Aoki, et al., 2003) and renal cell carcinomas (Ogushi, et al., 2005). Since it has been shown in immunocompetent BALB/c mice that Renca-EBAG9-transfected tumors or bladder cancer EJ-EBAG9 grew significantly larger compared to control tumors, it is reasonable to suggest that the tumor-promoting effect of EBAG9 might rely on the suppression of or an escape from antitumor immunity (Kumagai, et al., 2009; Ogushi, et al., 2005). This hypothesis warrants further verification in experimental animal models. Mechanistically, the tumor-promoting effects of EBAG9 might rely on tumor suppression caused by modulating cells of the immune system. This modulation is putatively linked to altered glycosylation, which itself is caused by an EBAG9-imposed inhibition of the biosynthetic transport route. O- and N-glycosylation have been implicated in immune system function and diseases (Lowe, 2001; Zhang, 2006) (chapter 1.3.2). More specifically, the inactivation of FucT-VII (a1-3-fucosyl-transferase) leads to defects in leukocyte trafficking, but to moderate increases in peripheral T cell numbers (Maly, et al., 1996). The deletion of C2GlcNAcT (β1-6-N-acetylglucosaminyltransferase) attenuates

activity of E- and P-selectin ligands on neutrophils (Ellies, et al., 1998) and Mgat5 (N-acetylglucosaminyltransferase V)-null mice exhibit a glomerulonephritis characteristic of autoimmune syndromes, and an exaggerated cellular immune response (Granovsky, et al., 2000). Most strikingly, Rüder et al. (2009) showed that *Ebag9–/–* mice exhibit a substantially stronger cytolytic memory T cell response compared with *Ebag9*+/+ or naive mice, which points towards a modulation of CD8 memory pool by EBAG9. Referring to this observation, it was noted that ST3Gal-I-deficient mice show a reduced CTL activity and impaired $CD8^+$ memory T cell formation (Priatel, et al., 2000). Galvan et al. (1998) demonstrated that the differentiation of activated effector $CD8^+$ T cells occurs with a significant resialylation of core 1 O-glycans mediated by ST3Gal-I (Galvan, et al., 1998). Furthermore, Hong et al (2009) showed that EBAG9 knockdown prolonged the survival of tumor-bearing mice and induced more intensive infiltration of $CD8^+$ T cells in the tumor. This demonstrates that EBAG9 facilitates tumor growth the metastasis of experimental murine mammary carcinoma by suppressing cytotoxic T cell activity (Hong, et al., 2009). From these studies it might be inferred that by interfering with the secretory pathway and consequently glycosylation, EBAG9 impairs $CD8^+$ T cell function, which contributes to tumor escape.

In conclusion, EBAG9 interference with the secretory pathway and subsequently glycosylation might not only alter the surface of tumor cells, but might also impair T cell function at the same time. Both processes could be linked mechanistically through estrogen-dependent expression of EBAG9 in tumor cells, and in T cells as well. This strategy would potentiate the tumor-promoting effect of EBAG9 (Fig. 5-4).

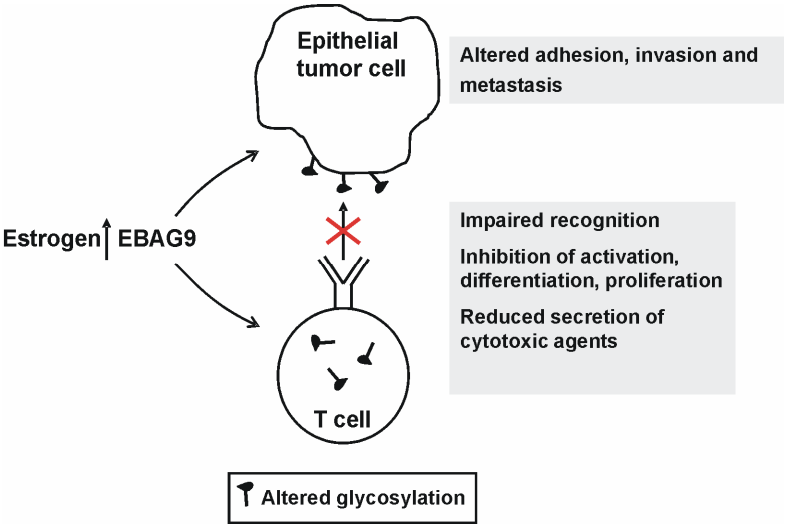

Fig. 5-4: Effect of EBAG9 on tumor progression. The impact of EBAG9 on glycosylation of on the one hand epithelial tumor cells and on the other hand cytotoxic T cells, would finally potentiate the tumor-promoting effect of EBAG9.

Finally, since tumor cells overexpressing EBAG9 seem to be able to evade the immune system, they are more difficult to treat. There is now growing evidence indicating that several chemotherapeutic agents as well as radiotherapy are more efficient against tumors that grow in immunocompetent hosts as compared to the same tumors growing in immunodeficient mice. This might imply that the immune system plays a pivotal role in combating tumors (Finn, 2007; Ryan, et al., 2007), and many therapeutic strategies rely on the activation of the immune system (Apetoh, et al., 2007; Panaretakis, et al., 2009). Regarding EBAG9 as an estrogen-inducible gene (chapter 1.1.2) and its possible impact on the immune system, EBAG9 could be particularly important for the development of malignancies under estrogen regulation and consequent treatment. EBAG9 expressed in response to elevated levels of estrogens in cytotoxic CTLs would provide an essential advantage to the development of these tumors, since elevated EBAG9 in these immune cells impairs their cytotoxic activity by reducing the formation/exocytosis of secretory lysosomes. In fact, anti-estrogens, such as tamoxifen and toremifene, have been demonstrated to augment immune oncolysis by CTLs (Baral, et al., 1994).

5.6 Outlook

In the past, EBAG9 has been used as an independent prognostic marker for disease-specific survival, since EBAG9 overexpression significantly correlated with tumor progression in several epithelial cancers (Akahira, et al., 2004; Ogushi, et al., 2005; Suzuki, et al., 2004; Takahashi, et al., 2003; Tsuneizumi, et al., 2001). Here, the deposition of common tumor-associated glycan antigens has been demonstrated (Engelsberg, et al., 2003). Functionally, those sugars were suggested to contribute to the pathogenesis of tumors through mediation of adhesion, invasion and metastasis (Baldus, et al., 2000; Cavallaro and Christofori, 2001; Hakomori, 2002; Tsuiji, et al., 2003). Despite its putative role in tumor progression, the pathophysiological function of EBAG9 has not yet been well defined. Recently, EBAG9 has been introduced as a negative regulator of regulated secretion (Ruder, et al., 2005) and implicated in endosomal-lysosomal biogenesis and membrane fusion (Ruder, et al., 2009). However, data obtained in these studies could not be reconciled with the effects observed in epithelial cell lines, including O-linked glycan generation. So far, little if any attention has been paid to a possible role of the regulation of the biosynthetic secretory pathway in the

pathogenesis of tumors. However, the importance of new avenues for cancer treatment by discovering novel pathways of tumor progression cannot be overestimated.

This thesis focuses on the secretory transport pathway, and thereby contributes essential insights into human diseases that arise from deregulation of this pathway. Within this work, EBAG9 is introduced as a negative regulator involved in COPI-dependent ER-to-Golgi transport in epithelial cells. This represents a novel pathogenetic principle which integrates hormone-dependent gene expression, the generation of tumor-associated marker molecules, vesicle transport and the immune system. So far, the molecular principle of EBAG9 function in epithelial cells is understood to some degree, except for the exact molecular mechanism of EBAG9 function on COPI vesicles. However, regarding cancer research, the most promising direction for future research is to investigate the impact of EBAG9 on the immune system. The data presented in this thesis strongly suggest that EBAG9 contributes to tumor escape by interfering with the secretory pathway. It is suggested that by interfering with the secretory pathway and consequently glycosylation, EBAG9 impairs $CD8^+$ T cell functions which contributes to tumor escape. However, this hypothesis has to be proved using animal models, in studies such as investigations into the phenotype of an EBAG9-overexpressing transgenic mouse. In this *in vivo* approach, the tissue-specific overexpression of EBAG9 in T lymphocytes, epithelial colon or mamma cells would be of intense interest. Finally, a detailed analysis of N- and O-glycosylating enzymes and changes in surface glycosylation patterns, which could be expected to be altered in these mice, would be beneficial. Since the immune system plays such a crucial role in tumor progression, such studies might lead to novel therapeutic strategies.

References

Akahira, J. I.; Aoki, M.; Suzuki, T.; Moriya, T.; Niikura, H.; Ito, K.; Inoue, S.; Okamura, K.; Sasano, H. and Yaegashi, N. (2004): Expression of EBAG9/RCAS1 is associated with advanced disease in human epithelial ovarian cancer, Br J Cancer (vol. 90), No. 11, pp. 2197-202. URL: http://www.ncbi.nlm.nih.gov/entrez/query.fcgi?cmd=Retrieve&db=PubMed&dopt=Citation&list_uids=15164121

Akashi, T.; Oimomi, H.; Nishiyama, K.; Nakashima, M.; Arita, Y.; Sumii, T.; Kimura, T.; Ito, T.; Nawata, H. and Watanabe, T. (2003): Expression and diagnostic evaluation of the human tumor-associated antigen RCAS1 in pancreatic cancer, Pancreas (vol. 26), No. 1, pp. 49-55. URL: http://www.ncbi.nlm.nih.gov/entrez/query.fcgi?cmd=Retrieve&db=PubMed&dopt=Citation&list_uids=12499917

Alberts, Bruce (2002): Molecular biology of the cell, 4th. ed., Garland Science, New York, ISBN: 9780815332183 (hardbound)

0815332181 (hardbound)

9780815340720 (pbk.P

0815340729 (pbk.P. URL: http://www.ncbi.nlm.nih.gov/books/bv.fcgi?call=bv.View..ShowTOC&rid=mboc4.TOC&depth=2

Alvarez, G.; Lascurain, R.; Perez, A.; Degand, P.; Montano, L. F.; Martinez-Cairo, S. and Zenteno, E. (1999): Relevance of sialoglycoconjugates in murine thymocytes during maturation and selection in the thymus, Immunol Invest (vol. 28), No. 1, pp. 9-18. URL: http://www.ncbi.nlm.nih.gov/entrez/query.fcgi?cmd=Retrieve&db=PubMed&dopt=Citation&list_uids=10073678

Andrews, N. W. and Chakrabarti, S. (2005): There's more to life than neurotransmission: the regulation of exocytosis by synaptotagmin VII, Trends Cell Biol (vol. 15), No. 11, pp. 626-31. URL: http://www.ncbi.nlm.nih.gov/entrez/query.fcgi?cmd=Retrieve&db=PubMed&dopt=Citation&list_uids=16168654

Aniento, F.; Gu, F.; Parton, R. G. and Gruenberg, J. (1996): An endosomal beta COP is involved in the pH-dependent formation of transport vesicles destined for late endosomes, J Cell Biol (vol. 133), No. 1, pp. 29-41. URL: http://www.ncbi.nlm.nih.gov/entrez/query.fcgi?cmd=Retrieve&db=PubMed&dopt=Citation&list_uids=8601610

Aoe, T.; Cukierman, E.; Lee, A.; Cassel, D.; Peters, P. J. and Hsu, V. W. (1997): The KDEL receptor, ERD2, regulates intracellular traffic by recruiting a GTPase-activating protein for ARF1, EMBO J (vol. 16), No. 24, pp. 7305-16. URL: http://www.ncbi.nlm.nih.gov/entrez/query.fcgi?cmd=Retrieve&db=PubMed&dopt=Citation&list_uids=9405360

Aoe, T.; Huber, I.; Vasudevan, C.; Watkins, S. C.; Romero, G.; Cassel, D. and Hsu, V. W. (1999): The KDEL receptor regulates a GTPase-activating protein for ADP-ribosylation factor 1 by interacting with its non-catalytic domain, J Biol Chem (vol. 274), No. 29, pp. 20545-9. URL: http://www.ncbi.nlm.nih.gov/entrez/query.fcgi?cmd=Retrieve&db=PubMed&dopt=Citation&list_uids=10400684

Aoki, T.; Inoue, S.; Imamura, H.; Fukushima, J.; Takahashi, S.; Urano, T.; Hasegawa, K.; Ogushi, T.; Ouchi, Y. and Makuuchi, M. (2003): EBAG9/RCAS1 expression in hepatocellular carcinoma: correlation with tumour dedifferentiation and proliferation, Eur J Cancer (vol. 39), No. 11, pp. 1552-61. URL: http://www.ncbi.nlm.nih.gov/entrez/query.fcgi?cmd=Retrieve&db=PubMed&dopt=Citation&list_uids=12855262

Apetoh, L.; Ghiringhelli, F.; Tesniere, A.; Obeid, M.; Ortiz, C.; Criollo, A.; Mignot, G.; Maiuri, M. C.; Ullrich, E.; Saulnier, P.; Yang, H.; Amigorena, S.; Ryffel, B.; Barrat, F. J.; Saftig, P.; Levi, F.; Lidereau, R.; Nogues, C.; Mira, J. P.; Chompret, A.; Joulin, V.; Clavel-Chapelon, F.; Bourhis, J.; Andre, F.; Delaloge, S.; Tursz, T.; Kroemer, G. and Zitvogel, L. (2007): Toll-like receptor 4-dependent contribution of the immune system to anticancer chemotherapy and radiotherapy, Nat Med (vol. 13), No. 9, pp. 1050-9. URL:

http://www.ncbi.nlm.nih.gov/entrez/query.fcgi?cmd=Retrieve&db=PubMed&dopt=Citation&list_uids=17704786

Appenzeller-Herzog, C. and Hauri, H. P. (2006): The ER-Golgi intermediate compartment (ERGIC): in search of its identity and function, J Cell Sci (vol. 119), No. Pt 11, pp. 2173-83. URL: http://www.ncbi.nlm.nih.gov/entrez/query.fcgi?cmd=Retrieve&db=PubMed&dopt=Citation&list_uids=16723730

Aridor, M.; Bannykh, S. I.; Rowe, T. and Balch, W. E. (1995): Sequential coupling between COPII and COPI vesicle coats in endoplasmic reticulum to Golgi transport, J Cell Biol (vol. 131), No. 4, pp. 875-93. URL: http://www.ncbi.nlm.nih.gov/entrez/query.fcgi?cmd=Retrieve&db=PubMed&dopt=Citation&list_uids=7490291

Aridor, M. and Hannan, L. A. (2000): Traffic jam: a compendium of human diseases that affect intracellular transport processes, Traffic (vol. 1), No. 11, pp. 836-51. URL: http://www.ncbi.nlm.nih.gov/entrez/query.fcgi?cmd=Retrieve&db=PubMed&dopt=Citation&list_uids=11208074

Asp, L. and Nilsson, T. (2008): Golgi gets wired up, Nat Cell Biol (vol. 10), No. 8, pp. 885-7. URL: http://www.ncbi.nlm.nih.gov/entrez/query.fcgi?cmd=Retrieve&db=PubMed&dopt=Citation&list_uids=18670448

Baekkeskov, S. and Kanaani, J. (2009): Palmitoylation cycles and regulation of protein function (Review), Mol Membr Biol (vol. 26), No. 1, pp. 42-54. URL: http://www.ncbi.nlm.nih.gov/entrez/query.fcgi?cmd=Retrieve&db=PubMed&dopt=Citation&list_uids=19169934

Baldus, S. E.; Zirbes, T. K.; Hanisch, F. G.; Kunze, D.; Shafizadeh, S. T.; Nolden, S.; Monig, S. P.; Schneider, P. M.; Karsten, U.; Thiele, J.; Holscher, A. H. and Dienes, H. P. (2000): Thomsen-Friedenreich antigen presents as a prognostic factor in colorectal carcinoma: A clinicopathologic study of 264 patients, Cancer (vol. 88), No. 7, pp. 1536-43. URL: http://www.ncbi.nlm.nih.gov/entrez/query.fcgi?cmd=Retrieve&db=PubMed&dopt=Citation&list_uids=10738210

Bannykh, S. I. and Balch, W. E. (1997): Membrane dynamics at the endoplasmic reticulum-Golgi interface, J Cell Biol (vol. 138), No. 1, pp. 1-4. URL: http://www.ncbi.nlm.nih.gov/entrez/query.fcgi?cmd=Retrieve&db=PubMed&dopt=Citation&list_uids=9214376

Baral, E.; Nagy, E. and Berczi, I. (1994): Target cells are sensitized for cytotoxic T-lymphocyte-mediated destruction by estradiol and tamoxifen, Int J Cancer (vol. 58), No. 1, pp. 64-8. URL: http://www.ncbi.nlm.nih.gov/entrez/query.fcgi?cmd=Retrieve&db=PubMed&dopt=Citation&list_uids=8014017

Barlowe, C. (2000): Traffic COPs of the early secretory pathway, Traffic (vol. 1), No. 5, pp. 371-7. URL: http://www.ncbi.nlm.nih.gov/entrez/query.fcgi?cmd=Retrieve&db=PubMed&dopt=Citation&list_uids=11208122

Barlowe, C.; Orci, L.; Yeung, T.; Hosobuchi, M.; Hamamoto, S.; Salama, N.; Rexach, M. F.; Ravazzola, M.; Amherdt, M. and Schekman, R. (1994): COPII: a membrane coat formed by Sec proteins that drive vesicle budding from the endoplasmic reticulum, Cell (vol. 77), No. 6, pp. 895-907. URL: http://www.ncbi.nlm.nih.gov/entrez/query.fcgi?cmd=Retrieve&db=PubMed&dopt=Citation&list_uids=8004676

Barnstable, C. J.; Bodmer, W. F.; Brown, G.; Galfre, G.; Milstein, C.; Williams, A. F. and Ziegler, A. (1978): Production of monoclonal antibodies to group A erythrocytes, HLA and other human cell surface antigens-new tools for genetic analysis, Cell (vol. 14), No. 1, pp. 9-20. URL: http://www.ncbi.nlm.nih.gov/entrez/query.fcgi?cmd=Retrieve&db=PubMed&dopt=Citation&list_uids=667938

Barr, F. A. (2002): The Golgi apparatus: going round in circles?, Trends Cell Biol (vol. 12), No. 3, pp. 101-4. URL: http://www.ncbi.nlm.nih.gov/entrez/query.fcgi?cmd=Retrieve&db=PubMed&dopt=Citation&list_uids=11859015

Bax, M.; Garcia-Vallejo, J. J.; Jang-Lee, J.; North, S. J.; Gilmartin, T. J.; Hernandez, G.; Crocker, P. R.; Leffler, H.; Head, S. R.; Haslam, S. M.; Dell, A. and van Kooyk, Y. (2007): Dendritic cell maturation results in pronounced changes in glycan expression affecting recognition by siglecs and galectins, J Immunol (vol. 179), No. 12, pp. 8216-24. URL: http://www.ncbi.nlm.nih.gov/entrez/query.fcgi?cmd=Retrieve&db=PubMed&dopt=Citation&list_uids=18056365

Beck, R.; Adolf, F.; Weimer, C.; Bruegger, B. and Wieland, F. T. (2009): ArfGAP1 activity and COPI vesicle biogenesis, Traffic (vol. 10), No. 3, pp. 307-15. URL: http://www.ncbi.nlm.nih.gov/entrez/query.fcgi?cmd=Retrieve&db=PubMed&dopt=Citation&list_uids=19055691

Beck, R.; Ravet, M.; Wieland, F. T. and Cassel, D. (2009): The COPI system: molecular mechanisms and function, FEBS Lett (vol. 583), No. 17, pp. 2701-9. URL: http://www.ncbi.nlm.nih.gov/entrez/query.fcgi?cmd=Retrieve&db=PubMed&dopt=Citation&list_uids=19631211

Beck, R.; Sun, Z.; Adolf, F.; Rutz, C.; Bassler, J.; Wild, K.; Sinning, I.; Hurt, E.; Brugger, B.; Bethune, J. and Wieland, F. (2008): Membrane curvature induced by Arf1-GTP is essential for vesicle formation, Proc Natl Acad Sci U S A (vol. 105), No. 33, pp. 11731-6. URL: http://www.ncbi.nlm.nih.gov/entrez/query.fcgi?cmd=Retrieve&db=PubMed&dopt=Citation&list_uids=18689681

Bednarek, S. Y.; Orci, L. and Schekman, R. (1996): Traffic COPs and the formation of vesicle coats, Trends Cell Biol (vol. 6), No. 12, pp. 468-73. URL: http://www.ncbi.nlm.nih.gov/entrez/query.fcgi?cmd=Retrieve&db=PubMed&dopt=Citation&list_uids=15157504

Bennett, M. K.; Calakos, N. and Scheller, R. H. (1992): Syntaxin: a synaptic protein implicated in docking of synaptic vesicles at presynaptic active zones, Science (vol. 257), No. 5067, pp. 255-9. URL: http://www.ncbi.nlm.nih.gov/entrez/query.fcgi?cmd=Retrieve&db=PubMed&dopt=Citation&list_uids=1321498

Benting, J. H.; Rietveld, A. G. and Simons, K. (1999): N-Glycans mediate the apical sorting of a GPI-anchored, raft-associated protein in Madin-Darby canine kidney cells, J Cell Biol (vol. 146), No. 2, pp. 313-20. URL: http://www.ncbi.nlm.nih.gov/entrez/query.fcgi?cmd=Retrieve&db=PubMed&dopt=Citation&list_uids=10427087

Bergers, G. and Coussens, L. M. (2000): Extrinsic regulators of epithelial tumor progression: metalloproteinases, Curr Opin Genet Dev (vol. 10), No. 1, pp. 120-7. URL: http://www.ncbi.nlm.nih.gov/entrez/query.fcgi?cmd=Retrieve&db=PubMed&dopt=Citation&list_uids=10679388

Berthoud, V. M.; Minogue, P. J.; Laing, J. G. and Beyer, E. C. (2004): Pathways for degradation of connexins and gap junctions, Cardiovasc Res (vol. 62), No. 2, pp. 256-67. URL: http://www.ncbi.nlm.nih.gov/entrez/query.fcgi?cmd=Retrieve&db=PubMed&dopt=Citation&list_uids=15094346

Bethune, J.; Wieland, F. and Moelleken, J. (2006): COPI-mediated transport, J Membr Biol (vol. 211), No. 2, pp. 65-79. URL: http://www.ncbi.nlm.nih.gov/entrez/query.fcgi?cmd=Retrieve&db=PubMed&dopt=Citation&list_uids=17041781

Bigay, J. and Antonny, B. (2005): Real-time assays for the assembly-disassembly cycle of COP coats on liposomes of defined size, Methods Enzymol (vol. 404), pp. 95-107. URL: http://www.ncbi.nlm.nih.gov/entrez/query.fcgi?cmd=Retrieve&db=PubMed&dopt=Citation&list_uids=16413261

Bigay, J.; Gounon, P.; Robineau, S. and Antonny, B. (2003): Lipid packing sensed by ArfGAP1 couples COPI coat disassembly to membrane bilayer curvature, Nature (vol. 426), No. 6966, pp. 563-6. URL: http://www.ncbi.nlm.nih.gov/entrez/query.fcgi?cmd=Retrieve&db=PubMed&dopt=Citation&list_uids=14654841

Bijlmakers, M. J. (2009): Protein acylation and localization in T cell signaling (Review), Mol Membr Biol (vol. 26), No. 1, pp. 93-103. URL:

http://www.ncbi.nlm.nih.gov/entrez/query.fcgi?cmd=Retrieve&db=PubMed&dopt=Citation&list_uids=19115146

Blott, E. J. and Griffiths, G. M. (2002): Secretory lysosomes, Nat Rev Mol Cell Biol (vol. 3), No. 2, pp. 122-31. URL: http://www.ncbi.nlm.nih.gov/entrez/query.fcgi?cmd=Retrieve&db=PubMed&dopt=Citation&list_uids=11836514

Boehm, M. and Bonifacino, J. S. (2001): Adaptins: the final recount, Mol Biol Cell (vol. 12), No. 10, pp. 2907-20. URL: http://www.ncbi.nlm.nih.gov/entrez/query.fcgi?cmd=Retrieve&db=PubMed&dopt=Citation&list_uids=11598180

Bonfanti, L.; Mironov, A. A., Jr.; Martinez-Menarguez, J. A.; Martella, O.; Fusella, A.; Baldassarre, M.; Buccione, R.; Geuze, H. J.; Mironov, A. A. and Luini, A. (1998): Procollagen traverses the Golgi stack without leaving the lumen of cisternae: evidence for cisternal maturation, Cell (vol. 95), No. 7, pp. 993-1003. URL: http://www.ncbi.nlm.nih.gov/entrez/query.fcgi?cmd=Retrieve&db=PubMed&dopt=Citation&list_uids=9875853

Bonifacino, J. S. and Glick, B. S. (2004): The mechanisms of vesicle budding and fusion, Cell (vol. 116), No. 2, pp. 153-66. URL: http://www.ncbi.nlm.nih.gov/entrez/query.fcgi?cmd=Retrieve&db=PubMed&dopt=Citation&list_uids=14744428

Bonifacino, J. S. and Lippincott-Schwartz, J. (2003): Coat proteins: shaping membrane transport, Nat Rev Mol Cell Biol (vol. 4), No. 5, pp. 409-14. URL: http://www.ncbi.nlm.nih.gov/entrez/query.fcgi?cmd=Retrieve&db=PubMed&dopt=Citation&list_uids=12728274

Bremser, M.; Nickel, W.; Schweikert, M.; Ravazzola, M.; Amherdt, M.; Hughes, C. A.; Sollner, T. H.; Rothman, J. E. and Wieland, F. T. (1999): Coupling of coat assembly and vesicle budding to packaging of putative cargo receptors, Cell (vol. 96), No. 4, pp. 495-506. URL: http://www.ncbi.nlm.nih.gov/entrez/query.fcgi?cmd=Retrieve&db=PubMed&dopt=Citation&list_uids=10052452

Brockhausen, I. (1999): Pathways of O-glycan biosynthesis in cancer cells, Biochim Biophys Acta (vol. 1473), No. 1, pp. 67-95. URL: http://www.ncbi.nlm.nih.gov/entrez/query.fcgi?cmd=Retrieve&db=PubMed&dopt=Citation&list_uids=10580130

Brockhausen, I. (2006): Mucin-type O-glycans in human colon and breast cancer: glycodynamics and functions, EMBO Rep (vol. 7), No. 6, pp. 599-604. URL: http://www.ncbi.nlm.nih.gov/entrez/query.fcgi?cmd=Retrieve&db=PubMed&dopt=Citation&list_uids=16741504

Brockhausen, I.; Yang, J.; Dickinson, N.; Ogata, S. and Itzkowitz, S. H. (1998): Enzymatic basis for sialyl-Tn expression in human colon cancer cells, Glycoconj J (vol. 15), No. 6, pp. 595-603. URL: http://www.ncbi.nlm.nih.gov/entrez/query.fcgi?cmd=Retrieve&db=PubMed&dopt=Citation&list_uids=9881766

Brockhausen, I.; Yang, J. M.; Burchell, J.; Whitehouse, C. and Taylor-Papadimitriou, J. (1995): Mechanisms underlying aberrant glycosylation of MUC1 mucin in breast cancer cells, Eur J Biochem (vol. 233), No. 2, pp. 607-17. URL: http://www.ncbi.nlm.nih.gov/entrez/query.fcgi?cmd=Retrieve&db=PubMed&dopt=Citation&list_uids=7588808

Budnik, A. and Stephens, D. J. (2009): ER exit sites--localization and control of COPII vesicle formation, FEBS Lett (vol. 583), No. 23, pp. 3796-803. URL: http://www.ncbi.nlm.nih.gov/entrez/query.fcgi?cmd=Retrieve&db=PubMed&dopt=Citation&list_uids=19850039

Burgoyne, R. D. and Morgan, A. (2003): Secretory granule exocytosis, Physiol Rev (vol. 83), No. 2, pp. 581-632. URL: http://www.ncbi.nlm.nih.gov/entrez/query.fcgi?cmd=Retrieve&db=PubMed&dopt=Citation&list_uids=12663867

Buxton, P.; Zhang, X. M.; Walsh, B.; Sriratana, A.; Schenberg, I.; Manickam, E. and Rowe, T. (2003): Identification and characterization of Snapin as a ubiquitously expressed SNARE-binding protein that interacts with SNAP23 in non-neuronal cells, Biochem J (vol. 375), No. Pt 2, pp. 433-40. URL: http://www.ncbi.nlm.nih.gov/entrez/query.fcgi?cmd=Retrieve&db=PubMed&dopt=Citation&list_uids=12877659

Cabrera, M.; Muniz, M.; Hidalgo, J.; Vega, L.; Martin, M. E. and Velasco, A. (2003): The retrieval function of the KDEL receptor requires PKA phosphorylation of its C-terminus, Mol Biol Cell (vol. 14), No. 10, pp. 4114-25. URL: http://www.ncbi.nlm.nih.gov/entrez/query.fcgi?cmd=Retrieve&db=PubMed&dopt=Citation&list_uids=14517323

Cai, H.; Reinisch, K. and Ferro-Novick, S. (2007): Coats, tethers, Rabs, and SNAREs work together to mediate the intracellular destination of a transport vesicle, Dev Cell (vol. 12), No. 5, pp. 671-82. URL: http://www.ncbi.nlm.nih.gov/entrez/query.fcgi?cmd=Retrieve&db=PubMed&dopt=Citation&list_uids=17488620

Cao, H.; Thompson, H. M.; Krueger, E. W. and McNiven, M. A. (2000): Disruption of Golgi structure and function in mammalian cells expressing a mutant dynamin, J Cell Sci (vol. 113 (Pt 11)), pp. 1993-2002. URL: http://www.ncbi.nlm.nih.gov/entrez/query.fcgi?cmd=Retrieve&db=PubMed&dopt=Citation&list_uids=10806110

Capitani, M. and Sallese, M. (2009): The KDEL receptor: new functions for an old protein, FEBS Lett (vol. 583), No. 23, pp. 3863-71. URL: http://www.ncbi.nlm.nih.gov/entrez/query.fcgi?cmd=Retrieve&db=PubMed&dopt=Citation&list_uids=19854180

Cavallaro, U. and Christofori, G. (2001): Cell adhesion in tumor invasion and metastasis: loss of the glue is not enough, Biochim Biophys Acta (vol. 1552), No. 1, pp. 39-45. URL: http://www.ncbi.nlm.nih.gov/entrez/query.fcgi?cmd=Retrieve&db=PubMed&dopt=Citation&list_uids=11781114

Chan, A. M. and Weber, T. (2002): A putative link between exocytosis and tumor development, Cancer Cell (vol. 2), No. 6, pp. 427-8. URL: http://www.ncbi.nlm.nih.gov/entrez/query.fcgi?cmd=Retrieve&db=PubMed&dopt=Citation&list_uids=12498708

Chapman, E. R. (2002): Synaptotagmin: a Ca(2+) sensor that triggers exocytosis?, Nat Rev Mol Cell Biol (vol. 3), No. 7, pp. 498-508. URL: http://www.ncbi.nlm.nih.gov/entrez/query.fcgi?cmd=Retrieve&db=PubMed&dopt=Citation&list_uids=12094216

Chardin, P.; Paris, S.; Antonny, B.; Robineau, S.; Beraud-Dufour, S.; Jackson, C. L. and Chabre, M. (1996): A human exchange factor for ARF contains Sec7- and pleckstrin-homology domains, Nature (vol. 384), No. 6608, pp. 481-4. URL: http://www.ncbi.nlm.nih.gov/entrez/query.fcgi?cmd=Retrieve&db=PubMed&dopt=Citation&list_uids=8945478

Chavrier, P.; Parton, R. G.; Hauri, H. P.; Simons, K. and Zerial, M. (1990): Localization of low molecular weight GTP binding proteins to exocytic and endocytic compartments, Cell (vol. 62), No. 2, pp. 317-29. URL: http://www.ncbi.nlm.nih.gov/entrez/query.fcgi?cmd=Retrieve&db=PubMed&dopt=Citation&list_uids=2115402

Cichon, G.; Schmidt, H. H.; Benhidjeb, T.; Loser, P.; Ziemer, S.; Haas, R.; Grewe, N.; Schnieders, F.; Heeren, J.; Manns, M. P.; Schlag, P. M. and Strauss, M. (1999): Intravenous administration of recombinant adenoviruses causes thrombocytopenia, anemia and erythroblastosis in rabbits, J Gene Med (vol. 1), No. 5, pp. 360-71. URL: http://www.ncbi.nlm.nih.gov/entrez/query.fcgi?cmd=Retrieve&db=PubMed&dopt=Citation&list_uids=10738553

Cole, N. B.; Sciaky, N.; Marotta, A.; Song, J. and Lippincott-Schwartz, J. (1996): Golgi dispersal during microtubule disruption: regeneration of Golgi stacks at peripheral endoplasmic reticulum exit sites, Mol Biol Cell (vol. 7), No. 4, pp. 631-50. URL: http://www.ncbi.nlm.nih.gov/entrez/query.fcgi?cmd=Retrieve&db=PubMed&dopt=Citation&list_uids=8730104

Cosson, P. and Letourneur, F. (1994): Coatomer interaction with di-lysine endoplasmic reticulum retention motifs, Science (vol. 263), No. 5153, pp. 1629-31. URL: http://www.ncbi.nlm.nih.gov/entrez/query.fcgi?cmd=Retrieve&db=PubMed&dopt=Citation&list_uids=8128252

Couse, J. F. and Korach, K. S. (1999): Estrogen receptor null mice: what have we learned and where will they lead us?, Endocr Rev (vol. 20), No. 3, pp. 358-417. URL: http://www.ncbi.nlm.nih.gov/entrez/query.fcgi?cmd=Retrieve&db=PubMed&dopt=Citation&list_uids=10368776

Coussens, L. M. and Werb, Z. (1996): Matrix metalloproteinases and the development of cancer, Chem Biol (vol. 3), No. 11, pp. 895-904. URL: http://www.ncbi.nlm.nih.gov/entrez/query.fcgi?cmd=Retrieve&db=PubMed&dopt=Citation&list_uids=8939708

Coussens, L. M. and Werb, Z. (2002): Inflammation and cancer, Nature (vol. 420), No. 6917, pp. 860-7. URL: http://www.ncbi.nlm.nih.gov/entrez/query.fcgi?cmd=Retrieve&db=PubMed&dopt=Citation&list_uids=12490959

Cudic, M.; Ertl, H. C. and Otvos, L., Jr. (2002): Synthesis, conformation and T-helper cell stimulation of an O-linked glycopeptide epitope containing extended carbohydrate side-chains, Bioorg Med Chem (vol. 10), No. 12, pp. 3859-70. URL: http://www.ncbi.nlm.nih.gov/entrez/query.fcgi?cmd=Retrieve&db=PubMed&dopt=Citation&list_uids=12413838

Cukierman, E.; Huber, I.; Rotman, M. and Cassel, D. (1995): The ARF1 GTPase-activating protein: zinc finger motif and Golgi complex localization, Science (vol. 270), No. 5244, pp. 1999-2002. URL: http://www.ncbi.nlm.nih.gov/entrez/query.fcgi?cmd=Retrieve&db=PubMed&dopt=Citation&list_uids=8533093

Dalziel, M.; Whitehouse, C.; McFarlane, I.; Brockhausen, I.; Gschmeissner, S.; Schwientek, T.; Clausen, H.; Burchell, J. M. and Taylor-Papadimitriou, J. (2001): The relative activities of the C2GnT1 and ST3Gal-I glycosyltransferases determine O-glycan structure and expression of a tumor-associated epitope on MUC1, J Biol Chem (vol. 276), No. 14, pp. 11007-15. URL: http://www.ncbi.nlm.nih.gov/entrez/query.fcgi?cmd=Retrieve&db=PubMed&dopt=Citation&list_uids=11118434

Daniels, R.; Svedine, S. and Hebert, D. N. (2004): N-linked carbohydrates act as lumenal maturation and quality control protein tags, Cell Biochem Biophys (vol. 41), No. 1, pp. 113-38. URL: http://www.ncbi.nlm.nih.gov/entrez/query.fcgi?cmd=Retrieve&db=PubMed&dopt=Citation&list_uids=15371643

de Renzis, S.; Sonnichsen, B. and Zerial, M. (2002): Divalent Rab effectors regulate the sub-compartmental organization and sorting of early endosomes, Nat Cell Biol (vol. 4), No. 2, pp. 124-33. URL: http://www.ncbi.nlm.nih.gov/entrez/query.fcgi?cmd=Retrieve&db=PubMed&dopt=Citation&list_uids=11788822

Delacour, D.; Gouyer, V.; Leteurtre, E.; Ait-Slimane, T.; Drobecq, H.; Lenoir, C.; Moreau-Hannedouche, O.; Trugnan, G. and Huet, G. (2003): 1-benzyl-2-acetamido-2-deoxy-alpha-D-galactopyranoside blocks the apical biosynthetic pathway in polarized HT-29 cells, J Biol Chem (vol. 278), No. 39, pp. 37799-809. URL: http://www.ncbi.nlm.nih.gov/entrez/query.fcgi?cmd=Retrieve&db=PubMed&dopt=Citation&list_uids=12855686

Dennis, J. W.; Granovsky, M. and Warren, C. E. (1999): Glycoprotein glycosylation and cancer progression, Biochim Biophys Acta (vol. 1473), No. 1, pp. 21-34. URL: http://www.ncbi.nlm.nih.gov/entrez/query.fcgi?cmd=Retrieve&db=PubMed&dopt=Citation&list_uids=10580127

Dinter, A. and Berger, E. G. (1998): Golgi-disturbing agents, Histochem Cell Biol (vol. 109), No. 5-6, pp. 571-90. URL: http://www.ncbi.nlm.nih.gov/entrez/query.fcgi?cmd=Retrieve&db=PubMed&dopt=Citation&list_uids=9681636

Donaldson, J. G.; Cassel, D.; Kahn, R. A. and Klausner, R. D. (1992): ADP-ribosylation factor, a small GTP-binding protein, is required for binding of the coatomer protein beta-COP to Golgi membranes, Proc Natl Acad Sci U S A (vol. 89), No. 14, pp. 6408-12. URL:

http://www.ncbi.nlm.nih.gov/entrez/query.fcgi?cmd=Retrieve&db=PubMed&dopt=Citation&list_uids=1631136

Dube, D. H. and Bertozzi, C. R. (2005): Glycans in cancer and inflammation--potential for therapeutics and diagnostics, Nat Rev Drug Discov (vol. 4), No. 6, pp. 477-88. URL: http://www.ncbi.nlm.nih.gov/entrez/query.fcgi?cmd=Retrieve&db=PubMed&dopt=Citation&list_uids=15931257

Duden, R.; Hosobuchi, M.; Hamamoto, S.; Winey, M.; Byers, B. and Schekman, R. (1994): Yeast beta- and beta'-coat proteins (COP). Two coatomer subunits essential for endoplasmic reticulum-to-Golgi protein traffic, J Biol Chem (vol. 269), No. 39, pp. 24486-95. URL: http://www.ncbi.nlm.nih.gov/entrez/query.fcgi?cmd=Retrieve&db=PubMed&dopt=Citation&list_uids=7929113

Duffield, A.; Caplan, M. J. and Muth, T. R. (2008): Protein trafficking in polarized cells, Int Rev Cell Mol Biol (vol. 270), pp. 145-79. URL: http://www.ncbi.nlm.nih.gov/entrez/query.fcgi?cmd=Retrieve&db=PubMed&dopt=Citation&list_uids=19081536

Egea, G.; Franci, C.; Gambus, G.; Lesuffleur, T.; Zweibaum, A. and Real, F. X. (1993): cis-Golgi resident proteins and O-glycans are abnormally compartmentalized in the RER of colon cancer cells, J Cell Sci (vol. 105 (Pt 3)), pp. 819-30. URL: http://www.ncbi.nlm.nih.gov/entrez/query.fcgi?cmd=Retrieve&db=PubMed&dopt=Citation&list_uids=7691849

Ellgaard, L.; Molinari, M. and Helenius, A. (1999): Setting the standards: quality control in the secretory pathway, Science (vol. 286), No. 5446, pp. 1882-8. URL: http://www.ncbi.nlm.nih.gov/entrez/query.fcgi?cmd=Retrieve&db=PubMed&dopt=Citation&list_uids=10583943

Ellies, L. G.; Tsuboi, S.; Petryniak, B.; Lowe, J. B.; Fukuda, M. and Marth, J. D. (1998): Core 2 oligosaccharide biosynthesis distinguishes between selectin ligands essential for leukocyte homing and inflammation, Immunity (vol. 9), No. 6, pp. 881-90. URL: http://www.ncbi.nlm.nih.gov/entrez/query.fcgi?cmd=Retrieve&db=PubMed&dopt=Citation&list_uids=9881978

Engelsberg, A.; Hermosilla, R.; Karsten, U.; Schulein, R.; Dorken, B. and Rehm, A. (2003): The Golgi protein RCAS1 controls cell surface expression of tumor-associated O-linked glycan antigens, J Biol Chem (vol. 278), No. 25, pp. 22998-3007. URL: http://www.ncbi.nlm.nih.gov/entrez/query.fcgi?cmd=Retrieve&db=PubMed&dopt=Citation&list_uids=12672804

Enjoji, M.; Nakashima, M.; Nishi, H.; Choi, I.; Oimomi, H.; Sugimoto, R.; Kotoh, K.; Taguchi, K.; Nakamuta, M.; Nawata, H. and Watanabe, T. (2002): The tumor-associated antigen, RCAS1, can be expressed in immune-mediated diseases as well as in carcinomas of biliary tract, J Hepatol (vol. 36), No. 6, pp. 786-92. URL: http://www.ncbi.nlm.nih.gov/entrez/query.fcgi?cmd=Retrieve&db=PubMed&dopt=Citation&list_uids=12044529

Evans, R. M. (1988): The steroid and thyroid hormone receptor superfamily, Science (vol. 240), No. 4854, pp. 889-95. URL: http://www.ncbi.nlm.nih.gov/entrez/query.fcgi?cmd=Retrieve&db=PubMed&dopt=Citation&list_uids=3283939

Field, M. C. and Wainwright, L. J. (1995): Molecular cloning of eukaryotic glycoprotein and glycolipid glycosyltransferases: a survey, Glycobiology (vol. 5), No. 5, pp. 463-72. URL: http://www.ncbi.nlm.nih.gov/entrez/query.fcgi?cmd=Retrieve&db=PubMed&dopt=Citation&list_uids=8563132

Finn, O. J. (2007): Human tumor immunology at the molecular divide, J Immunol (vol. 178), No. 5, pp. 2615-6. URL: http://www.ncbi.nlm.nih.gov/entrez/query.fcgi?cmd=Retrieve&db=PubMed&dopt=Citation&list_uids=17312098

Fransen, J. A.; Hauri, H. P.; Ginsel, L. A. and Naim, H. Y. (1991): Naturally occurring mutations in intestinal sucrase-isomaltase provide evidence for the existence of an intracellular sorting signal in the isomaltase subunit, J Cell Biol (vol. 115), No. 1, pp. 45-57. URL:

http://www.ncbi.nlm.nih.gov/entrez/query.fcgi?cmd=Retrieve&db=PubMed&dopt=Citation&list_uids=1717481

Freire, T.; Bay, S.; von Mensdorff-Pouilly, S. and Osinaga, E. (2005): Molecular basis of incomplete O-glycan synthesis in MCF-7 breast cancer cells: putative role of MUC6 in Tn antigen expression, Cancer Res (vol. 65), No. 17, pp. 7880-7. URL: http://www.ncbi.nlm.nih.gov/entrez/query.fcgi?cmd=Retrieve&db=PubMed&dopt=Citation&list_uids=16140958

Friedl, P.; den Boer, A. T. and Gunzer, M. (2005): Tuning immune responses: diversity and adaptation of the immunological synapse, Nat Rev Immunol (vol. 5), No. 7, pp. 532-45. URL: http://www.ncbi.nlm.nih.gov/entrez/query.fcgi?cmd=Retrieve&db=PubMed&dopt=Citation&list_uids=15999094

Frigerio, G.; Grimsey, N.; Dale, M.; Majoul, I. and Duden, R. (2007): Two human ARFGAPs associated with COP-I-coated vesicles, Traffic (vol. 8), No. 11, pp. 1644-55. URL: http://www.ncbi.nlm.nih.gov/entrez/query.fcgi?cmd=Retrieve&db=PubMed&dopt=Citation&list_uids=17760859

Fukuda, M. (2002): Roles of mucin-type O-glycans in cell adhesion, Biochim Biophys Acta (vol. 1573), No. 3, pp. 394-405. URL: http://www.ncbi.nlm.nih.gov/entrez/query.fcgi?cmd=Retrieve&db=PubMed&dopt=Citation&list_uids=12417424

Galien, R. and Garcia, T. (1997): Estrogen receptor impairs interleukin-6 expression by preventing protein binding on the NF-kappaB site, Nucleic Acids Res (vol. 25), No. 12, pp. 2424-9. URL: http://www.ncbi.nlm.nih.gov/entrez/query.fcgi?cmd=Retrieve&db=PubMed&dopt=Citation&list_uids=9171095

Galvan, M.; Murali-Krishna, K.; Ming, L. L.; Baum, L. and Ahmed, R. (1998): Alterations in cell surface carbohydrates on T cells from virally infected mice can distinguish effector/memory CD8+ T cells from naive cells, J Immunol (vol. 161), No. 2, pp. 641-8. URL: http://www.ncbi.nlm.nih.gov/entrez/query.fcgi?cmd=Retrieve&db=PubMed&dopt=Citation&list_uids=9670938

Gilchrist, A.; Au, C. E.; Hiding, J.; Bell, A. W.; Fernandez-Rodriguez, J.; Lesimple, S.; Nagaya, H.; Roy, L.; Gosline, S. J.; Hallett, M.; Paiement, J.; Kearney, R. E.; Nilsson, T. and Bergeron, J. J. (2006): Quantitative proteomics analysis of the secretory pathway, Cell (vol. 127), No. 6, pp. 1265-81. URL: http://www.ncbi.nlm.nih.gov/entrez/query.fcgi?cmd=Retrieve&db=PubMed&dopt=Citation&list_uids=17174899

E:\Jana\PhD_thesis\Publications\Jana\09_Developmental_Cell\280909_Script_AR.doc

Girod, A.; Storrie, B.; Simpson, J. C.; Johannes, L.; Goud, B.; Roberts, L. M.; Lord, J. M.; Nilsson, T. and Pepperkok, R. (1999): Evidence for a COP-I-independent transport route from the Golgi complex to the endoplasmic reticulum, Nat Cell Biol (vol. 1), No. 7, pp. 423-30. URL: http://www.ncbi.nlm.nih.gov/entrez/query.fcgi?cmd=Retrieve&db=PubMed&dopt=Citation&list_uids=10559986

Glick, B. S.; Elston, T. and Oster, G. (1997): A cisternal maturation mechanism can explain the asymmetry of the Golgi stack, FEBS Lett (vol. 414), No. 2, pp. 177-81. URL: http://www.ncbi.nlm.nih.gov/entrez/query.fcgi?cmd=Retrieve&db=PubMed&dopt=Citation&list_uids=9315681

Glinskii, O. V.; Turk, J. R.; Pienta, K. J.; Huxley, V. H. and Glinsky, V. V. (2004): Evidence of porcine and human endothelium activation by cancer-associated carbohydrates expressed on glycoproteins and tumour cells, J Physiol (vol. 554), No. Pt 1, pp. 89-99. URL: http://www.ncbi.nlm.nih.gov/entrez/query.fcgi?cmd=Retrieve&db=PubMed&dopt=Citation&list_uids=14678494

Goldberg, J. (2000): Decoding of sorting signals by coatomer through a GTPase switch in the COPI coat complex, Cell (vol. 100), No. 6, pp. 671-9. URL: http://www.ncbi.nlm.nih.gov/entrez/query.fcgi?cmd=Retrieve&db=PubMed&dopt=Citation&list_uids=10761932

Goldenberg, N. M. and Silverman, M. (2009): Rab34 and its effector munc13-2 constitute a new pathway modulating protein secretion in the cellular response to hyperglycemia, Am J Physiol Cell Physiol (vol.

297), No. 4, pp. C1053-8. URL: http://www.ncbi.nlm.nih.gov/entrez/query.fcgi?cmd=Retrieve&db=PubMed&dopt=Citation&list_uids=19641095

Goodwin, J. S.; Drake, K. R.; Rogers, C.; Wright, L.; Lippincott-Schwartz, J.; Philips, M. R. and Kenworthy, A. K. (2005): Depalmitoylated Ras traffics to and from the Golgi complex via a nonvesicular pathway, J Cell Biol (vol. 170), No. 2, pp. 261-72. URL: http://www.ncbi.nlm.nih.gov/entrez/query.fcgi?cmd=Retrieve&db=PubMed&dopt=Citation&list_uids=16027222

Granovsky, M.; Fata, J.; Pawling, J.; Muller, W. J.; Khokha, R. and Dennis, J. W. (2000): Suppression of tumor growth and metastasis in Mgat5-deficient mice, Nat Med (vol. 6), No. 3, pp. 306-12. URL: http://www.ncbi.nlm.nih.gov/entrez/query.fcgi?cmd=Retrieve&db=PubMed&dopt=Citation&list_uids=10700233

Griffiths, G.; Pepperkok, R.; Locker, J. K. and Kreis, T. E. (1995): Immunocytochemical localization of beta-COP to the ER-Golgi boundary and the TGN, J Cell Sci (vol. 108 (Pt 8)), pp. 2839-56. URL: http://www.ncbi.nlm.nih.gov/entrez/query.fcgi?cmd=Retrieve&db=PubMed&dopt=Citation&list_uids=7593324

Gu, F.; Crump, C. M. and Thomas, G. (2001): Trans-Golgi network sorting, Cell Mol Life Sci (vol. 58), No. 8, pp. 1067-84. URL: http://www.ncbi.nlm.nih.gov/entrez/query.fcgi?cmd=Retrieve&db=PubMed&dopt=Citation&list_uids=11529500

Guan, J. L.; Machamer, C. E. and Rose, J. K. (1985): Glycosylation allows cell-surface transport of an anchored secretory protein, Cell (vol. 42), No. 2, pp. 489-96. URL: http://www.ncbi.nlm.nih.gov/entrez/query.fcgi?cmd=Retrieve&db=PubMed&dopt=Citation&list_uids=3928168

Hakomori, S. (1989): Aberrant glycosylation in tumors and tumor-associated carbohydrate antigens, Adv Cancer Res (vol. 52), pp. 257-331. URL: http://www.ncbi.nlm.nih.gov/entrez/query.fcgi?cmd=Retrieve&db=PubMed&dopt=Citation&list_uids=2662714

Hakomori, S. (1996): Tumor malignancy defined by aberrant glycosylation and sphingo(glyco)lipid metabolism, Cancer Res (vol. 56), No. 23, pp. 5309-18. URL: http://www.ncbi.nlm.nih.gov/entrez/query.fcgi?cmd=Retrieve&db=PubMed&dopt=Citation&list_uids=8968075

Hakomori, S. (2002): Glycosylation defining cancer malignancy: new wine in an old bottle, Proc Natl Acad Sci U S A (vol. 99), No. 16, pp. 10231-3. URL: http://www.ncbi.nlm.nih.gov/entrez/query.fcgi?cmd=Retrieve&db=PubMed&dopt=Citation&list_uids=12149519

Hanahan, D. and Weinberg, R. A. (2000): The hallmarks of cancer, Cell (vol. 100), No. 1, pp. 57-70. URL: http://www.ncbi.nlm.nih.gov/entrez/query.fcgi?cmd=Retrieve&db=PubMed&dopt=Citation&list_uids=10647931

Hanover, J. A.; Willingham, M. C. and Pastan, I. (1984): Kinetics of transit of transferrin and epidermal growth factor through clathrin-coated membranes, Cell (vol. 39), No. 2 Pt 1, pp. 283-93. URL: http://www.ncbi.nlm.nih.gov/entrez/query.fcgi?cmd=Retrieve&db=PubMed&dopt=Citation&list_uids=6149810

Harter, C. and Reinhard, C. (2000): The secretory pathway from history to the state of the art, Subcell Biochem (vol. 34), pp. 1-38. URL: http://www.ncbi.nlm.nih.gov/entrez/query.fcgi?cmd=Retrieve&db=PubMed&dopt=Citation&list_uids=10808330

Harter, C. and Wieland, F. (1996): The secretory pathway: mechanisms of protein sorting and transport, Biochim Biophys Acta (vol. 1286), No. 2, pp. 75-93. URL: http://www.ncbi.nlm.nih.gov/entrez/query.fcgi?cmd=Retrieve&db=PubMed&dopt=Citation&list_uids=8652612

Hauri, H.; Appenzeller, C.; Kuhn, F. and Nufer, O. (2000): Lectins and traffic in the secretory pathway, FEBS Lett (vol. 476), No. 1-2, pp. 32-7. URL:

http://www.ncbi.nlm.nih.gov/entrez/query.fcgi?cmd=Retrieve&db=PubMed&dopt=Citation&list_uids=10878245

Hauri, H. P.; Kappeler, F.; Andersson, H. and Appenzeller, C. (2000): ERGIC-53 and traffic in the secretory pathway, J Cell Sci (vol. 113 (Pt 4)), pp. 587-96. URL: http://www.ncbi.nlm.nih.gov/entrez/query.fcgi?cmd=Retrieve&db=PubMed&dopt=Citation&list_uids=10652252

Hebert, D. N.; Foellmer, B. and Helenius, A. (1995): Glucose trimming and reglucosylation determine glycoprotein association with calnexin in the endoplasmic reticulum, Cell (vol. 81), No. 3, pp. 425-33. URL: http://www.ncbi.nlm.nih.gov/entrez/query.fcgi?cmd=Retrieve&db=PubMed&dopt=Citation&list_uids=7736594

Hebert, D. N.; Garman, S. C. and Molinari, M. (2005): The glycan code of the endoplasmic reticulum: asparagine-linked carbohydrates as protein maturation and quality-control tags, Trends Cell Biol (vol. 15), No. 7, pp. 364-70. URL: http://www.ncbi.nlm.nih.gov/entrez/query.fcgi?cmd=Retrieve&db=PubMed&dopt=Citation&list_uids=15939591

Helenius, A. and Aebi, M. (2001): Intracellular functions of N-linked glycans, Science (vol. 291), No. 5512, pp. 2364-9. URL: http://www.ncbi.nlm.nih.gov/entrez/query.fcgi?cmd=Retrieve&db=PubMed&dopt=Citation&list_uids=11269317

Helenius, A. and Aebi, M. (2004): Roles of N-linked glycans in the endoplasmic reticulum, Annu Rev Biochem (vol. 73), pp. 1019-49. URL: http://www.ncbi.nlm.nih.gov/entrez/query.fcgi?cmd=Retrieve&db=PubMed&dopt=Citation&list_uids=15189166

Henderson, B. E. and Feigelson, H. S. (2000): Hormonal carcinogenesis, Carcinogenesis (vol. 21), No. 3, pp. 427-33. URL: http://www.ncbi.nlm.nih.gov/entrez/query.fcgi?cmd=Retrieve&db=PubMed&dopt=Citation&list_uids=10688862

Hirst, J.; Motley, A.; Harasaki, K.; Peak Chew, S. Y. and Robinson, M. S. (2003): EpsinR: an ENTH domain-containing protein that interacts with AP-1, Mol Biol Cell (vol. 14), No. 2, pp. 625-41. URL: http://www.ncbi.nlm.nih.gov/entrez/query.fcgi?cmd=Retrieve&db=PubMed&dopt=Citation&list_uids=12589059

Hoffman, G. R.; Rahl, P. B.; Collins, R. N. and Cerione, R. A. (2003): Conserved structural motifs in intracellular trafficking pathways: structure of the gammaCOP appendage domain, Mol Cell (vol. 12), No. 3, pp. 615-25. URL: http://www.ncbi.nlm.nih.gov/entrez/query.fcgi?cmd=Retrieve&db=PubMed&dopt=Citation&list_uids=14527408

Hong, X.; Liu, Y.; Hu, G.; Zhao, D.; Shen, J.; Shen, F.; Cao, X. and Wang, Q. (2009): EBAG9 inducing hyporesponsiveness of T cells promotes tumor growth and metastasis in 4T1 murine mammary carcinoma, Cancer Sci (vol. 100), No. 5, pp. 961-9. URL: http://www.ncbi.nlm.nih.gov/entrez/query.fcgi?cmd=Retrieve&db=PubMed&dopt=Citation&list_uids=19445026

Hosobuchi, M.; Kreis, T. and Schekman, R. (1992): SEC21 is a gene required for ER to Golgi protein transport that encodes a subunit of a yeast coatomer, Nature (vol. 360), No. 6404, pp. 603-5. URL: http://www.ncbi.nlm.nih.gov/entrez/query.fcgi?cmd=Retrieve&db=PubMed&dopt=Citation&list_uids=1461285

Hsu, V. W.; Lee, S. Y. and Yang, J. S. (2009): The evolving understanding of COPI vesicle formation, Nat Rev Mol Cell Biol (vol. 10), No. 5, pp. 360-4. URL: http://www.ncbi.nlm.nih.gov/entrez/query.fcgi?cmd=Retrieve&db=PubMed&dopt=Citation&list_uids=19293819

Huet, G.; Gouyer, V.; Delacour, D.; Richet, C.; Zanetta, J. P.; Delannoy, P. and Degand, P. (2003): Involvement of glycosylation in the intracellular trafficking of glycoproteins in polarized epithelial cells, Biochimie (vol. 85), No. 3-4, pp. 323-30. URL: http://www.ncbi.nlm.nih.gov/entrez/query.fcgi?cmd=Retrieve&db=PubMed&dopt=Citation&list_uids=12770771

Hughes, H. and Stephens, D. J. (2008): Assembly, organization, and function of the COPII coat, Histochem Cell Biol (vol. 129), No. 2, pp. 129-51. URL: http://www.ncbi.nlm.nih.gov/entrez/query.fcgi?cmd=Retrieve&db=PubMed&dopt=Citation&list_uids=18060556

Ikeda, K.; Sato, M.; Tsutsumi, O.; Tsuchiya, F.; Tsuneizumi, M.; Emi, M.; Imoto, I.; Inazawa, J.; Muramatsu, M. and Inoue, S. (2000): Promoter analysis and chromosomal mapping of human EBAG9 gene, Biochem Biophys Res Commun (vol. 273), No. 2, pp. 654-60. URL: http://www.ncbi.nlm.nih.gov/entrez/query.fcgi?cmd=Retrieve&db=PubMed&dopt=Citation&list_uids=10873660

Ikonen, E. and Simons, K. (1998): Protein and lipid sorting from the trans-Golgi network to the plasma membrane in polarized cells, Semin Cell Dev Biol (vol. 9), No. 5, pp. 503-9. URL: http://www.ncbi.nlm.nih.gov/entrez/query.fcgi?cmd=Retrieve&db=PubMed&dopt=Citation&list_uids=9835637

Ilardi, J. M.; Mochida, S. and Sheng, Z. H. (1999): Snapin: a SNARE-associated protein implicated in synaptic transmission, Nat Neurosci (vol. 2), No. 2, pp. 119-24. URL: http://www.ncbi.nlm.nih.gov/entrez/query.fcgi?cmd=Retrieve&db=PubMed&dopt=Citation&list_uids=10195194

Inoue, H. and Randazzo, P. A. (2007): Arf GAPs and their interacting proteins, Traffic (vol. 8), No. 11, pp. 1465-75. URL: http://www.ncbi.nlm.nih.gov/entrez/query.fcgi?cmd=Retrieve&db=PubMed&dopt=Citation&list_uids=17666108

Irimura, T.; Denda, K.; Iida, S.; Takeuchi, H. and Kato, K. (1999): Diverse glycosylation of MUC1 and MUC2: potential significance in tumor immunity, J Biochem (vol. 126), No. 6, pp. 975-85. URL: http://www.ncbi.nlm.nih.gov/entrez/query.fcgi?cmd=Retrieve&db=PubMed&dopt=Citation&list_uids=10578046

Itin, C.; Foguet, M.; Kappeler, F.; Klumperman, J. and Hauri, H. P. (1995): Recycling of the endoplasmic reticulum/Golgi intermediate compartment protein ERGIC-53 in the secretory pathway, Biochem Soc Trans (vol. 23), No. 3, pp. 541-4. URL: http://www.ncbi.nlm.nih.gov/entrez/query.fcgi?cmd=Retrieve&db=PubMed&dopt=Citation&list_uids=8566411

Izumi, M.; Nakanishi, Y.; Yoshino, I.; Nakashima, M.; Watanabe, T. and Hara, N. (2001): Expression of tumor-associated antigen RCAS1 correlates significantly with poor prognosis in nonsmall cell lung carcinoma, Cancer (vol. 92), No. 2, pp. 446-51. URL: http://www.ncbi.nlm.nih.gov/entrez/query.fcgi?cmd=Retrieve&db=PubMed&dopt=Citation&list_uids=11466701

Jackson, C. L. (2009): Mechanisms of transport through the Golgi complex, J Cell Sci (vol. 122), No. Pt 4, pp. 443-52. URL: http://www.ncbi.nlm.nih.gov/entrez/query.fcgi?cmd=Retrieve&db=PubMed&dopt=Citation&list_uids=19193869

Jackson, C. L. and Casanova, J. E. (2000): Turning on ARF: the Sec7 family of guanine-nucleotide-exchange factors, Trends Cell Biol (vol. 10), No. 2, pp. 60-7. URL: http://www.ncbi.nlm.nih.gov/entrez/query.fcgi?cmd=Retrieve&db=PubMed&dopt=Citation&list_uids=10652516

Jahn, R. and Scheller, R. H. (2006): SNAREs--engines for membrane fusion, Nat Rev Mol Cell Biol (vol. 7), No. 9, pp. 631-43. URL: http://www.ncbi.nlm.nih.gov/entrez/query.fcgi?cmd=Retrieve&db=PubMed&dopt=Citation&list_uids=16912714

Jelinek-Kelly, S.; Akiyama, T.; Saunier, B.; Tkacz, J. S. and Herscovics, A. (1985): Characterization of a specific alpha-mannosidase involved in oligosaccharide processing in Saccharomyces cerevisiae, J Biol Chem (vol. 260), No. 4, pp. 2253-7. URL: http://www.ncbi.nlm.nih.gov/entrez/query.fcgi?cmd=Retrieve&db=PubMed&dopt=Citation&list_uids=3882690

Jensen, T.; Nielsen, M.; Gad, M.; Hansen, P.; Komba, S.; Meldal, M.; Odum, N. and Werdelin, O. (2001): Radically altered T cell receptor signaling in glycopeptide-specific T cell hybridoma induced by antigen with minimal differences in the glycan group, Eur J Immunol (vol. 31), No. 11, pp. 3197-206. URL:

http://www.ncbi.nlm.nih.gov/entrez/query.fcgi?cmd=Retrieve&db=PubMed&dopt=Citation&list_uids=11745336

Johannes, L. (2002): The epithelial cell cytoskeleton and intracellular trafficking. I. Shiga toxin B-subunit system: retrograde transport, intracellular vectorization, and more, Am J Physiol Gastrointest Liver Physiol (vol. 283), No. 1, pp. G1-7. URL: http://www.ncbi.nlm.nih.gov/entrez/query.fcgi?cmd=Retrieve&db=PubMed&dopt=Citation&list_uids=12065285

Johnsen, M.; Lund, L. R.; Romer, J.; Almholt, K. and Dano, K. (1998): Cancer invasion and tissue remodeling: common themes in proteolytic matrix degradation, Curr Opin Cell Biol (vol. 10), No. 5, pp. 667-71. URL: http://www.ncbi.nlm.nih.gov/entrez/query.fcgi?cmd=Retrieve&db=PubMed&dopt=Citation&list_uids=9818179

Ju, T.; Aryal, R. P.; Stowell, C. J. and Cummings, R. D. (2008): Regulation of protein O-glycosylation by the endoplasmic reticulum-localized molecular chaperone Cosmc, J Cell Biol (vol. 182), No. 3, pp. 531-42. URL: http://www.ncbi.nlm.nih.gov/entrez/query.fcgi?cmd=Retrieve&db=PubMed&dopt=Citation&list_uids=18695044

Ju, T. and Cummings, R. D. (2002): A unique molecular chaperone Cosmc required for activity of the mammalian core 1 beta 3-galactosyltransferase, Proc Natl Acad Sci U S A (vol. 99), No. 26, pp. 16613-8. URL: http://www.ncbi.nlm.nih.gov/entrez/query.fcgi?cmd=Retrieve&db=PubMed&dopt=Citation&list_uids=12464682

Ju, T.; Cummings, R. D. and Canfield, W. M. (2002): Purification, characterization, and subunit structure of rat core 1 Beta1,3-galactosyltransferase, J Biol Chem (vol. 277), No. 1, pp. 169-77. URL: http://www.ncbi.nlm.nih.gov/entrez/query.fcgi?cmd=Retrieve&db=PubMed&dopt=Citation&list_uids=11673471

Julien, S.; Grimshaw, M. J.; Sutton-Smith, M.; Coleman, J.; Morris, H. R.; Dell, A.; Taylor-Papadimitriou, J. and Burchell, J. M. (2007): Sialyl-Lewis(x) on P-selectin glycoprotein ligand-1 is regulated during differentiation and maturation of dendritic cells: a mechanism involving the glycosyltransferases C2GnT1 and ST3Gal I, J Immunol (vol. 179), No. 9, pp. 5701-10. URL: http://www.ncbi.nlm.nih.gov/entrez/query.fcgi?cmd=Retrieve&db=PubMed&dopt=Citation&list_uids=17947642

Julien, S.; Krzewinski-Recchi, M. A.; Harduin-Lepers, A.; Gouyer, V.; Huet, G.; Le Bourhis, X. and Delannoy, P. (2001): Expression of sialyl-Tn antigen in breast cancer cells transfected with the human CMP-Neu5Ac: GalNAc alpha2,6-sialyltransferase (ST6GalNac I) cDNA, Glycoconj J (vol. 18), No. 11-12, pp. 883-93. URL: http://www.ncbi.nlm.nih.gov/entrez/query.fcgi?cmd=Retrieve&db=PubMed&dopt=Citation&list_uids=12820722

Keller, P.; Toomre, D.; Diaz, E.; White, J. and Simons, K. (2001): Multicolour imaging of post-Golgi sorting and trafficking in live cells, Nat Cell Biol (vol. 3), No. 2, pp. 140-9. URL: http://www.ncbi.nlm.nih.gov/entrez/query.fcgi?cmd=Retrieve&db=PubMed&dopt=Citation&list_uids=11175746

Khvotchev, M. V.; Ren, M.; Takamori, S.; Jahn, R. and Sudhof, T. C. (2003): Divergent functions of neuronal Rab11b in Ca2+-regulated versus constitutive exocytosis, J Neurosci (vol. 23), No. 33, pp. 10531-9. URL: http://www.ncbi.nlm.nih.gov/entrez/query.fcgi?cmd=Retrieve&db=PubMed&dopt=Citation&list_uids=14627637

Kino, T. and Chrousos, G. P. (2009): Tumor-associated, estrogen receptor-related antigen EBAG9: linking intracellular vesicle trafficking, immune homeostasis, and malignancy, Mol Interv (vol. 9), No. 6, pp. 294-8. URL: http://www.ncbi.nlm.nih.gov/entrez/query.fcgi?cmd=Retrieve&db=PubMed&dopt=Citation&list_uids=20048134

Kirchhausen, T.; Boll, W.; van Oijen, A. and Ehrlich, M. (2005): Single-molecule live-cell imaging of clathrin-based endocytosis, Biochem Soc Symp, No. 72, pp. 71-6. URL:

http://www.ncbi.nlm.nih.gov/entrez/query.fcgi?cmd=Retrieve&db=PubMed&dopt=Citation&list_uids=15649131

Klumperman, J.; Schweizer, A.; Clausen, H.; Tang, B. L.; Hong, W.; Oorschot, V. and Hauri, H. P. (1998): The recycling pathway of protein ERGIC-53 and dynamics of the ER-Golgi intermediate compartment, J Cell Sci (vol. 111 (Pt 22)), pp. 3411-25. URL: http://www.ncbi.nlm.nih.gov/entrez/query.fcgi?cmd=Retrieve&db=PubMed&dopt=Citation&list_uids=9788882

Komm, B. S.; Terpening, C. M.; Benz, D. J.; Graeme, K. A.; Gallegos, A.; Korc, M.; Greene, G. L.; O'Malley, B. W. and Haussler, M. R. (1988): Estrogen binding, receptor mRNA, and biologic response in osteoblast-like osteosarcoma cells, Science (vol. 241), No. 4861, pp. 81-4. URL: http://www.ncbi.nlm.nih.gov/entrez/query.fcgi?cmd=Retrieve&db=PubMed&dopt=Citation&list_uids=3164526

Kornfeld, R. and Kornfeld, S. (1985): Assembly of asparagine-linked oligosaccharides, Annu Rev Biochem (vol. 54), pp. 631-64. URL: http://www.ncbi.nlm.nih.gov/entrez/query.fcgi?cmd=Retrieve&db=PubMed&dopt=Citation&list_uids=3896128

Koval, M. and Pagano, R. E. (1991): Intracellular transport and metabolism of sphingomyelin, Biochim Biophys Acta (vol. 1082), No. 2, pp. 113-25. URL: http://www.ncbi.nlm.nih.gov/entrez/query.fcgi?cmd=Retrieve&db=PubMed&dopt=Citation&list_uids=2007175

Ktistakis, N. T.; Kao, C. Y.; Wang, R. H. and Roth, M. G. (1995): A fluorescent lipid analogue can be used to monitor secretory activity and for isolation of mammalian secretion mutants, Mol Biol Cell (vol. 6), No. 2, pp. 135-50. URL: http://www.ncbi.nlm.nih.gov/entrez/query.fcgi?cmd=Retrieve&db=PubMed&dopt=Citation&list_uids=7787242

Kumagai, J.; Urano, T.; Ogushi, T.; Takahashi, S.; Horie-Inoue, K.; Fujimura, T.; Azuma, K.; Muramatsu, M.; Ouchi, Y.; Kitamura, T. and Inoue, S. (2009): EBAG9 is a tumor-promoting and prognostic factor for bladder cancer, Int J Cancer (vol. 124), No. 4, pp. 799-805. URL: http://www.ncbi.nlm.nih.gov/entrez/query.fcgi?cmd=Retrieve&db=PubMed&dopt=Citation&list_uids=19030177

Kupfer, A. and Singer, S. J. (1989): Cell biology of cytotoxic and helper T cell functions: immunofluorescence microscopic studies of single cells and cell couples, Annu Rev Immunol (vol. 7), pp. 309-37. URL: http://www.ncbi.nlm.nih.gov/entrez/query.fcgi?cmd=Retrieve&db=PubMed&dopt=Citation&list_uids=2523714

Lee, M. C.; Miller, E. A.; Goldberg, J.; Orci, L. and Schekman, R. (2004): Bi-directional protein transport between the ER and Golgi, Annu Rev Cell Dev Biol (vol. 20), pp. 87-123. URL: http://www.ncbi.nlm.nih.gov/entrez/query.fcgi?cmd=Retrieve&db=PubMed&dopt=Citation&list_uids=15473836

Leteurtre, E.; Gouyer, V.; Delacour, D.; Hemon, B.; Pons, A.; Richet, C.; Zanetta, J. P. and Huet, G. (2003): Induction of a storage phenotype and abnormal intracellular localization of apical glycoproteins are two independent responses to GalNAcalpha-O-bn, J Histochem Cytochem (vol. 51), No. 3, pp. 349-61. URL: http://www.ncbi.nlm.nih.gov/entrez/query.fcgi?cmd=Retrieve&db=PubMed&dopt=Citation&list_uids=12588963

Letourneur, F.; Gaynor, E. C.; Hennecke, S.; Demolliere, C.; Duden, R.; Emr, S. D.; Riezman, H. and Cosson, P. (1994): Coatomer is essential for retrieval of dilysine-tagged proteins to the endoplasmic reticulum, Cell (vol. 79), No. 7, pp. 1199-207. URL: http://www.ncbi.nlm.nih.gov/entrez/query.fcgi?cmd=Retrieve&db=PubMed&dopt=Citation&list_uids=8001155

Lewin, D. A.; Sheff, D.; Ooi, C. E.; Whitney, J. A.; Yamamoto, E.; Chicione, L. M.; Webster, P.; Bonifacino, J. S. and Mellman, I. (1998): Cloning, expression, and localization of a novel gamma-adaptin-like molecule, FEBS Lett (vol. 435), No. 2-3, pp. 263-8. URL: http://www.ncbi.nlm.nih.gov/entrez/query.fcgi?cmd=Retrieve&db=PubMed&dopt=Citation&list_uids=9762922

Lewis, M. J. and Pelham, H. R. (1990): A human homologue of the yeast HDEL receptor, Nature (vol. 348), No. 6297, pp. 162-3. URL: http://www.ncbi.nlm.nih.gov/entrez/query.fcgi?cmd=Retrieve&db=PubMed&dopt=Citation&list_uids=2172835

Lewis, M. J. and Pelham, H. R. (1992): Ligand-induced redistribution of a human KDEL receptor from the Golgi complex to the endoplasmic reticulum, Cell (vol. 68), No. 2, pp. 353-64. URL: http://www.ncbi.nlm.nih.gov/entrez/query.fcgi?cmd=Retrieve&db=PubMed&dopt=Citation&list_uids=1310258

Lippincott-Schwartz, J. (1998): Cytoskeletal proteins and Golgi dynamics, Curr Opin Cell Biol (vol. 10), No. 1, pp. 52-9. URL: http://www.ncbi.nlm.nih.gov/entrez/query.fcgi?cmd=Retrieve&db=PubMed&dopt=Citation&list_uids=9484595

Lippincott-Schwartz, J.; Donaldson, J. G.; Schweizer, A.; Berger, E. G.; Hauri, H. P.; Yuan, L. C. and Klausner, R. D. (1990): Microtubule-dependent retrograde transport of proteins into the ER in the presence of brefeldin A suggests an ER recycling pathway, Cell (vol. 60), No. 5, pp. 821-36. URL: http://www.ncbi.nlm.nih.gov/entrez/query.fcgi?cmd=Retrieve&db=PubMed&dopt=Citation&list_uids=2178778

Liu, W.; Duden, R.; Phair, R. D. and Lippincott-Schwartz, J. (2005): ArfGAP1 dynamics and its role in COPI coat assembly on Golgi membranes of living cells, J Cell Biol (vol. 168), No. 7, pp. 1053-63. URL: http://www.ncbi.nlm.nih.gov/entrez/query.fcgi?cmd=Retrieve&db=PubMed&dopt=Citation&list_uids=15795316

Lowe, J. B. (2001): Glycosylation, immunity, and autoimmunity, Cell (vol. 104), No. 6, pp. 809-12. URL: http://www.ncbi.nlm.nih.gov/entrez/query.fcgi?cmd=Retrieve&db=PubMed&dopt=Citation&list_uids=11290318

Luna, A.; Matas, O. B.; Martinez-Menarguez, J. A.; Mato, E.; Duran, J. M.; Ballesta, J.; Way, M. and Egea, G. (2002): Regulation of protein transport from the Golgi complex to the endoplasmic reticulum by CDC42 and N-WASP, Mol Biol Cell (vol. 13), No. 3, pp. 866-79. URL: http://www.ncbi.nlm.nih.gov/entrez/query.fcgi?cmd=Retrieve&db=PubMed&dopt=Citation&list_uids=11907268

Lupas, A.; Van Dyke, M. and Stock, J. (1991): Predicting coiled coils from protein sequences, Science (vol. 252), No. 5009, pp. 1162-4. URL: http://www.ncbi.nlm.nih.gov/entrez/query.fcgi?cmd=Retrieve&db=PubMed&dopt=Citation&list_uids=17797907

Majoul, I.; Sohn, K.; Wieland, F. T.; Pepperkok, R.; Pizza, M.; Hillemann, J. and Soling, H. D. (1998): KDEL receptor (Erd2p)-mediated retrograde transport of the cholera toxin A subunit from the Golgi involves COPI, p23, and the COOH terminus of Erd2p, J Cell Biol (vol. 143), No. 3, pp. 601-12. URL: http://www.ncbi.nlm.nih.gov/entrez/query.fcgi?cmd=Retrieve&db=PubMed&dopt=Citation&list_uids=9813083

Makler, V.; Cukierman, E.; Rotman, M.; Admon, A. and Cassel, D. (1995): ADP-ribosylation factor-directed GTPase-activating protein. Purification and partial characterization, J Biol Chem (vol. 270), No. 10, pp. 5232-7. URL: http://www.ncbi.nlm.nih.gov/entrez/query.fcgi?cmd=Retrieve&db=PubMed&dopt=Citation&list_uids=7890632

Malhotra, V.; Serafini, T.; Orci, L.; Shepherd, J. C. and Rothman, J. E. (1989): Purification of a novel class of coated vesicles mediating biosynthetic protein transport through the Golgi stack, Cell (vol. 58), No. 2, pp. 329-36. URL: http://www.ncbi.nlm.nih.gov/entrez/query.fcgi?cmd=Retrieve&db=PubMed&dopt=Citation&list_uids=2752426

Mallard, F.; Antony, C.; Tenza, D.; Salamero, J.; Goud, B. and Johannes, L. (1998): Direct pathway from early/recycling endosomes to the Golgi apparatus revealed through the study of shiga toxin B-fragment transport, J Cell Biol (vol. 143), No. 4, pp. 973-90. URL: http://www.ncbi.nlm.nih.gov/entrez/query.fcgi?cmd=Retrieve&db=PubMed&dopt=Citation&list_uids=9817755

Malsam, J.; Satoh, A.; Pelletier, L. and Warren, G. (2005): Golgin tethers define subpopulations of COPI vesicles, Science (vol. 307), No. 5712, pp. 1095-8. URL:

http://www.ncbi.nlm.nih.gov/entrez/query.fcgi?cmd=Retrieve&db=PubMed&dopt=Citation&list_uids=15718469

Maly, P.; Thall, A.; Petryniak, B.; Rogers, C. E.; Smith, P. L.; Marks, R. M.; Kelly, R. J.; Gersten, K. M.; Cheng, G.; Saunders, T. L.; Camper, S. A.; Camphausen, R. T.; Sullivan, F. X.; Isogai, Y.; Hindsgaul, O.; von Andrian, U. H. and Lowe, J. B. (1996): The alpha(1,3)fucosyltransferase Fuc-TVII controls leukocyte trafficking through an essential role in L-, E-, and P-selectin ligand biosynthesis, Cell (vol. 86), No. 4, pp. 643-53. URL: http://www.ncbi.nlm.nih.gov/entrez/query.fcgi?cmd=Retrieve&db=PubMed&dopt=Citation&list_uids=8752218

Marino, J. H.; Tan, C.; Davis, B.; Han, E. S.; Hickey, M.; Naukam, R.; Taylor, A.; Miller, K. S.; Van De Wiele, C. J. and Teague, T. K. (2008): Disruption of thymopoiesis in ST6Gal I-deficient mice, Glycobiology (vol. 18), No. 9, pp. 719-26. URL: http://www.ncbi.nlm.nih.gov/entrez/query.fcgi?cmd=Retrieve&db=PubMed&dopt=Citation&list_uids=18535087

Marra, P.; Salvatore, L.; Mironov, A., Jr.; Di Campli, A.; Di Tullio, G.; Trucco, A.; Beznoussenko, G.; Mironov, A. and De Matteis, M. A. (2007): The biogenesis of the Golgi ribbon: the roles of membrane input from the ER and of GM130, Mol Biol Cell (vol. 18), No. 5, pp. 1595-608. URL: http://www.ncbi.nlm.nih.gov/entrez/query.fcgi?cmd=Retrieve&db=PubMed&dopt=Citation&list_uids=17314401

Marth, J. D. and Grewal, P. K. (2008): Mammalian glycosylation in immunity, Nat Rev Immunol (vol. 8), No. 11, pp. 874-87. URL: http://www.ncbi.nlm.nih.gov/entrez/query.fcgi?cmd=Retrieve&db=PubMed&dopt=Citation&list_uids=18846099

Martin, O. C. and Pagano, R. E. (1994): Internalization and sorting of a fluorescent analogue of glucosylceramide to the Golgi apparatus of human skin fibroblasts: utilization of endocytic and nonendocytic transport mechanisms, J Cell Biol (vol. 125), No. 4, pp. 769-81. URL: http://www.ncbi.nlm.nih.gov/entrez/query.fcgi?cmd=Retrieve&db=PubMed&dopt=Citation&list_uids=8188745

Martinez-Menarguez, J. A.; Geuze, H. J.; Slot, J. W. and Klumperman, J. (1999): Vesicular tubular clusters between the ER and Golgi mediate concentration of soluble secretory proteins by exclusion from COPI-coated vesicles, Cell (vol. 98), No. 1, pp. 81-90. URL: http://www.ncbi.nlm.nih.gov/entrez/query.fcgi?cmd=Retrieve&db=PubMed&dopt=Citation&list_uids=10412983

Martinez-Menarguez, J. A.; Prekeris, R.; Oorschot, V. M.; Scheller, R.; Slot, J. W.; Geuze, H. J. and Klumperman, J. (2001): Peri-Golgi vesicles contain retrograde but not anterograde proteins consistent with the cisternal progression model of intra-Golgi transport, J Cell Biol (vol. 155), No. 7, pp. 1213-24. URL: http://www.ncbi.nlm.nih.gov/entrez/query.fcgi?cmd=Retrieve&db=PubMed&dopt=Citation&list_uids=11748250

Matlin, K. S. and Simons, K. (1983): Reduced temperature prevents transfer of a membrane glycoprotein to the cell surface but does not prevent terminal glycosylation, Cell (vol. 34), No. 1, pp. 233-43. URL: http://www.ncbi.nlm.nih.gov/entrez/query.fcgi?cmd=Retrieve&db=PubMed&dopt=Citation&list_uids=6883510

Matsushima, T.; Nakashima, M.; Oshima, K.; Abe, Y.; Nishimura, J.; Nawata, H.; Watanabe, T. and Muta, K. (2001): Receptor binding cancer antigen expressed on SiSo cells, a novel regulator of apoptosis of erythroid progenitor cells, Blood (vol. 98), No. 2, pp. 313-21. URL: http://www.ncbi.nlm.nih.gov/entrez/query.fcgi?cmd=Retrieve&db=PubMed&dopt=Citation&list_uids=11435298

McMahon, H. T. and Mills, I. G. (2004): COP and clathrin-coated vesicle budding: different pathways, common approaches, Curr Opin Cell Biol (vol. 16), No. 4, pp. 379-91. URL: http://www.ncbi.nlm.nih.gov/entrez/query.fcgi?cmd=Retrieve&db=PubMed&dopt=Citation&list_uids=15261670

Mermall, V.; Post, P. L. and Mooseker, M. S. (1998): Unconventional myosins in cell movement, membrane traffic, and signal transduction, Science (vol. 279), No. 5350, pp. 527-33. URL:

http://www.ncbi.nlm.nih.gov/entrez/query.fcgi?cmd=Retrieve&db=PubMed&dopt=Citation&list_uids=9438839

Moelleken, J.; Malsam, J.; Betts, M. J.; Movafeghi, A.; Reckmann, I.; Meissner, I.; Hellwig, A.; Russell, R. B.; Sollner, T.; Brugger, B. and Wieland, F. T. (2007): Differential localization of coatomer complex isoforms within the Golgi apparatus, Proc Natl Acad Sci U S A (vol. 104), No. 11, pp. 4425-30. URL: http://www.ncbi.nlm.nih.gov/entrez/query.fcgi?cmd=Retrieve&db=PubMed&dopt=Citation&list_uids=17360540

Molinari, M. (2007): N-glycan structure dictates extension of protein folding or onset of disposal, Nat Chem Biol (vol. 3), No. 6, pp. 313-20. URL: http://www.ncbi.nlm.nih.gov/entrez/query.fcgi?cmd=Retrieve&db=PubMed&dopt=Citation&list_uids=17510649

Monlauzeur, L.; Breuza, L. and Le Bivic, A. (1998): Putative O-glycosylation sites and a membrane anchor are necessary for apical delivery of the human neurotrophin receptor in Caco-2 cells, J Biol Chem (vol. 273), No. 46, pp. 30263-70. URL: http://www.ncbi.nlm.nih.gov/entrez/query.fcgi?cmd=Retrieve&db=PubMed&dopt=Citation&list_uids=9804786

Montoya, M. C.; Sancho, D.; Vicente-Manzanares, M. and Sanchez-Madrid, F. (2002): Cell adhesion and polarity during immune interactions, Immunol Rev (vol. 186), pp. 68-82. URL: http://www.ncbi.nlm.nih.gov/entrez/query.fcgi?cmd=Retrieve&db=PubMed&dopt=Citation&list_uids=12234363

Moody, A. M.; Chui, D.; Reche, P. A.; Priatel, J. J.; Marth, J. D. and Reinherz, E. L. (2001): Developmentally regulated glycosylation of the CD8alphabeta coreceptor stalk modulates ligand binding, Cell (vol. 107), No. 4, pp. 501-12. URL: http://www.ncbi.nlm.nih.gov/entrez/query.fcgi?cmd=Retrieve&db=PubMed&dopt=Citation&list_uids=11719190

Moolenaar, C. E.; Ouwendijk, J.; Wittpoth, M.; Wisselaar, H. A.; Hauri, H. P.; Ginsel, L. A.; Naim, H. Y. and Fransen, J. A. (1997): A mutation in a highly conserved region in brush-border sucrase-isomaltase and lysosomal alpha-glucosidase results in Golgi retention, J Cell Sci (vol. 110 (Pt 5)), pp. 557-67. URL: http://www.ncbi.nlm.nih.gov/entrez/query.fcgi?cmd=Retrieve&db=PubMed&dopt=Citation&list_uids=9092938

Moremen, K. W. (2002): Golgi alpha-mannosidase II deficiency in vertebrate systems: implications for asparagine-linked oligosaccharide processing in mammals, Biochim Biophys Acta (vol. 1573), No. 3, pp. 225-35. URL: http://www.ncbi.nlm.nih.gov/entrez/query.fcgi?cmd=Retrieve&db=PubMed&dopt=Citation&list_uids=12417404

Munro, S. and Pelham, H. R. (1987): A C-terminal signal prevents secretion of luminal ER proteins, Cell (vol. 48), No. 5, pp. 899-907. URL: http://www.ncbi.nlm.nih.gov/entrez/query.fcgi?cmd=Retrieve&db=PubMed&dopt=Citation&list_uids=3545499

Nakakubo, Y.; Hida, Y.; Miyamoto, M.; Hashida, H.; Oshikiri, T.; Kato, K.; Suzuoki, M.; Hiraoka, K.; Ito, T.; Morikawa, T.; Okushiba, S.; Kondo, S. and Katoh, H. (2002): The prognostic significance of RCAS1 expression in squamous cell carcinoma of the oesophagus, Cancer Lett (vol. 177), No. 1, pp. 101-5. URL: http://www.ncbi.nlm.nih.gov/entrez/query.fcgi?cmd=Retrieve&db=PubMed&dopt=Citation&list_uids=11809537

Nakashima, M.; Sonoda, K. and Watanabe, T. (1999): Inhibition of cell growth and induction of apoptotic cell death by the human tumor-associated antigen RCAS1, Nat Med (vol. 5), No. 8, pp. 938-42. URL: http://www.ncbi.nlm.nih.gov/entrez/query.fcgi?cmd=Retrieve&db=PubMed&dopt=Citation&list_uids=10426319

Nelson, W. J. and Yeaman, C. (2001): Protein trafficking in the exocytic pathway of polarized epithelial cells, Trends Cell Biol (vol. 11), No. 12, pp. 483-6. URL: http://www.ncbi.nlm.nih.gov/entrez/query.fcgi?cmd=Retrieve&db=PubMed&dopt=Citation&list_uids=11719053

Newsom-Davis, T. E.; Wang, D.; Steinman, L.; Chen, P. F.; Wang, L. X.; Simon, A. K. and Screaton, G. R. (2009): Enhanced immune recognition of cryptic glycan markers in human tumors, Cancer Res (vol.

69), No. 5, pp. 2018-25. URL: http://www.ncbi.nlm.nih.gov/entrez/query.fcgi?cmd=Retrieve&db=PubMed&dopt=Citation&list_uids=19223535

Nickel, W.; Brugger, B. and Wieland, F. T. (2002): Vesicular transport: the core machinery of COPI recruitment and budding, J Cell Sci (vol. 115), No. Pt 16, pp. 3235-40. URL: http://www.ncbi.nlm.nih.gov/entrez/query.fcgi?cmd=Retrieve&db=PubMed&dopt=Citation&list_uids=12140255

Nickel, W.; Malsam, J.; Gorgas, K.; Ravazzola, M.; Jenne, N.; Helms, J. B. and Wieland, F. T. (1998): Uptake by COPI-coated vesicles of both anterograde and retrograde cargo is inhibited by GTPgammaS in vitro, J Cell Sci (vol. 111 (Pt 20)), pp. 3081-90. URL: http://www.ncbi.nlm.nih.gov/entrez/query.fcgi?cmd=Retrieve&db=PubMed&dopt=Citation&list_uids=9739081

Nilsson, S.; Kuiper, G. and Gustafsson, J. A. (1998): ERbeta: a novel estrogen receptor offers the potential for new drug development, Trends Endocrinol Metab (vol. 9), No. 10, pp. 387-95. URL: http://www.ncbi.nlm.nih.gov/entrez/query.fcgi?cmd=Retrieve&db=PubMed&dopt=Citation&list_uids=18406312

Nilsson, S.; Makela, S.; Treuter, E.; Tujague, M.; Thomsen, J.; Andersson, G.; Enmark, E.; Pettersson, K.; Warner, M. and Gustafsson, J. A. (2001): Mechanisms of estrogen action, Physiol Rev (vol. 81), No. 4, pp. 1535-65. URL: http://www.ncbi.nlm.nih.gov/entrez/query.fcgi?cmd=Retrieve&db=PubMed&dopt=Citation&list_uids=11581496

Nilsson, T.; Au, C. E. and Bergeron, J. J. (2009): Sorting out glycosylation enzymes in the Golgi apparatus, FEBS Lett (vol. 583), No. 23, pp. 3764-9. URL: http://www.ncbi.nlm.nih.gov/entrez/query.fcgi?cmd=Retrieve&db=PubMed&dopt=Citation&list_uids=19878678

Nishimura, N.; Bannykh, S.; Slabough, S.; Matteson, J.; Altschuler, Y.; Hahn, K. and Balch, W. E. (1999): A di-acidic (DXE) code directs concentration of cargo during export from the endoplasmic reticulum, J Biol Chem (vol. 274), No. 22, pp. 15937-46. URL: http://www.ncbi.nlm.nih.gov/entrez/query.fcgi?cmd=Retrieve&db=PubMed&dopt=Citation&list_uids=10336500

Ogushi, T.; Takahashi, S.; Takeuchi, T.; Urano, T.; Horie-Inoue, K.; Kumagai, J.; Kitamura, T.; Ouchi, Y.; Muramatsu, M. and Inoue, S. (2005): Estrogen receptor-binding fragment-associated antigen 9 is a tumor-promoting and prognostic factor for renal cell carcinoma, Cancer Res (vol. 65), No. 9, pp. 3700-6. URL: http://www.ncbi.nlm.nih.gov/entrez/query.fcgi?cmd=Retrieve&db=PubMed&dopt=Citation&list_uids=15867365

Ohshima, K.; Nakashima, M.; Sonoda, K.; Kikuchi, M. and Watanabe, T. (2001): Expression of RCAS1 and FasL in human trophoblasts and uterine glands during pregnancy: the possible role in immune privilege, Clin Exp Immunol (vol. 123), No. 3, pp. 481-6. URL: http://www.ncbi.nlm.nih.gov/entrez/query.fcgi?cmd=Retrieve&db=PubMed&dopt=Citation&list_uids=11298137

Ohtsubo, K. and Marth, J. D. (2006): Glycosylation in cellular mechanisms of health and disease, Cell (vol. 126), No. 5, pp. 855-67. URL: http://www.ncbi.nlm.nih.gov/entrez/query.fcgi?cmd=Retrieve&db=PubMed&dopt=Citation&list_uids=16959566

Ohya, T.; Miaczynska, M.; Coskun, U.; Lommer, B.; Runge, A.; Drechsel, D.; Kalaidzidis, Y. and Zerial, M. (2009): Reconstitution of Rab- and SNARE-dependent membrane fusion by synthetic endosomes, Nature (vol. 459), No. 7250, pp. 1091-7. URL: http://www.ncbi.nlm.nih.gov/entrez/query.fcgi?cmd=Retrieve&db=PubMed&dopt=Citation&list_uids=19458617

Okada, K.; Nakashima, M.; Komuta, K.; Hashimoto, S.; Okudaira, S.; Baba, N.; Hishikawa, Y.; Koji, T.; Kanematsu, T. and Watanabe, T. (2003): Expression of tumor-associated membrane antigen, RCAS1, in human colorectal carcinomas and possible role in apoptosis of tumor-infiltrating lymphocytes, Mod Pathol (vol. 16), No. 7, pp. 679-85. URL:

http://www.ncbi.nlm.nih.gov/entrez/query.fcgi?cmd=Retrieve&db=PubMed&dopt=Citation&list_uids=12861064

Olkkonen, V. M. and Ikonen, E. (2000): Genetic defects of intracellular-membrane transport, N Engl J Med (vol. 343), No. 15, pp. 1095-104. URL: http://www.ncbi.nlm.nih.gov/entrez/query.fcgi?cmd=Retrieve&db=PubMed&dopt=Citation&list_uids=11027745

Orci, L.; Stamnes, M.; Ravazzola, M.; Amherdt, M.; Perrelet, A.; Sollner, T. H. and Rothman, J. E. (1997): Bidirectional transport by distinct populations of COPI-coated vesicles, Cell (vol. 90), No. 2, pp. 335-49. URL: http://www.ncbi.nlm.nih.gov/entrez/query.fcgi?cmd=Retrieve&db=PubMed&dopt=Citation&list_uids=9244307

Ou, W. J.; Cameron, P. H.; Thomas, D. Y. and Bergeron, J. J. (1993): Association of folding intermediates of glycoproteins with calnexin during protein maturation, Nature (vol. 364), No. 6440, pp. 771-6. URL: http://www.ncbi.nlm.nih.gov/entrez/query.fcgi?cmd=Retrieve&db=PubMed&dopt=Citation&list_uids=8102790

Oyler, G. A.; Higgins, G. A.; Hart, R. A.; Battenberg, E.; Billingsley, M.; Bloom, F. E. and Wilson, M. C. (1989): The identification of a novel synaptosomal-associated protein, SNAP-25, differentially expressed by neuronal subpopulations, J Cell Biol (vol. 109), No. 6 Pt 1, pp. 3039-52. URL: http://www.ncbi.nlm.nih.gov/entrez/query.fcgi?cmd=Retrieve&db=PubMed&dopt=Citation&list_uids=2592413

Palade, G. (1975): Intracellular aspects of the process of protein synthesis, Science (vol. 189), No. 4200, pp. 347-58. URL: http://www.ncbi.nlm.nih.gov/entrez/query.fcgi?cmd=Retrieve&db=PubMed&dopt=Citation&list_uids=1096303

Palmer, D. J.; Helms, J. B.; Beckers, C. J.; Orci, L. and Rothman, J. E. (1993): Binding of coatomer to Golgi membranes requires ADP-ribosylation factor, J Biol Chem (vol. 268), No. 16, pp. 12083-9. URL: http://www.ncbi.nlm.nih.gov/entrez/query.fcgi?cmd=Retrieve&db=PubMed&dopt=Citation&list_uids=8505331

Palmer, R. E.; Lee, S. B.; Wong, J. C.; Reynolds, P. A.; Zhang, H.; Truong, V.; Oliner, J. D.; Gerald, W. L. and Haber, D. A. (2002): Induction of BAIAP3 by the EWS-WT1 chimeric fusion implicates regulated exocytosis in tumorigenesis, Cancer Cell (vol. 2), No. 6, pp. 497-505. URL: http://www.ncbi.nlm.nih.gov/entrez/query.fcgi?cmd=Retrieve&db=PubMed&dopt=Citation&list_uids=12498718

Panaretakis, T.; Kepp, O.; Brockmeier, U.; Tesniere, A.; Bjorklund, A. C.; Chapman, D. C.; Durchschlag, M.; Joza, N.; Pierron, G.; van Endert, P.; Yuan, J.; Zitvogel, L.; Madeo, F.; Williams, D. B. and Kroemer, G. (2009): Mechanisms of pre-apoptotic calreticulin exposure in immunogenic cell death, EMBO J (vol. 28), No. 5, pp. 578-90. URL: http://www.ncbi.nlm.nih.gov/entrez/query.fcgi?cmd=Retrieve&db=PubMed&dopt=Citation&list_uids=19165151

Park, K. J.; Krishnan, V.; O'Malley, B. W.; Yamamoto, Y. and Gaynor, R. B. (2005): Formation of an IKKalpha-dependent transcription complex is required for estrogen receptor-mediated gene activation, Mol Cell (vol. 18), No. 1, pp. 71-82. URL: http://www.ncbi.nlm.nih.gov/entrez/query.fcgi?cmd=Retrieve&db=PubMed&dopt=Citation&list_uids=15808510

Peaper, D. R. and Cresswell, P. (2008): Regulation of MHC class I assembly and peptide binding, Annu Rev Cell Dev Biol (vol. 24), pp. 343-68. URL: http://www.ncbi.nlm.nih.gov/entrez/query.fcgi?cmd=Retrieve&db=PubMed&dopt=Citation&list_uids=18729726

Pelham, H. R. (1996): The dynamic organisation of the secretory pathway, Cell Struct Funct (vol. 21), No. 5, pp. 413-9. URL: http://www.ncbi.nlm.nih.gov/entrez/query.fcgi?cmd=Retrieve&db=PubMed&dopt=Citation&list_uids=9118249

Pelham, H. R. and Rothman, J. E. (2000): The debate about transport in the Golgi--two sides of the same coin?, Cell (vol. 102), No. 6, pp. 713-9. URL:

http://www.ncbi.nlm.nih.gov/entrez/query.fcgi?cmd=Retrieve&db=PubMed&dopt=Citation&list_uids=11030615

Pepperkok, R.; Scheel, J.; Horstmann, H.; Hauri, H. P.; Griffiths, G. and Kreis, T. E. (1993): Beta-COP is essential for biosynthetic membrane transport from the endoplasmic reticulum to the Golgi complex in vivo, Cell (vol. 74), No. 1, pp. 71-82. URL: http://www.ncbi.nlm.nih.gov/entrez/query.fcgi?cmd=Retrieve&db=PubMed&dopt=Citation&list_uids=8334707

Pernet-Gallay, K.; Antony, C.; Johannes, L.; Bornens, M.; Goud, B. and Rios, R. M. (2002): The overexpression of GMAP-210 blocks anterograde and retrograde transport between the ER and the Golgi apparatus, Traffic (vol. 3), No. 11, pp. 822-32. URL: http://www.ncbi.nlm.nih.gov/entrez/query.fcgi?cmd=Retrieve&db=PubMed&dopt=Citation&list_uids=12383348

Peter, F.; Plutner, H.; Zhu, H.; Kreis, T. E. and Balch, W. E. (1993): Beta-COP is essential for transport of protein from the endoplasmic reticulum to the Golgi in vitro, J Cell Biol (vol. 122), No. 6, pp. 1155-67. URL: http://www.ncbi.nlm.nih.gov/entrez/query.fcgi?cmd=Retrieve&db=PubMed&dopt=Citation&list_uids=8376457

Peterson, J. R.; Ora, A.; Van, P. N. and Helenius, A. (1995): Transient, lectin-like association of calreticulin with folding intermediates of cellular and viral glycoproteins, Mol Biol Cell (vol. 6), No. 9, pp. 1173-84. URL: http://www.ncbi.nlm.nih.gov/entrez/query.fcgi?cmd=Retrieve&db=PubMed&dopt=Citation&list_uids=8534914

Peyroche, A.; Paris, S. and Jackson, C. L. (1996): Nucleotide exchange on ARF mediated by yeast Gea1 protein, Nature (vol. 384), No. 6608, pp. 479-81. URL: http://www.ncbi.nlm.nih.gov/entrez/query.fcgi?cmd=Retrieve&db=PubMed&dopt=Citation&list_uids=8945477

Polishchuk, R.; Di Pentima, A. and Lippincott-Schwartz, J. (2004): Delivery of raft-associated, GPI-anchored proteins to the apical surface of polarized MDCK cells by a transcytotic pathway, Nat Cell Biol (vol. 6), No. 4, pp. 297-307. URL: http://www.ncbi.nlm.nih.gov/entrez/query.fcgi?cmd=Retrieve&db=PubMed&dopt=Citation&list_uids=15048124

Polishchuk, R. S.; Capestrano, M. and Polishchuk, E. V. (2009): Shaping tubular carriers for intracellular membrane transport, FEBS Lett (vol. 583), No. 23, pp. 3847-56. URL: http://www.ncbi.nlm.nih.gov/entrez/query.fcgi?cmd=Retrieve&db=PubMed&dopt=Citation&list_uids=19840796

Presley, J. F.; Cole, N. B.; Schroer, T. A.; Hirschberg, K.; Zaal, K. J. and Lippincott-Schwartz, J. (1997): ER-to-Golgi transport visualized in living cells, Nature (vol. 389), No. 6646, pp. 81-5. URL: http://www.ncbi.nlm.nih.gov/entrez/query.fcgi?cmd=Retrieve&db=PubMed&dopt=Citation&list_uids=9288971

Presley, J. F.; Smith, C.; Hirschberg, K.; Miller, C.; Cole, N. B.; Zaal, K. J. and Lippincott-Schwartz, J. (1998): Golgi membrane dynamics, Mol Biol Cell (vol. 9), No. 7, pp. 1617-26. URL: http://www.ncbi.nlm.nih.gov/entrez/query.fcgi?cmd=Retrieve&db=PubMed&dopt=Citation&list_uids=9658158

Presley, J. F.; Ward, T. H.; Pfeifer, A. C.; Siggia, E. D.; Phair, R. D. and Lippincott-Schwartz, J. (2002): Dissection of COPI and Arf1 dynamics in vivo and role in Golgi membrane transport, Nature (vol. 417), No. 6885, pp. 187-93. URL: http://www.ncbi.nlm.nih.gov/entrez/query.fcgi?cmd=Retrieve&db=PubMed&dopt=Citation&list_uids=12000962

Priatel, J. J.; Chui, D.; Hiraoka, N.; Simmons, C. J.; Richardson, K. B.; Page, D. M.; Fukuda, M.; Varki, N. M. and Marth, J. D. (2000): The ST3Gal-I sialyltransferase controls CD8+ T lymphocyte homeostasis by modulating O-glycan biosynthesis, Immunity (vol. 12), No. 3, pp. 273-83. URL: http://www.ncbi.nlm.nih.gov/entrez/query.fcgi?cmd=Retrieve&db=PubMed&dopt=Citation&list_uids=10755614

Pulvirenti, T.; Giannotta, M.; Capestrano, M.; Capitani, M.; Pisanu, A.; Polishchuk, R. S.; San Pietro, E.; Beznoussenko, G. V.; Mironov, A. A.; Turacchio, G.; Hsu, V. W.; Sallese, M. and Luini, A. (2008): A traffic-activated Golgi-based signalling circuit coordinates the secretory pathway, Nat Cell Biol (vol.

10), No. 8, pp. 912-22. URL: http://www.ncbi.nlm.nih.gov/entrez/query.fcgi?cmd=Retrieve&db=PubMed&dopt=Citation&list_uids=18641641

Rabouille, C. and Klumperman, J. (2005): Opinion: The maturing role of COPI vesicles in intra-Golgi transport, Nat Rev Mol Cell Biol (vol. 6), No. 10, pp. 812-7. URL: http://www.ncbi.nlm.nih.gov/entrez/query.fcgi?cmd=Retrieve&db=PubMed&dopt=Citation&list_uids=16167055

Rak, J.; Filmus, J.; Finkenzeller, G.; Grugel, S.; Marme, D. and Kerbel, R. S. (1995): Oncogenes as inducers of tumor angiogenesis, Cancer Metastasis Rev (vol. 14), No. 4, pp. 263-77. URL: http://www.ncbi.nlm.nih.gov/entrez/query.fcgi?cmd=Retrieve&db=PubMed&dopt=Citation&list_uids=8821090

Randazzo, P. A. and Kahn, R. A. (1994): GTP hydrolysis by ADP-ribosylation factor is dependent on both an ADP-ribosylation factor GTPase-activating protein and acid phospholipids, J Biol Chem (vol. 269), No. 14, pp. 10758-63. URL: http://www.ncbi.nlm.nih.gov/entrez/query.fcgi?cmd=Retrieve&db=PubMed&dopt=Citation&list_uids=8144664

Raykhel, I.; Alanen, H.; Salo, K.; Jurvansuu, J.; Nguyen, V. D.; Latva-Ranta, M. and Ruddock, L. (2007): A molecular specificity code for the three mammalian KDEL receptors, J Cell Biol (vol. 179), No. 6, pp. 1193-204. URL: http://www.ncbi.nlm.nih.gov/entrez/query.fcgi?cmd=Retrieve&db=PubMed&dopt=Citation&list_uids=18086916

Razi, M.; Chan, E. Y. and Tooze, S. A. (2009): Early endosomes and endosomal coatomer are required for autophagy, J Cell Biol (vol. 185), No. 2, pp. 305-21. URL: http://www.ncbi.nlm.nih.gov/entrez/query.fcgi?cmd=Retrieve&db=PubMed&dopt=Citation&list_uids=19364919

Rehm, A.; Stern, P.; Ploegh, H. L. and Tortorella, D. (2001): Signal peptide cleavage of a type I membrane protein, HCMV US11, is dependent on its membrane anchor, Embo J (vol. 20), No. 7, pp. 1573-82. URL: http://www.ncbi.nlm.nih.gov/entrez/query.fcgi?cmd=Retrieve&db=PubMed&dopt=Citation&list_uids=11285222

Reichardt, P.; Dornbach, B. and Gunzer, M. (2007): The molecular makeup and function of regulatory and effector synapses, Immunol Rev (vol. 218), pp. 165-77. URL: http://www.ncbi.nlm.nih.gov/entrez/query.fcgi?cmd=Retrieve&db=PubMed&dopt=Citation&list_uids=17624952

Reimer, T. A.; Anagnostopoulos, I.; Erdmann, B.; Lehmann, I.; Stein, H.; Daniel, P.; Dorken, B. and Rehm, A. (2005): Reevaluation of the 22-1-1 antibody and its putative antigen, EBAG9/RCAS1, as a tumor marker, BMC Cancer (vol. 5), No. 1, p. 47. URL: http://www.ncbi.nlm.nih.gov/entrez/query.fcgi?cmd=Retrieve&db=PubMed&dopt=Citation&list_uids=15904507

Reinhard, C.; Schweikert, M.; Wieland, F. T. and Nickel, W. (2003): Functional reconstitution of COPI coat assembly and disassembly using chemically defined components, Proc Natl Acad Sci U S A (vol. 100), No. 14, pp. 8253-7. URL: http://www.ncbi.nlm.nih.gov/entrez/query.fcgi?cmd=Retrieve&db=PubMed&dopt=Citation&list_uids=12832619

Rink, J.; Ghigo, E.; Kalaidzidis, Y. and Zerial, M. (2005): Rab conversion as a mechanism of progression from early to late endosomes, Cell (vol. 122), No. 5, pp. 735-49. URL: http://www.ncbi.nlm.nih.gov/entrez/query.fcgi?cmd=Retrieve&db=PubMed&dopt=Citation&list_uids=16143105

Robinson, M. S. (2004): Adaptable adaptors for coated vesicles, Trends Cell Biol (vol. 14), No. 4, pp. 167-74. URL: http://www.ncbi.nlm.nih.gov/entrez/query.fcgi?cmd=Retrieve&db=PubMed&dopt=Citation&list_uids=15066634

Robinson, M. S. and Bonifacino, J. S. (2001): Adaptor-related proteins, Curr Opin Cell Biol (vol. 13), No. 4, pp. 444-53. URL:

http://www.ncbi.nlm.nih.gov/entrez/query.fcgi?cmd=Retrieve&db=PubMed&dopt=Citation&list_uids=11454451

Rodriguez-Boulan, E.; Kreitzer, G. and Musch, A. (2005): Organization of vesicular trafficking in epithelia, Nat Rev Mol Cell Biol (vol. 6), No. 3, pp. 233-47. URL: http://www.ncbi.nlm.nih.gov/entrez/query.fcgi?cmd=Retrieve&db=PubMed&dopt=Citation&list_uids=15738988

Rodriguez-Boulan, E. and Powell, S. K. (1992): Polarity of epithelial and neuronal cells, Annu Rev Cell Biol (vol. 8), pp. 395-427. URL: http://www.ncbi.nlm.nih.gov/entrez/query.fcgi?cmd=Retrieve&db=PubMed&dopt=Citation&list_uids=1476804

Rodriguez Boulan, E. and Sabatini, D. D. (1978): Asymmetric budding of viruses in epithelial monlayers: a model system for study of epithelial polarity, Proc Natl Acad Sci U S A (vol. 75), No. 10, pp. 5071-5. URL: http://www.ncbi.nlm.nih.gov/entrez/query.fcgi?cmd=Retrieve&db=PubMed&dopt=Citation&list_uids=283416

Rojo, M.; Pepperkok, R.; Emery, G.; Kellner, R.; Stang, E.; Parton, R. G. and Gruenberg, J. (1997): Involvement of the transmembrane protein p23 in biosynthetic protein transport, J Cell Biol (vol. 139), No. 5, pp. 1119-35. URL: http://www.ncbi.nlm.nih.gov/entrez/query.fcgi?cmd=Retrieve&db=PubMed&dopt=Citation&list_uids=9382861

Rost, M.; Mann, S.; Lambert, C.; Doring, T.; Thome, N. and Prange, R. (2006): Gamma-adaptin, a novel ubiquitin-interacting adaptor, and Nedd4 ubiquitin ligase control hepatitis B virus maturation, J Biol Chem (vol. 281), No. 39, pp. 29297-308. URL: http://www.ncbi.nlm.nih.gov/entrez/query.fcgi?cmd=Retrieve&db=PubMed&dopt=Citation&list_uids=16867982

Roth, J. (2002): Protein N-glycosylation along the secretory pathway: relationship to organelle topography and function, protein quality control, and cell interactions, Chem Rev (vol. 102), No. 2, pp. 285-303. URL: http://www.ncbi.nlm.nih.gov/entrez/query.fcgi?cmd=Retrieve&db=PubMed&dopt=Citation&list_uids=11841244

Rottger, S.; White, J.; Wandall, H. H.; Olivo, J. C.; Stark, A.; Bennett, E. P.; Whitehouse, C.; Berger, E. G.; Clausen, H. and Nilsson, T. (1998): Localization of three human polypeptide GalNAc-transferases in HeLa cells suggests initiation of O-linked glycosylation throughout the Golgi apparatus, J Cell Sci (vol. 111 (Pt 1)), pp. 45-60. URL: http://www.ncbi.nlm.nih.gov/entrez/query.fcgi?cmd=Retrieve&db=PubMed&dopt=Citation&list_uids=9394011

Rubinstein, N.; Alvarez, M.; Zwirner, N. W.; Toscano, M. A.; Ilarregui, J. M.; Bravo, A.; Mordoh, J.; Fainboim, L.; Podhajcer, O. L. and Rabinovich, G. A. (2004): Targeted inhibition of galectin-1 gene expression in tumor cells results in heightened T cell-mediated rejection; A potential mechanism of tumor-immune privilege, Cancer Cell (vol. 5), No. 3, pp. 241-51. URL: http://www.ncbi.nlm.nih.gov/entrez/query.fcgi?cmd=Retrieve&db=PubMed&dopt=Citation&list_uids=15050916

Rudd, P. M.; Elliott, T.; Cresswell, P.; Wilson, I. A. and Dwek, R. A. (2001): Glycosylation and the immune system, Science (vol. 291), No. 5512, pp. 2370-6. URL: http://www.ncbi.nlm.nih.gov/entrez/query.fcgi?cmd=Retrieve&db=PubMed&dopt=Citation&list_uids=11269318

Ruder, C.; Hopken, U. E.; Wolf, J.; Mittrucker, H. W.; Engels, B.; Erdmann, B.; Wollenzin, S.; Uckert, W.; Dorken, B. and Rehm, A. (2009): The tumor-associated antigen EBAG9 negatively regulates the cytolytic capacity of mouse CD8+ T cells, J Clin Invest (vol. 119), No. 8, pp. 2184-203. URL: http://www.ncbi.nlm.nih.gov/entrez/query.fcgi?cmd=Retrieve&db=PubMed&dopt=Citation&list_uids=19620783

Ruder, C.; Reimer, T.; Delgado-Martinez, I.; Hermosilla, R.; Engelsberg, A.; Nehring, R.; Dorken, B. and Rehm, A. (2005): EBAG9 adds a new layer of control on large dense-core vesicle exocytosis via interaction with Snapin, Mol Biol Cell (vol. 16), No. 3, pp. 1245-57. URL: http://www.ncbi.nlm.nih.gov/entrez/query.fcgi?cmd=Retrieve&db=PubMed&dopt=Citation&list_uids=15635093

Rutz, C.; Satoh, A.; Ronchi, P.; Brugger, B.; Warren, G. and Wieland, F. T. (2009): Following the fate in vivo of COPI vesicles generated in vitro, Traffic (vol. 10), No. 8, pp. 994-1005. URL: http://www.ncbi.nlm.nih.gov/entrez/query.fcgi?cmd=Retrieve&db=PubMed&dopt=Citation&list_uids=19497049

Ryan, S. O.; Gantt, K. R. and Finn, O. J. (2007): Tumor antigen-based immunotherapy and immunoprevention of cancer, Int Arch Allergy Immunol (vol. 142), No. 3, pp. 179-89. URL: http://www.ncbi.nlm.nih.gov/entrez/query.fcgi?cmd=Retrieve&db=PubMed&dopt=Citation&list_uids=17106205

Saitoh, A.; Shin, H. W.; Yamada, A.; Waguri, S. and Nakayama, K. (2009): Three homologous ArfGAPs participate in coat protein I-mediated transport, J Biol Chem (vol. 284), No. 20, pp. 13948-57. URL: http://www.ncbi.nlm.nih.gov/entrez/query.fcgi?cmd=Retrieve&db=PubMed&dopt=Citation&list_uids=19299515

Sallese, M.; Giannotta, M. and Luini, A. (2009): Coordination of the secretory compartments via inter-organelle signalling, Semin Cell Dev Biol (vol. 20), No. 7, pp. 801-9. URL: http://www.ncbi.nlm.nih.gov/entrez/query.fcgi?cmd=Retrieve&db=PubMed&dopt=Citation&list_uids=19447052

Sannerud, R.; Saraste, J. and Goud, B. (2003): Retrograde traffic in the biosynthetic-secretory route: pathways and machinery, Curr Opin Cell Biol (vol. 15), No. 4, pp. 438-45. URL: http://www.ncbi.nlm.nih.gov/entrez/query.fcgi?cmd=Retrieve&db=PubMed&dopt=Citation&list_uids=12892784

Saraste, J.; Dale, H. A.; Bazzocco, S. and Marie, M. (2009): Emerging new roles of the pre-Golgi intermediate compartment in biosynthetic-secretory trafficking, FEBS Lett (vol. 583), No. 23, pp. 3804-10. URL: http://www.ncbi.nlm.nih.gov/entrez/query.fcgi?cmd=Retrieve&db=PubMed&dopt=Citation&list_uids=19887068

Saraste, J. and Svensson, K. (1991): Distribution of the intermediate elements operating in ER to Golgi transport, J Cell Sci (vol. 100 (Pt 3)), pp. 415-30. URL: http://www.ncbi.nlm.nih.gov/entrez/query.fcgi?cmd=Retrieve&db=PubMed&dopt=Citation&list_uids=1808196

Scales, S. J.; Pepperkok, R. and Kreis, T. E. (1997): Visualization of ER-to-Golgi transport in living cells reveals a sequential mode of action for COPII and COPI, Cell (vol. 90), No. 6, pp. 1137-48. URL: http://www.ncbi.nlm.nih.gov/entrez/query.fcgi?cmd=Retrieve&db=PubMed&dopt=Citation&list_uids=9323141

Scheiffele, P.; Peranen, J. and Simons, K. (1995): N-glycans as apical sorting signals in epithelial cells, Nature (vol. 378), No. 6552, pp. 96-8. URL: http://www.ncbi.nlm.nih.gov/entrez/query.fcgi?cmd=Retrieve&db=PubMed&dopt=Citation&list_uids=7477300

Schietinger, A.; Philip, M.; Yoshida, B. A.; Azadi, P.; Liu, H.; Meredith, S. C. and Schreiber, H. (2006): A mutant chaperone converts a wild-type protein into a tumor-specific antigen, Science (vol. 314), No. 5797, pp. 304-8. URL: http://www.ncbi.nlm.nih.gov/entrez/query.fcgi?cmd=Retrieve&db=PubMed&dopt=Citation&list_uids=17038624

Schledzewski, K.; Brinkmann, H. and Mendel, R. R. (1999): Phylogenetic analysis of components of the eukaryotic vesicle transport system reveals a common origin of adaptor protein complexes 1, 2, and 3 and the F subcomplex of the coatomer COPI, J Mol Evol (vol. 48), No. 6, pp. 770-8. URL: http://www.ncbi.nlm.nih.gov/entrez/query.fcgi?cmd=Retrieve&db=PubMed&dopt=Citation&list_uids=10229581

Schmitz, K. R.; Liu, J.; Li, S.; Setty, T. G.; Wood, C. S.; Burd, C. G. and Ferguson, K. M. (2008): Golgi localization of glycosyltransferases requires a Vps74p oligomer, Dev Cell (vol. 14), No. 4, pp. 523-34. URL: http://www.ncbi.nlm.nih.gov/entrez/query.fcgi?cmd=Retrieve&db=PubMed&dopt=Citation&list_uids=18410729

Schuck, S.; Gerl, M. J.; Ang, A.; Manninen, A.; Keller, P.; Mellman, I. and Simons, K. (2007): Rab10 is involved in basolateral transport in polarized Madin-Darby canine kidney cells, Traffic (vol. 8), No. 1, pp. 47-60. URL:

http://www.ncbi.nlm.nih.gov/entrez/query.fcgi?cmd=Retrieve&db=PubMed&dopt=Citation&list_uids=17132146

Schuck, S. and Simons, K. (2004): Polarized sorting in epithelial cells: raft clustering and the biogenesis of the apical membrane, J Cell Sci (vol. 117), No. Pt 25, pp. 5955-64. URL: http://www.ncbi.nlm.nih.gov/entrez/query.fcgi?cmd=Retrieve&db=PubMed&dopt=Citation&list_uids=15564373

Schweizer, A.; Fransen, J. A.; Bachi, T.; Ginsel, L. and Hauri, H. P. (1988): Identification, by a monoclonal antibody, of a 53-kD protein associated with a tubulo-vesicular compartment at the cis-side of the Golgi apparatus, J Cell Biol (vol. 107), No. 5, pp. 1643-53. URL: http://www.ncbi.nlm.nih.gov/entrez/query.fcgi?cmd=Retrieve&db=PubMed&dopt=Citation&list_uids=3182932

Schweizer, A.; Matter, K.; Ketcham, C. M. and Hauri, H. P. (1991): The isolated ER-Golgi intermediate compartment exhibits properties that are different from ER and cis-Golgi, J Cell Biol (vol. 113), No. 1, pp. 45-54. URL: http://www.ncbi.nlm.nih.gov/entrez/query.fcgi?cmd=Retrieve&db=PubMed&dopt=Citation&list_uids=2007626

Semenza, J. C.; Hardwick, K. G.; Dean, N. and Pelham, H. R. (1990): ERD2, a yeast gene required for the receptor-mediated retrieval of luminal ER proteins from the secretory pathway, Cell (vol. 61), No. 7, pp. 1349-57. URL: http://www.ncbi.nlm.nih.gov/entrez/query.fcgi?cmd=Retrieve&db=PubMed&dopt=Citation&list_uids=2194670

Serafini, T.; Stenbeck, G.; Brecht, A.; Lottspeich, F.; Orci, L.; Rothman, J. E. and Wieland, F. T. (1991): A coat subunit of Golgi-derived non-clathrin-coated vesicles with homology to the clathrin-coated vesicle coat protein beta-adaptin, Nature (vol. 349), No. 6306, pp. 215-20. URL: http://www.ncbi.nlm.nih.gov/entrez/query.fcgi?cmd=Retrieve&db=PubMed&dopt=Citation&list_uids=1898984

Sewell, R.; Backstrom, M.; Dalziel, M.; Gschmeissner, S.; Karlsson, H.; Noll, T.; Gatgens, J.; Clausen, H.; Hansson, G. C.; Burchell, J. and Taylor-Papadimitriou, J. (2006): The ST6GalNAc-I sialyltransferase localizes throughout the Golgi and is responsible for the synthesis of the tumor-associated sialyl-Tn O-glycan in human breast cancer, J Biol Chem (vol. 281), No. 6, pp. 3586-94. URL: http://www.ncbi.nlm.nih.gov/entrez/query.fcgi?cmd=Retrieve&db=PubMed&dopt=Citation&list_uids=16319059

Simerly, R. B.; Chang, C.; Muramatsu, M. and Swanson, L. W. (1990): Distribution of androgen and estrogen receptor mRNA-containing cells in the rat brain: an in situ hybridization study, J Comp Neurol (vol. 294), No. 1, pp. 76-95. URL: http://www.ncbi.nlm.nih.gov/entrez/query.fcgi?cmd=Retrieve&db=PubMed&dopt=Citation&list_uids=2324335

Simons, K. and Zerial, M. (1993): Rab proteins and the road maps for intracellular transport, Neuron (vol. 11), No. 5, pp. 789-99. URL: http://www.ncbi.nlm.nih.gov/entrez/query.fcgi?cmd=Retrieve&db=PubMed&dopt=Citation&list_uids=8240804

Sollner, T.; Bennett, M. K.; Whiteheart, S. W.; Scheller, R. H. and Rothman, J. E. (1993): A protein assembly-disassembly pathway in vitro that may correspond to sequential steps of synaptic vesicle docking, activation, and fusion, Cell (vol. 75), No. 3, pp. 409-18. URL: http://www.ncbi.nlm.nih.gov/entrez/query.fcgi?cmd=Retrieve&db=PubMed&dopt=Citation&list_uids=8221884

Sollner, T.; Whiteheart, S. W.; Brunner, M.; Erdjument-Bromage, H.; Geromanos, S.; Tempst, P. and Rothman, J. E. (1993): SNAP receptors implicated in vesicle targeting and fusion, Nature (vol. 362), No. 6418, pp. 318-24. URL: http://www.ncbi.nlm.nih.gov/entrez/query.fcgi?cmd=Retrieve&db=PubMed&dopt=Citation&list_uids=8455717

Sonoda, K.; Miyamoto, S.; Nakashima, M. and Wake, N. (2008): The biological role of the unique molecule RCAS1: a bioactive marker that induces connective tissue remodeling and lymphocyte apoptosis, Front Biosci (vol. 13), pp. 1106-16. URL:

http://www.ncbi.nlm.nih.gov/entrez/query.fcgi?cmd=Retrieve&db=PubMed&dopt=Citation&list_uids=17981616

Sonoda, K.; Nakashima, M.; Kaku, T.; Kamura, T.; Nakano, H. and Watanabe, T. (1996): A novel tumor-associated antigen expressed in human uterine and ovarian carcinomas, Cancer (vol. 77), No. 8, pp. 1501-9. URL: http://www.ncbi.nlm.nih.gov/entrez/query.fcgi?cmd=Retrieve&db=PubMed&dopt=Citation&list_uids=8608535

Spang, A. (2002): ARF1 regulatory factors and COPI vesicle formation, Curr Opin Cell Biol (vol. 14), No. 4, pp. 423-7. URL: http://www.ncbi.nlm.nih.gov/entrez/query.fcgi?cmd=Retrieve&db=PubMed&dopt=Citation&list_uids=12383792

Spang, A.; Matsuoka, K.; Hamamoto, S.; Schekman, R. and Orci, L. (1998): Coatomer, Arf1p, and nucleotide are required to bud coat protein complex I-coated vesicles from large synthetic liposomes, Proc Natl Acad Sci U S A (vol. 95), No. 19, pp. 11199-204. URL: http://www.ncbi.nlm.nih.gov/entrez/query.fcgi?cmd=Retrieve&db=PubMed&dopt=Citation&list_uids=9736713

Sprague, B. L. and McNally, J. G. (2005): FRAP analysis of binding: proper and fitting, Trends Cell Biol (vol. 15), No. 2, pp. 84-91. URL: http://www.ncbi.nlm.nih.gov/entrez/query.fcgi?cmd=Retrieve&db=PubMed&dopt=Citation&list_uids=15695095

Springer, G. F. (1984): T and Tn, general carcinoma autoantigens, Science (vol. 224), No. 4654, pp. 1198-206. URL: http://www.ncbi.nlm.nih.gov/entrez/query.fcgi?cmd=Retrieve&db=PubMed&dopt=Citation&list_uids=6729450

Stein, M.; Wandinger-Ness, A. and Roitbak, T. (2002): Altered trafficking and epithelial cell polarity in disease, Trends Cell Biol (vol. 12), No. 8, pp. 374-81. URL: http://www.ncbi.nlm.nih.gov/entrez/query.fcgi?cmd=Retrieve&db=PubMed&dopt=Citation&list_uids=12191914

Stephens, D. J.; Lin-Marq, N.; Pagano, A.; Pepperkok, R. and Paccaud, J. P. (2000): COPI-coated ER-to-Golgi transport complexes segregate from COPII in close proximity to ER exit sites, J Cell Sci (vol. 113 (Pt 12)), pp. 2177-85. URL: http://www.ncbi.nlm.nih.gov/entrez/query.fcgi?cmd=Retrieve&db=PubMed&dopt=Citation&list_uids=10825291

Stephens, D. J. and Pepperkok, R. (2001): Illuminating the secretory pathway: when do we need vesicles?, J Cell Sci (vol. 114), No. Pt 6, pp. 1053-9. URL: http://www.ncbi.nlm.nih.gov/entrez/query.fcgi?cmd=Retrieve&db=PubMed&dopt=Citation&list_uids=11228150

Stinchcombe, J. C.; Bossi, G.; Booth, S. and Griffiths, G. M. (2001): The immunological synapse of CTL contains a secretory domain and membrane bridges, Immunity (vol. 15), No. 5, pp. 751-61. URL: http://www.ncbi.nlm.nih.gov/entrez/query.fcgi?cmd=Retrieve&db=PubMed&dopt=Citation&list_uids=11728337

Storrie, B. and Nilsson, T. (2002): The Golgi apparatus: balancing new with old, Traffic (vol. 3), No. 8, pp. 521-9. URL: http://www.ncbi.nlm.nih.gov/entrez/query.fcgi?cmd=Retrieve&db=PubMed&dopt=Citation&list_uids=12121415

Storrie, B.; Pepperkok, R. and Nilsson, T. (2000): Breaking the COPI monopoly on Golgi recycling, Trends Cell Biol (vol. 10), No. 9, pp. 385-91. URL: http://www.ncbi.nlm.nih.gov/entrez/query.fcgi?cmd=Retrieve&db=PubMed&dopt=Citation&list_uids=10932096

Storrie, B.; White, J.; Rottger, S.; Stelzer, E. H.; Suganuma, T. and Nilsson, T. (1998): Recycling of golgi-resident glycosyltransferases through the ER reveals a novel pathway and provides an explanation for nocodazole-induced Golgi scattering, J Cell Biol (vol. 143), No. 6, pp. 1505-21. URL: http://www.ncbi.nlm.nih.gov/entrez/query.fcgi?cmd=Retrieve&db=PubMed&dopt=Citation&list_uids=9852147

Sudhof, T. C. (1995): The synaptic vesicle cycle: a cascade of protein-protein interactions, Nature (vol. 375), No. 6533, pp. 645-53. URL: http://www.ncbi.nlm.nih.gov/entrez/query.fcgi?cmd=Retrieve&db=PubMed&dopt=Citation&list_uids=7791897

Sun, F. C.; Wei, S.; Li, C. W.; Chang, Y. S.; Chao, C. C. and Lai, Y. K. (2006): Localization of GRP78 to mitochondria under the unfolded protein response, Biochem J (vol. 396), No. 1, pp. 31-9. URL: http://www.ncbi.nlm.nih.gov/entrez/query.fcgi?cmd=Retrieve&db=PubMed&dopt=Citation&list_uids=16433633

Suzuki, T.; Inoue, S.; Kawabata, W.; Akahira, J.; Moriya, T.; Tsuchiya, F.; Ogawa, S.; Muramatsu, M. and Sasano, H. (2001): EBAG9/RCAS1 in human breast carcinoma: a possible factor in endocrine-immune interactions, Br J Cancer (vol. 85), No. 11, pp. 1731-7. URL: http://www.ncbi.nlm.nih.gov/entrez/query.fcgi?cmd=Retrieve&db=PubMed&dopt=Citation&list_uids=11742495

Suzuki, T.; Miki, Y.; Moriya, T.; Shimada, N.; Ishida, T.; Hirakawa, H.; Ohuchi, N. and Sasano, H. (2004): Estrogen-related receptor alpha in human breast carcinoma as a potent prognostic factor, Cancer Res (vol. 64), No. 13, pp. 4670-6. URL: http://www.ncbi.nlm.nih.gov/entrez/query.fcgi?cmd=Retrieve&db=PubMed&dopt=Citation&list_uids=15231680

Takahashi, S.; Urano, T.; Tsuchiya, F.; Fujimura, T.; Kitamura, T.; Ouchi, Y.; Muramatsu, M. and Inoue, S. (2003): EBAG9/RCAS1 expression and its prognostic significance in prostatic cancer, Int J Cancer (vol. 106), No. 3, pp. 310-5. URL: http://www.ncbi.nlm.nih.gov/entrez/query.fcgi?cmd=Retrieve&db=PubMed&dopt=Citation&list_uids=12845666

Takatsu, H.; Futatsumori, M.; Yoshino, K.; Yoshida, Y.; Shin, H. W. and Nakayama, K. (2001): Similar subunit interactions contribute to assembly of clathrin adaptor complexes and COPI complex: analysis using yeast three-hybrid system, Biochem Biophys Res Commun (vol. 284), No. 4, pp. 1083-9. URL: http://www.ncbi.nlm.nih.gov/entrez/query.fcgi?cmd=Retrieve&db=PubMed&dopt=Citation&list_uids=11409905

Takatsu, H.; Sakurai, M.; Shin, H. W.; Murakami, K. and Nakayama, K. (1998): Identification and characterization of novel clathrin adaptor-related proteins, J Biol Chem (vol. 273), No. 38, pp. 24693-700. URL: http://www.ncbi.nlm.nih.gov/entrez/query.fcgi?cmd=Retrieve&db=PubMed&dopt=Citation&list_uids=9733768

Tanigawa, G.; Orci, L.; Amherdt, M.; Ravazzola, M.; Helms, J. B. and Rothman, J. E. (1993): Hydrolysis of bound GTP by ARF protein triggers uncoating of Golgi-derived COP-coated vesicles, J Cell Biol (vol. 123), No. 6 Pt 1, pp. 1365-71. URL: http://www.ncbi.nlm.nih.gov/entrez/query.fcgi?cmd=Retrieve&db=PubMed&dopt=Citation&list_uids=8253837

Tanos, B. and Rodriguez-Boulan, E. (2008): The epithelial polarity program: machineries involved and their hijacking by cancer, Oncogene (vol. 27), No. 55, pp. 6939-57. URL: http://www.ncbi.nlm.nih.gov/entrez/query.fcgi?cmd=Retrieve&db=PubMed&dopt=Citation&list_uids=19029936

Tarentino, A. L.; Trimble, R. B. and Maley, F. (1978): endo-beta-N-Acetylglucosaminidase from Streptomyces plicatus, Methods Enzymol (vol. 50), pp. 574-80. URL: http://www.ncbi.nlm.nih.gov/entrez/query.fcgi?cmd=Retrieve&db=PubMed&dopt=Citation&list_uids=26849

Tisdale, E. J.; Plutner, H.; Matteson, J. and Balch, W. E. (1997): p53/58 binds COPI and is required for selective transport through the early secretory pathway, J Cell Biol (vol. 137), No. 3, pp. 581-93. URL: http://www.ncbi.nlm.nih.gov/entrez/query.fcgi?cmd=Retrieve&db=PubMed&dopt=Citation&list_uids=9151666

Toscano, M. A.; Bianco, G. A.; Ilarregui, J. M.; Croci, D. O.; Correale, J.; Hernandez, J. D.; Zwirner, N. W.; Poirier, F.; Riley, E. M.; Baum, L. G. and Rabinovich, G. A. (2007): Differential glycosylation of TH1, TH2 and TH-17 effector cells selectively regulates susceptibility to cell death, Nat Immunol (vol. 8), No. 8, pp. 825-34. URL:

http://www.ncbi.nlm.nih.gov/entrez/query.fcgi?cmd=Retrieve&db=PubMed&dopt=Citation&list_uids=17589510

Trimble, W. S.; Cowan, D. M. and Scheller, R. H. (1988): VAMP-1: a synaptic vesicle-associated integral membrane protein, Proc Natl Acad Sci U S A (vol. 85), No. 12, pp. 4538-42. URL: http://www.ncbi.nlm.nih.gov/entrez/query.fcgi?cmd=Retrieve&db=PubMed&dopt=Citation&list_uids=3380805

Tsuboi, S. and Fukuda, M. (1997): Branched O-linked oligosaccharides ectopically expressed in transgenic mice reduce primary T-cell immune responses, EMBO J (vol. 16), No. 21, pp. 6364-73. URL: http://www.ncbi.nlm.nih.gov/entrez/query.fcgi?cmd=Retrieve&db=PubMed&dopt=Citation&list_uids=9351819

Tsuboi, S. and Fukuda, M. (1998): Overexpression of branched O-linked oligosaccharides on T cell surface glycoproteins impairs humoral immune responses in transgenic mice, J Biol Chem (vol. 273), No. 46, pp. 30680-7. URL: http://www.ncbi.nlm.nih.gov/entrez/query.fcgi?cmd=Retrieve&db=PubMed&dopt=Citation&list_uids=9804842

Tsuchiya, F.; Ikeda, K.; Tsutsumi, O.; Hiroi, H.; Momoeda, M.; Taketani, Y.; Muramatsu, M. and Inoue, S. (2001): Molecular cloning and characterization of mouse EBAG9, homolog of a human cancer associated surface antigen: expression and regulation by estrogen, Biochem Biophys Res Commun (vol. 284), No. 1, pp. 2-10. URL: http://www.ncbi.nlm.nih.gov/entrez/query.fcgi?cmd=Retrieve&db=PubMed&dopt=Citation&list_uids=11374862

Tsuchiya, F.; Ikeda, K.; Tsutsumi, O.; Hiroi, H.; Momoeda, M.; Taketani, Y.; Muramatsu, M. and Inoue, S. (2001): Molecular cloning and characterization of mouse EBAG9, homolog of a human cancer associated surface antigen: expression and regulation by estrogen., Biochemical and Biophysical Research Communications (vol. 284), No. 1, pp. 2-10. URL: http://research.bmn.com/medline/search/record?uid=MDLN.11374862

Tsuiji, H.; Takasaki, S.; Sakamoto, M.; Irimura, T. and Hirohashi, S. (2003): Aberrant O-glycosylation inhibits stable expression of dysadherin, a carcinoma-associated antigen, and facilitates cell-cell adhesion, Glycobiology (vol. 13), No. 7, pp. 521-7. URL: http://www.ncbi.nlm.nih.gov/entrez/query.fcgi?cmd=Retrieve&db=PubMed&dopt=Citation&list_uids=12672699

Tsuneizumi, M.; Emi, M.; Nagai, H.; Harada, H.; Sakamoto, G.; Kasumi, F.; Inoue, S.; Kazui, T. and Nakamura, Y. (2001): Overrepresentation of the EBAG9 gene at 8q23 associated with early-stage breast cancers, Clin Cancer Res (vol. 7), No. 11, pp. 3526-32. URL: http://www.ncbi.nlm.nih.gov/entrez/query.fcgi?cmd=Retrieve&db=PubMed&dopt=Citation&list_uids=11705872

Tu, L.; Tai, W. C.; Chen, L. and Banfield, D. K. (2008): Signal-mediated dynamic retention of glycosyltransferases in the Golgi, Science (vol. 321), No. 5887, pp. 404-7. URL: http://www.ncbi.nlm.nih.gov/entrez/query.fcgi?cmd=Retrieve&db=PubMed&dopt=Citation&list_uids=18635803

Tulsiani, D. R.; Hubbard, S. C.; Robbins, P. W. and Touster, O. (1982): alpha-D-Mannosidases of rat liver Golgi membranes. Mannosidase II is the GlcNAcMAN5-cleaving enzyme in glycoprotein biosynthesis and mannosidases Ia and IB are the enzymes converting Man9 precursors to Man5 intermediates, J Biol Chem (vol. 257), No. 7, pp. 3660-8. URL: http://www.ncbi.nlm.nih.gov/entrez/query.fcgi?cmd=Retrieve&db=PubMed&dopt=Citation&list_uids=7061502

Turano, C.; Coppari, S.; Altieri, F. and Ferraro, A. (2002): Proteins of the PDI family: unpredicted non-ER locations and functions, J Cell Physiol (vol. 193), No. 2, pp. 154-63. URL: http://www.ncbi.nlm.nih.gov/entrez/query.fcgi?cmd=Retrieve&db=PubMed&dopt=Citation&list_uids=12384992

Ungar, D.; Oka, T.; Krieger, M. and Hughson, F. M. (2006): Retrograde transport on the COG railway, Trends Cell Biol (vol. 16), No. 2, pp. 113-20. URL: http://www.ncbi.nlm.nih.gov/entrez/query.fcgi?cmd=Retrieve&db=PubMed&dopt=Citation&list_uids=16406524

van Kooyk, Y. and Rabinovich, G. A. (2008): Protein-glycan interactions in the control of innate and adaptive immune responses, Nat Immunol (vol. 9), No. 6, pp. 593-601. URL: http://www.ncbi.nlm.nih.gov/entrez/query.fcgi?cmd=Retrieve&db=PubMed&dopt=Citation&list_uids=18490910

van Meel, E. and Klumperman, J. (2008): Imaging and imagination: understanding the endo-lysosomal system, Histochem Cell Biol (vol. 129), No. 3, pp. 253-66. URL: http://www.ncbi.nlm.nih.gov/entrez/query.fcgi?cmd=Retrieve&db=PubMed&dopt=Citation&list_uids=18274773

Volchuk, A.; Amherdt, M.; Ravazzola, M.; Brugger, B.; Rivera, V. M.; Clackson, T.; Perrelet, A.; Sollner, T. H.; Rothman, J. E. and Orci, L. (2000): Megavesicles implicated in the rapid transport of intracisternal aggregates across the Golgi stack, Cell (vol. 102), No. 3, pp. 335-48. URL: http://www.ncbi.nlm.nih.gov/entrez/query.fcgi?cmd=Retrieve&db=PubMed&dopt=Citation&list_uids=10975524

Ward, T. H.; Polishchuk, R. S.; Caplan, S.; Hirschberg, K. and Lippincott-Schwartz, J. (2001): Maintenance of Golgi structure and function depends on the integrity of ER export, J Cell Biol (vol. 155), No. 4, pp. 557-70. URL: http://www.ncbi.nlm.nih.gov/entrez/query.fcgi?cmd=Retrieve&db=PubMed&dopt=Citation&list_uids=11706049

Watanabe, T; Inoue, S; Hiroi, H; Orimo, A; Kawashima, H and Muramatsu, M (1998): Isolation of estrogen-responsive genes with a CpG island library, Molecular And Cellular Biology (vol. 18), No. 1, pp. 442-449.

Watanabe, T.; Inoue, S.; Hiroi, H.; Orimo, A.; Kawashima, H. and Muramatsu, M. (1998): Isolation of estrogen-responsive genes with a CpG island library, Mol Cell Biol (vol. 18), No. 1, pp. 442-9. URL: http://www.ncbi.nlm.nih.gov/entrez/query.fcgi?cmd=Retrieve&db=PubMed&dopt=Citation&list_uids=9418891

Waters, M. G.; Serafini, T. and Rothman, J. E. (1991): 'Coatomer': a cytosolic protein complex containing subunits of non-clathrin-coated Golgi transport vesicles, Nature (vol. 349), No. 6306, pp. 248-51. URL: http://www.ncbi.nlm.nih.gov/entrez/query.fcgi?cmd=Retrieve&db=PubMed&dopt=Citation&list_uids=1898986

Wearsch, P. A.; Jakob, C. A.; Vallin, A.; Dwek, R. A.; Rudd, P. M. and Cresswell, P. (2004): Major histocompatibility complex class I molecules expressed with monoglucosylated N-linked glycans bind calreticulin independently of their assembly status, J Biol Chem (vol. 279), No. 24, pp. 25112-21. URL: http://www.ncbi.nlm.nih.gov/entrez/query.fcgi?cmd=Retrieve&db=PubMed&dopt=Citation&list_uids=15056662

Weimer, C.; Beck, R.; Eckert, P.; Reckmann, I.; Moelleken, J.; Brugger, B. and Wieland, F. (2008): Differential roles of ArfGAP1, ArfGAP2, and ArfGAP3 in COPI trafficking, J Cell Biol (vol. 183), No. 4, pp. 725-35. URL: http://www.ncbi.nlm.nih.gov/entrez/query.fcgi?cmd=Retrieve&db=PubMed&dopt=Citation&list_uids=19015319

Wendler, F. and Tooze, S. (2001): Syntaxin 6: the promiscuous behaviour of a SNARE protein, Traffic (vol. 2), No. 9, pp. 606-11. URL: http://www.ncbi.nlm.nih.gov/entrez/query.fcgi?cmd=Retrieve&db=PubMed&dopt=Citation&list_uids=11555414

Wessels, E.; Duijsings, D.; Niu, T. K.; Neumann, S.; Oorschot, V. M.; de Lange, F.; Lanke, K. H.; Klumperman, J.; Henke, A.; Jackson, C. L.; Melchers, W. J. and van Kuppeveld, F. J. (2006): A viral protein that blocks Arf1-mediated COP-I assembly by inhibiting the guanine nucleotide exchange factor GBF1, Dev Cell (vol. 11), No. 2, pp. 191-201. URL: http://www.ncbi.nlm.nih.gov/entrez/query.fcgi?cmd=Retrieve&db=PubMed&dopt=Citation&list_uids=16890159

White, J.; Johannes, L.; Mallard, F.; Girod, A.; Grill, S.; Reinsch, S.; Keller, P.; Tzschaschel, B.; Echard, A.; Goud, B. and Stelzer, E. H. (1999): Rab6 coordinates a novel Golgi to ER retrograde transport pathway in live cells, J Cell Biol (vol. 147), No. 4, pp. 743-60. URL: http://www.ncbi.nlm.nih.gov/entrez/query.fcgi?cmd=Retrieve&db=PubMed&dopt=Citation&list_uids=10562278

White, T.; Bennett, E. P.; Takio, K.; Sorensen, T.; Bonding, N. and Clausen, H. (1995): Purification and cDNA cloning of a human UDP-N-acetyl-alpha-D-galactosamine:polypeptide N-acetylgalactosaminyltransferase, J Biol Chem (vol. 270), No. 41, pp. 24156-65. URL: http://www.ncbi.nlm.nih.gov/entrez/query.fcgi?cmd=Retrieve&db=PubMed&dopt=Citation&list_uids=7592619

Whitehouse, C.; Burchell, J.; Gschmeissner, S.; Brockhausen, I.; Lloyd, K. O. and Taylor-Papadimitriou, J. (1997): A transfected sialyltransferase that is elevated in breast cancer and localizes to the medial/trans-Golgi apparatus inhibits the development of core-2-based O-glycans, J Cell Biol (vol. 137), No. 6, pp. 1229-41. URL: http://www.ncbi.nlm.nih.gov/entrez/query.fcgi?cmd=Retrieve&db=PubMed&dopt=Citation&list_uids=9182658

Yamamoto, K.; Fujii, R.; Toyofuku, Y.; Saito, T.; Koseki, H.; Hsu, V. W. and Aoe, T. (2001): The KDEL receptor mediates a retrieval mechanism that contributes to quality control at the endoplasmic reticulum, EMBO J (vol. 20), No. 12, pp. 3082-91. URL: http://www.ncbi.nlm.nih.gov/entrez/query.fcgi?cmd=Retrieve&db=PubMed&dopt=Citation&list_uids=11406585

Yamamoto, K.; Hamada, H.; Shinkai, H.; Kohno, Y.; Koseki, H. and Aoe, T. (2003): The KDEL receptor modulates the endoplasmic reticulum stress response through mitogen-activated protein kinase signaling cascades, J Biol Chem (vol. 278), No. 36, pp. 34525-32. URL: http://www.ncbi.nlm.nih.gov/entrez/query.fcgi?cmd=Retrieve&db=PubMed&dopt=Citation&list_uids=12821650

Yang, J. S.; Lee, S. Y.; Gao, M.; Bourgoin, S.; Randazzo, P. A.; Premont, R. T. and Hsu, V. W. (2002): ARFGAP1 promotes the formation of COPI vesicles, suggesting function as a component of the coat, J Cell Biol (vol. 159), No. 1, pp. 69-78. URL: http://www.ncbi.nlm.nih.gov/entrez/query.fcgi?cmd=Retrieve&db=PubMed&dopt=Citation&list_uids=12379802

Yoshino, A.; Setty, S. R.; Poynton, C.; Whiteman, E. L.; Saint-Pol, A.; Burd, C. G.; Johannes, L.; Holzbaur, E. L.; Koval, M.; McCaffery, J. M. and Marks, M. S. (2005): tGolgin-1 (p230, golgin-245) modulates Shiga-toxin transport to the Golgi and Golgi motility towards the microtubule-organizing centre, J Cell Sci (vol. 118), No. Pt 10, pp. 2279-93. URL: http://www.ncbi.nlm.nih.gov/entrez/query.fcgi?cmd=Retrieve&db=PubMed&dopt=Citation&list_uids=15870108

Zerial, M. and McBride, H. (2001): Rab proteins as membrane organizers, Nat Rev Mol Cell Biol (vol. 2), No. 2, pp. 107-17. URL: http://www.ncbi.nlm.nih.gov/entrez/query.fcgi?cmd=Retrieve&db=PubMed&dopt=Citation&list_uids=11252952

Zhang, Q. and Wang, Y. (2008): High mobility group proteins and their post-translational modifications, Biochim Biophys Acta (vol. 1784), No. 9, pp. 1159-66. URL: http://www.ncbi.nlm.nih.gov/entrez/query.fcgi?cmd=Retrieve&db=PubMed&dopt=Citation&list_uids=18513496

Zhang, X. L. (2006): Roles of glycans and glycopeptides in immune system and immune-related diseases, Curr Med Chem (vol. 13), No. 10, pp. 1141-7. URL: http://www.ncbi.nlm.nih.gov/entrez/query.fcgi?cmd=Retrieve&db=PubMed&dopt=Citation&list_uids=16719775

Zinchuk, V. and Zinchuk, O. (2008): Quantitative colocalization analysis of confocal fluorescence microscopy images, Curr Protoc Cell Biol (vol. Chapter 4), p. Unit 4 19. URL: http://www.ncbi.nlm.nih.gov/entrez/query.fcgi?cmd=Retrieve&db=PubMed&dopt=Citation&list_uids=18551422

Zinchuk, V.; Zinchuk, O. and Okada, T. (2007): Quantitative colocalization analysis of multicolor confocal immunofluorescence microscopy images: pushing pixels to explore biological phenomena, Acta Histochem Cytochem (vol. 40), No. 4, pp. 101-11. URL: http://www.ncbi.nlm.nih.gov/entrez/query.fcgi?cmd=Retrieve&db=PubMed&dopt=Citation&list_uids=17898874

Zizioli, D.; Meyer, C.; Guhde, G.; Saftig, P.; von Figura, K. and Schu, P. (1999): Early embryonic death of mice deficient in gamma-adaptin, J Biol Chem (vol. 274), No. 9, pp. 5385-90. URL:

http://www.ncbi.nlm.nih.gov/entrez/query.fcgi?cmd=Retrieve&db=PubMed&dopt=Citation&list_uids=10026148

Appendix

Acknowledgement

There are many people who made this work possible and I would like to express my immense gratitude to them.

First, I have to appreciate my supervisor Dr. Armin Rehm. He not only provided this interesting project, but also offered very good working conditions and permanent attendance to discuss my work. He helped me to develop my skills and establish scientific thinking.

Second, I want to thank Prof. Dr. med. Bernd Dörken for the opportunity to work in his group and for provision of an excellent working environment.

Third, I express my gratitude to my PhD supervisor Prof. Dr. Thomas Börner for his direct assistance, if needed, and representation of this thesis at the department of Biology, Humboldt University of Berlin.

Furthermore, I am thankful for stimulating discussion and valuable suggestions by the PhD committee members Prof. Dr. Fritz Rathjen and Prof. Dr. Michael Gotthardt. As a member of the International PhD Program “Molecular Cell Biology”, I thank Max-Delbrück-Center for Molecular Medicine for financial and equipment support. Likewise, I express my full thankfulness to PD Dr. Uta Höpken for frequent attendance of our lab meetings, discussion of the project and critical evaluation of the work.

Without the cooperation of partners, some critical data could not be achieved. I am extremely grateful to the support of Dr. Sebastian Schuck for the excellent supervision at the MPI for Molecular Cell Biology and Genetics in Dresden and introduction into polarized transport and Dr. Anje Sporbert for direct support at Microscopy Core Facility (MCF). Additionally**,** I thank J. Lippincott-Schwartz, L. Johannes, T. Südhof, B. Storrie, D. Mc Niven, R.D. Cummings, J. Gruenberg and I. Morano for providing us with essential reagents.

I extremely appreciate the help of the whole “Rehm-lab” members, their friendship and the pleasant atmosphere. Especially to Angela Mensen, Steffi Wittstock for frequent discussions and former members Dr. Constantin Rüder and Dr. Tatjana Reimer for introducing me to this project and techniques. In addition, I thank Kerstin Gerlach for expert technical assistance.

Last but not least, I am very grateful to Russ Hodge proofreading the manuscript.

Finally, when I meet any obstacles either in research or in daily life, my mother, parents in law and husband are always available, encouraged me and are ready to help, such as with statistical advise. I address my deepest appreciation to them. Especially to my daughter, who makes every day of my life somewhat special.

.

Abbreviations

Arf	Adenosine diphosphate-ribosylation factor
AP	Adaptor complex
APC	Antigen-presenting cell
BFA	Brefeldin A
BSA	Bovine serum albumin
C2GNT1	2-β6-N-acetylglucosaminyltransferase
CCV	Clathrin-coated vesicle
COG	Conserved oligomeric Golgi
COP	Coat Protein Complex
CTL	Cytotoxic T-lymphocyte
EBAG9	Estrogen receptor-binding fragment-associated gene 9
EGC	ER-to-Golgi carriers
ERAD	ER-associated protein degradation
ERE	Estrogen Responsive Element
EndoH	Endoglycosidase H
ER	Endoplasmatic reticulum
ERGIC-53 (p58)	ER-Golgi intermediate compartment
FACS	Fluorescence activated cell sorting
FPV	Fowl plaque virus
FRAP	Fluorescence recovery after photobleaching
GalNAc-α-O-bn	1-benzyl-2-acetamido-2-deoxy-α-D-galactopyranoside
GalNAc-T	UDP-N-acetyl-α-D-galactosamine: polypeptide N Acetyl-galactosaminyl-transferase
GalT	β-1-4 Galactosyltransferase
GlcNAc	N-acetylglucosamine
GEF	Guanine-nucleotid-exchange factor
GFP	Green fluorescence protein
GM130	Golgi matrix protein 130 kDa
GST	Glutathione S-transferase
hGH / rGH	Human / rat Growth Hormone
HA	Hemaglutenin A
HC	Heavy chain
IC	Intermediate compartment

IS	Immunological synapse
KDELr	Lys-Asp-Glu-Leu -receptor
LacZ	ß-galactosidase
Lck	Lymphoid specific cytosolic protein tyrosine kinase
Man II	Mannosidase II
MHC class I	Major Histocompatibility Complex antigen class I
MPR	Mannose-6-phosphate receptor
NANA	Neuraminidase
NGF	NGF
PDI	Protein Disulphide-Isomerase
PKA	Protein kinase A
PM	Plasma membrane
PNA	Peanut Agglutinin
RCAS1	Receptor-binding cancer antigen expressed on SiSo cells
SCID	Severe Combined Immunodeficient
SFK	Src (sarcoma) family kinases
SNAP25	Synaptosome-associated protein 25 kDa
SNARE	Soluble N-ethylmaleimide-sensitive factor attachment protein receptors
ST3Gal I	α2,3-sialyltransferase
STB	Shiga toxin B-fragment
TCR	T-cell receptor
TF	Thomsen-Friedenreich; O-glycan
TGN	Trans-Golgi-network
Tn	GalNAc; O-glycan
T-synthase	β1,3galactosyltransferase
VSVG	Vesicular Stomatitis Virus G protein
VTC	Vesicular-Tubular Clusters
VVA	Vivia Villosa Lectin

Index of figures

Index of tables

Eidesstattliche Erklärung

Hiermit erkläre ich, die vorliegende Arbeit selbstständig und ohne unerlaubte Hilfe angefertigt zu haben und alle Hilfsmittel und Inhalte aus anderen Quellen als solche gekennzeichnet zu haben. Des weiteren versichere ich, dass die vorliegende Arbeit nie Gegenstand eines früheren Promotionsverfahrens war.

Die Promotionsordnung der Mathematisch-Naturwissenschaftlichen Fakultät I der Humboldt-Universität zu Berlin habe ich gelesen und akzeptiert.

Jana Wolf Berlin, den 16.6.2010